RHODES UNIVERSITY

DEPARTMENT OF BIOCHEMISTRY, MICROBIOLOGY AND BIOTECHNOLOGY

PhD THESIS

Academic Year 2007

W M J A S B MANIPURA

Bioprocess development for removal of nitrogenous compounds from precious metal refinery wastewater

Supervisor: Dr. J. E. Burgess

January 2007

This thesis is submitted in fulfilment of the requirement for the Degree of DOCTOR OF PHILOSOPHY.

ABSTRACT

Removal of nitrogenous compounds from precious metal refinery (PMR) wastewater is important in terms of avoiding eutrophication (environmental protection), metal recovery (increased overall process efficiency and value recovery) and reuse of treated water (maximum use of natural resources). Extreme pH conditions (4 to 13 depending on the wastewater stream), high chemical oxygen demand (> 10,000 mg/l), numerous metals and high concentrations of those metals (> 20 mg/l of platinum group metals) in the wastewater are the main challenges for biological removal of nitrogenous compounds from PMR wastewater. Nitrogenous compounds such as NH_4^+-N and NO_3^--N are strong metal ligands, which make it difficult to recover metals from the wastewater. Therefore, a bioprocess was developed for removal of nitrogenous compounds from carefully simulated PMR wastewater.

A preliminary investigation of metal wastewater was carried out to determine its composition and physico-chemical properties, the ability to nitrify and denitrify under different pH conditions and denitrification with different carbon source compounds and amounts. Even at pH 4, nitrification could be carried out. A suitable hydraulic retention time was found to be 72 hours. There was no significant difference between sodium acetate and sodium lactate as carbon sources for denitrification. Based on these results, a reactor comparison study was carried out using simulated PMR wastewater in three types of reactors: continuously stirred tank reactor (CSTR), packed-bed reactor (PBR) and airlift suspension reactor (ALSR). These reactors were fed with 30 mg/l of Rh bound in an NH_4^+ based compound (Claus salt: pentaaminechlororhodium (III) dichloride). Total nitrogen removal efficiencies of > 68 %, > 79 % and > 45 % were obtained in the CSTR, PBR and ALSR, respectively. Serially connected CSTR-PBR and PBR-CSTR reactor configurations were then studied to determine the best configuration for maximum removal of nitrogenous compounds from the wastewater. The PBR-CSTR configuration gave consistent biomass retention and automatic pH control in the CSTR. Ammonium removal efficiencies > 95 % were achieved in both reactors. As poor nitrate removal was observed a toxicity study was carried out using respirometry and the half saturation inhibition coefficients for Pt, Pd, Rh and Ru were found to be 15.81, 25.00, 33.34 and 39.25 mg/l, respectively.

A mathematical model was developed to describe the nitrogen removal in PMR wastewater using activated sludge model number 1 (ASM1), two step nitrification and metal toxicity. An operational protocol was developed based on the literature review, experimental work and simulation results. The optimum reactor configuration under the set conditions (20 mg/l of Rh and < 100 mg/l of NH_4^+-N) was found to be PBR-CSTR-PBR process, which achieved overall NH_4^+-N and NO_3^--N removal efficiencies of > 90 % and 95 %, respectively. Finally, a rudimentary microbial characterisation was carried out on subsamples from the CSTR and $PBR_{Secondary}$. It was found that the CSTR biomass

consisted of both rods and cocci while $PBR_{Secondary}$ consisted of rods only. Based on these experimental works, further research needs and recommendations were made for optimisation of the developed bioprocess for removal of nitrogenous compounds from PMR wastewater.

ACKNOWLEDGEMENTS

On the way to this milestone of my life, there were many people who were behind my shoulders. Even though it is difficult to mention everybody at this stage, I must mention at least few of them who made my life a comfortable and meaningful one. First, my sincere thanks and gratitude go to my supervisor and research group leader, Dr. J.E. Burgess who put confidence in me assigning a very interesting research project. This led me to learn different disciplines in a short period of time. She was behind me at all the happy and hard times which I had to face during my stay at Rhodes. Her encouragement, prompt action and meticulous guidance always paved the way for me to achieve what I wanted to do. Thus an excellent training which I received under her supervision is priceless. Simply, "thank you very much Dr. Jo", as I used to call you.

The Joint Research Committee offered financial assistance for conference attendance. Dr. Kevin Whittington-Jones introduced me to Dr. Burgess, had the patience and time for replying to my numerous e-mails and he negotiated with Dr. Burgess on my behalf to join the environmental biotechnology research group (EBRG) of Rhodes University. My sincere appreciation should also go to Prof. Chris Buckley of Natal University in South Africa, who was quite keen to help me in using WEST and generously loaning us WEST software for simulation work. Prof. Mike Burton (Department of Mathematics, Rhodes University) encouraged and helped me to learn MATLAB which was quite useful for me in data analysis and simulation work.

Dr. Dave Robinson, Ms. Kerry Slatter and Dr. Neville Plint of Anglo Platinum Ltd. extended their constructive comments during progress meetings and thus their encouragement for improving the experiments was commendable. Anglo Platinum Ltd. without their generous funding, this research would not have been possible. Dr. Vera Barbosa and Dr. Roman Tandlich facilitated the research work during their tenure as laboratory managers at the EBRG. My special thanks also go to Dr. Tandlich helping me in initial microbial characterisation work. Dr. Oliver Hart who fabricated the reactors which were long lasting!

Ms. Louise Howis, our departmental secretary always put a smile on our faces using her usual humorous e-mails around the clock and her patience and diligent attention whenever the need arose. Mr. Anthony Sullivan (Department of Physics and Electronics) helped me in instrumentation work and Anthony had time for me to clarify whenever I had difficulties. Mr. Terry Butterworth (Zoology and Entomology) who always opened his workshop whenever I wanted to do modifications or any fabrication work of reactors. Mr. John Hemple (Geology) was kind enough to arrange the facilities for VSS measurements. Without all these people's assistance the work could have been a nightmare for me.

In the EBRG, Cherie-Lynn, James, Bronwyn, Eric, Rylan, for making the lab a home away from home for me. Thanks a lot Cherie and James for your generous assistance in my work. One and only one Sri Lankan who was with me at Rhodes, Darshan (Big D) always had some time to share all the ups and downs. And all those who changed my life positively (even with a smile!).

My sincere thanks also go to Prof. Ajith De Alwis, Dr. Sumith Pilapitiya, Prof. Malik Ranasinghe and Lashan Jayawardhana to all of whom I am indebted for their courage, motivation and directions for persuading me to do a doctoral study.

At last but not least my parents, who took care of me with their unconditional love, support and with the best they could afford as well as teaching me not to hate people but to develop the patience which always paid off handsomely at all the difficult times. Finally, I am indebted to my brothers; Anuruddha, Yasas and my sister; Gayani for their encouragement, patience and support.

TABLE OF CONTENTS

LIST OF FIGURES

LIST OF TABLES

ABBREVIATIONS AND NOTATIONS

Abbreviation	Description	Unit
ALSR	Airlift suspension reactor	
AMD	Acid-mine drainage	
ANAMMOX	ANaerobic AMMonium OXidation	
ANRP	Autotrophic nitrogen removal process	
ASM1	Activated Sludge Model number 1	
ASP	activated sludge processes	
ASR	Activated sludge respiration	
AOB	Ammonium oxidising bacteria	
AUR	Ammonium utilisation rate	mg/l/h
b	Endogenous-decay coefficient	1/d
BOD	Biochemical oxygen demand	mg/l
CA	Cellular automata	
CFD	Computational fluid dynamics	
CH_3OH	Methanol	
CSTR	Continuously stirred tank reactor	
CANON	Completely autotrophic nitrogen removal over nitrite	
COD	Chemical oxygen demand	mg/l
DO	Dissolved oxygen	mg/l
DOC	Dissolved organic carbon	mg/l
DWAF	Department of Water Affairs and Forestry	
E_{act}	Activation energy	J/moles
EPS	Extracellular polysaccharides	
FBR	Fluidised-bed reactor	
FEM	Finite element methods	
GAC	Granular activated carbon	
GDP	Gross domestic product	USD
GHG	Green house gas	
GWP	Global warming potential	
HAAO	Heterotrophic anaerobic ammonium oxidation	
HRT	Hydraulic retention time	h
IWA	International Water Association	
k_a	Ammonification constant	
K_i	Inhibition coefficients	mg/l
K_La	Oxygen mass transfer coefficient	mg/(l.h)

K_m	Michaelis constant, that concentration of substrate giving half maximum rate	mg/l
KBES	Knowledge based expert system	
LPS	Lipopolysaccharides	
MABR	Membrane aerated bioreactor	
MFD	Material flow diagram	
MBR	Membrane bioreactor	
MBBR	Moving-bed bioreactor	
MLSS	Mixed liquor suspended solids	mg/l
MLVSS	Mixed liquor volatile suspended solids	mg/l
NAF	Nitrite accumulation factor	
NH_3	Ammonia	mg/l
NH_4^+	Ammonium	mg/l
NO_2	Nitrogen dioxide	
NO_2^-	Nitrite	mg/l
NO_3^-	Nitrate	mg/l
NOB	Nitrite oxidising bacteria	
NFR	Nitrate formation rate	mg/l/h
NUR	Nitrate utilisation rate	mg/l/h
OLAND	Oxygen limited autotrophic nitrification denitrification	
OU	Oxygen uptake	mg/l
OUR	Oxygen uptake rate	mg/l/h
$[O_2]_g$	Oxygen concentration in the gas phase	mg/l
P_{O_2}	Partial pressure of oxygen	Pa
PBR	Packed bed reactor	
PGM	Platinum group metals	
PID	Proportional integral derivative	
PMR	Precious metal refinery	
PFD	Process flow diagram	
R	Universal gas constant	Pa.l/g/K
RRI	Reactor resistance to inhibition	
RSA	Republic of South Africa	
RTMC	Real-time monitoring and control	
S_I	Inhibitor concentration	mg/l
S_O	Dissolved oxygen concentration	mg/l
S_s	Substrate concentration	mg/l
SBR	Sequencing batch reactor	

SBR	Sequencing batch reactor	
SHARON	Single reactor High activity Ammonia Removal Over Nitrite	
SND	Simultaneous nitrification and denitrification	
SOU	specific oxygen uptake	mg/l/h
SOUR	specific oxygen uptake	mg/(l.h.mgVSS)
SRT	Solid retention time	d
t	Time	s
T	Temperature	°C
TAN	Total ammonium nitrogen	mg/l
TN	Total nitrogen	mg/l
TSS	Total suspended solids	mg/l
UCT	University of Cape Town	
UASB	Upflow anaerobic sludge blanket	
v	Reaction rate	mg/l/h
v_{max}	Maximum reaction rate	mg/l/h
V_g	Gas phase volume	l
V_l	Liquid phase volume	l
VFA	Volatile fatty acid	
WHO	World Health Organisation	
WRC	Water Research Commission of the RSA	
WWTP	Wastewater treatment plant	
X	Suspended biomass concentration	mg/l
X_H	Heterotrophic biomass concentration	mg/l
X_{ANX}	Anammox biomass concentration	mg/l
X_{AOB}	Ammonium oxidising biomass concentration	mg/l
X_i	Inert biomass concentration	mg/l
X_{NOB}	Nitrite oxidising biomass concentration	mg/l
$\hat{\mu}$	Maximum specific growth rate	1/d
μ_{decay}	Specific growth rate due to decay	1/d
μ_{syn}	Specific growth rate due to synthesis	1/d

This thesis is dedicated to my loving parents.

CHAPTER 1

Big things happen when you do the little things right.

- Don Gabor, Motivational speaker.

1.0 Introduction and Synopsis

1.1 Background

The Republic of South Africa (RSA) has achieved a significant development in mineral based resource economics due to the large abundance of concentrated mineral deposits in the country such as gold, platinum group metals (PGMs: Pt, Pd, Rh, Ir, Ru and Os), uranium, diamonds, coal etc. (Stilwell *et al.*, 2000). Hence mineral extraction, processing and refining technologies have been developed well in the country over a century, making South Africa one of the main mineral producing, processing and technology providing hubs of the mining world (Walker and Minnitt, 2006). South African mining plays an important role in the country's economy in terms of gross domestic product (GDP) contribution, employment creation and foreign exchange. According to government statistics, the industry contributed about 26 billion USD to the GDP in the year 2004 and has created about 415,000 employment opportunities (Statistics South Africa, 2004). The total export earnings in the year 2000 were about 14.5 billion USD, which accounted 47 % of the total exports value (Coakley, 2000). Given these facts, it is imperative to consider the significant impact of the mining industry on the socio-economic status of the South African people.

Even though the mining industry has influenced the South African economy positively, environmental strains imposed by this sector are immense with respect to land usage (e.g. Witwatersrand basin – gold fields stretch 350 km long, 200 km wide and have been mined up to depths of about 3500 m (WRC, 2005a), fresh water consumption (it has been estimated that the groundwater resource potential and utilisable groundwater exploitation potential in South Africa are 49 billion m^3/annum and 10.3 billion m^3/annum respectively (WRC, 2005b)) , mine waste (tailings), wastewater produced during refining, surface and ground water pollution (e.g. acid-mine drainage - AMD), and emissions to the atmosphere (e.g. CH_4, CO_2, CO, SO_2, NH_3; Winde and van der Walt, 2004). Therefore, the mining industry is one of the main pollution contributors in the country irrespective of its positive economic contribution to the country's progress. Nitrogen pollution from any contributor is a major concern due to eutrophication, ground water pollution and subsequent health hazards. High nitrate (NO_3^-) concentrations (20 mg/l < $[NO_3^-]$ < 200 mg/l) in ground water have been reported in many parts of the country. Nitrate is considered to be dangerous to people's health, resulting in infant methaemoglobinaemia when its concentration exceeds 40 mg NO_3^--N/l (WRC, 2005c). Even though excess NO_3^- pollution occurs due to point sources such as sewage sludge dying beds, land application of sludge, and irrigation of partly treated wastewater (WRC, 2005c), nitrogen pollution due to mining and metal refinery industries also should not be underestimated. Nitrogenous compounds are produced in this sector due to the use of nitrogen based compounds as blasting agents in mining and solvents in metal extraction. Therefore, stringent discharge standards have been set by regulating bodies such as the Department of Water Affairs and Forestry (DWAF) to minimise the pollution by different

industrial sectors including mining and metal processing, textile, paper, livestock, etc. Therefore, mining and metal processing industries are under constant pressure to develop environmentally sound technologies while maintaining their market competitiveness. Table 1.1 presents a summary of selected minimum discharge standards set by the DWAF and the drinking water quality as set by the World Health Organisation (WHO). It can be seen that several nitrogenous compounds are considered with enough priority to be subject to individual discharge limits – NH_4^+, NO_3^- and NO_2^-.

Table 1.1: Selected minimum discharge standards for wastewater by DWAF (1996) and WHO (2006).

No.	(Bio)Chemical parameter	Units	Permissible value		Remarks
			DWAF[1]	WHO[2]	
1	pH	-	4–11	6.5–8.0	Depends on the specific site[1].
2	Temperature	°C	5–30	N/A*	Site specific[1].
3	Dissolved oxygen (DO)	%	80 – 120	N/A*	Saturation of specific site[1].
4	Total Suspended solids (TSS)	mg/l	100	N/A*	
5	Total dissolved solids (TDS)	mg/l	N/A*	600	
6	Ammonium (NH_4^+-N)	µg/l	100	1165	Acute effect value[1]. No immediate health relevance[2].
7	Nitrite (NO_2^--N)	µg/l	N/A*	913.4	
8	Nitrate (NO_3^--N)	mg/l	10	11.3	
9	Sulphate (SO_4^-)	mg/l	N/A*	250	
10	Phosphate (PO_4^{2-}-P)	mg/l	5	N/A*	

*N/A – Not available

In addition, some nitrogenous compounds are strong metal ligands (e.g. NO_3^-), leading to the waste of a considerable amount of valuable metal found in the refinery wastewater as complexes, making it difficult to recover. Therefore, the removal of nitrogenous compounds from metal refinery wastewater is a three-fold benefit, namely: treatment of wastewater to meet discharge standards, recovery of valuable metals in the wastewater (which would otherwise be wasted in the downstream) and appropriate reuse of treated water in the refinery process or discharge to suitable receiving water bodies.

There are several different technological options available for nitrogen removal, and process selection is decided based on the nitrogen species concentration in the wastewater. According to Mulder (2003), three main categories can be identified: total ammonium-nitrogen concentrations (TAN) < 100 mg/l (category I: e.g. domestic wastewater), concentrations in the range of 100 – 5000 mg/l (category II: e.g. landfill leachate) and concentrated TAN where TAN > 5000 mg/l (category III: e.g. livestock industry). Biological treatment is usually used where nitrogen species concentration is < 5000 mg/l

(van Hulle, 2005) thus conventional biological treatment is preferred over the chemical nitrogen elimination by magnesium-ammonium-phosphate precipitation or air stripping (Wyffels *et al.*, 2004). Physico-chemical processes such as ion exchange are mainly used in category III and category II wastewater treatment (depending on the treatment effectiveness and cost recovery in category II). The precious metal refinery (PMR) wastewater which is the subject of this study comes under category II (see Chapter 3: Preliminary investigations of PMR wastewater).

The rationale behind this research was based on the factors discussed above, considering the needs of pollution control due to nitrogenous compounds release to the environment by the PMR wastewater, improved metal recovery after removal of nitrogenous compounds from the PMR wastewater and potential reuse of the treated water in the refining process, or release to the environment after meeting the minimum discharge standards set by regulating agencies, such as DWAF.

It was hypothesised that the nitrogenous compounds in the PMR wastewater could be removed biologically, assisting the downstream recovery of precious metals contained in the wastewater.

1.2 Objectives of the research

The four main objectives of the research were as follows:

1.2.1 Development of a nitrogen compounds removal system for PMR wastewater,

1.2.2 Development of a mathematical model to describe the process,

1.2.3 Development of an operational protocol for the system and

1.2.4 Downstream metal recovery using the developed system.

Chapter 3: Figure 3.1 shows an approximate material flow diagram (MFD) in the PMR production process highlighting the unit operations where wastewater is produced. The MFD is useful in achieving the above research objectives, for an input-output analysis at different unit operations, diverting wastewater for metal recovery and end of pipe treatment as appropriate.

1.3 Synopsis

Figure 1.2 shows the thesis chapter organisation for developing a bioprocess for removal of nitrogenous compounds from the carefully simulated PMR wastewater, operational protocol and subsequent downstream metal recovery.

Chapter 2 reviews the literature, considering the general characteristics of the PMR wastewater, different technologies available, microbiology of biological nitrogen removal processes and their optimum conditions, potential novel nitrogen removal processes and their chemical kinetics, process

and reactor selection, process control and the knowledge gap analysis with respect to biological treatment of the PMR wastewater.

Chapter 3 presents the preliminary investigations consisting of PMR wastewater characterisation, testing of potential of biological nitrogenous compound removal, effect of different pH on nitrification and denitrification, and evaluation of different carbon sources for denitrification. The results of the characterisation indicated that biological wastewater treatment could be possible but did not point to one process unit in particular, so the next phase of the research comprised a process comparison study.

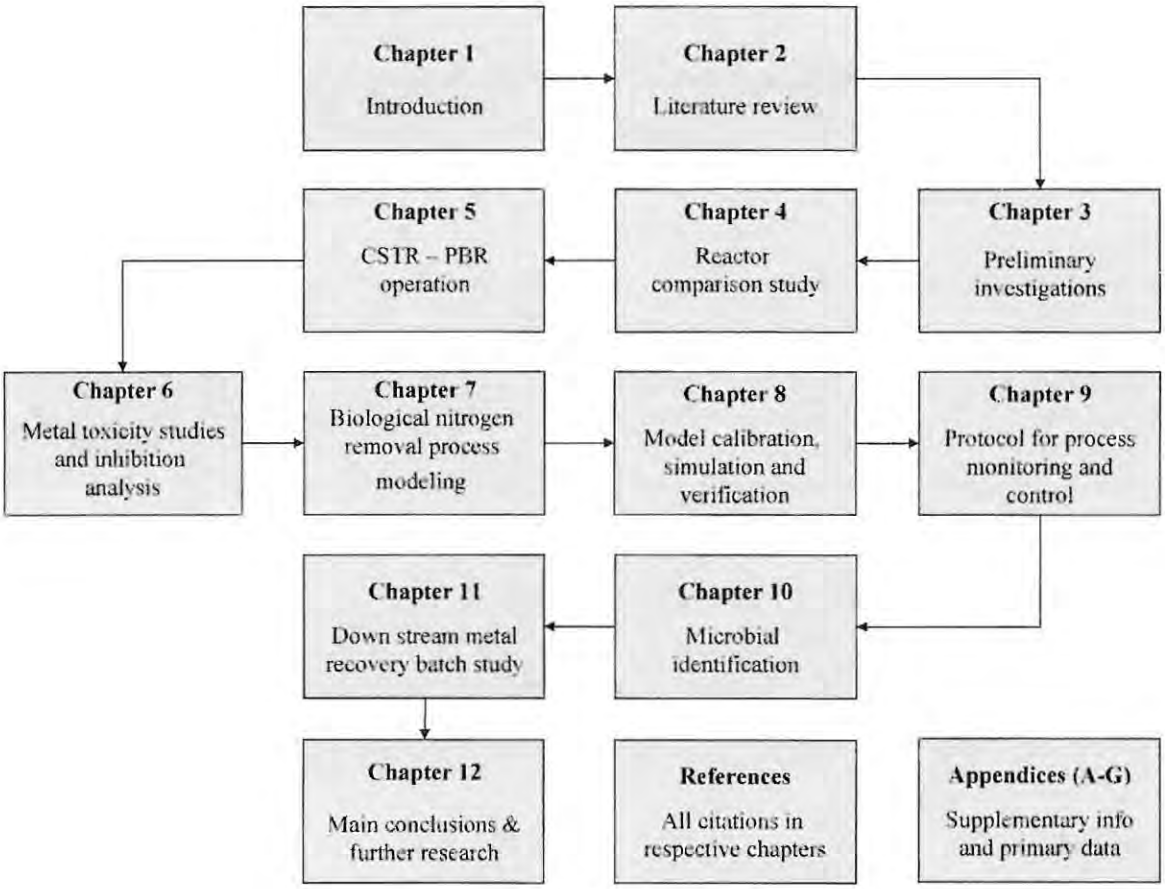

Figure 1.1: Thesis structure

Chapter 4 presents the reactor comparison study conducted to evaluate a suitable reactor type for nitrification and denitrification of simulated PMR wastewater using a rhodium (Rh) based ammonium compound (Claus salt: pentaaminechlrorhodium dichloride). The best result obtained for total nitrogen removal was 79 %, leading to the conclusion that a single-stage system could not achieve both nitrification and denitrification.

Chapter 5 describes the continuous operation of a continuously stirred tank (CSTR) and packed-bed reactor (PBR) combined as dual-stage system used to investigate nitrification and denitrification.

While 99 % ammonium removal was obtained, only 32 % nitrate removal could be achieved. Attempts to improve the process by changing the unit sequence had limited success, and one possible cause identified was the toxicity of the PGMs to the denitrifying organisms. It was also clear that empirical process optimisation was not a time and cost effective option, so a mathematical model was chosen as the efficient alternative.

Chapter 6 reports the results obtained for precious metal toxicity and various component analysis studies carried out for activated sludge based on respirometry batch tests. Inhibition coefficients of selected PGMs were identified empirically for inclusion in the mathematical model of the process.

Chapter 7 presents the mathematical model development of nitrogenous compounds removal from PMR wastewater based on Activated Sludge Model number 1, autotrophic nitrogen removal and metal toxicity due to precious metals.

Chapter 8 presents the simulation, approximate calibration and sensitivity analysis of the model described in Chapter 7 using the experimental data and MATLAB 7.0 / Simulink 6.0 simulation environment.

Chapter 9 sets out an operation protocol for process monitoring and control of the reactor configuration used in Chapter 8. Further, it summarises performances of different reactor configurations studied during the bioprocess development.

Chapter 10 describes preliminary microbial characterisation using a set of identification methods to investigate biomass sampled from the process configuration used in Chapter 9.

Chapter 11 presents the metal recovery batch tests carried out using simulated PMR wastewater to assess the effectiveness of metal recovery after nitrogenous compounds removal.

Chapter 12 discusses the important findings of the research and provides research recommendations for optimising the bioprocess developed for removal of nitrogenous compounds from simulated PMR wastewater.

Appendices A to F provide the supplementary information and primary data sheets used in the analysis of the results presented in the preceding chapters.

CHAPTER 2

An edition of this chapter has been published as:

Manipura, A., Roman, H.J., Duncan, J.R., Burgess, J.E., 2005. Potential biological processes available for removal of nitrogenous compounds from metal industry wastewater. Process Safety and Environmental Protection, 83 (B5): 472-480.

A problem is an opportunity in work clothes.

- Henry Kaiser (1882-1967), American industrialist.

2.0 Literature review

2.1 Introduction

Nitrogen is an essential element for all life forms on earth as a building block of proteins (Rožić *et al.*, 2000). However, excess amounts of nitrogen are not only toxic to organisms (Rožić *et al.*, 2000) but also lead to eutrophication of ecosystems, which in recent times has caused interest in nitrogen biotransformations (Kowalchuk and Stephen, 2001). The European Union and other developed countries called for the revision of wastewater discharge requirements due to rising nitrogen pollution as indicated by the deterioration of water quality of different aquifers, eutrophication of receiving water bodies, and nitrogen related health problems (Bilanovic *et al.*, 1999; Jeong *et al.*, 2006). Further, Bilanovic *et al.* stated that the solution to the high-quality water shortage depends on the elimination of N-compounds and other pollutants, efficient water recycling and comprehensive implementation of effective biological treatments into daily wastewater practices. Usually mineral processing wastewater contains nitrogenous compounds such as ammonium (NH_4^+) and nitrate (NO_3^-) as a result of the use of nitrogenous compounds (e.g. ammonium hydroxide as a precipitant, ammonium sulphate as an ion exchange resin eluent and nitrate based blasting agents during mining). Therefore, wastewater produced by mineral processing must be treated properly prior to discharge to the environment, according to the minimum standards set by government monitoring and regulating agencies. However, treatment of heavy industrial wastewaters is somewhat complicated by their inherent characteristics and variability, as these inhibit the traditional biological treatment processes used in municipal wastewater treatment. Low pH and high NH_4^+ and NO_3^- concentrations (Koren *et al.*, 2000) are typical characteristics of mineral and metal processing wastewaters. Metal refinery wastewater contains a large quantity of nitrogenous compounds which will lead to eutrophication of environmental waters if discharged without sufficient treatment and prevent the recovery of metals from the effluent, as some of the nitrogenous compounds (e.g. NO_3^-) are strong metal ligands (Kasia *et al.*, 2005). Further, high NH_4^+ or nitrite (NO_2^-) concentrated industrial wastewater inhibits the nitrification process in conventional municipal wastewater treatment (Carrera *et al.*, 2003).

Presently numerous industrial manufacturing sites use a variety of different water management strategies to reduce fresh water intake in their processes and the volumes of wastewater generated, hence discharging reduced volumes of effluent to the environment, minimising the deterioration of water quality in the process circuits and treating the water to the required level of reuse and then, final discharge (Pulles *et al.*, 1996). Maximised water recycling and reuse of treated wastewater can lead to minimum discharge of polluted water to the environment and intake of potable water. This often ensures meeting the minimum environmental standards. As a result of water reuse, financially and environmentally significant potable water savings can be made.

Conventional metal recovery technologies (physicochemical processes; precipitation, coagulation, reduction, ion exchange, evaporation, and membrane processes) have several disadvantages such as low metal extraction efficiency, high reagent requirements, high costs, generation of toxic sludge and the problem of safe disposal of process by-products (Cho and Kim, 2003). Conversely, biological treatment technologies have distinct advantages over conventional methods, as these are highly selective, more efficient, easy to operate, and cost effective. Therefore, these factors have led researchers to explore the possibilities of use of microbial techniques in industrial wastewater treatment (Brombacher *et al.*, 1997; Fux *et al.*, 2006; Goel and Flora, 2005). Further favourable characteristics of microbes (such as higher growth rate, low generation (doubling) time, well diversified species under different environmental conditions and capability of metabolising different substrates) have been the concern of many researchers (Saglam *et al.*, 1999; Suhasini *et al.*, 1999; Tien, 2002) for using biological processes in metal industry wastewater treatment.

Removing the nitrogenous compounds from wastewater usually involves a two-step biological process, namely nitrification-denitrification, by transforming the nitrogenous compounds to dinitrogen gas (Maier *et al.*, 2000). The nitrification process is mainly carried out by autotrophic aerobic bacteria, while denitrification is mainly carried out by anaerobic heterotrophic bacteria. Therefore, the use of a dual reactor system for each operation is common practice, which enables independent control of both the nitrification and denitrification processes. As nitrification is carried out by autotrophic nitrifying bacteria, the presence or addition of organic matter retards the growth of nitrifying bacteria by allowing the heterotrophic bacteria which compete for other nutrients contained in the reactor to dominate, and ultimately the nitrification process is failed or operated under optimum conditions. As nitrification is an aerobic process and denitrification is anoxic, perhaps it is wise to operate the two processes independently.

In order to find an appropriate technique for treatment of mineral and metal industry wastewaters, factors to consider include the chemical (oxidation state, ionization energy), physical (precipitation of metals under different pH conditions, solubility) and biological (microbial response to different metal concentration, accumulation of metals by metabolically active biomass) properties of metals, characteristics and composition of the industrial effluent, seasonal composition variations of the wastewater, suitable species of microbes and their optimum environmental conditions (pH and temperature), reactor types to be used and their operational characteristics. Therefore, in implementing technologies for treating nitrogenous mining and refining wastewater, it is necessary to consider capital cost, both the optimum operational environment and the operational cost of those technologies. This may achieve the dual objectives of meeting the regulating standards and the recovery of metals from the wastewater, which will otherwise be wasted downstream. Further, it would ensure the maximum recycling of treated wastewater, minimising the demand for potable water.

Therefore, the objectives of this chapter are to present the biological process selection aspects of removal of nitrogenous compounds from metal refining wastewaters, to review the microbial types used, removal efficiency and reactor types in early biological treatment processes and to identify the critical parameters to be considered in selecting and tailoring a bioreactor type for removing nitrogenous compounds from metal industry wastewaters.

2.2 Process Microbiology

As previously mentioned, nitrification – denitrification is a two-step process. First, NH_4^+ is converted to NO_2^- by ammonium oxidising bacteria (AOB). Then, NO_2^- is oxidised to NO_3^- by nitrite oxidising bacteria (NOB). Conversion of NH_4^+ into NO_3^- is known as nitrification. In the denitrification process, NO_3^- is converted to dinitrogen gas ($N_{2(g)}$) in two steps by denitrifying bacteria, first NO_3^- to NO_2^- and then NO_2^- to $N_{2(g)}$. The overall process can be summarised as shown in Figure 2.1.

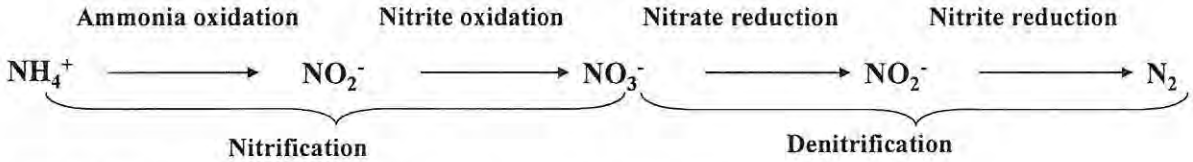

Figure 2.1: Overall nitrification and denitrification process.

Chemolitho-autotrophic AOB, which have the ability to utilise NH_4^+ as a sole source of energy and carbon dioxide as the main source of carbon, are responsible for the rate-limiting step of nitrification. Generally, AOB are obligate aerobes, but there are some species that may be highly tolerant to low oxygen or anoxic environments (Kowalchuck and Stephen, 2001; van Graaf *et al.,* 1995). Ammonia oxidising bacteria were classified into different genera based on cell morphology, such as *Nitrosomonas*, *Nitrosococcus*, *Nitrosospira*, *Nitrosovibrio*, and *Nitrosolobus.* However, based on 16S rRNA sequence homology, *Nitrosospira*, *Nitrosovibrio*, and *Nitrosolobus* have since been proposed to combine into one common genus *Nitrosospira* (Bothe *et al.,* 2000). Nitrifying bacteria (aerobic AOB and NOB) belong to a very restricted group of autotrophs. *Nitrosomonas* and *Nitrosospira* are the best known AOB (Schramm *et al.,* 1998) while *Nitrobacter* (Burerell *et al.,* 1998) and *Nitrospira* are the most well known NOB (Sliekers *et al.,* 2002).

Egli *et al.* (2003) reported that the AOB *Nitrosomonas eutropha* and *Nitrosomonas europea*, were observed only at pH 7.5 and 30 °C. Further, they suggested that pH is more important than temperature in selecting *N. eutropha* and *N. europea.* Ammonium oxidising bacteria produce large quantities of extracellular polysaccharides (EPS) when growing in surface biofilm communities. High EPS bacteria have a greater tolerance to low pH (Hesselsoe and Sorensen, 1999). Further, AOB populations tend to reside in the more external regions of flocs or biofilms, where oxygen levels are

typically high, whereas NOB typically reside internally and adjacent to AOB, where lower oxygen conditions are detected. However, nitrification is mainly limited to the outer 100-150 μm of flocs or films (Schramm *et al.*, 1998; Kowalchuck and Stephen, 2001).

Denitrifiers belong to a diverse group of facultative anaerobic bacteria which have the ability to use nitrogen oxides (NO_3^- and NO_2^-) as electron acceptors, and produce $N_{2(g)}$ as the end product (Etchebehere *et al.*, 2001). Therefore, denitrifying bacteria spread in well diversified genera with a spectrum of heterotrophic and autotrophic metabolism (Szekeres *et al.*, 2002). The denitrifying bacteria most frequently isolated from soil belong to the genera *Alicaligenes* and *Pseudomonas* (Casasus, *et al.*, 2005). However, predominant members isolated from activated sludge belong to the *Rubrivivax* subgroup in the β-purple subdivision, the *Rhodobacter* group in the α-purple subdivision, and the *Pseudomonas* subgroup in the γ-purple subdivision (Martienssen *et al.*, 1999; Etchebehere *et al.*, 2001).

The *Planctomycetales* are responsible for anaerobic NH_4^+ oxidation processes. The order *Planctomycetales* includes four genera: *Planctomyces, Pirellula, Gemmata* and *Isosphaera* (Schmidt *et al.*, 2002). Two species of *Planctomyces* are *Brocadia Anammoxidans* and *Kuenenia stuttgartiensis* (Fujii *et al.*, 2002). Strous *et al.* (2006) assembled the genome of the uncultured Anammox bacterium *Kuenenia stuttgartiensis* from a complex bioreactor community. This has shown the evolutionary history of the Planctomycetes, allowing a better understand of the organisms' special properties. Further, they identified candidate genes responsible for ladderane biosynthesis and biological hydrazine metabolism, and versatility. Under oxygen-limited conditions, the AOB oxidise NH_4^+ to NO_2^- and keep oxygen concentrations low, while *B. Anammoxidans* convert the produced NO_2^- and the remaining NH_4^+ to $N_{2(g)}$ (Schmidt *et al.*, 2002). It has been estimated that Anammox is responsible for 50 % fixed nitrogen removal in the ocean (Strous *et al.*, 2006). The Anammox pathway is used in different nitrogen removal systems such as the oxygen limited autotrophic nitrification denitrification process - OLAND (Kuai and Verstraete, 1998), completely autotrophic nitrogen removal over nitrite - CANON (Third *et al.*, 2001; Sliekers *et al.*, 2002) and Anammox process in gas-lift and sequencing batch reactors (Dapena-Mora *et al.*, 2004).

Both mixed and pure cultures of *Nitrosomonas eutropha* are capable of denitrification under oxygen limited conditions. According to Jetten *et al.* (2001), in the presence of nitrogen dioxide (NO_2), the anaerobic activity of *N. eutropha* was boosted to 2.2 nmol/NH_4^+/min/mg protein. However, this is 50-fold slower than the obligate anaerobe *B. Anammoxidans* and 200 times slower than the aerobic activity of *N. eutropha* itself (Jetten *et al.*, 2001).

Metal toxicity to microbes plays an important role in metal industry wastewater treatment (Principi *et al.*, 2006). Metal uptake by primary sludge is significantly affected by pH (Wang *et al.*, 2006) and

therefore metal uptake by microbes has a major role in nitrogen removal of PMR wastewaters which has a wide pH range (from acidic to caustic). The toxicity of heavy metals to the nitrification and denitrification processes in activated sludge systems has been studied extensively (Beg *et al.*, 1998; Gumaelius *et al.*, 1996; Lewandowski, 1985; 1987; Lim *et al.*, 2003; Principi *et al.*, 2006; Stephen *et al.*, 1999; White *et al.*, 1997). Gumaelius *et al.* (1996) studied the effects of cadmium (Cd) in denitrification process under pure culture conditions and found a significant decrease of NO_2^- conversion at a concentration of 10 mg/l. Chromium (CrIV) toxicity also has been studied and it was found that the Cr concentration affects both nitrification and organic oxidation (Beg *et al.*, 1998). The nitrifying microorganisms are generally more susceptible to metal inhibition than the heterotrophic microorganisms responsible for COD oxidation (Dahl *et al.*, 1997). Although a constant low-level exposure to metals does not typically affect microbial activity due to biomass acclimation (Neufeld and Hermann, 1975), shock loads of metals can lead to complete failure of biological processes (Bagay and Sherrard, 1981; Battistoni *et al.*, 1993). For example, Juliastuti *et al.* (2003) illustrated that the net maximum specific growth rate of autotrophic biomass decreases as the concentration of heavy metals increases. The growth rate of their autotrophic biomass was 92 % inhibited at 1.2 mg/l Zn^{2+}. The net maximum specific growth rate was severely reduced by Zn^{2+} at concentrations above 0.3 mg/l. Eysenbach (1994) also reported 0.08 mg/l Zn^{2+} as the minimum inhibition threshold value, and 0.08–0.5 mg/l Zn^{2+} as the range of inhibition levels. These findings illustrate the extensive studies done on commonly found heavy and base metals. Monti-bragadin *et al.* (1987) worked on mutagenic effects of Rh(I) and Ru (II) on bacteria. However, the toxic effect of precious metals on nitrification and denitrification or on activated sludge processes (ASP) have been hardly reported in the public literature. This is a critical area to be investigated in developing a bioprocess to remove nitrogenous compounds from the precious metal refinery (PMR) wastewaters. A comparison of half-saturated inhibition coefficients of different metals commonly found in traditional wastewater treatment plants and PGM data are presented in the discussion of Chapter 6 (Table 6.9).

Monitoring strategies have been developed to accurately and rapidly determine the microbial inhibition potential of a wastewater stream. For instance, short-term batch respirometric assays have been used to quantify nitrification inhibition (Chandran and Smets, 2000; Checchi and Marsili-Libelli, 2005; Gernaey *et al.*, 1997). Other assays rely on measurement of NH_4^+-N or NO_2^--N after short term incubation of pure cultures of *Nitrosomonas* and *Nitrobacter* with test toxicants (Grunditz and Dalhammar, 2001) as well as in mixed cultures as found in industrial wastewaters (Horsch *et al.*, 2004), Microtox™ determination of bioluminescence using *Photobacterium phosphoreum* (Sillanpaa and Oikari, 1996) and detection of stress protein generation in response to toxic shocks (Bott and Love, 2001). The foremost disadvantage of such tests is that they consider acute inhibitory responses only. Other studies have demonstrated that such short-term data may not adequately reflect the response observed in continuous flow reactors subject to prolonged toxic exposure (Vandevivere *et*

al., 1998), and in addition they fail to account for acclimatisation of consortia to individual wastewaters.

Table 2.1 presents a summary of bacteria and enzymes involved in nitrification and denitrification processes. Figure 2.2 shows the overall analysis of nitrification – denitrification in terms of process steps, aerobic / anaerobic / anoxic conditions, participating micro-organisms, and their autotrophic / heterotrophic conditions.

2.3 Available technologies for nitrogenous compounds removal

Existing different technologies vary in their cost aspects, chemical and energy requirements, operational experiences, and process reliability (Mulder, 2003). A range of new microbial processes have been described and investigated at laboratory and pilot scales as well as field scale (Fux *et al.*, 2002; Jetten *et al.*, 2004; Lucas *et al.*, 2005; Metcalf and Eddy Inc., 2004; Sliekers *et al.*, 2003; Strous et al., 1997; Windey *et al.*, 2005; Wyffels *et al.*, 2004) such as aerobic denitrification and heterotrophic nitrification (SND – simultaneous nitrification / denitrification) and anaerobic ammonium oxidation (Anammox) and completely autotrophic nitrogen removal over nitrite (CANON) etc. The well established ASP is still being used successfully around the world with different configurations (Metcalf and Eddy Inc., 2004; Rittmann and McCarthy, 2001). The following section briefly describes these different processes used for nitrification and denitrification, according to the conversions involved, process configuration and operational control.

2.3.1 Activated sludge process (ASP) with different configurations

The ASP has been used for wastewater treatment since the early 20th century (Jeppsson, 1996; Metcalf and Eddy Inc., 1991; Rittmann and McCarthy, 2001). The ASP is strictly aerobic, although anoxic variations are used in the denitrification process (Rittmann and McCarthy, 2001). This process consists of an aeration tank, settling tank and sludge return from the settling tank back to the aeration tank. This basic configuration has been reconfigured to optimise a particular interest such as removal of NH_4^+ or NO_3^- or phosphorous in number of processes such as the UCT process, modified UCT process, two-stage Phoredox (A/O) process, five stage Phoredox (modified Bardenpho) process, three-stage Phoredox (A^2/O) process and Johannesburg process. These processes have been modified based on physical configuration, oxygen addition or distribution and organic loading (biochemical oxygen demand-BOD) (Rittmann and McCarthy, 2001). Jeppsson (1996) and Rittmann and McCarthy (2001) presented a detailed discussion on ASP in wastewater treatment describing different models and configurations used around the world. Due to the wide spread application and acceptance of this process, the International Water Association (IWA) developed a series of mathematical models (ASM1, ASM2, ASM2d, ASM3, etc.) for better understanding and application of ASP in treating

Table 2.1: Bacteria and enzymes involved in nitrification and denitrification process (Bothe *et al.*, 2000).

Enzyme	Reaction performed	Genes	Function of gene product	Bacteria from which genes were sequenced (see footnote).
NO_3^- reductase	$NO_3^- + 2e^- + 2H^+ \rightarrow NO_2^- + H_2O$	*narG*	Catalytic centre	1- 7 & 12 others partly
		narH	Confers e- from NarI to NarG	1- 7 and partly 8
		narJ	Function unknown	1- 7
		narI	Membrane anchor, QH_2 oxidation	1- 7
Heme NO_2^- reductase	$NO_2^- + e^- + 2H^+ \rightarrow NO + H_2O$	*nirS*	Catalytic centre	4, 9, 10 & four others partly
Cu NO_2^- reductase	$NO_2^- + e^- + 2H^+ \rightarrow NO + H_2O$	*nirK*	Catalytic centre	11-17
NO reductase	$2NO + 2e^- + 2H^+ \rightarrow N_2O + H_2O$	*norB*	Catalytic centre	4, 5, 9, 10, 13, 17, 18, partly 20
		norC	Catalytic centre	2 × 4, 5, 10,13, 15, 2 × 17, 19
N_2O reductase	$N_2O + 2e^- + 2H^+ \rightarrow N_2 + H_2O$	*nosZ*	Catalytic centre	2 × 4, 5, 9, 10, 11, 13, 21 & 43 others partly
Ammonia monooxygenase	$NH_3 + 2[H] + O_2 \rightarrow NH_2OH + H_2O$	*amoA*	Active site	22- 28, 69 others partly
		amoB	Involved in activity	23, 24, 26 & two others partly
		amoC	Function unknown	26, 29, 30 & two others partly
Hydroxylamine oxireudctase	$NH_2OH + H_2O \rightarrow HNO_2 + 4[H]$	*hao*	Catalytic centre	26, 31 & one other partly

1. *Bacillus subtilis*
2. *Escherichia coli*
3. *Mycobacterium tuberculosis*
4. *Paracoccus denitrificans*
5. *Pseudomonas aeruginosa*
6. *Staphylococcus caenosus*
7. *Thermus thermophilus*
8. *Pseudomonas fluorescen*
9. *Ralstonia eutropha*
10. *Pseudomonas stutzeri*
11. *Achromobacter cycloclastes*
12. *Alcaligens faecalis*
13. *Bradyrhizobium japonicum*
14. *Pseudomonas chlororaphis*
15. *Pseudomonas* sp.
16. *Rhizobium hedysari*
17. *Rhodobacter sphaeroides*
18. *Nitrobacter hamburgensis*
19. *Paracoccus halodenitrificans*
20. *Synechocyctis* spp.
21. *Sinorhizobium meliloti*
22. *Pseudomonas putida*
23. *Nitrococcus oceani*
24. *Nitrococcus* sp. C-113
25. *Nitrosospira multiformis*
26. *Nitrosomonas europea*
27. *Nitrosospira briensis*
28. *Nitrosospira tenuis*
29. *Nitrospira* sp. NpAV
30. *Nitrosomonas* sp. TK 794
31. *Nitrosomonas* sp. EN-11

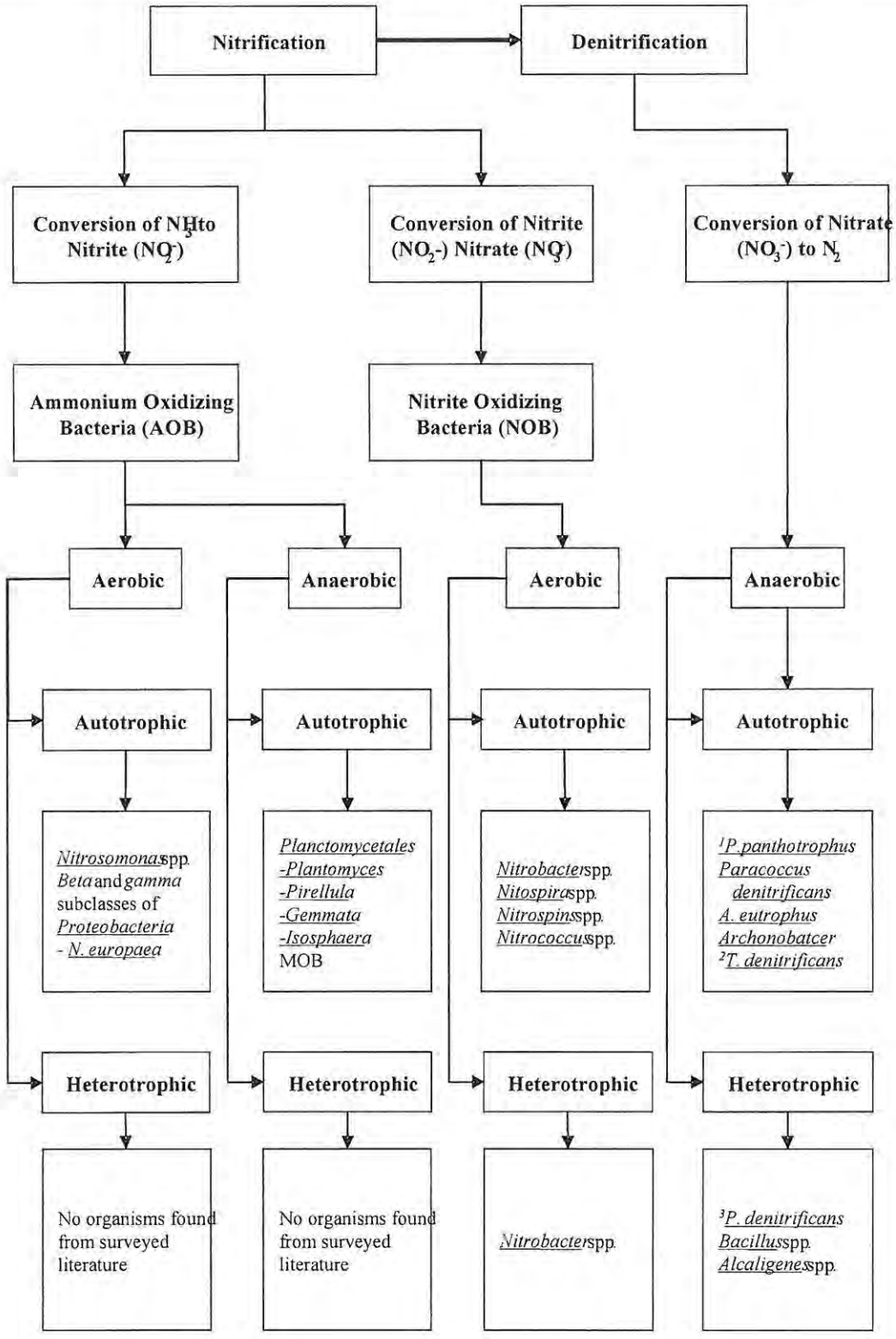

[1]P – Pseudomonas;[2]T – Thiobacillus[3]P - Paracoccus

Figure 2.2: Identification of microbes: Biological removal of nitrogenous compounds from precious metal refinery wastewater.

various wastewater streams (Brun *et al.*, 2002; Ekama and Wentzel, 2004; Gernaey *et al.*, 2004; Henze *et al.*, 1987; Moussa *et al.*, 2005; Sin *et al.*, 2005).

2.3.2 Oxygen Limited Autotrophic Nitrification Denitrification (OLAND®) process

The basic principle of the process is based on supplying oxygen such that nitrification only proceeds up to the NO_2^- step. Subsequently, due to the lack of an electron acceptor, the NO_2^- is consumed to oxidise another mole of NH_4^+ (Verstraete and Philips, 1998). Ammonium removals in the OLAND system are reported to take place via the following steps.

$$2\ NH_4^+ + 1.5\ O_2 \rightarrow NO_2^- + H_2O + 2\ H^+ + NH_4^+ \quad (2.1)$$

$$NH_4^+ + NO_2^- \rightarrow N_2 + 2\ H_2O \quad (2.2)$$

The whole process can be summarised as

$$2\ NH_4^+ + 1.5O_2 \rightarrow N_2 + 3H_2O + 2H^+ \quad (2.3)$$

In the OLAND system, the autotrophic conversion of NH_4^+- N to N_2 may be effected mainly by AOB, not by NOB (Kuai and Verstraete, 1998). The *Nitrosomonas* species obtain sufficient energy for cell maintenance using the above reactions. The key parameter to control the process is oxygen. However, this is rather difficult under mixed culture conditions. Therefore, a pH controlled aeration approach seems to be feasible for controlling this process (Verstraete and Philips, 1998).

2.3.3 ANaerobic AMMonium OXidation (Anammox®) process

The Anammox process was first reported as a process which converts NH_4^+ to $N_{2\,(g)}$ with NO_3^- serving as the electron acceptor under autotrophic anaerobic conditions (Verstraete and Philips, 1998). This process is based on energy conservation through anoxic NH_4^+ oxidation with NO_2^- as the electron acceptor. Hydrazine and hydroxylamine are intermediate products in the process (Shivaraman and Shivaraman, 2003).

Table 2.2 shows some of the possible reaction steps that could occur in the Anammox process. Enzymes such as ammonia monooxygenase, hydroxylamine oxidoreductase and nitrite reductase may be involved (Jetten *et al.*, 1999). According to Jetten *et al.* (2001), the electron acceptor, nitrite, is reduced to hydroxylamine and later reacts with the electron donor, NH_4^+, producing $N_{2\,(g)}$. Hydrazine is the intermediate product in the final step and is oxidised to $N_{2\,(g)}$, producing electrons for the initial reduction of nitrite to hydroxylamine.

Table 2.2: Possible reactions of anaerobic ammonium oxidation via NO and HNO as intermediate (Anammox process).

Reaction	Associated enzyme
NO as intermediate	
$NO + NH_3 + 3H^+ + 3e^- \rightarrow N_2H_2 + H_2O$	ammonia monooxygenase-like enzyme
$N_2H_2 \rightarrow N_2 + 4H^+ + 4e^-$	hydroxylamine oxidoreductase like enzyme
$NO^-_2 + 2H^+ + e^- \rightarrow NO + H_2O$	nitrite reductase
$NH_3 + NO^-_2 + H^+ \rightarrow N_2 + 2\ H_2O$	
HNO as intermediate	
$HNO + NH_3 \rightarrow N_2H_2 + H_2O$	ammonia monooxygenase-like enzyme
$N_2H_2 \rightarrow N_2 + 4H^+ + 4e^-$	hydroxylamine oxidoreductase like enzyme
$NO^-_2 + 2H^+ + 2\ e^- \rightarrow HNO + OH^-$	nitrite reductase
$NH_3 + NO^-_2 \rightarrow N_2 + H_2O + OH$	
$NH_3 + 1.32\ NO_2^- \rightarrow 1.02\ N_2 + 0.26NO_3^- + 2H_2O$	

Sources: Jetten *et al.*, 1999; Sliekers *et al.*, 2003.

Anammox activity decreases with increased nitrite concentrations. Strous *et al.* (1999) observed that the process was not completely inhibited until the NO_2^- concentration was 0.1 g NO^-_2 – N/l. The ratio of NH_4^+ and NO_2^- needed for the Anammox process is one to one (Jetten *et al.*, 2002). Therefore, monitoring and controlling of the NO_2^- concentration is an important factor in the Anammox process. Perhaps on-line monitoring and controlling of NH_4^+ and NO_2^- concentrations would enable efficient process operation.

Jetten *et al.* (2001) found the highest Anammox activity at pH 7.0 – 8.5 and temperature 30 – 37 °C in a fluidised bed reactor with a removal rate of 2.6 kg N_{tot}/m^3/day. This was later corroborated by Schmidt *et al.* (2002), who reported a high Anammox activity in a pH range between 6.4 and 8.3 and temperature range between 20 and 43°C. Under the optimum conditions, specific activity is about 3.6 mmol/g protein /h, the biomass yield is about 0.666 C-mol/mol NH_4^+, and specific growth rate is about 0.0027 h^{-1}.

The Anammox process is inhibited by higher NO_2^- concentrations (20 mM) and exposure to longer period (12 hours) of high concentrations also inhibits the process completely (Jetten *et al.*, 1999). Application of the Anammox process in nitrogen removal systems could reduce 90 % of operational cost (Jetten *et al.*, 2001). This is due to the fact that the process requires neither aeration nor an external carbon source.

2.3.4 Single reactor High activity Ammonia Removal Over Nitrite (SHARON®) process

The single reactor high activity ammonia removal over nitrite (SHARON) process is based on the denitrification pathway. This *short-circuit* process could save energy and electron donor, provided nitrification stops at the nitrite stage. Usually *Nitrobacter* immediately convert the NO_2^- to NO_3^-. Therefore, holding the nitrification at the intermediate stage is not successful (Verstraete and Philips, 1998). However, at high temperatures, *Nitrobacter* has a distinctly lower growth rate than *Nitrosomonas*. Therefore by implementing a completely mixed reactor at shorter residence time and high temperatures, one could eliminate *Nitrobacter* growth. Hence, the SHARON process is a chemostat without biomass retention, in which the dilution rate is higher than the maximum growth rate of the NOB, but lower than the growth rate of AOB (Jetten *et al.*, 2002). Partial oxidation of NH_4^+ to NO_2^- and subsequent reduction of the NO_2^- to molecular nitrogen ($N_{2\,(g)}$) was seen as the desired *short-cut*, especially for treating wastewater with a low C/N ratio. The main features of SHARON process are high operational temperature (30-35 °C) and very short sludge age (1 – 3 days) or sludge recirculation (Pollice *et al.*, 2002). The nitrification reactions are given below. Reaction (2.4) saves 25% of oxygen compared to reaction (2.5).

$$NH_4^+ + 1.5\ O_2 \rightarrow NO_2^- + H_2O + 2H^+ \quad (2.4)$$

$$NH_4^+ + 2\ O_2 \rightarrow NO_3^- + H_2O + 2H^+ \quad (2.5)$$

Denitrification can be compared as follow. Reaction (2.6) saves 40 % of CH_3OH compared to reaction (2.7).

$$6\ NO_2^- + 3\ CH_3OH + 3\ CO_2 \rightarrow 3\ N_2 + 6\ HCO_3^- + 3\ H_2O \quad (2.6)$$

$$6\ NO_3^- + 5\ CH_3OH + CO_2 \rightarrow 3\ N_2 + 6\ HCO_3^- + 7\ H_2O \quad (2.7)$$

The SHARON process follows reactions (2.4) and (2.6). Denitrification and pH control could be maintained by imposing intermittent aeration (Verstraete and Philips, 1998). The NH_4^+ and NO_3^- ratio in the effluent could be fine-tuned by adjusting the pH between 6.5 and 7.5 (Jetten *et al.*, 2002). The SHARON process suits to remove nitrogen from high NH_4^+ concentrated (> 0.5 g N/l) wastewaters. At temperatures above 25° C, the process effectively outcompetes the NOB, resulting in stable nitritation (i.e. process of NO_2^- production) with NO_2^- as the end-product (Jetten *et al.*, 1999). Lower oxygen demand (25 % energy saving during aeration), reduced organic substrate requirement for heterotrophic denitrification (up to -40 %), lower biomass production (up to -300 %), increased denitrification kinetics and carrying the process out in a single reactor without any sludge retention (Jetten *et al.*,

1999) are the main operational advantages of the SHARON process. The main disadvantage of the SHARON process is the accumulation of NO_2^- and its presumed toxic effect on the biomass, even at relatively low concentrations (10 – 30 mg N- NO_2^-/l).

2.3.5 Completely Autotrophic Nitrogen removal Over Nitrite (CANON®) Process

Aerobic bacteria oxidise NH_3 to NO_2^-, whereas anaerobic / anoxic bacteria convert NH_3 and NO_2^- to $N_{2\,(g)}$. According to Sliekers *et al.* (2003), the process in which NH_3 is converted to $N_{2\,(g)}$ by maintaining both types of organisms in one reactor under oxygen limited conditions is called Completely Autotrophic Nitrogen removal Over Nitrite (CANON). The CANON process comprises the Anammox process in combination with nitrification, occurring in a single biofilm system (Hao *et al.*, 2001). Ammonia is partly oxidised to NO_2^- by aerobic AOB and the remaining NH_3 and the NO_2^- produced are converted to N_2 gas by anaerobic AOB (Jetten *et al.*, 2001). The overall reaction that takes place in the CANON process is given below (Sliekers *et al.*, 2003).

$$NH_3 + 0.85\ O_2 \rightarrow \quad 0.11\ NO_3^- + 0.44\ N_2 + 0.14\ H^+ + 1.43\ H_2O \qquad (2.8)$$

In the CANON process, kinetics parameters and biofilm characteristics (density and porosity) are in generally insensitive to the total effluent concentrations. This is due to the diffusion limit of the biofilm. A small biofilm volume effects the nitrogen conversion and leads to limited space for growth of Anammox organisms. Dissolved oxygen (DO) and NH_4^+ surface load are the two key process factors governing the behaviour of the CANON process. Autotrophic microorganisms involved in the CANON process have different growth rates and temperature coefficients, therefore changing the temperature also affects the process performance (Hao *et al.*, 2002). The process should be kept at a higher NH_4^+ flux than oxygen at all times in order to maintain oxygen-limited conditions in the reactor (Sliekers *et al.*, 2003). The advantage of the CANON process is that it is not necessary to add an external carbon source, hence it is an excellent process for removal of nitrogen compounds from industrial wastewaters characterised by a low organic content (Sliekers *et al.*, 2003).

2.4 Selection of suitable nitrogen removal process

Treatment systems differ in their purpose, design, influent material, method, duration of biomass retention and numerous other factors. A suitable nitrogen removal process could be selected based on the TN removal efficiency, NH_4^+ conversion per unit reactor volume per day, operational cost per kg of NH_4^+ removal, capital cost of the system, and effluent conditions (pH, composition, temperature). Total nitrogen removal efficiency is defined as the difference between fluxes of dissolved inorganic nitrogenous compounds (NH_4^+, NO_3^-, and NO_2^-) in the influent and the effluent, divided by the fluxes of NH_4^+ in the influent (Benthum *et al.*, 1998). Therefore, when selecting and designing bioreactor systems for nitrification-denitrification processes, how the biofilm is developed (species, thickness,

oxygen diffusion), what medium is to be used (in case of packed-bed bioreactors), how to achieve complete mixing without excessive shear stress on the biofilm and how to control the thickness of the biofilm must be considered.

The type of bioreactor used depends on the process adopted. For example, if an aerobic autotrophic nitrification process is used, sufficient oxygen conditions with minimum shear stress on the microbes should be provided. On the other hand, if anaerobic heterotrophic denitrification is adapted it could either be a packed bed column or a fluidised bed reactor. For example, Kasia *et al.* (2005) used a CSTR with > 80 % NH_4^+ removal for metal refinery wastewater. However, they found gravel-packed column reactor was not suitable for NO_3^- removal under the used configuration with just < 15 % NO_3^- removal. Table 2.3 shows a qualitative comparison of different nitrogen removal systems. The critical parameters for denitrification of metal refinery wastewater were found to be NO_3^- concentration, temperature, influent flow rate and mean cell retention time (Kasia *et al.*, 2005). A study done by Pearce (2004) based on full-scale trickling filters stated nitrogen removal and denitrification is strongly influenced by BOD load, irrigation velocity and media size of the trickling filters. Trickling filters are extensively used in municipal wastewater treatment around the world due to low cost, robustness, simple operation and control, small number of moving parts (pump and rotary distributor), capability to produce high quality nitrified effluent, requires minimal skilled maintenance (due to the efficient oxygen transfer), and high energy efficiency (Pearce, 2004).

As shown in Table 2.3, the Anammox reactor has the highest reactor capacity per unit volume. Model-based evaluation done on the CANON showed that Anammox is the major contributor to the TN removal in stable biofilm systems and conventional denitrification only takes a share of <20 % in the TN removal (Hao and van Loosdrecht, 2004). On the other hand, SHARON, Anammox, OLAND and CANON processes produce less sludge and no need of COD requirement and pH control compared to the conventional nitrification – denitrification process. The main difference between OLAND and CANON processes is that OLAND makes use of denitrification activity of conventional aerobic nitrifiers whereas CANON incorporates the Anammox process (Jetten *et al.*, 2001).

Based on the above discussion, it appears to be that each of the above processes is governed by the sequence of each reaction taking place under the different oxygen conditions (such as aerobic, anaerobic and anoxic). Therefore, by controlling each reaction step, the desired mode of process operation could be achieved (for example SHARON and OLAND processes differ in how the oxygen supply is controlled and selective inhibition of the undesirable bacteria in the reactor system). Combined nitritation and Anammox can be used in a two reactor system to control the different physiological requirements of both microorganisms types (e.g. presence *vs.* absence of oxygen). This would require less oxygen input for the nitritation process and no additional organic carbon is

necessary for denitrification (Egli *et al.*, 2003). Even though high specific NO_2^- production can be achieved in short term, the difficulty of establishing long term nitritation in a moving-bed biofilm reactor was demonstrated negating usual microbial selection criteria: high NH_4^+ loading rate, high free NH_3 or low DO (Fux *et al.*, 2004). A CSTR or SBR with suspended biomass was recommended for full-scale operation of Anammox (Fux *et al.*, 2004; 2002). The combined process, like SHARON – Anammox, CANON – Anammox, would eliminate the need for external carbon sources partially or completely and have a lower operational cost (Jetten *et al.*, 2001).

Table 2.3: Overview of the N conversion in **kg - N / m^3 reactor /day** in different reactor setups.

Process	**Reactor Type**	**Nitrogen conversion**
Single Autotrophic Process		
Anammox	Fluidised Bed Reactor (FBR)	4.8
Anammox	Sequencing Batch Reactor (SBR)	7
Anammox	Gas-lift Reactor	8.9
Nitrification	Biofilm Airlift System (BAS)	5
Combined Autotrophic Process		
CANON	SBR	0.07
CANON	Gas-lift Reactor	1.5
SHARON	CSTR + SBR	1
OLAND	SBR	0.05
Deammonification	RBC	0.3
Combined Autotrophic / Heterotrophic Process		
Nitrification-denitrification	BAS	3.75

Source: Sliekers *et al.* (2003).

Nitrogen conversion rate [kg N / m^3 reactor / day] in the reactor system is an important design parameter to decide the type of process for nitrification – denitrification. As compiled by Sliekers *et al.* (2003), Table 2.4 shows a comparison of different processes based on the trophic status (autotrophic vs. heterotrophic) and single vs. combined processes.

It is shown that the biofilm airlift reactors give the maximum conversion rate under the Anammox process. Perhaps this is due to the fact that gas film reactors support both suspended and fixed film growth bacteria and are subjected to uniform mixing of the substrate in the reactor. This is supported by the results of fluidised bed reactors, which also achieve both the above conditions. Anammox

conversion is about 20 times faster than the traditional removal processes. However, when selecting the gas for gas lift or fluidisation, the cost of gas needs to be considered. For example, when a gas lift reactor is used in Anammox, 95% argon (Ar) and 5% carbon dioxide (CO_2) have been used (Sliekers *et al.*, 2003). According to Jetten *et al.* (2001), the combined SHARON – Anammox process would cost about 0.75 € / kg N removal compared to 2 – 5 € / kg N for other processes at pilot scale.

Table 2.4: Qualitative comparison of different nitrogen removal systems.

System	**SHARON**	**Anammox**	**CANON**	**Conventional nitrification denitrification**
No. of reactors	1	1	1	2
Feed	Wastewater	NH_4NO_2 mixture	Wastewater	Wastewater
Discharge	NH_4^+, NO_2^-	N_2, NO_3^-	N_2, NO_3^-	NO_3^-, N_2O,N_2
Conditions	Oxic	Anoxic	O_2 limited	Oxic; anoxic
O_2 requirement	Low	None	Low	High
pH control	None	None	None	Yes
Biomass retention	None	Yes	Yes	None
*COD requirement	None	None	None	Yes
Sludge production	Low	Low	Low	High
Reactor capacity (kg N /m^3 /day)	1	6-12	1-3	0.05-4
Bacteria	Aerobic NH_4^+ oxidisers	*Planctomycetes*	Aerobic NH_4^+ oxidisers, *Planctomycetes*	Nitrifiers + various heterotrophs

Source: Jetten *et al.*, 2002. * COD – Chemical oxygen demand

Denitrification is usually carried out by heterotrophic anaerobic bacteria which need an external carbon source for their optimum growth. Early researchers (Hallin *et al.*, 1996; Aesøy *et al.*, 1998; Nogueira *et al.*, 2002) reported the possibility of using different carbon sources for denitrification. However, the choice of carbon source depends on the cost and availability of particular sources. Acetic acid, acetone, ethanol, methanol, glucose monohydrate, sucrose and sewage sludge have been used as carbon sources. Commercially bought carbon compounds are generally too expensive for use at full scale, but municipal and agricultural sludges are rich in volatile fatty acids (VFA) and hence have a good potential as carbon sources at little or no cost (Bilanovic *et al.*, 1999).

2.5 Bioreactor selection

Elimination of nitrogenous compounds in the form of $N_{2\,(g)}$ is often the key goal in the nitrification – denitrification process. Different reactor types and configurations are used in order to achieve this (Koren *et al.*, 2000; Metcalf and Eddy Inc., 2004). A comparison study over 20 years between nitrifying-only and combined nitrifying/denitrifying processes (NDN) showed that the NDN operations always have lower aeration costs, and generally have the lowest combined operational cost. Table 2.5 summarises this study (Rosso and Stenstrom, 2005). Therefore, the oxic-anoxic interface is thought to be critical for efficient coupling of nitrification - denitrification process. The rate of nitrification is highly dependent on stirring speed and it improves with increased mixing at a constant DO of 0.75 mg/l (Barber and Stuckey, 2000b). Increased gas mixing improves the overall nitrification by enhanced mass transfer, as the co-substrate and gaseous oxygen are both in the bulk phase. Hence, tracking of denitrifying populations and their activities is important in bioreactor ecology. However, the organisms which are more suitable for a particular reactor design or performance are yet to be identified (Kowalchuck and Stephen, 2001). For example, enrichment of Anammox biomass has been achieved in a relatively short time (60 days) in a SBR (Dapena-Mora *et al.*, 2004b). The SBR has been the focus many authors for enrichment of Anammox (Arrojo *et al.*, 2006; Strous *et al.*, 1998). Identification and compilation of metabolic pathways, physiology of aggregated biomass (esp. very efficient biomass retention time in the Anammox process due to extremely low growth rate (approximately 11 days doubling time, Schmidt *et al.*, 2004), and nature of intermediate products (e.g. hydroxylamine and hydrazine in Anammox) are important in the design and scale-up of bioprocesses (Strous *et al.*, 1999). More rapid methods to quantify nitrifiers in activated sludge have been developed in recent years compared to time consuming fluorescence in situ hybridisation (FISH) and confocal laser scanning microscopy (CLSM) (Manser *et al.*, 2005b). Special reactor configurations have been extensively studied for increased biomass retention in Anammox (Schmidt *et al.*, 2004) such as moving-bed biofilm reactor (MBBR), CSTR, upflow anaerobic sludge blanket (UASB), fluidised-bed, fixed bed, SBR and rotating biological reactors (Fux *et al.*, 2004a; 2004b; 2002; Schmidt *et al.*, 2004; Strous *et al.*, 1997; 2002; Siegrist *et al.*, 1998). Immobilised biomass reactors such as UASB are more suitable alternative than suspended biomass reactors (CSTR), due to poor settleability of denitrifying suspended sludge when nitrification-denitrification is performed via NO_2^- accumulation (Ruiz *et al.*, 2006).

Therefore, factors such as maximum nitrification-denitrification per unit reactor volume, operation and maintenance cost, capital and installation cost, increased microbial and substrate transport, process control and instrumentation, handling and fabrication limitations, ancillary equipment (such as pumps, valves) and safety have to be considered in selection from the many suitable reactor types outlined below. Detailed description of different bioreactors and their suitability for different process engineering applications including wastewater treatment engineering already exist (Chen *et al.*, 2003;

Lubbert and Jorgensen, 2001; Metcalf and Eddy Inc., 2004; Moo-Young and Chisti, 2004; and Rossi, 2001), so they are discussed only briefly here.

Table 2.5: Cost-analysis results for ASP (adapted from Rosso and Stenstrom, 2005).

Parameter	Conventional	Nitrifying only	Nitrifying/denitrifying
Sludge disposal cost (USD/d)	140	78	69
Oxygen requirement (kgO_2/d)	3800	5034	3469
Field transfer efficiency (%)	15.3	17.6	18.8
Aeration cost (USD/d)	39	52	36
CH_4 production credit (USD/d)	96	36	32
Total cost (USD/d)	**83**	**94**	**73**

Plant flow: 20 000 m^3/d; influent concentration: 350 mg_{BOD}/l; effluent concentration: 20 mg_{BOD}/l; theoretical yield: 0.7 /d (for carbonaceous growth), 0.15 /d (for nitrifying growth); decay coefficient: 0.13 /d (for carbonaceous growth), 0.05 /d (for nitrifying growth); power cost: 0.15 USD/kWh; sludge disposal cost: 20 USD/ wet t; methane gas value: 0.25 USD/m^3; final methane resale value: 0.06 USD/m^3; required blower energy: 1.17 kW/m^3.

The anaerobic baffled reactor is a high rate bioreactor with the advantages of better resilience to hydraulic and organic shock loadings, longer biomass retention times, lower sludge yields, and the ability to partially separate the various phases of anaerobic catabolism (Barber and Stuckey, 2000a).

Fluidised bed reactors (FBRs) have long commissioning phases for certain industrial wastewaters, as it takes a long time to develop the nitrifying biofilm on the carriers when wastewater does not contain sufficient quantities of organic compounds (Tsuneda *et al.*, 2003). However, FBRs have the advantage of supporting both fixed film and suspended microbial populations. Tsuneda *et al.* (2003) further stated that FBRs have a larger gas-liquid interface and hence may be operated at a lower aeration volume than other types of bioreactors.

A membrane aerated bioreactor (MABR) is composed of porous hollow-fibre membranes, the outer surface of which is covered by biofilm. The membrane serves as a carrier to immobilise the bacteria as well as being the oxygen supplying material (Brindle *et al.*, 1998). Manser *et al.* (2005) showed that diffusion resistance in MBRs is negligible as the membrane separation leads to small floc sizes. Oxygen penetrates through the membrane into the biofilm that forms on the membrane surface. Bacteria in the biofilm consume the oxygen to oxidise the pollutants diffusing from the bulk solution (Terada *et al.*, 2003). Further, Terada *et al.* stated when applying MABRs for high strength organic wastewaters, the aerobic zone close to the biofilm-membrane interface supports nitrification, whereas the anoxic zone close to the biofilm-liquid interface allows denitrification. Membrane aerated

bioreactors can hence be used as a single reactor system for both nitrification and denitrification for strong organic wastewaters.

Continuous stirred tank reactors (CSTRs) are the most common reactor type in process engineering, perhaps due to well established theory and a long history of practical applications in various industries. Rushton type turbines are mainly used as the stirring mechanism which creates better fluid dynamics with less dead zones. However, when a CSTR is used in the nitrification process, the possible shear stresses acting on the suspended aerobic microbes need to be considered. It is logical to assume that due to the low EPS produced by autotrophic aerobic bacteria, the cell damage due to the shear stresses produced by the turbine is greater. Therefore the stirring speed (revolutions per minute of turbine), geometry, and size of the turbine would affect the shear stresses on the microbial cells. However, nitrifying bacteria are usually outcompeted in CSTRs by heterotrophic bacteria, due to their slow growth rates and metabolic activity. Arrojo *et al.* (2006) studied the effect of mechanical stress on Anammox granules in a SBR using a Rushton type impeller and found stirring speeds up to 180 rpm have no negative effects on the performance of Anammox process. However, a 60 % decrease in Anammox activity was observed when the stirring speed was increased to 250 rpm.

Packed-bed reactors (PBRs) are used for fixed films. Though they are not more efficient than the FBRs, they have the advantages of low operational cost, low energy consumption, high efficiency of biological water treatment and compactness of the reactor (Bourrel *et al.*, 2000). The main disadvantage of PBR is the preferential flow occurring in the reaction bed. Dispersion rings at appropriate intervals can be used to limit the preferential flow of the influent in the medium (Woodbury and Dahab, 2001).

In PBRs, the medium plays a major role in immobilising and maintaining micro-organisms in the reaction bed. The medium provides a surface for growing the fixed film bacteria and as temporary nutrient storage in the reactor. Medium selection is based on the properties and cost of a particular medium. Hydrophilicity, support for the developing biofilm (easy adhesion), improved micropores for better nutrient and microbial dispersion and attachment are some of the properties that can be considered when selecting suitable media for a given application. Granular activated carbon (GAC) contains the largest proportion of micropores, which can adsorb a wide variety of organic compounds. Granular activated carbon can be used not only as a supporting medium for the denitrifying organisms but basically as a medium of temporary storage for the supplied organic material, which is subsequently recovered through desorption and consumption, and as a carbon source for denitrification following the mechanism of bioregeneration (Sison *et al.*, 1996). In addition to GAC, ceramic granules, sand, high density polyethylene granules and zeolite are often used as supporting

media in PBRs (Park *et al.*, 2003). Table 2.6 shows a qualitative comparison of different types of reactors used in wastewater treatment.

Table 2.6: Qualitative comparison of different bioreactors used in wastewater treatment

Parameter	CSTR	PBR	FBR	PFR
Operation cost	HIGH	LOW	HIGH	LOW
Space requirement	LOW	LOW	LOW	HIGH
Efficiency	VARY	VARY	VARY	VARY
Energy use	HIGH	LOW	HIGH	LOW
Maintenance	HIGH	LOW	HIGH	LOW

2.6 Scale-up, process control and implementation

Scaling up from laboratory or pilot to full scale should include considerations such as effective monitoring of nitrogen compounds, efficient biomass retention, a good balance between aerobic and anaerobic ammonium oxidation and long term stability of the process. A rigorous pilot plant study should establish the design criteria for full-scale implementation of the technology and to determine the performance of the technology under real wastewater conditions (Jetten *et al.*, 2002). Further, the process designer should consider the risk assessment, balancing the risk of contamination of the process by undesired organisms (e.g. heterotrophic biomass in autotrophic processes such as Anammox, OLAND), products (e.g. NO_2^- and NO_3^-), the cost of contamination and cost of preventing contamination (Winkler, 1983). However, in order to achieve the optimum results obtained during the lab scale experiments in scaled up reactors as well, appropriate scale up strategies, process monitoring and control through carefully design and implemented instrumentation are required. Process scale up using dimensional analysis and computational fluid dynamics (CFD) models would eliminate the unnecessary over-designs and simulate the reactor performance prior to construction (Lane *et al.*, 2005). A number of CFD models have been developed for various types of reactors (airlift, fluidised bed, CSTR, spinner-flask) in recent history (Garcia-Calvo *et al.*, 1999; Lane *et al.*, 2005; Sucosky *et al.*, 2004; Werther and Hartge, 2003; Xia *et al.*, 2006). Real-time monitoring and control (RTMC) of wastewater treatment plants are primarily based on insight into the process as summarised in a proper model, sensors that provide on-line data, adequate monitoring and control strategies and actuators that implement the controller output (Vanrolleghem and Lee, 2003). Detailed discussion of on-line measurements, process monitoring and control for wastewater treatment processes can be found in Vanrolleghem and Lee (2003) and Wilderer *et al.* (2002). Table 2.6 presents a summary of on-line monitoring equipment for wastewater treatment processes.

Closed-loop process control enhances the process economics in terms of minimum energy usage (e.g. aeration, stirring, pumping and recirculation of effluents), maximum growth of desired bacteria (oxic-

anoxic conditions, pH and temperature control), and desired yield ($N_{2\,(g)}$). Use of RTMC would reduce the capital cost of construction where an over-designed approach was adopted (in early days) to guarantee the minimum discharge water quality regardless of shock and variations of influent water quality. Probably, retrofitting the old treatment plants with RTM would increase the capacity to treat more influent loads than those designed to be handled. Control of biological removal of nitrogen from wastewater treatment plants in early days was largely limited by the availability of reliable on-line sensors for collection of necessary information for optimum operation of the plant (Verstraete and Philips, 1998) and hence over-designed approaches had been adopted. Nevertheless, during the last decade the development of reliable sensors and the reduced cost of PCs have enabled the average plant operators to be able to access the RTMC and instrumentation (Jeppsson *et al.*, 2002; Vanrolleghem and Lee, 2003).

Table 2.6: State of the art of on-line monitoring equipment for wastewater treatment process (adapted from Vanrolleghem and Lee, 2003).

Physical measurements			**Physico-chemical measurements**			**(Bio-)chemical measurements**		
Variable	**Process**	**Range**	**Variable**	**Process**	**Range**	**Variable**	**Process**	**Range**
Temperature	G	∀	pH	G	∀	Respirometry	2, 3	∀
Pressure	G	∀	Conductivity	G	∀	Toxicity	2, 3	∀
Liquid level	G	∀	DO	2, 3	∀	BOD st	2, 3	∀
Flow rates	G	∀	Fluorescence	2, 3	∃	COD	1, 2, 3	∃
Suspended solids	G	∃	Redox	1, 3	∀	TOC	1, 2, 3	∀
Sludge blanket	4	∃	NH_4^+	3	∀	NH_4^+	3	∀
Sludge volume	4	∃	NO_3^-	3	∃	NO_3^-	3	∀
Settling velocity	4	O	NO_2^-	3	∃	NO_2^-	3	∀
Sludge morphology	G	O	Digester gas:	1,2,3		Micro-scale NOx	3	∀
Calorimetry	1, 2, 3	O	CH_4, H_2S, H_2, CO_2		∀	HCO_3^-	1, 3	∃
UV absorption	G	∃				VFA	1, 3	O

Process: Unit processes in wastewater treatments plants where the sensors can be implemented 1: Anaerobic, 2: Activated sludge, 3: Nutrient removal, 4: Sedimentaion, G: All processes. Applicability range:∀, State of the technology; ∃: Application in certain cases; O: requires development work.

Nitrifying bacteria are very highly vulnerable to inhibition due to process variables such as temperature, pH, DO, substrate concentration (NH_4^+ and NO_2^-) and the presence of organic and toxic (e.g. metals) compounds (Oguz *et al.*, 2006). Therefore, nitrification is considered as the rate limiting step of nitrogen removal process. Measuring of mixed liquor suspended solids (MLSS), total suspended solids (TSS) and volatile suspended solids (VSS) content is an indication of the microbial

population density in the reactor. Seixo *et al.* (2004) obtained a linear relationship between the autotrophic fraction and C_{org} / N of the load which can be used for biomass assignment and for the development of on-line estimators.

Temperature based selective inhibition of undesired biomass (e.g. NOBs) is one of the possible ways to control the NO_2^- accumulation in the nitritaion process. This can be achieved due to the different temperature dependence of AOB and NOB. Nitrite oxidisers have a higher decay rate than AOB at temperature below about 20 °C and a lower decay rate above 20 °C (Manser *et al.*, 2006). This suggests that operation of CANON, SHARON or OLAND is easier at lower temperatures or the process can be varied according to seasonal weather changes (Farabegoli *et al.* (2004) reported average NH_4^+ removal efficiency of 82 % and 32 % in summer and winter, respectively in a submerged aerated biofilter). The DO regulation according to variations in NH_4^+ load is vital for optimum operation of CANON process (Nielsen *et al.*, 2005). Further, Nielsen *et al.* (2005) stated that monitoring of NO_2^- and NO_3^- status would be necessitated to prevent process failure due to NO_2^- poisoning of Anammox and overloading of DO, which would lead to NO_2^- oxidation to NO_3^-. On the other hand, in conventional nitrification-denitrification processes, DO inhibition of the denitrification process could be one of the difficulties faced while maintaining anaerobic / anoxic conditions. Undesirable products (e.g. CO_2) removal in the denitrification reactor would probably enhance the process considerably. Large shear stresses developed on biofilms by rapid stirring and pumping large volumes of wastewater in full scale plants has to be considered carefully in the dimensional analysis of the scaling-up process. Kim *et al.* (2001) showed that pump shear in MBRs affects the microbial activity, COD removal efficiency, specific oxygen uptake and sludge yield, due to the breakage of microbial flocs.

Precise control of process parameters (e.g. pH, oxygen conditions, carbon source) for nitrification and denitrification processes is therefore vital for optimum transformation of nitrogenous compounds into $N_{2\,(gas)}$. Successful nitrification requires a high oxygen concentration of about 4.57 kg O_2 / kg NH_3-N. Availability of oxygen in a reactor is limited by mass transport and generally oxygen can penetrate a biofilm of 0.1 to 0.2 mm with a diffusion coefficient of 66% of that in water for freely suspended cells (Barber and Stuckey, 2000b). The mass transfer depends strongly on variable parameters such as floc size and floc density, which may vary greatly form plant to plant (Manser *et al.*, 2005). Ammonia oxidisers need gaseous oxygen (Brindle *et al.*, 1998) while NOB require chemically bound oxygen (NO_2^-). Un-ionised ammonia, nitrous acid and excessive COD can all inhibit the nitrification process (Barber and Stuckey, 2000b). Denitrification consists of four stages producing chemical intermediates NO_2^-, nitric oxide (NO), nitrous oxide (N_2O) and finally $N_{2\,(g)}$. Different stages of denitrification and lack of enzymes lead to accumulation of intermediate products. Oxygen is a strong inhibitor of the

process and the aerobic denitrification rate is only about 0.3 – 3 % of the anoxic rate (Barber and Stuckey, 2000b).

The use of dissolved oxygen, pH, ORP (oxygen reduction potential) probes and on-line sensors for monitoring NH_4^+, NO_3^- and NO_2^- concentrations for operation and maintenance of wastewater treatment plants is widespread. However, use of those ion selective electrodes (ISE) is limited to certain applications especially where similar ions do not interfere with the desired ion being measured. Further, some ISEs (e.g. NH_4^+) interfere with microbial micronutrients such as Na^+ and K^+. This prevents on-line measurements where pre-treatment of those ions in the sample can not be precipitated. High temperature coefficient also leads to large errors due to temperature variations (e.g. 1 °C difference in temperature results in a 2 % error at the 0.001 M level of NH_4^+ electrode; pHoenix Electrode Co., 2005). Alternatively, biosensors are also good candidates for monitoring nitrogen compounds in wastewater systems. Recently, long-term stable biosensors for NO_x^- and NO_2^- based on bacterial reduction of the ionic species to N_2O gas have been developed (Jetten *et al.*, 2002). The desired features of on-line sensors are accuracy and precision, sterilisability (heat and pressure resistant), mechanical robustness, low adhesion of bacterial cells and other fouling species (e.g. proteins), leak proof, stable signal over long periods, linear characteristics and fast dynamics (Rieger *et al.*, 2005). Rapid fouling of submerged probes or of sidestream systems set up to feed samples into external sensor systems contribute to serious problems with reliability (Pedersen and Petersen, 1996). Microbial toxicity monitors such as Microtox™ and Amtox™ are available and evade probe fouling problems, but they are expensive, time consuming to operate and delicate. Non-invasive monitoring via sampling the gas mixture released from the wastewater treatment process unit is a more promising alternative, as all wastewater or biofilm fouling and toxicity problems can be avoided (Burgess *et al.*, 2002). Perhaps in nitrification and denitrification, it is more important to develop better process control strategies than to search for new processes with different microbes.

Previous researchers have used different control strategies (Fuerhacker *et al.*, 2000; Wu and Huang, 2003) in bioreactor control. Bourrel *et al.* (2000) showed the state variables important in the denitrification process as NO_3^-, NO_2^-, carbon, porosity, active biomass and total biomass. In traditional process control systems, a feedback or feedforward strategy is used. Proportional integrated derivative (PID) controllers are mainly used where more rigorous and accurate control signals are required. However, better process control could be achieved using a knowledge based expert system (KBES) coupled with PID controllers. A simple, rule-based KBES could be developed from the available literature (knowledge base) for the nitrification and denitrification processes. Baeza *et al.* (2002) reported on a wastewater treatment plant that was effectively controlled using an on-line KBES and optimised using operating rules such as DO, flow-rates and stirring rates. The KBES acted as the master in a supervisory set point control. It was fed with monitored in-line data (pH, temperature, DO,

ORP, aeration and flow rates) and on-line data (NO_3^-, NO_2^- and NH_4^+ concentrations). The advantage of embedding a KBES to PID controller is that it can feed not only quantitative data but also the qualitative data (e.g. odours, colours and microbiological observations etc.) for smooth process performance.

Growing IT techniques could be used in modelling, simulation, process control and instrumentation of wastewater treatment plants (WWTPs). On the other hand, the volume of information evolved in wastewater treatment could be used effectively by incorporating into knowledge based information system for better monitoring and controlling of the WWTPs. Integration of process knowledge with simulating tools (such as MATLAB, Mathworks Inc., USA, WEST, Hemmis Inc., Belgium, Aquasim, EAWAG, Switzerland) and process control software (LabVIEW, National Instruments Inc., USA) will enhance the process stability and to make educated judgements on the process on real-time basis.

Therefore, identification of process controlling parameters for metal mining and refining wastewater is an important activity. Operational parameters such as optimal pH range, temperature, required DO content and intermediate products (e.g. NO_3^- and NO_2^- content) could be used as the state variables to control the process. Based on the optimum values for maximum removal of nitrogenous compounds from the PMR wastewater, the process control parameters in each operation (nitrification and denitrification), should be changed by appropriate control action (e.g. pH correction adding lime, aeration switch on – off , hot / cold water supply for temperature control, etc).

2.7 Gap analysis

A detailed characterisation of PMR wastewater is required in order to decide the type of bioreactors and process configurations. This study should be performed to analyse seasonal as well as spot variations at different refinery process points where wastewater is produced. However, accessing to highly technology guarded PMR process prevents this type of study thus final wastewater collected at evaporation ponds would be a practical choice. No or little precious metal toxicity data for activated sludge or novel processes have been reported in the published literature. These areas need further investigation as metal toxicity threshold for PGMs would be vital for operation of different processes for biological removal of nitrogenous compounds from the PMR, which consists of a number of metals including base and heavy metals. Activated sludge process and metal toxicity models could be coupled to study various toxicity effects on biological nitrogen removal process. Different process configurations might be useful to control adverse effects imposed by PMR wastewater (extreme pH, high COD etc) on microbial populations responsible for each step of nitrogen removal. Even though novel processes are potential candidates for high strength inorganic wastewaters, none of the novel processes (Anammox, CANON, OLAND and SHARON) have been tested for high strength PMR wastewater. Further, no specific genera or species of microbes which can tolerate the toxicity of

specific metals (e.g. PGMs) have been reported. This opens up a wide research area to explore the potential different microbial genera or species coupled with novel processes in PMR wastewater treatment. Some of the queries arising from the literature review are: do the heterotrophic microbes produce more EPS than the autotrophic microbes? Can the high EPS producing bacteria tolerate extreme pH conditions? Do the EPS have a role in metal transport phenomena through cellular membrane? Are the AOB more sensitive to metal toxicity than NOB? If heterotrophic anoxic ammonium oxidisers exist can they tolerate extreme pH and high metal content than the aerobic autotrophic AOB? Therefore, it is worthwhile to find out if particular genera or species tolerate PGMs toxicity and whether they are environment specific, such as a particular type of reactor (CSTR *vs.* PBR *vs.* FBR, etc.) for maximum biomass yield.

2.8 Interim Conclusions

Figure 2.3 summarises a general strategy for process development for nitrification and denitrification of as yet uncharacterised wastewaters. It is important to know which species of microbes give the maximum conversion of ammonia into nitrogen gas per unit reactor volume of a particular reactor configuration under aerobic or anaerobic conditions.

According to the available literature, CANON can be operated as a single step autotrophic process. Anammox, CANON and SHARON do not need an additional carbon source. However, the microbes responsible for the process have extremely slow growth rates. Additionally, closer process control is more difficult to balance for CANON, as two processes are run simultaneously in one reactor. Therefore, it is sometimes a better option to separate the two processes (nitrification and denitrification) by using a two-reactor system so that each process variable in each reactor can be controlled independently.

It is worthwhile to find out how the recirculation step in each process, intermittent aeration in nitrification, optimum recirculation ratio and the introduction of pure carbon for denitrification affect the overall nitrification process using the actual industrial wastewater to be treated at pilot scale so that an optimum operational protocol for maximum yield of dinitrogen gas (maximum conversion of ammonia) can be developed.

It may be possible to develop empirical equations relating the correlations between the process parameters such as biomass yield, temperature, pH, and ammonium, nitrate, nitrite and nitrogen gas concentrations for a given reactor configuration. These could then be used as the characteristic equations of a particular reactor configuration, to enhance process control and build a data library for a KBES.

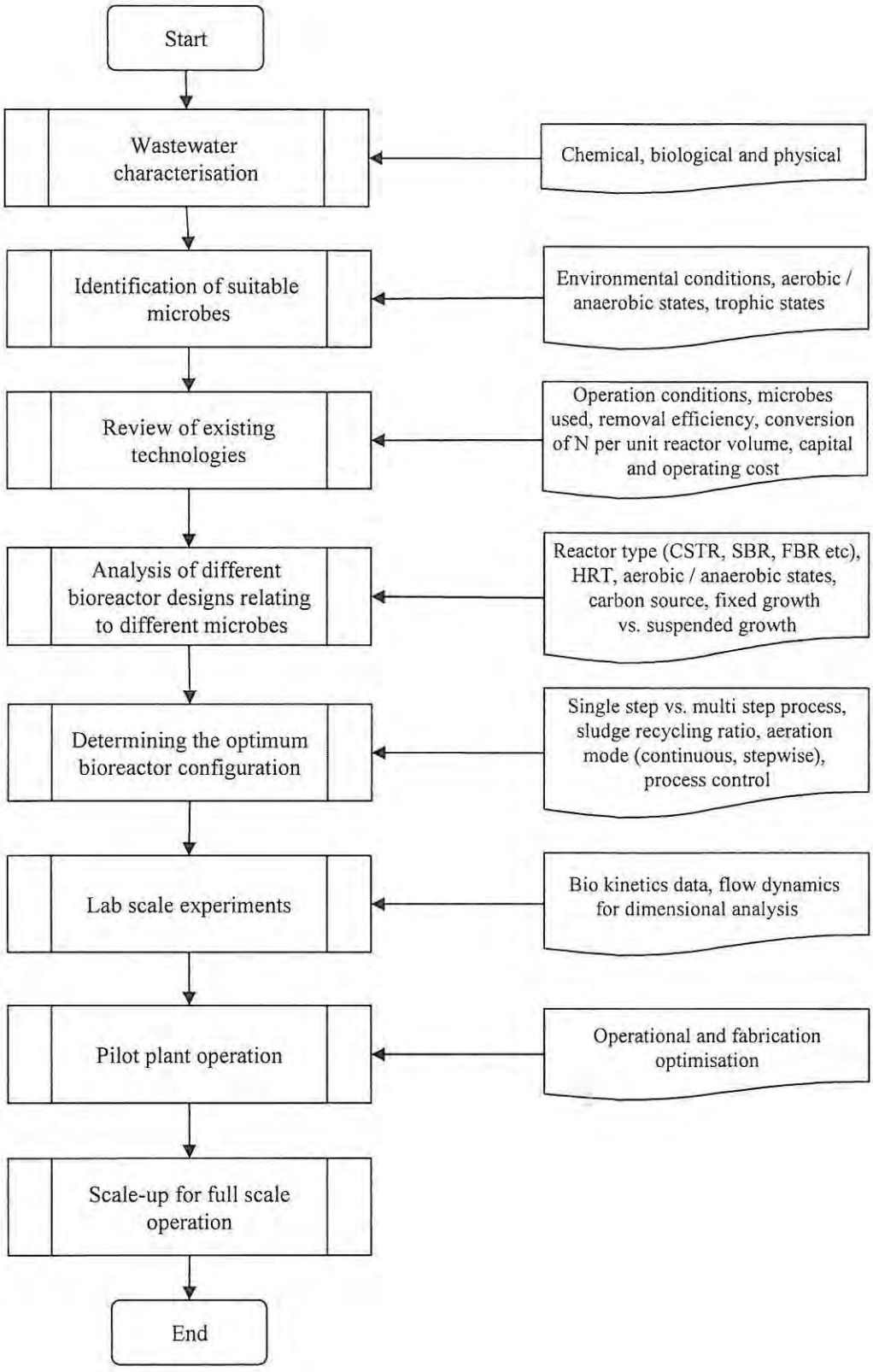

Figure 2.3: Bioprocess development for N removal in PMR wastewater.

CHAPTER 3

Our doubts are our traitors, make us lose the good we oft might win, by fearing to attempt

- William Shakespeare (1564-1616).

3.0 Preliminary investigations of precious metal refinery wastewater

3.1. Introduction

Most problems in environmental biotechnology/engineering practice involve relationships between living organisms and their environment; hence the analytical procedures needed to obtain quantitative information are often a complex mixture of chemical and biochemical methods. Therefore, data interpretation is usually related to the effect on micro-organisms or human beings or other flora and fauna (Sawyer *et al.*, 1994).

In developing a bioprocess to remove nitrogenous compounds from precious metal refinery (PMR) wastewater, it was necessary to characterise the wastewater. The PMR wastewater is produced in various unit operations such as metal extraction using solvents, plant cleaning and drainage, etc. Due to certain technical limitations (e.g. process inefficiency) complete recovery of valuable metals and/or solvents from the wastewater is not possible. General characterisation consisted of identification of constituents (e.g. metals, ammonium, nitrate, nitrite, organic compounds), physical parameters (e.g. settlability, suspended solids, volatile solids, colour and turbidity), chemical parameters (e.g. pH, COD, oxidation-reduction potential (ORP)) and biological parameters (e.g. biochemical oxygen demand (BOD), microbial populations) in the wastewater. Usually high concentrations of ammonium (NH_4^+ -N) and nitrate (NO_3^- -N) are present in the metal refinery wastewater due to widespread use of other nitrogen-containing reagents in the refinery process (Koren *et al.*, 2000). Further, maximum nitrification and denitrification rates are two key parameters for designing an optimum nitrogen removal system for high strength industrial wastewater (Carrera *et al.*, 2003). The volume and strength of industrial wastewater are usually defined in terms of units of production (e.g. kilograms of COD per tonne of pulp produced in the paper and pulp industry) and the variation in characteristic by a statistical distribution (Eckenfelder, 2000). Further, Eckenfelder (2000) stated there will be a statistical variation in waste-flow characteristics in any given plant and the magnitude of this variation will depend on the diversity of products manufactured, process operating contributing wastes, and process operation mode (batch *vs.* continuous).

The objectives of this chapter are to present the results obtained during preliminary investigations of the PMR wastewater intended for the biological removal of nitrogenous compounds. As the overall aim of this research was to develop a bioprocess, nitrification and denitrification activities with respect to the PMR wastewater were also evaluated under different conditions such as pH variation in nitrification, different carbon sources and different amounts of the carbon source in denitrification. Five preliminary experiments were carried out in order to achieve these research objectives and those are described from Section 3.2 to Section 3.6. First, initial characterisation of PMR wastewater was carried out (Section 3.2). Based on those results, nitrification of acidic wastewater stream was

evaluated under different pH conditions (Section 3.3). Then denitrification of nitrified wastewater (Section 3.4) was evaluated using three different carbon sources (sodium lactate, sodium acetate and methanol). These carbon sources were selected based on availability in the laboratory, easiness for hydrolysis compared to complex organic carbon sources such as sewage sludge, denitrification performance obtained in previous works and considering cost recovery of metal, after effective denitrification. The cost of carbon source can easily be recovered on the basis of value of PGM. Once the best carbon source was identified, the denitrification was carried out using the nitrified wastewater (Section 3.5). Then amount of carbon source was optimised by using different amounts for denitrification which described in Section 3.6.

3.2 Characterisation of the precious metal refinery (PMR) wastewater

A preliminary study to characterise PMR wastewater was performed using samples provided by Anglo Platinum Ltd., from their Rustenburg refinery. Samples from two streams were provided for preliminary study, namely acidic and caustic final effluent, which flow into a value recovery plant for metal reclaim and then into evaporation dams. The evaporation dams are a temporary storage facility for the final PMR wastewater awaiting further treatment and recovery of residual metals. Figure 3.1 presents a simplified process flow diagram (PFD) for the PMR process and points at which wastewater is produced.

3.2.1 Materials and methods

Ammonium (NH^+_4-N), nitrite (NO^-_2-N), nitrate (NO^-_3-N) and COD concentrations were measured using colorimetric reagent kits (Merck Chemicals (Pty) Ltd, Johannesburg) based on the principles of *Standard Methods* (APHA *et al.*, 1998). Spectroquant® reagent test numbers 14752 (NH^+_4-N), 14773 (NO^-_3-N) and 14538/9 (COD) were used, which are analogous to *Standard Methods* numbers 4500-NH_3-F, 4500-NO_3-E and 5220-D, respectively. The pH was measured using an electrode (CyberScan 2500, Eutech Instruments, Singapore). Platinum (Pt), palladium (Pd) and rhodium (Rh) concentrations were measured using an atomic absorption spectrophotometer (GBC 909 AA, Australia). A set of standards was prepared for Pt, Pd and Rh using 1000 mg/l stock solutions (EC Lab Services (Pty) Ltd., Port Elizabeth, South Africa) of each metal diluted to provide calibration standards of 10, 20, 30, 40, and 50 mg/l.

3.2.2 Results and discussion

Two streams of wastewaters (acidic and caustic) were analysed to determine the properties of each wastewater. Table 3.1 presents some of the parameters analysed. These results were obtained using single spot samples from each stream provided by the sponsoring metal refinery company. However, in order to get a clear picture of wastewater constituents, periodic and long term wastewater characterisation study is recommended.

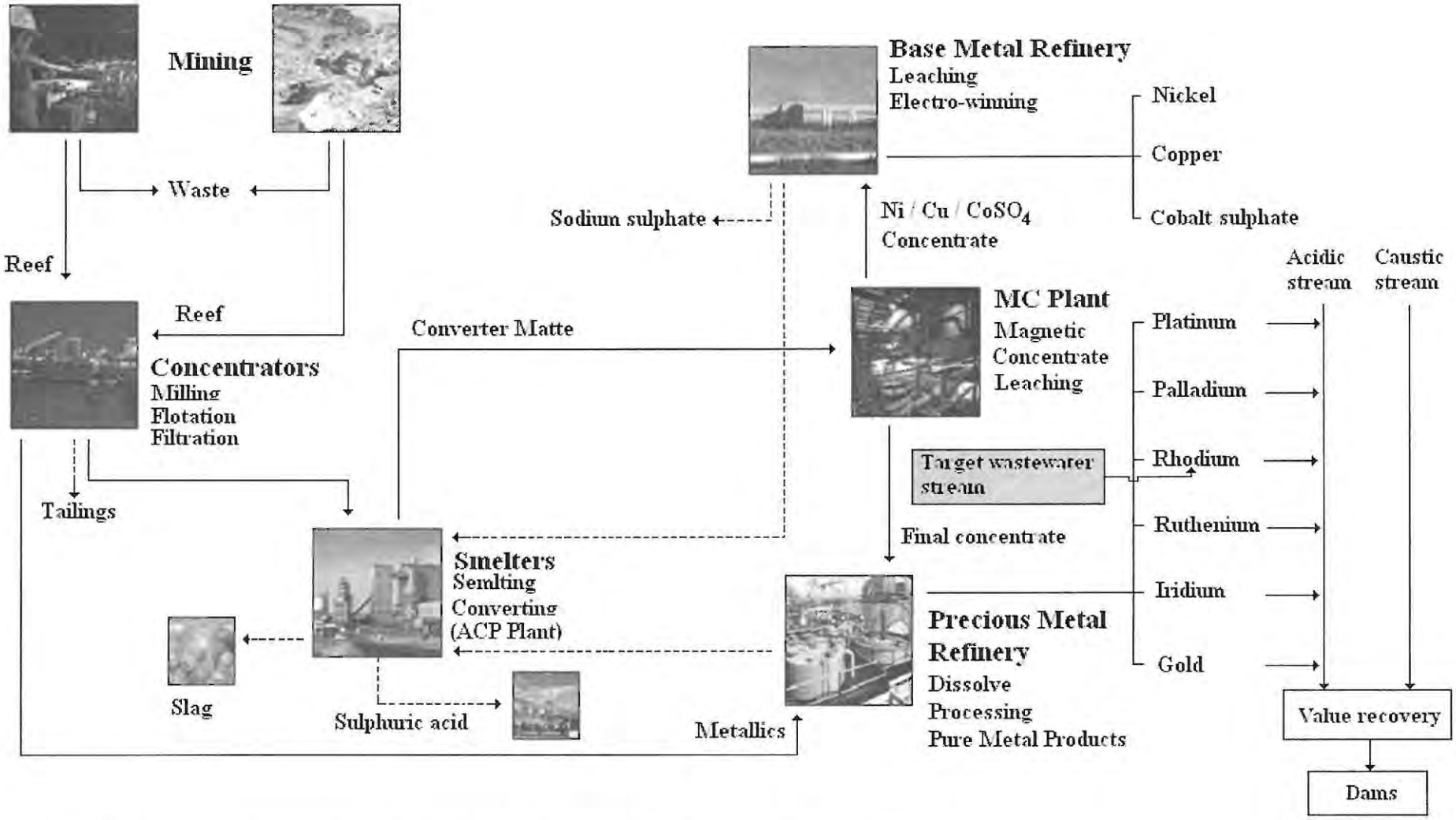

Figure 3.1: Simplified precious metal refinery process (source: Anglo Platinum Ltd., 2004)

Table 3.1: Preliminary characterisation of the PMR wastewater

Parameter	Acidic wastewater	Caustic wastewater
pH	4.00	12.50
NH_4^+ - N / (mg/l)	1.80	0.07
NO_3^- - N / (mg/l)	53	1721
COD / (mg/l)	16300	16230
Pt / (mg/l)	33.70	81.30
Pd / (mg/l)	66.20	64.90
Rh / (mg/l)	26.60	20.71

The two wastewaters were at the extreme ends of the pH range. As far as nitrification and denitrification processes are concerned, it is much easier to treat a suitably neutralised wastewater than to treat them separately. This makes sense in terms of capital and operational cost, and a simplified single treatment system rather than two separate systems for each wastewater type. However, it would be important to keep the pH of the mixed wastewater between 7 and 8 for optimum microbial activities. Further, pH correction in the denitrification reactor could be achieved using the acidic wastewater as a neutralisation step prior to biological treatment. The two wastewaters were mixed to create a neutralised single wastewater in order to determine the mixing potential. Table 3.2.shows the volume of caustic wastewater required for different pH (between 7.00 and 8.51) of mixed wastewater with initial acidic wastewater volume of 20 ml. Knowing the average daily flow rates of each wastewater, a neutralised stream could be made by mixing acidic and caustic streams suitably. However, the heat of reaction needs to be found when neutralising the pH of each stream and hence a suitable reactor has to be decided, as it was observed that a strong exothermic reaction occurred when mixing the two wastewaters. Possibly this heat energy could be used in other utility activities depending on the volume of each stream produced per day. However, this has to be evaluated further considering the possible chemical reactions, health and safety issues, and process economics.

Table 3.2: Caustic stream volume to result in different pH of mixed stream solution.

pH	Volume of caustic wastewater / (ml)
7.00	8.0
7.53	5.5
8.01	4.4
8.51	3.6

It was observed that there was low NH_4^+ -N content in both wastewaters (4 mg/l and 12.5 mg/l). The caustic stream had a high NO_3^- - N (about 1721 mg/l) content. Both wastewaters had a very high COD

(> 16,000 mg/l). Very high COD could be attributed to use of organic solvents in precious metal extraction process (Dobson and Burgess, 2007). Biodegradability of those organic solvents used in PMR process was demonstrated elsewhere (Dobson, 2006). Based on this preliminary analysis, the first requirement would be to neutralise each wastewater by mixing suitable volumetric flow rates of both acidic and caustic, as described above. Then, the pH, content of nitrogen compounds and COD of the mixed wastewater would need to be measured while keeping the pH between 7 and 8. The process configuration and operation have to be decided depending on the form and quantities of nitrogen compounds (NH_4^+ -N and NO_3^- - N) available in each wastewater (acidic and caustic). If the influent NH_4^+ -N content is too low for nitrification of acidic wastewater as shown Table 3.1, only denitrification would be required, as a high NO_3^- - N content was observed in both wastewaters. However, in order to decide the best process configuration (i.e. nitrification and denitrification or only denitrification), it would be necessary to analyse the wastewater for a considerable period of time (e.g. one year) to determine the pattern of NH_4^+ -N and NO_3^- - N contents in each wastewater stream.

3.3 Nitrification of acidic wastewater under different pH conditions

This experiment was carried out to investigate the optimum pH conditions for maximum conversion of NH_4^+ -N in the nitrification process using the acidic stream of the PMR wastewater, and to study the effect of pH variation in the PMR wastewater nitrification process.

3.3.1 Materials and methods

Ammonium concentration changes with time were studied at different pH conditions (4, 5, 6 and 7) by triplicating (as 1, 2 and 3) each sample. The pH was adjusted using NaOH to 5, 6 and 7 to mimic different initial pH status. Then samples of 200 ml of wastewater were mixed with 200 ml of trickling filter humus sludge for inoculation. Each sample was then aerated and the NH_4^+ -N content was measured at 12 hour intervals initially and then at 24 hour intervals, until the concentration reached < 0.05 mg/l. For uniform mixing, the whole set of samples (12) were mixed at 140 rpm on a shaker (Labcon, Lab Design Engineering, Maraisburg, RSA). Once the nitrification test was completed, the nitrified wastewater was stored at 4 ° C for use in denitrification.

3.3.2 Results and discussion

Figure 3.2 shows that even at pH 4, NH_4^+ -N removal efficiency was > 85 % after 48 hours. Further, the final average pH had been increased from 4.00 to 5.64. When pH was increased in the PMR wastewater using NaOH, the initial content of NH_4^+ -N could have decreased due to the conversion of NH_4^+ -N into ammonia gas (NH_3) and their pH dependency (see Appendix B for pH and temperature dependency of the NH_4^+ -N and NH_3 equilibrium). Appendix A: Table A.1 shows the primary data related to this experiment.

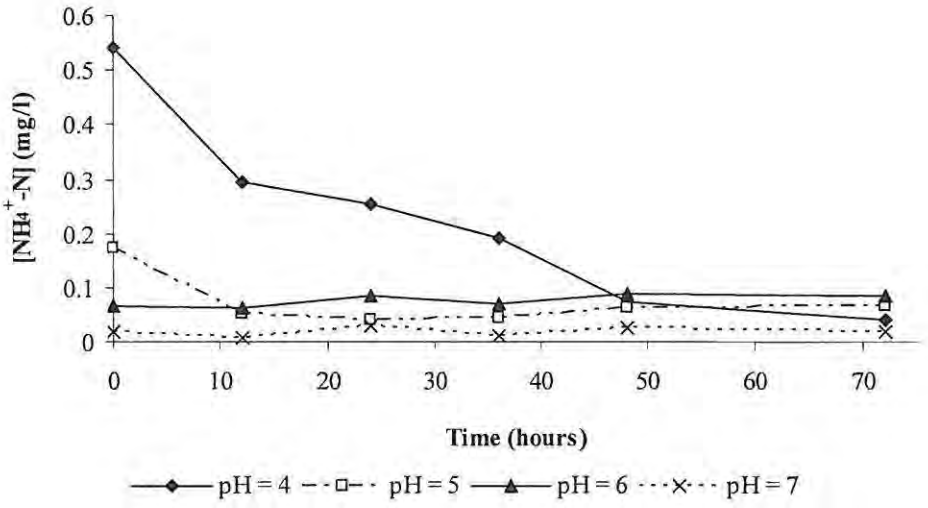

Figure 3.2: Ammonium removal under different pH conditions.

High tolerance of ammonium oxidisers to low pH and hence effective removal of NH_4^+ -N could have been due to the higher volume of activated sludge used (1:1 with the acidic stream) in the experiment. Extracellular polysaccharides (EPS) can act as a pH buffer for extreme conditions (Hesselsoe and Sorensen, 1999). This was observed when the pH increased from 4.00 to 5.64 after 72 hours. Ammonia oxidising bacteria (AOB) produce large quantities of EPS when growing in surface biofilms (Hesselsoe and Sorensen, 1999). Further, the AOB *Nitrosomonas eutropha* and *Nitrosomonas europea* were observed only at pH 7.5 and 30° C (Egli *et al.*, 2003). However, the experiments for the PMR wastewaters were carried out at a room temperature of about 22° C. Therefore, neither pH nor temperature was conducive to the growth of the above AOB as reported in literature. Therefore, effective NH_4^+ -N removal even at pH 4 could have been due to involvement of different AOB or reduced activity of the above subgroups with high biomass content in the inoculum. Nitrification in acidic soils has been reviewed by De Boer and Kowalchuk (2001), who discussed the possibility of nitrification at low pH, citing different scenarios such as adapting to growth and nitrification by immobilisation in alginate or by exposure to fluctuating pH when high cell densities were present, improved nitrification at low pH in biofilms *cf.* cells in suspension and EPS in which the bacteria may be provided with suitable conditions for nitrification at low pH. A preliminary study on microbial community analysis in a continuously stirring tank reactor (CSTR) and packed-bed reactor (PBR) is presented in Chapter 10. This batch experiment was carried out to mimic a CSTR by shaking at 140 rpm. This enhanced the effective substrate mass transfer from the bulk liquid to biomass. In biomass suspension systems, the surface area to volume ratio of the biomass is 10 – 100 times higher than in biofilm systems; hence the substrate uptake rate was not limited by mass transfer (Siegrist and Gujer, 1987). Further, Siegrist and Gujer (1987) stated if ions are involved in mass transfer (e.g.

NH_4^+-N and NO_3^- - N), electrostatic interactions between ions can increase or decrease molecular diffusion.

3.4 Evaluation of denitrification using different carbon sources

Facultative bacteria are able to switch their oxidative metabolism to NO_3^- respiration in the absence of oxygen requiring an external carbon source as an electron donor (Gallert and Winter, 2005). Thus, this experiment was carried out to identify a suitable carbon source for denitrification of the PMR wastewater. Sodium acetate, sodium lactate and ethanol were chosen based on availability and easy hydrolysis. Cheap carbon sources such as molasses and sewage sludge are more difficult to metabolise by denitrifiers due to their complex chemical structures. This was evidenced by previous work by Kasia *et al.* (2005) who used sewage sludge as carbon source and thus showed poor NO_3^- - N removal using actual PMR wastewater in a PBR. When considering the amount of precious metals contained in the wastewater, use of sodium lactate is justified due to the value recovery of metals and improved denitrification.

3.4.1 Materials and methods

First, each sample (200 ml) was adjusted to pH 7 using NaOH. Then samples were inoculated with 200 ml of trickling filter humus sludge to make the total volume 400 ml. Sodium acetate, sodium lactate and ethanol (all carbon sources were analytical grade supplied by Merck Chemicals (Pty) Ltd., Johannesburg) were added to each sample as 1% of total volume (400 ml). All the samples were kept under anoxic conditions and the NO_3^- - N content was measured at 24 hour intervals. Samples were run in triplicate.

3.4.2 Results and discussion

Usually denitrification is carried out by heterotrophic bacteria. A carbon supply is vital for heterotrophic denitrification, as it determines the efficiency of denitrification rather than individual enzymatic activities (Martienssen and Schöps, 1999). Therefore, the introduction of an external carbon source (electron donor) for energy production is necessary for nitrogen removal. Figure 3.3 shows the nitrate removal with time using three carbon sources (sodium acetate, sodium lactate and ethanol). Sodium acetate and sodium lactate enabled lower NO_3^- - N concentrations to be reached compared to ethanol. Sodium acetate enabled 73.5 % NO_3^- - N removal after 168 hours.

However, after 168 hours, NO_3^- - N started to form instead of be removed. A similar trend was also observed using the other two carbon sources. This could be due to the conversion of hydrolysed particulate organic nitrogen, as a result of microbial decay and subsequent release to the bulk liquid. Sodium lactate allowed 57 % NO_3^- - N removal within 72 hours compared to ethanol, which took 144 hours to achieve its highest removal efficiency of 62.5 %. The relevant primary data are shown in Appendix A: Table A.2.

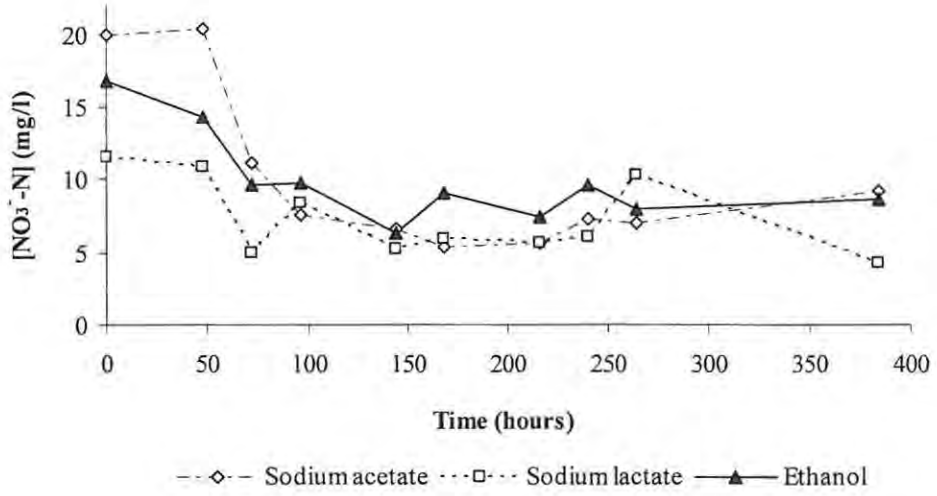

Figure 3.3: Nitrate removal from nitrified acidic wastewater with different carbon sources.

As sodium lactate was available in the laboratory, the following statistical test was carried out using MS-Excel to decide the significance of the differences observed between sodium acetate and sodium lactate. Tables 3.3 and 3.4 show the variations in mean NO_3^- - N concentration using sodium acetate and sodium lactate during the experimental period of 384 hours and a t-test summary carried out for the two carbon sources for decision making.

Table 3.3: Mean [NO_3^- - N] in mg/l for 384 hour-period.

Time	Mean [NO_3^- - N] / (mg/l)	
Hours	Sodium acetate	Sodium lactate
0	20.00	11.60
48	20.37	10.87
72	11.17	5.00
96	7.57	8.40
144	6.57	5.27
168	5.30	5.90
216	5.67	5.70
240	7.33	6.00
264	6.97	10.30
384	9.23	4.23
Mean	10.02	7.33
Variance	31.59	7.38
Observations	10	10

According to Table 3.4, it can be concluded that there was no significant difference between sodium acetate and sodium lactate as carbon sources for the experiments carried out. Therefore, sodium lactate was chosen based on availability in the laboratory for further studies on denitrifying activities.

Table 3.4: t-Test: Paired two sample for means.

Parameter	Value
Pearson correlation	0.6680
Hypothesised mean difference	0
Df	9
T Stat	*1.9741*
P(T<=t) one-tail	0.0399
T Critical one-tail	1.8331
P(T<=t) two-tail	0.0798
T Critical two-tail	*2.2622*

In the denitrification process, quite a number of bacterial genera (*Pseudomonas*, *Paracoccus*, *Flavobacterium*, *Alcaligenes* and *Bacillus* spp.) use NO_3^- - N as the terminal electron acceptor in their respiration in the absence of oxygen (Sanchez *et al.*, 2000). Therefore, denitrification is carried out under anoxic conditions so that NO_3^- - N and nitrite (NO_2^- - N) are used by denitrifying bacteria in their energy production processes which ultimately lead to evolution of di-nitrogen gas (N_2). Methanol (CH_3OH), ethanol (C_2H_5OH), sodium acetate (CH_3COONa), sodium lactate ($C_3H_5NaO_3$), molasses, acetic acid (CH_3COOH) and hydrolysed sludge can be used as carbon sources in denitrifying reactors depending on many factors such as cost, availability and nitrate (and nitrite) removal effectiveness etc (Akunna *et al.*, 1993; Sanchez *et al.*, 2000). Aesøy *et al.* (1998) mentioned only the volatile fatty acids (VFAs) are utilised in denitrifying biofilm process. Further, readily available organic matter (low molecular weight fatty acids) gives the highest denitrification rates (Aesøy *et al.*, 1998).

3.5 Evaluation of denitrification using nitrified wastewater with the best carbon source

The objective of this experiment was to evaluate denitrification using the best carbon source as identified in section 3.4. As there was no statistically significant difference between the sodium lactate and sodium acetate, sodium lactate was used as the carbon source. Further, a simple organic compound was used to avoid the extra burden on microbes due to complex, but cheap organic compounds such as molasses and sewage sludge as already the denitrifiers were subjected to precious metal toxicity and extreme pH conditions.

3.5.1 Materials and methods

Nitrified wastewater produced (volume of 200 ml) in section 3.3 was centrifuged (Beckman, Model J2-J21 Centrifuge, Beckman Coulter Inc., USA) at 9,000 rpm (using J-14 rotor) for five minutes. Then inoculum (humus sludge taken from trickling filters of Grahamstown Municipal Wastewater Treatment Works, South Africa) was added to the wastewater as 20 % of its volume. Sodium lactate (60 % w/v, Merck) was added to each sample as a carbon source. The quantity of carbon source was determined taking 1 % (6 g/l) of total volume (ie. volume of nitrified wastewater plus inoculum). Then denitrification was carried out under anoxic conditions while continuously mixing the samples at 140 rpm on a shaker (Labcon, Lab Design Engineering, Maraisburg, South Africa) for improved mass transfer between the bulk liquid and biomass and *vice versa*. Nitrate content of the bulk liquid was measured at 24 hour intervals. The test was carried out for 168 hours to observe the nitrate concentration change until steady state occurred.

3.5.2 Results and discussion

Nitrified wastewater was denitrified using sodium lactate as the carbon source. The NO_3^- - N concentration decrease with time is shown in Figure 3.4. The labelling of pH 4, 5, 6 and 7 does not represent the actual pH conditions in each sample, but the original pH condition used for nitrification. The relevant primary data are shown in Appendix A: Table A.3.

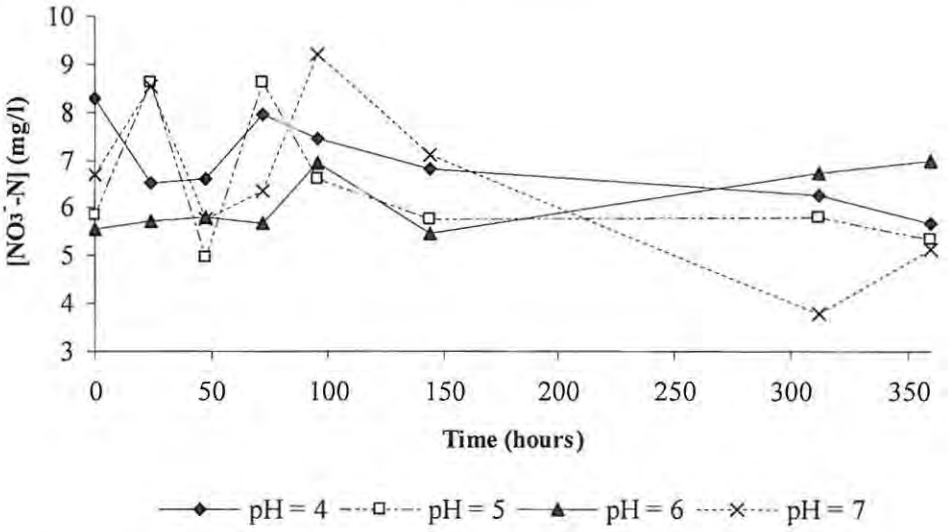

Figure 3.4: Nitrate removal using sodium lactate in nitrified effluent.

Gradual nitrate removal was observed at pH 7 compared to other pH ranges. At pH 4, the original NO_3^- - N content decreased from 8.3 mg/l to 5.7 mg/l (31.3 % reduction) over 360 hours. This shows that denitrification activity was greatly retarded at pH 4. It was evident that denitrifying bacteria are more active closer to neutral pH (Koren *et al.*, 2000). At pH 5, the highest NO_3^- - N decrease (i.e. from 5.83 mg/l to 4.97 mg/l) was observed in the first 48 hours. After that a NO_3^- - N increase was observed

instead of removal. This could be due to the hydrolysis of particulate nitrogen and subsequent addition to the bulk liquid as described earlier.

A significant NO_3^- - N removal activity could not be observed even at pH 6. Instead, intermittent NO_3^- removal and formation were observed during the experimental period of 360 hours. However, the low initial NO_3^- - N content in each sample (≤ 10 mg/l) could have led to low denitrification activity due to insufficient nitrogen for cellular synthesis of denitrifying bacteria (Figure 3.2 *cf.* Figure 3.3).

3.6 Denitrification under different amounts of the best carbon source

This experiment was carried out to identify a suitable amount of carbon source in terms of NO_3^- - N removal efficiency in the acidic wastewater stream without pH adjustment.

3.6.1 Materials and methods

Equal volumes (100 ml of each) of acidic wastewater and inoculum (trickling filter humus sludge, Grahamstown Municipal Wastewater Treatment Works, South Africa) were mixed to make one sample. Six samples were prepared, and sodium lactate (60 % w/v) added at 1.5, 2, 2.5, 3, 3.5 and 4 % of the total volume. Denitrification was then carried out for 120 hours under anoxic conditions while all the samples were uniformly mixed on a shaker at 140 rpm. Nitrate content and pH of bulk liquid were monitored at 24 hour intervals. No pH adjustment was done during this experiment.

3.6.2 Results and discussion

Figure 3.5 shows the NO_3^- - N removal with different amounts of sodium lactate. Under different percentages (by volume) of sodium lactate, 3 % concentration showed the highest NO_3^- - N removal (69 %) within 72 hours.

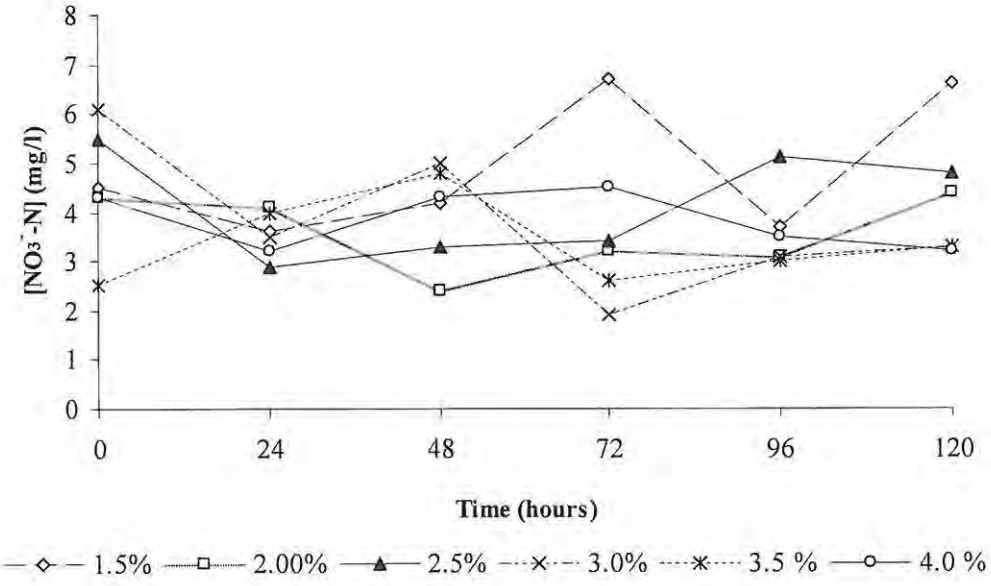

Figure 3.5: Nitrate removal with different percentages (by volume) of sodium lactate.

Sodium lactate at 2.5 % showed approximately constant NO_3^- concentration until 72 hours after reaching the minimum NO_3^- - N concentration (decreased from 5.5 mg/l to 3.3 mg/l in 48 hours). None of the different sodium lactate concentrations showed any significant pH change during the experimental period (the change is 3.95 to 4.37). However, as denitrification is a bicarbonate ion (HCO_3^-) producing process, pH increase was expected. The relevant primary data are shown in Appendix A: Table A.4.

Two of the drawbacks of this experiment were non-availability of biomass information in each sample and low initial NO_3^- - N concentration. Even though equal volumes of sludge were used as the inoculum, there was no guarantee of having equal quantities of biomass in each sample. Hence it is difficult to deduce the denitrification activity unless NO_3^- - N removal is calculated on a per unit biomass basis (eg. NO_3^--N mg/mg VSS or NO_3^--N mg/mg MLSS). It can not be distinguished whether low or high denitrification activity was due to low or high biomass or sodium lactate different concentrations. Further, low initial NO_3^- - N concentration (< 7 mg/l) could have led to low denitrification activity as mentioned in section 3.4.

3.7 Interim conclusions

According to the preliminary investigations, nitrogenous compounds removal in the PMR wastewater can be achieved either in a single stage, where ammonium is low (< 1 mg/l) and nitrate high (> 1000 mg/l) using the denitrification only option or dual stage, where ammonium and nitrate concentrations are significant, using the nitrification-denitrification option. However, a study on long term variations of influent concentrations has to be performed for decision making and detailed design processes. Further, treatment of a single wastewater stream would be more feasible than treating two separate streams as acidic and caustic wastewaters. Based on the batch experiments, nitrification of acidic wastewater could be carried out even at pH 4, indicating that there was no need of pH adjustment, as the nitrifying microbes were able to acclimatise to low pH conditions. Forty-eight hours was a suitable hydraulic retention time (HRT) for nitrification at pH 4 using acidic wastewater, attaining > 85 % NH_4^+-N removal. For denitrification, there was no statistically significant difference between sodium lactate and sodium acetate as a carbon source. Therefore, sodium lactate was used as the carbon source for denitrification. Hydraulic retention time can be taken as 24 hours based on the nitrate conversion, as there was cyclic increase and decrease after a certain time. For a 1:1 a ratio of wastewater and inoculum, addition of 3 % carbon source by volume gave the best nitrate conversion under the set conditions. There was no significant pH change in the denitrification process, unlike in the nitrification process. The conditions of HRT, carbon supply and inoculum: initial feed ratio information were taken forward into the next phase of the research, to investigate the possible reactor configurations. The types of selected single stage reactors and their performances are described in the next chapter.

CHAPTER 4

An edition of this chapter has been published as:

Manipura, A., Barbosa, V.L., Burgess, J.E., 2006.Comparison of biological ammonium removal from synthetic metal refinery wastewater using three different types of reactor. Minerals Engineering, doi:10.1016/j.mineng.2006.11.008.

I do the very best I know how-the very best I can; and I mean to keep doing so until the end.

- Abraham Lincoln (1809-1865).

4.0 Reactor comparison study of biological nitrogenous compounds removal from synthetic precious metal refinery wastewater

4.1 Introduction

When selecting a suitable reactor type for removal of nitrogenous compounds from PMR wastewater, many factors such as removal rate per unit reactor volume, technical feasibility, operational cost, robustness, maintenance and operation, process monitoring and control, and lifetime of the reactor type must be considered. The CSTR has been extensively used in chemical and biological applications due to its favourable rates of mass transfer between different phases (such as gas / liquid / solid *vice versa*), its position as a well-established technology, well understood fluid dynamics (important in mixing and scaling-up), and easy process monitoring and control. The main disadvantage of the CSTR is high operational cost for aeration and continuous stirring. The PBR has the advantages of easy construction, the support of attached growth bacteria by providing high specific surface area, use of support media such as granular activated carbon (GAC), which acts as micronutrient and substrate storage, and creating an anoxic/anaerobic environment to facilitate denitrification effectively. The main disadvantages of the PBR are the inability to control process parameters (e.g. pH), preferential flow inside the bed and hence uneven distribution of influent and nutrients. Airlift suspension reactors have been used for nitrogen removal with slightly different designs in recent years (Campos *et al.*, 2000; van Benthum *et al.*, 1998) as they can support suspension and attached growth organisms simultaneously, achieve high N removal rates per unit reactor volume, and it is relatively easy to control desired parameters such as pH and mixing. The fluid bed and biomass carrier particles are in suspension in the ALSR by the rising air (or gas) which is dispersed from the bottom. Therefore, relatively high pressure air (or gas) has to be used in the ALSR. Nitrification is mainly carried out by autotrophic aerobic bacteria, while denitrification is mainly carried out by anoxic/anaerobic heterotrophic bacteria. Therefore the use of a dual reactor system for each operation is common practice, enabling independent control of both processes. However, the organisms which are more suitable for a particular reactor design or performance are yet to be identified (Kowalchuck and Stephen, 2001). Usually CSTRs and ALSRs without a biomass carrier are used for biological treatment with suspended biomass and PBRs and ALSRs with biomass a carrier are used for attached growth organisms.

In this chapter, biological removal of nitrogen bound into compounds (NH^+_4-N, NO^-_2-N and NO^-_3-N) from metal refinery wastewater was investigated using carefully simulated wastewater in three types of bioreactor (CSTR, PBR and ALSR). Ammonium and nitrate bound metal complexes are formed during the metal refinery process as most of the intermediate compounds are chloramines. Thus PMR wastewater contains nitrogenous compound bound metal as described in Chapter 2. The objective of

this chapter is to present the results of NH^+_4-N removal, NO^-_3-N formation / removal and NO^-_2-N accumulation / removal in each reactor using synthetic metal refinery wastewater containing ammonium-bound heavy metals (30 mg/l), as found in samples of real metal refinery wastewater.

4.2 Materials and methods

Three reactor types were selected considering biomass suspension, biofilm growth and mixed biomass growth (suspended and fixed growth). Thus comparison study could reveal the suitable reactor type for removal of nitrogenous compounds at different stages. A CSTR, a PBR filled with granular activated carbon (GAC) and an ALSR with GAC as the biomass support were used (Figure 4.1). The hydraulic retention time (HRT) for the CSTR and PBR was kept at 72 hours (based on preliminary tests). Each reactor was maintained with a 1:1 recycling ratio. Air was supplied to the CSTR and ALSR at a rate of 200 ml/min by a compressor. The ALSR consisted of an inner tube which acted as the draught tube for biomass carrier particle suspension, and an outer cylinder which was the downcomer of the circulating liquid. Granular activated carbon (0.5 - 1.5 mm diameter) was used as the biofilm carrier. Compressed air was pumped into the bottom of the draught tube through a circular nozzle. Initially, the ALSR was run for 48 hours without influent but re-circulating the wastewater within the reactor. Then the ALSR was fed at a rate to maintain a HRT of 48 hours. Nitrifying trickling filter humus sludge from Grahamstown Municipal Wastewater Treatment Works, South Africa, was used as an inoculum and mixed with metal refinery wastewater as shown in Table 4.1.

Table 4.1: Initial influent compositions.

Component (unit)	CSTR	PBR	ALSR
Inoculum (l)	4	2.0	2
Refinery wastewater (l)	2	0.9	3*
Distilled water (l)	1	1.5	2
Total active reactor volume (l)	7	**4.4**	7

* Effluent from CSTR was used instead of refinery wastewater.

Each reactor was then fed (Table 4.1) and the systems were run for two weeks, separately recycling the effluents. All the reactors were then half emptied and the synthetic wastewater was supplied as feed. The feed contained 30 mg/l heavy metal as found in the initial PMR wastewater characterisation study and 100 mg/l NH^+_4-N. Nutrient solution made up using UniLAB grade reagents (Merck Chemicals (Pty) Ltd, Johannesburg: 4 g/l $NaHCO_3$, 13.5 g/l Na_2HPO_4, 0.7 g/l KH_2PO_4, 0.1 g/l $MgSO_4.7H_2O$, 0.0014 g/l $FeCl_3.6H_2O$, and 0.011 g/l $CaCl_2.2H_2O$) was fed to each reactor with the ammonium: nutrient solution ratio at 10:1 (Koren *et al.*, 2000). Nutrients were added to the CSTR and ALSR at 10 % of the influent feed rate. Sodium lactate (60 % w/v, UniLAB, Merck) was pumped to the PBR at 3 % of the feed flow rate to provide a carbon source for heterotrophic denitrification (based

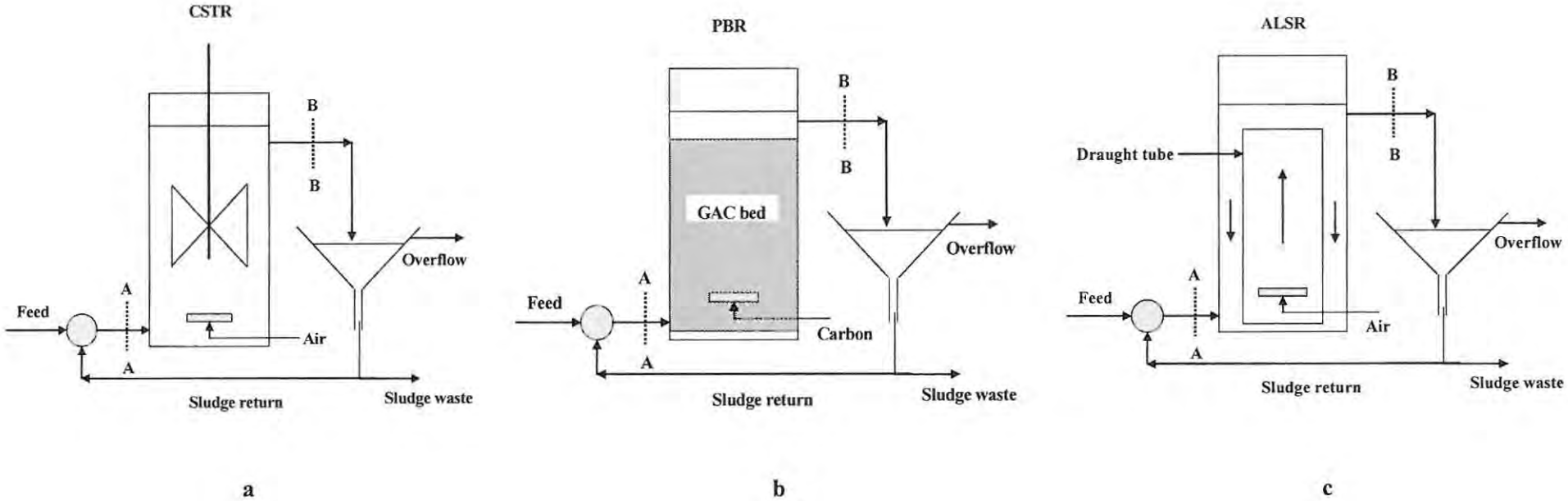

a b c

Figure 4.1: Schematic diagrams of the CSTR (a), PBR (b) and ALSR (c). Annotations A--A and B--B indicate sampling points.

on the previous results - see Chapter 2: Preliminary investigations). Sludge collected in the clarifiers downstream of the CSTR and ALSR was returned to the respective reactors to prevent biomass washout. All the experiments were carried out at room temperature of approximately 20 °C. Samples were taken from the points indicated (Figure 4.1) three times per week for analysis. The pH also was monitored daily in the CSTR and ALSR. When the pH exceeded 8.5, 32 % (w/w) HCl was added to the reactor to restore the pH to 7.5 ± 0.5. Ammonium-N, NO_2^--N and NO_3^--N concentrations were measured using spectrophotometric kits (Merck) based on the principles of *Standard Methods* (APHA *et al.*, 1998). Spectroquant® test numbers 14752 (NH^+_4-N), 14776 (NO^-_2-N) and 14773 (NO^-_3-N) were used (analogous to *Standard Methods* 4500-NH_3-F, 4500-NO_2-B, 4500-NO_3-E and 5220-D, respectively). The concentration of mixed liquor suspended solids (MLSS) in the CSTR was determined according to *Standard Methods* (2540-D) and pH measured using an electrode (CyberScan 2500, Eutech Instruments, Singapore).

4.3 Results

4.3.1 Continuously Stirred Tank Reactor

Initially the CSTR showed low NH_4^+ -N removal (Figure 4.2a). This could have been due to the slow growth rate of NH_4^+ oxidizers (Sliekers *et al.*, 2003), possible toxic effects of high metal concentration (30 mg/l) and unrealistically low influent NH^+_4-N concentration. Hence, it could have taken a longer time than anticipated to achieve process stability. See Appendix B: Table B.1 for primary data.

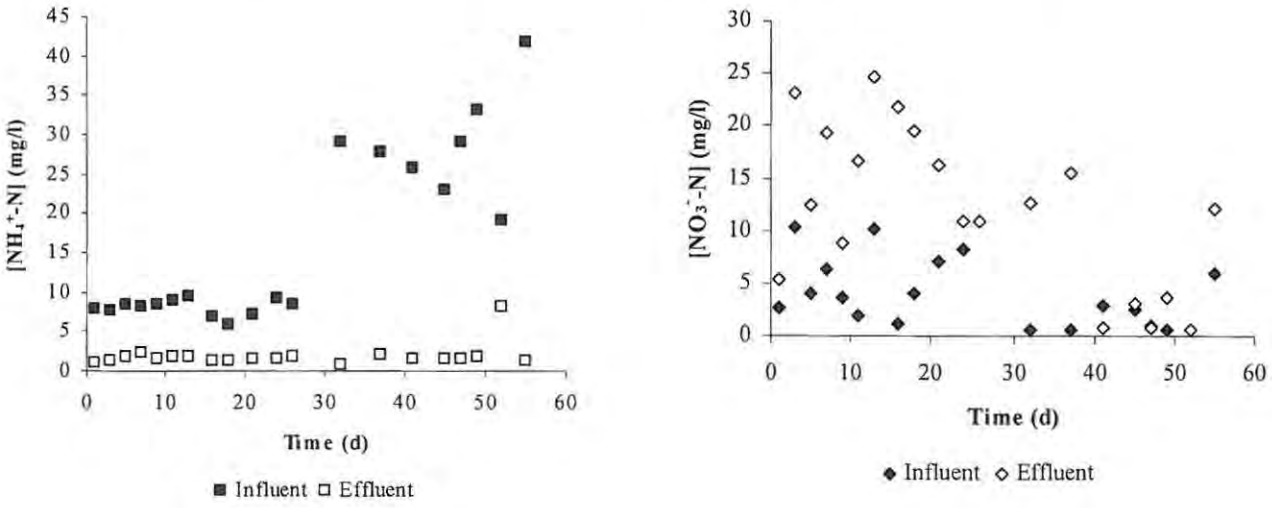

a B

Figure 4.2: Ammonium removal (a) and nitrate production (b) in the CSTR.

Low NH^+_4-N removal (< 80 %) was observed until day 22, due to low influent NH^+_4-N concentration. Good growth of ammonia oxidizing bacteria (AOB) could have been retarded, as enough nitrogen

(NH^+_4-N) for cellular synthesis may not have been available in the reactor. Once the influent NH^+_4-N concentration was increased to the same concentration as measured in real wastewater samples, a significant improvement in NH^+_4-N removal efficiency was observed. The mean NH^+_4-N removal efficiency during the whole test period was 93 %. No consistent NO_3^- formation was observed (Figure 4.2b). This was probably due to the slower growth rate of NO_2^- oxidizing bacteria (NOB) compared to AOB. Nitrite accumulation was observed despite nitrate oxidation. However, the NO_3^- concentrations were < 0.58 mg/l. A 50 – 75 % increase in nitrite in the CSTR compared to influent NO_2^- concentration was observed. The mixed liquor pH varied within 7.32 - 8.94. Since the optimum pH condition for AOB is 7.5 (Egli *et al.*, 2003), pH was controlled by dosing HCl.

4.3.2 Packed Bed Reactor

Figure 4.3a illustrates the NH^+_4-N removal observed in the PBR. Significant NH^+_4-N removal (> 85 %) was observed from day 1. However, a dramatic reduction of NH^+_4-N removal efficiency was observed from day 5 to 30. This could have been due to insufficient nitrogen in the PBR for cellular synthesis of AOB as a result of low content of NH^+_4-N in the influent, as mentioned earlier.

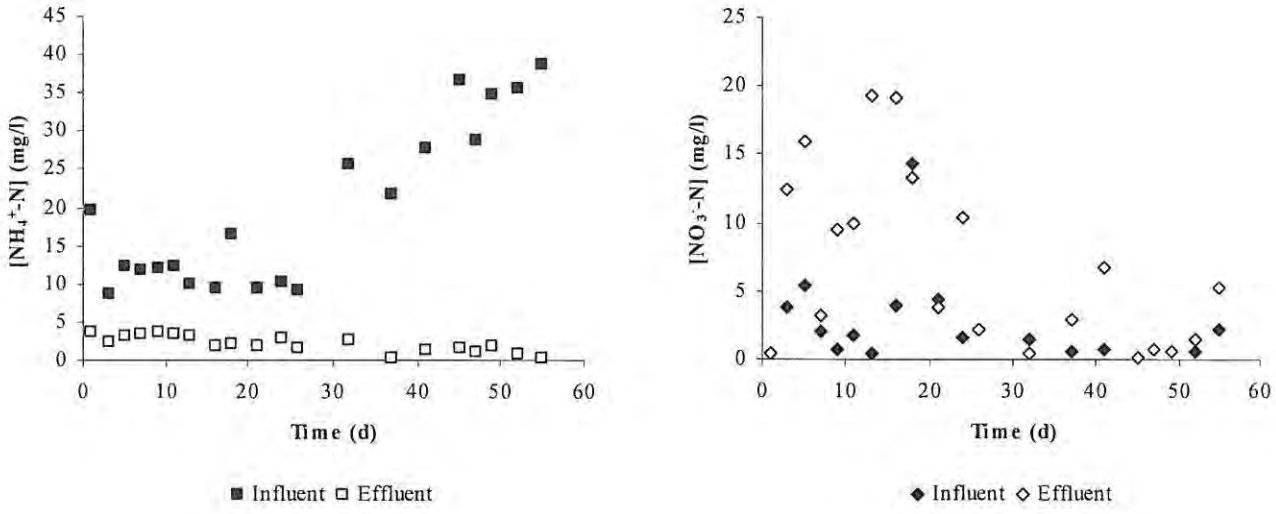

a B

Figure 4.3: Ammonium removal (a) and nitrate production (b) in the PBR.

Either heterotrophic or autotrophic anaerobic ammonium oxidizers may have removed ammonium anaerobically. Analysis is yet to be carried out to identify the micro-organisms in the PBR. Increased influent NH^+_4-N concentration improved the removal efficiency. No NO_2^--N accumulation was observed as it was in the CSTR. Inconsistent NO_3^--N formation was observed (Figure 4.3b).Nitrate formation was seen in the PBR during the first 28 days, as opposed to the NO_3^--N removal expected in the denitrification process. However, towards the end of the experiment, there was a decrease in NO_3^--N in the PBR effluent (see Appendix B: Table B.2 for primary data).

The pH in the PBR was not controlled as in the CSTR; it varied within 5.45 - 5.99. This may have been due to the production of low molecular fatty acids (Barber and Stuckey, 2000). However, neither methane nor carbon dioxide production was monitored in this experiment and therefore this idea cannot be supported by data.

4.3.3 Airlift Suspension Reactor

Figure 4.4a shows the NH^+_4-N removal in the ALSR. The ALSR HRT was 48 h (*cf.* CSTR and PBR; 72 h), as the ALSR supported both suspended and fixed biomass (on the surface of GAC). The ALSR took 21 days to attain consistent NH^+_4-N removal. However, once it reached steady state, the ALSR showed continuous NH^+_4-N removal over the remainder of the experimental period.

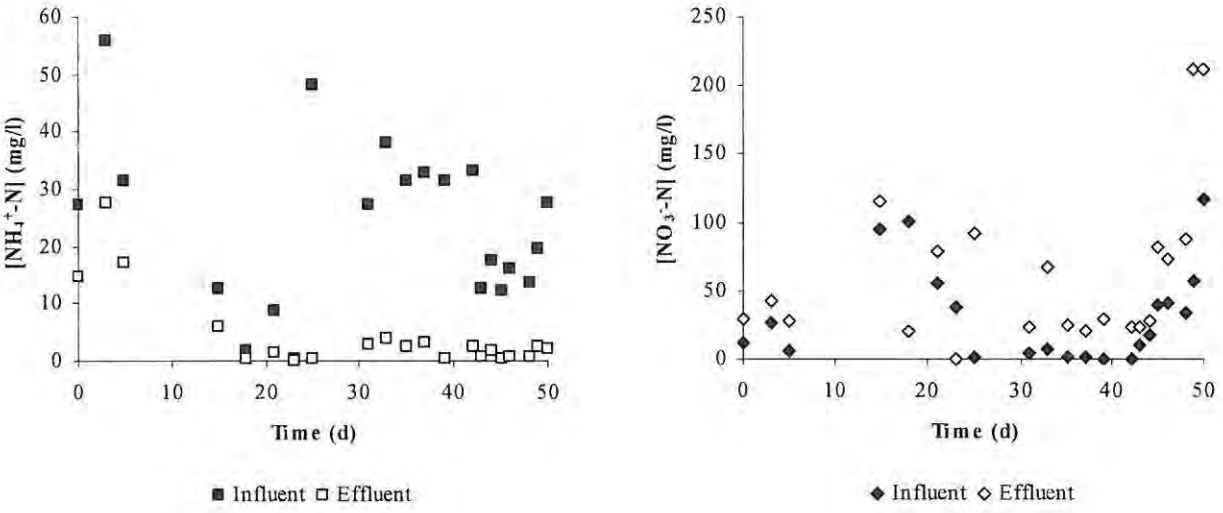

A **B**

Figure 4.4: Ammonium removal (a) and nitrate production (b) in the ALSR.

Nearly 100 % NO_3^- increase (Figure 4.4b) was observed during the experimental period. Introduction of the inner circulation draught tube improved mixing, but led to consistent NO_3^--N formation at the expense of NO_2^- compared to operating without the inner draught tube. The pH varied between 7.29 and 8.65, as it was controlled using HCl (See Appendix B: Table B.3 for primary data).

4.4 Discussion

Three different reactors under similar influent conditions without removal optimisation of each nitrogen species (i.e. NH^+_4-N, NO_2^--N and NO_3^--N) showed >80 % NH^+_4-N removal alone. Ammonium and NO_3^--N removal is carried out by different microbial consortia. The organisms which are more suitable for a particular reactor design or performance are yet to be identified (Kowalchuck and Stephen, 2001). Therefore, identification of the fundamental steps in nitrification and denitrification under extreme pH conditions, high metal concentrations and high NO_3^--N concentrations (> 1000 mg/l) is critical to the development of a sustainable continuous nitrogen

removal process for metal refinery wastewater. Preliminary batch experiments (Chapter 3: Preliminary investigations of PMR wastewater) indicated that NH^+_4-N could be decreased to 0.05 mg/l in 72 hours at pH 4 in a nitrification NH^+_4-N oxidation step, and that subsequent denitrification achieved effluent NO_3^--N concentrations of ≥3.6 mg/l. This was verified using the CSTR, ALSR and PBR. However, this process was inhibited by extreme pH, high concentrations of nitrogen compounds (e.g. 1721 mg/l nitrate was measured in one wastewater), high chemical oxygen demand (COD), of up to 16000 mg/l, and high metal concentration (≈30 mg/l total heavy metals concentration). High COD inhibits nitrification by allowing heterotrophic organisms to outcompete the nitrifying bacteria, and hence excessive aeration is needed for effective nitrification.

The AOB produce large quantities of extracellular polymeric substances (EPS) when growing in biofilm communities. High EPS bacteria tolerate low pH (Hesselsoe and Sorensen, 1999). Nitrite oxidizers are more sensitive than AOB to free ammonia and free nitrous acid, hence they are inhibited if the prevailing pH in the reactor increases (higher free ammonia) or decreases (higher free nitrous acid) (Bernet *et al.*, 2005). As the influent NH^+_4-N concentration increased in each reactor, NH^+_4-N removal efficiencies improved. This was observed after 26 and 32 days in the CSTR and PBR, respectively. The ALSR was operated after the CSTR and PBR, so the higher NH_4^+ concentration was used from day 0. The improvement of NH^+_4-N removal efficiencies (Figure 4.5) can be explained as efficient growth and retention of nitrifying bacteria. The initial retardation of growth can be attributed to the artificially low concentration of NH^+_4-N used originally, which may have been insufficient for biomass growth. The specific growth rate of each cell is governed by the NH^+_4-N loading rate (Tsuneda *et al.*, 2003). The ALSR took 18 days to reach >80 % removal efficiency, whereas the CSTR and PBR took 9 and 16 days, respectively. Tsuneda *et al.* (2003) also found that it takes longer to develop a nitrifying biofilm in fluidised bed reactors, particularly when the wastewater contains no organic compounds.

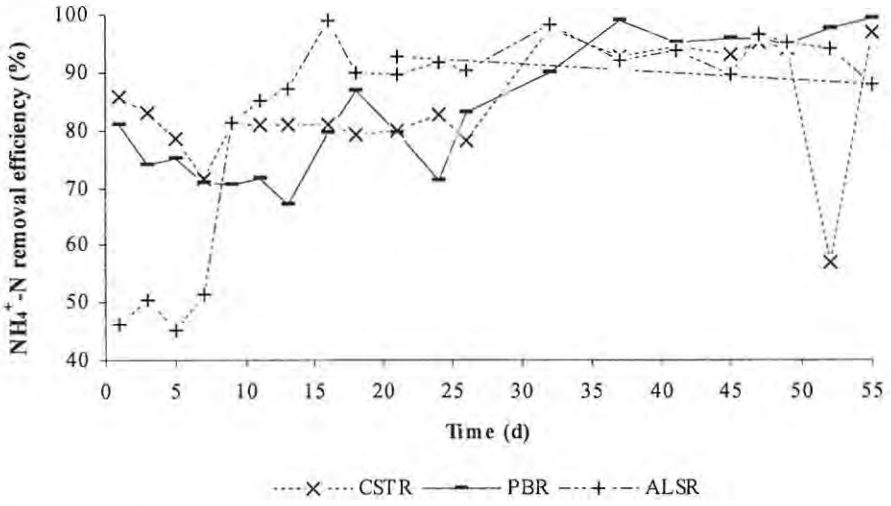

Figure 4.5: Comparison of ammonium removal efficiencies in the three reactor types.

A similar study (van Benthum *et al.*, 1998) obtained complete NH^+_4-N removal in a biofilm airlift reactor in which the pH was 7.5 ± 0.5. However, the operating temperature (30 °C) and hydraulic retention time (5 h) were different from this study (20 °C and 48 h). Further, van Benthum *et al.* (1998) used a CSTR (pre-denitrification) prior to ALSR (nitrification). Each reactor had a recirculation ratio of 6.5, *cf.* 1. The higher recycling ratio used by van Benthum *et al.* (1998) could have led to higher influent NH^+_4-N concentrations provided to their ALSR, so that NH^+_4-N removal was improved (this study showed increased NH^+_4-N removal occurred when the influent NH^+_4-N concentration increased). A recirculation ratio of 1:1 diluted the influent NH^+_4-N concentration entering the ALSR in this study. Therefore, this ALSR received lower NH^+_4-N and had lower removal efficiency. High recirculation ratios improve the influent NH^+_4-N concentration, while low ratios improve biomass retention in the reactor. These two studies demonstrate the compromise between increased ammonium influent concentration and better biomass retention by adjusting the recirculation ratio. The net influent NH^+_4-N concentration to the reactor should be sufficient to allow biomass synthesis for better removal of NH^+_4-N. At higher temperature (30° C) AOB have better growth than at 20° C. This could also account for the complete NH^+_4-N removal reported by van Benthum *et al.* (1998), compared to this study.

During the first 30 days, the ALSR produced higher amounts of NO_2^--N (1.4 mg/l, *cf.* influent 0.16 mg/l) than the CSTR (0.48 mg/l *cf.* influent 0.15 mg/l; Figure 4.6a and 4.6b). This was observed after introducing the inner draught tube to enhance mixing. The nitrite formation factor (NAF) was defined as the ratio between the NO_2^--N concentration in the reactor and the NO_2^--N concentration in the feed and was used to ascertain nitrite accumulation. The ALSR showed inconsistent NO_2^--N production.

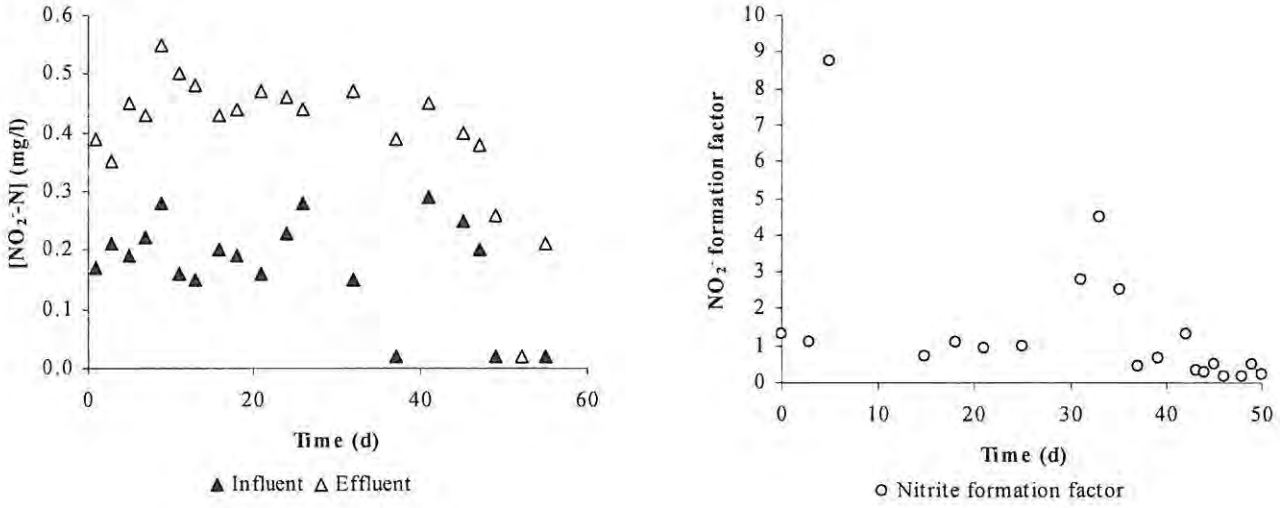

Figure 4.6: Nitrite production in the CSTR (a) and ALSR (b).

This can be observed from day 32 onwards (NAF <1), as there was no NO_2^--N accumulation in the ALSR. Conversely, the CSTR showed consistent NO_2^--N accumulation over the 55 days with a maximum of 0.39 mg/l *cf.* influent 0.02 mg/l. Nitrite accumulation (<100 mg/l) is intended in operating the completely autotrophic nitrogen removal over nitrite (CANON), single reactor high activity ammonia removal over nitrite (SHARON) and oxygen limited nitrification and denitrification (OLAND) processes. Nitrite oxidisers and reducers compete for the common substrate, NO_2^--N. Adopting the correct aerobic and anoxic HRT in biofilm airlift reactors, the nitrifiers grow in biofilms, while denitrifiers grow in suspension (van Benthum *et al.*, 1998). The DO in the ALSR was above 4 mg/l, as air was used to suspend the particles and to supply the electron acceptor. Therefore, the initial NO_2^--N accumulation recorded in the ALSR cannot be explained by oxygen limitation, although it is possible to have lower oxygen concentration in the inner layers of the biofilm than in the bulk liquid. The NOB may have taken a longer time to acclimatise to the high metal concentrations, leading to lower initial NO_3^--N formation, allowing NO_2^--N accumulation in the CSTR and ALSR. Similar NO_2^--N accumulation in a biofilm airlift suspension reactor with a HRT of 8.3 h (*cf.* 48 h) was observed by van Benthum *et al.* (1998). Nitrite oxidation to NO_3^--N is performed when the DO concentration is >3 mg/l, although the concentration in the biofilm is much lower. However, after 14 days, ammonium removal efficiency exceeded 50 %. The slow start up NH^+_4-N removal is due to slowly growing autotrophic NH_4^+ and NO_2^- oxidisers. Nitrate formation in the ALSR occurred later than NH^+_4-N removal due to relatively slower growth rates of NO_2^- oxidisers which convert the intermediate NO_2^--N to NO_3^--N (Figure 4.4b). Increased NO_3^- input into each reactor can be attributed to the 1:1 recirculation ratio. Under lower DO conditions (<3 mg/l) a lower amount of nitrate is produced (van Benthum *et al.*, 1998), but NO_2^- is produced because NO_2^- oxidation is inhibited due to lack of oxygen. It has been shown that NOB grow more slowly than AOB at lower oxygen concentrations and that the optimum DO concentration for maximum NO_2^--N accumulation depends on the NH^+_4-N loading rate (Bernet *et al.*, 2005).

The PBR showed a more consistent pH than the CSTR and ALSR, in which the pH had to be controlled. However, the ALSR was operated at values above over the optimum pH for nitrification (Figure 4.7). A significant increase in NO_2^--N formation was observed in the ALSR during the first 21 days, but it subsequently decreased. Similarly, the pH increased and the desired range (7.5 -8.5) was maintained by adding 4 ml HCl (32 %) to the ALSR daily.

After 28 days of ALSR operation, the pH decreased dramatically. This is expected in the nitrification process, which produces H^+ ions. After a further 7 days, consistent pH (7.29 – 7.65) prevailed, which was more suitable for Anammox and AOB, whereas the PBR had a lower pH, < 6, although the NH^+_4-N removal efficiency was > 90 %. This affected the NH^+_4 *vs.* NH_3 pH dependant equilibrium. Table 4.2 compares the performance of the three reactors.

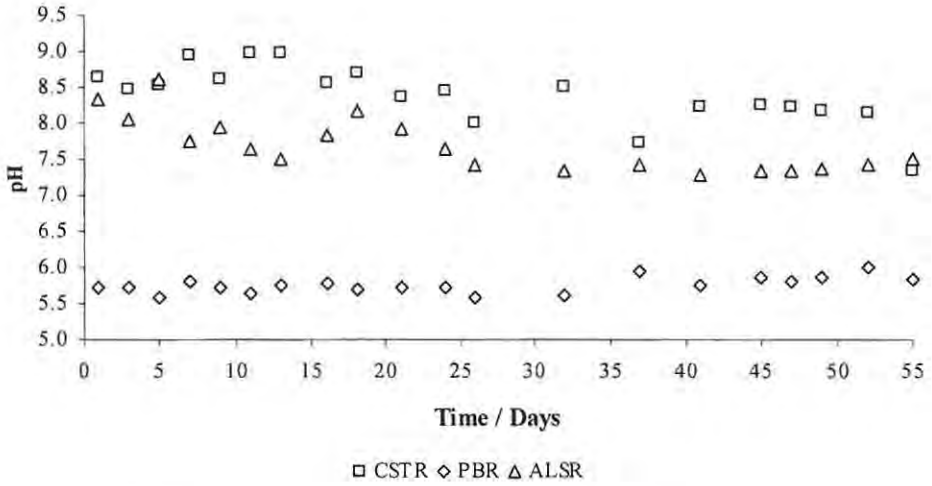

Figure 4.7: pH variation in the CSTR, PBR and ALSR.

Table 4.2: Summary of comparison of the performance of the three reactors.

Parameter	CSTR	PBR	ALSR
Ammonium removal efficiency (% after 28 days)	> 93	> 89	> 87
Nitrite accumulation	50 - 75 % of input	None	Varied
Nitrate formation	Good	Good	Good
Average total nitrogen (TN) removal efficiency (%)	> 68 %	> 79 %	> 45 %**
pH variation	pH increases	Consistent	pH increases

** Excluding days in which $TN_{influent} < TN_{effluent}$.

Kasia *et al.* (2005) reported similar NH^+_4-N removal results as in the CSTR and PBR of this study using actual refinery wastewater. They removed >97 % NH^+_4-N in a CSTR with a 27 h HRT. Initially they used a higher NH^+_4-N concentration (101 mg/l) and thus achieved higher removal efficiency. However, after 16 days they operated under low NH^+_4-N input (due to a different refinery wastewater batch) and their removal efficiency decreased (*cf.* 18.18 % minimum and 92.27 % maximum). In this study, the opposite approach was used as influent NH^+_4-N concentration was increased after 28 days, leading to higher removal efficiency (*cf.* minimum 71.6 % in day 7 and 96.88 % in day 55; Figure 4.5).

Usually NH^+_4-N and NO_3^--N removal is the first performance indicator to show the metal poisoning of the nitrification and denitrification processes in municipal wastewater treatment. Beside the NH^+_4-N

removal, poor NO_2^--N conversion could also indicate toxic inhibition by metals. Biochemical data such as oxygen uptake rates, NH^+_4-N utilisation rates, and NO_3^--N production rates, volatile suspended solids obtained for different metal concentrations of Cu, Ni and Zn showed that higher sensitivity of nitrifiers to these metals (Principi *et al.*, 2006). Even micronutrients at high concentrations lead to toxic effect while some toxic metal at very low concentrations show some stimulant activity in biochemical processes shifting the normal metabolic pathways (Hughes and Poole, 1989). At various pH conditions, soluble metal species can be shifted from one form to another, blocking active sites of the enzymes responsible in the conversion of NH^+_4-N to $N_{2(g)}$ pathway. However, the effects of different metal complexes formed under different pH are not known in nitrification and denitrification, and require further investigation. Lewandowski (1985; 1987) stated that biological wastewater treatment operated in the presence of toxic compounds acting as noncompetitive inhibitors can perform complete substrate conversion when the toxic concentration does not exceed the Reactor Resistance to Inhibition (RRI) value. The RRI is defined as the minimum concentration of inhibitive compound at which process efficiency is reduced. When the HRT is greater than the time required for complete substrate conversion, tolerance is achieved. Therefore, the better NH^+_4-N removal efficiency observed may have been a result of the lower metal concentration (RRI) for the given HRT in each reactor; i.e. each reactor might have had higher resistance to concentration metals under the set HRT for NH^+_4-N oxidation. On the other hand, the set HRT for denitrification could have been exceeded the RRI for the PBR avoiding the NO_3^--N removal. Therefore, it is worthwhile to determine the RRI value for various metal concentrations under different HRTs. Lewandowski (1986) showed that RRI varies linearly with HRT in a PBR.

Total nitrogen (i.e. TN = NH_4^+-N + NO_2^--N + NO_3^--N) in the influent and effluent were found to asses the overall nitrogen removal in each reactor considering the nitrogen fraction in each component (i.e. NH_4^+-N, NO_2^--N and NO_3^--N) as shown in Table 4.3. The TN was calculated using the nitrogen fraction in each nitrogenous compound and multiplying it by the respective influent and effluent concentrations. The respective, influent and effluent nitrogenous compounds concentrations of each reactor are given in Appendix B: Tables B.1 to B.3. The CSTR and PBR showed higher and more consistent total nitrogen removal efficiency > 68 % and 79 % respectively, compared to the ALSR. During the last 10 days of the operational period (i.e. from day 45 to 55), the PBR removed > 94 % of TN from the influent. The ALSR did not show a similar trend, mainly due to manual sludge introduction back to the reactor, which prevented the actual influent TN measurement at A-A as shown in Figure 4.1c. Even though effluent TN of the ALSR exceeded the influent TN in certain samples (days 13, 47, 52, and 55) due to the inaccurate measurement scheme adopted, the average trend showed the removal of TN in the ALSR (see Table 4.3).

Table 4.3: Nitrogen balance over influent and effluent of the CSTR, PBR and ALSR.

Day	CSTR				PBR				ALSR			
	pH	Total influent N (mg/l)	Total effluent N (mg/l)	Overall N removal eff. (%)	pH	Total influent N (mg/l)	Total effluent N (mg/l)	Overall N removal eff. (%)	pH	Total influent N (mg/l)	Total effluent N (mg/l)	Overall N removal eff. (%)
1	8.64	6.70	2.19	67.3	5.71	15.34	3.02	80.3	8.34	23.90	18.20	23.9
3	8.46	8.37	6.36	24.0	5.71	7.54	4.57	39.4	8.06	50.03	31.61	36.8
5	8.52	7.48	4.36	41.8	5.58	10.70	5.95	44.4	8.60	25.57	20.07	21.5
7	8.94	7.80	6.28	19.6	5.81	9.72	3.41	64.9	7.76	34.85	33.36	4.3
9	8.60	7.44	3.38	54.7	5.73	9.56	4.92	48.5	7.94	26.65	7.73	71.0
11	8.97	7.39	5.24	29.0	5.65	9.89	4.94	50.0	7.63	20.30	19.72	2.9
13	8.98	9.63	7.12	26.0	5.74	7.81	6.91	11.5	7.50	8.78	22.06	-151.2
16	8.55	5.59	6.04	-8.1	5.77	8.29	5.86	29.3	7.82	37.73	21.11	44.1
18	8.70	5.47	5.47	-0.1	5.70	16.07	4.72	70.6	8.16	22.24	7.63	65.7
21	8.35	7.07	4.91	30.5	5.71	8.30	2.36	71.6	7.92	31.38	18.64	40.6
24	8.44	9.09	3.82	57.9	5.72	8.21	4.62	43.8	7.65	24.57	7.68	68.7
26	7.99	8.97	3.97	55.7	5.59	7.56	1.71	77.4	7.43	25.76	7.00	72.8
32	8.51	22.68	3.56	84.3	5.61	20.22	2.11	89.5	7.33	24.63	6.95	71.8
37	7.73	21.73	5.17	76.2	5.94	17.07	0.85	95.0	7.43	25.88	7.27	71.9
41	8.21	20.62	1.40	93.2	5.76	21.77	2.59	88.1	7.29	12.16	5.80	52.3
45	8.24	18.42	2.04	88.9	5.86	28.37	1.23	95.7	7.34	17.51	7.78	55.6
47	8.23	22.81	1.38	93.9	5.81	22.63	1.10	95.2	7.34	18.37	18.75	-2.1
49	8.18	25.84	2.37	90.8	5.86	27.24	1.59	94.2	7.36	21.82	17.07	21.8
52	8.13	14.90	6.51	56.3	5.99	27.71	1.01	96.3	7.41	18.33	20.39	-11.3
55	7.32	33.74	3.81	88.7	5.83	30.55	1.44	95.3	7.49	28.20	49.68	-76.2

The difference between the influent and effluent TN concentration of the CSTR, PBR and ALSR could be attributed to the release of nitrogen in the form of $N_{2\,(g)}$, $NO_{(g)}$, $N_2O_{(g)}$ or $NH_{3\,(g)}$ (pH and temperature dependant) from each of the reactors. As gas composition analysis was not carried out, it can not be determined which gas was the dominant component. However, considering the average pH of each reactors, it can be assumed that the contribution of $NH_{3\,(g)}$ was minimal (see Appendix B.4, which presents the pH and temperature dependant $NH_4^{+}{}_{(aq)} \leftrightarrow NH_{3\,(g)}$ equilibrium and the composition of each component in each phase (gas *vs.* aqueous) under different pH and temperature conditions). This can be calculated using the Equations (4.1), (4.2) and (4.3) as given below (Farabegoli *et al.*, 2004).

$$NH_4^{+} + OH^{-} \quad \leftrightarrow \quad NH_{3\,free} + H_2O \tag{4.1}$$

$$[NH_3 - N]_{free} = \frac{[NH_4 - N] \bullet 10^{pH}}{\left(\frac{K_a}{K_w}\right) + 10^{pH}} \tag{4.2}$$

$$\frac{K_a}{K_w} = \exp\left[\frac{6334}{273 + T}\right] \tag{4.3}$$

Emission of N_2O has been estimated 0.1 % to 0.4 % of the TN in the influent where low oxygenation levels (DO of 1 mg/l) occurred (Tallec *et al.*, 2006). The CSTR and ALSR were operated well above 1 mg/l of DO. Therefore, it could be assumed that there was not significant amount of N_2O release.

Nitrite oxidising bacteria typically reside internally and adjacent to AOB aggregates where lower oxygen conditions are detected. Further, nitrification is mainly limited to the outer 100 – 150 μm of aggregates (Kowalchuck and Stephen, 2001). It can be reasonably assumed that internal layers of aggregates would have been subjected to anoxic conditions where layer thickness exceeds > 150 μm. Therefore, growth of a denitrifying consortium is possible in the inner layers of the microbial aggregates (thickness > 150 μm). Hao *et al.* (2004) stated that Anammox could occur in the deeper layers of a nitrifying biofilm that is limited by oxygen mass transfer. According to the results of the TN balance over the CSTR, > 68 % TN removal occurred. Irrespective of NO_3^{-}-N formation in the CSTR, there has been a TN removal (e.g. the average influent and effluent concentrations of NH_4^{+}-N, NO_2^{-}-N, NO_3^{-}-N are 16.2, 0.17, 4.25 mg/l and 1.87, 0.40, 11.94 mg/l respectively). This suggests that some kind of autotrophic nitrogen removal had occurred in the CSTR, as there was no carbon source supplied to the CSTR. A similar result could be observed in the ALSR where no carbon source was introduced. On the other hand, PBR showed > 79 % TN removal with sodium lactate as the carbon

source. Based on these observations, it could be hypothesised that either autotrophic or heterotrophic nitrogen removal occurred in the CSTR, ALSR and PBR respectively.

The ALSR produced the highest amount (>8 times with respect to influent) of NO_2^--N at the beginning. This is probably due to oxygen-limited conditions caused by supply air pressure variation (air was supplied to the reactor by a central air compressor which produced different output air pressure due to variations of the demand) and pH control in the ALSR at various times which might have inhibited the NO_2^- oxidisers preventing NO_3^--N formation. Further, the ALSR could be modelled as a hybrid reactor (i.e. suspension and attached biomass growth), as it contained GAC fluidised by air. Therefore, the ALSR might be a good candidate for the CANON process, which is a biofilm-associated activity (van Loosedrecht *et al.*, 2002). The biofilm grown on the surface of GAC would be subjected to different aerobic conditions, as inner biofilm layers receive less oxygen, which enhances CANON, whereas the outer layers of the biofilm are exposed to a higher oxygen concentration, which promotes NH_4^+ oxidation. Generally, autotrophic bacteria that produce little EPS carry out nitrification. This leads to a weaker biofilm matrix on the surface of particles which are subjected to higher hydrodynamic shear stress. Therefore, reduced aeration rates could help to reduce stress on the biofilm formed in the fluidised bed reactors while promoting the partial nitrification. Tsuneda *et al.* (2003) reported a suitable aeration volume promoting the nitrifying granulation. They showed that nitrifying granules formed in fluidised bed reactors exhibited higher sedimentation ability than nitrifying sludge, indicating that granules could be effectively retained when used in a CSTR under completely mixed conditions.

4.5 Interim conclusions

All the reactors studied removed NH^+_4-N effectively from the simulated metal refinery wastewater with > 85 % removal efficiency under the set conditions. The overall TN removal efficiencies in the CSTR, PBR and ALSR were > 68 %, > 79 % and 45 % respectively. Either autotrophic or heterotrophic nitrogen removal was observed in the three reactors studied. However, metal toxicity data for nitrification and denitrification for complex metal mixtures are not yet published. Hence the mechanism of the enzymatic inhibition of NH^+_4-N and TN removal occurring in the process cannot be ascertained. Robust behaviour of the PBR with consistent pH conditions and high anoxic NH^+_4-N and TN removal, compared to the CSTR and ALSR, suggested the PBR as a good candidate for wastewater treatment where pH is low with high heavy metal concentrations. The presence of metal inhibitor at a concentration of 30 mg/l did not significantly alter the NH^+_4-N removal in any of the reactors. However, based on the results of the comparison study, it is now necessary to determine the metal toxicity threshold for microbial consortium without compromising NH^+_4-N, NO_2^--N and NO_3^--N removal. Therefore, it is necessary to investigate the long term acclimatisation of nitrifying and denitrifying consortia high metal content by running reactors for a longer period. It is too early draw

conclusions based on these results for deciding the best reactor, as the system was not run for process optimisation considering each reactor type. Therefore, in order to confirm the effectiveness of each reactor type, each system needs to run under the optimum conditions. In addition, it was clear that while NH^{+}_{4}-N removal was achieved, it was not possible to perform nitrification and denitrification with acceptable efficiencies in the same reactor unit. A dual-stage system comprising a CSTR and a PBR, the best units in terms of TN removal emerging in this chapter and good candidates for maintaining different DO regimes as required for nitrification (aerobic) and denitrification (anoxic) was designed. The next chapter describes the performance of the dual-stage reactor system.

CHAPTER 5

An edition of this chapter has been presented as:

Manipura, A., Duncan, J.R., Roman, H., Burgess, J.E., 2005. Bioprocess development for nitrogen compounds removal from metal refinery wastewater. 7th World Congress on Recovery, Recycling and Re-integration, Beijing, China, Sept 25-29.

Get a good idea and stay with it. Dog it, and work at it until it's done, and done right.

- Walt Disney (1901-1966).

5.0 Nitrification and denitrification of precious metal refinery wastewater in a dual-stage system using a model compound

5.1 Introduction

Removing the nitrogenous compounds from wastewater usually involves a two-step biological process, namely nitrification-denitrification, by transforming the nitrogenous compounds to dinitrogen gas (Maier *et al.*, 2000). The nitrification process is mainly carried out by autotrophic aerobic bacteria, while denitrification is mainly carried out by heterotrophic facultative bacteria (Rittmann and McCarthy, 2001). Therefore, the use of a dual reactor system is common practice, as it enables independent control of both the nitrification and denitrification processes. As nitrification is carried out by autotrophic nitrifying bacteria, the presence or addition of organic matter depresses the growth of nitrifying bacteria by allowing the heterotrophic bacteria (which compete for other nutrients and oxygen contained in the reactor) to dominate, and ultimately the nitrification process is inhibited. Nitrogen removal from wastewaters containing large concentrations of inorganic compounds is problematic when using the standard nitrification and denitrification process, as inorganic compounds do not contain any organic matter used by heterotrophic microbes in the denitrification process. However, novel processes like anaerobic ammonium oxidation (Anammox), single reactor high activity ammonium removal over nitrite (SHARON), completely autotrophic nitrogen removal over nitrite (CANON) and oxygen limited autotrophic nitrification-denitrification (OLAND) processes use no carbon source (in autotrophic processes Anammox, CANON and OLAND) or a lower amount of carbon (SHARON) in removing the nitrogenous compounds (Hao *et al.*, 2001; Jetten *et al.*, 2002;1999; Kuai and Verstraete, 1998; Mulder, 2003; Sliekers *et al.*, 2002; 2003; Schmidt *et al.*, 2002). These processes are either still in pilot scale or have not been tested for metal refinery wastewaters, which are high strength in terms of nitrogenous compounds and metal concentrations (Manipura *et al.*, 2005a). However, the potential for use of these autotrophic processes is critical in metal refinery wastewaters in which no or very little organic compounds exist (Koren *et al.*, 2000). Very low specific growth rates (e.g. maximum growth rate of anammox is about 0.019 day^{-1} (Strous *et al.*, 1998)) and the non-availability of metal toxicity data for high strength industrial wastewaters are the main hurdles to use of these novel processes in treating metal refinery wastewaters.

The actual metal refinery wastewater contains numerous metals such as Pt, Pd, Rh, Os, Ru, Ir (PGMs), Cu, Zn, Ni, Cr, Pb and Cd (base and heavy metals), at various concentrations (Milbourne *et al.*, 2003). Therefore, it is difficult to assess the degree of toxicity imposed by each metal when using the actual refinery wastewater for biological nitrogenous compounds removal processes. The toxicity effect and efficiency of nitrification and denitrification processes can be relatively easily evaluated

using a model compound containing only one of the main metals found in the actual metal refinery wastewater. Further, by varying the concentration of the metal in the model wastewater, the degree of toxicity for each process (nitrification and denitrification) can be ascertained. Metal toxicity studies were therefore carried out by targeting the metals contained in the wastewater (refer Chapter 6: Metal toxicity studies of trickling filter humus sludge using respirometry).

In this research, biological removal of nitrogen compounds (ammonium, nitrite and nitrate) from PMR wastewater was investigated using simulated PMR wastewater containing pentaamine chlororhodium (III) dichloride (Claus salt) as the rhodium (Rh) source. This chapter presents the results of ammonium and nitrate removal from the simulated PMR wastewater containing 30 mg/l ammonium-bound rhodium, as found in the real refinery wastewater. As mentioned in earlier chapters, metal refinery wastewater contains ammonium-bound chlorometal complexes due to the use of ammonium sulphate and hydrochloric acids based reagents during refinery process. The study was carried out using an aerated CSTR and a PBR filled with GAC for creating nitrifying and denitrifying environments, respectively.

5.2 Materials and methods

This experiment used a serially connected CSTR and PBR. Nitrification was carried out in a CSTR of 7 litres working volume, and denitrification was carried out in a PBR of 8 litres (4.4 litres working volume) packed with GAC (see Figure 5.1).

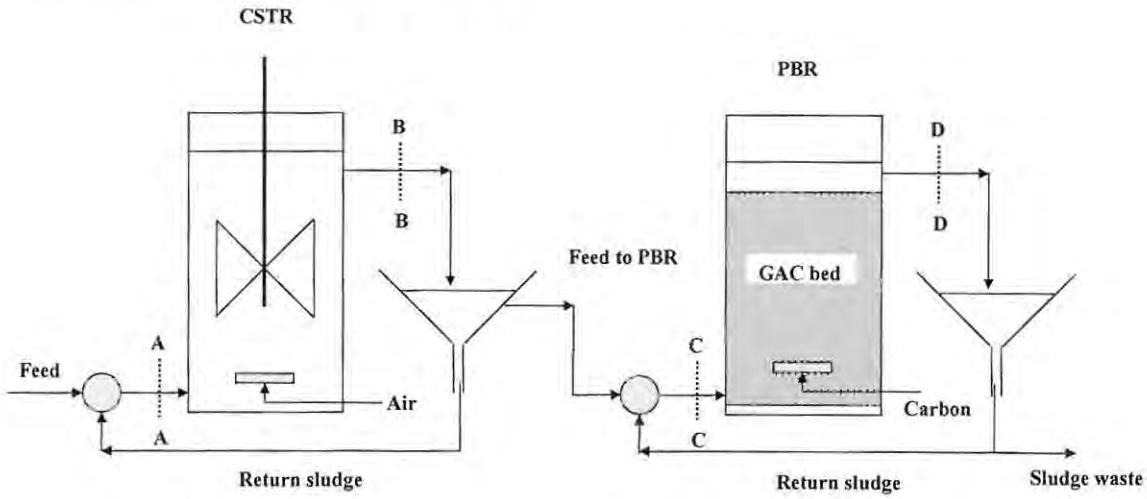

Figure 5.1: Sketch of CSTR, PBR reactor set up and sampling points (A-A, B-B, C-C and D-D).

Humus sludge from nitrifying trickling filters at Grahamstown Municipal Wastewater Treatment Works was used to inoculate the CSTR (4 l sludge) and PBR (2 l sludge). Each reactor was then fed with influent comprising PMR wastewater and deionised waster, as shown in Table 5.1. Sodium lactate (60 % w/v, analytical grade, Merck Chemicals (Pty) Ltd, Johannesburg) was added to the PBR

as the carbon source for heterotrophic denitrification. The amount added to the reactor was 3 % of the working volume (based on the results in Chapter 3). The system was run for two weeks without influent, but separately recirculating the output within the reactors.

Table 5.1: Initial feed compositions used as influent in the CSTR and PBR.

Component	CSTR	PBR
PMR wastewater (l)	2.0	0.9
Deionised water (l)	1.0	1.5

Then, both reactors were half emptied and the synthetic wastewater was fed to the CSTR for 24 hours, after which the CSTR effluent was fed to the PBR. The hydraulic retention time (HRT) for both reactors was kept at 72 hours (based on the results in Chapter 3). Each reactor was maintained with a 1:1 feed: effluent recycling ratio. Air was supplied to the CSTR at a rate of 200 ml/min by a compressor. The feed for the continuous process was prepared using 85.714 mg of Claus Salt (pentaamine chlororhodium (III) dichloride - $[RhCl(NH_3)_5]Cl_2$) dissolved in one litre of deionised water to obtain 30 mg/l of rhodium (Rh). Nutrient solution containing 4 g/l $NaHCO_3$, 13.5 g/l Na_2HPO_4, 0.7 g/l KH_2PO_4, 0.1 g/l $MgSO_4.7H_2O$, 0.0014 g/l $FeCl_3.6H_2O$, and 0.011 g/l $CaCl_2.2H_2O$ was fed to each reactor with a ratio of feed solution rate to nutrient solution rate of 10:1 (Koren *et al.*, 2000). All the nutrients were prepared using analytical grade chemicals (UniLAB, Merck). The experiment was carried out at room temperature and pressure (22 ± 2 °C; 1 atm). Samples were taken for analysis at the points (A-A, B-B, C-C and D-D) as indicated in Figure 5.1 three times per week.

Ammonium (NH_4^+-N), nitrite (NO_2^--N), nitrate (NO_3^--N) and chemical oxygen demand (COD) concentrations were measured using colorimetric reagent kits (Merck) based on the principles of *Standard Methods* (APHA *et al.*, 1998). Spectroquant® reagent test numbers 14752 (NH_4^+-N), 14776 (NO_2^--N), 14773 (NO_3^--N) and 14538/9 (COD) were used, which are analogous to *Standard Methods* numbers 4500-NH_3-F, 4500-NO_2-B, 4500-NO_3-E and 5220-D, respectively. The concentration of mixed liquor suspended solids (MLSS) in the CSTR was measured according to *Standard Methods* (2540-D) and pH measured using an electrode (CyberScan 2500, Eutech Instruments, Singapore). Sludge collected in the clarifier downstream of the CSTR was recycled to the CSTR prevent biomass washout. Ammonium removal, NO_3^--N formation and nitrate removal efficiencies were calculated as shown in Equations (5.1), (5.2) and (5.3), respectively. After running two reactors for 37 days, the sequence of operation was swapped. That is, the initial CSTR – PBR sequence was changed to PBR – CSTR by feeding the influent (simulated wastewater) to the PBR instead of the CSTR. This enabled pH control and improved biomass retention in the CSTR.

$$\text{Ammonium removal efficiency (\%)} = \frac{[\text{Influent } NH_4^+] - [\text{Effluent } NH_4^+] \times 100}{[\text{Influent } NH_4^+]} \quad (5.1)$$

$$\text{Nitrate formation efficiency (\%)} = \frac{[\text{Effluent } NO_3^-] - [\text{Influent } NO_3^-] \times 100}{[\text{Influent } NO_3^-]} \quad (5.2)$$

$$\text{Nitrate removal efficiency (\%)} = \frac{[\text{Influent } NO_3^-] - [\text{Effluent } NO_3^-] \times 100}{[\text{Influent } NO_3^-]} \quad (5.3)$$

5.3 Results

The primary data and observations are shown in Appendix C. The results are discussed below considering the ammonium removal and nitrate formation / removal, pH and MLSS variations in the CSTR and the PBR during 89 days of operational period. The operational period of 89 days were divided into three separate periods. From day 0 to 37, the influent was fed to the CSTR and the effluent from the CSTR was fed to the PBR with 1:1 recycling ratio as described under the Materials and Methods section. From day 37 to day 65, operation sequence was swapped. i.e. the influent (the feed) was sent to the PBR first, and then the effluent from the PBR was fed to the CSTR with 1:1 recycling ratio. During the final operational period, the SRT was set to 8 days in the both reactors.

5.3.1 Continuous stirred tank reactor (CSTR) operation

Ammonium removal in the CSTR during the first 37 days was very unstable due to the acclimatisation stage for higher metal concentration by the NH_4^+ oxidisers. This is evident with just > 5 % of overall NH_4^+-N removal efficiency during the first 37 days of the CSTR operation as shown in Figure 5.2.

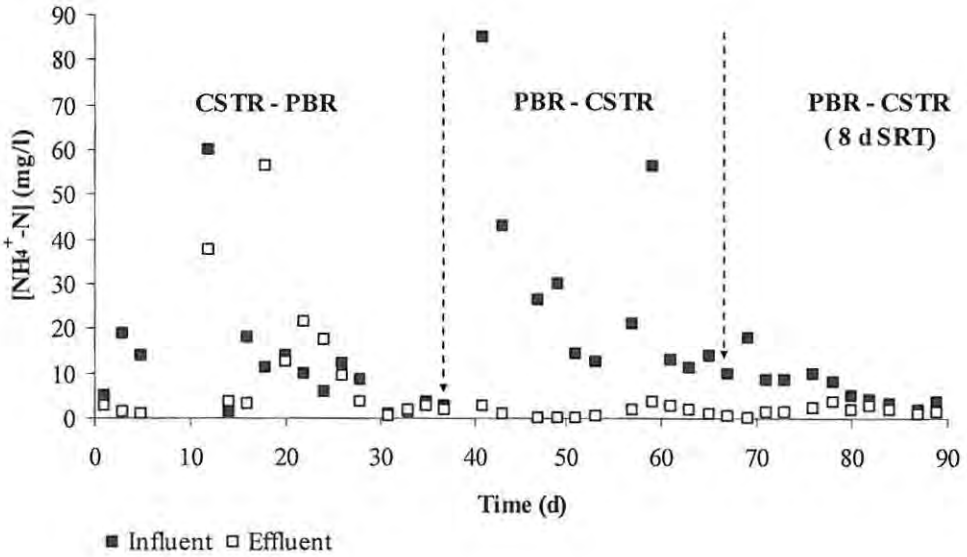

Figure 5.2: Ammonium removal in the CSTR during the period of day 0 to 89.

The average NH_4^+-N concentrations of the influent and effluent of the CSTR were 11.7 mg/l and 11.08 mg/l respectively. Highly variable NH_4^+-N influent concentration (1 mg/l to 60 mg/l) was due to the 1:1 recycling ratio of the feed and effluent from the CSTR clarifier. However, influent NH_4^+-N concentration was gradually reduced to the lowest amount of 1 mg/l on 28th day. This trend was observed until the 37th day of the CSTR operation.

The MLSS in the CSTR was varied between 450 mg/l to 2530 mg/l (the highest on the 22nd day). Then, gradually MLSS was also reduced to 1469 mg/l on the 37th day. The MLSS decreased by 39 % from 2400 mg/l (day 24) to 1469 mg/l (day 37) in 13 days (see Figure 5.3). The pH was changed from 4.15 to 9.71 during the first 37 days while the corresponding values for day 37 to day 89 were 7.38 and 8.69, respectively.

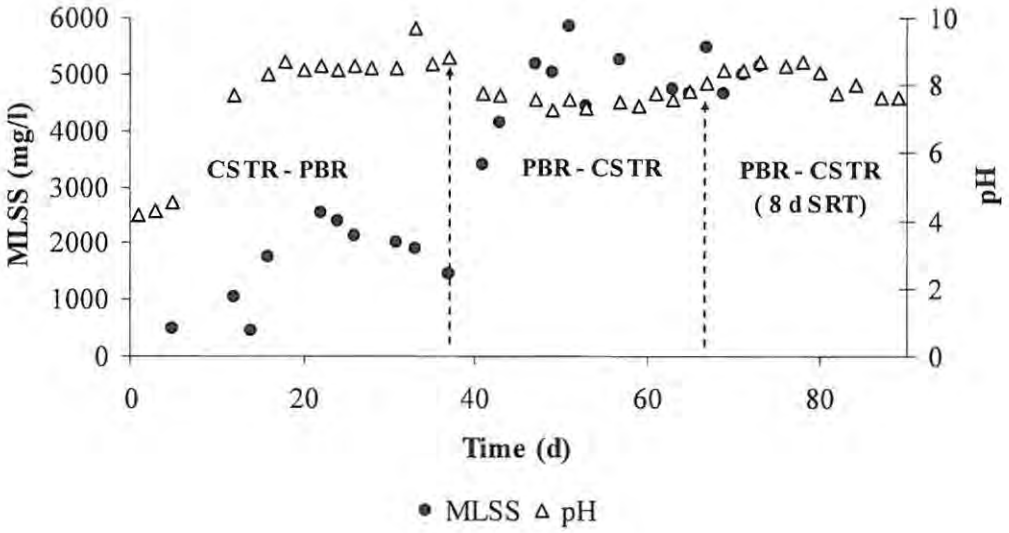

Figure 5.3: pH and MLSS variation in the CSTR.

Meanwhile, the biofilm in the PBR was observed to grow well and > 99 % of anoxic NH_4^+-N removal occurred during the 37 days of operation of the PBR. This is probably due to the higher tolerance of autotrophic or heterotrophic anoxic NH_4^+ oxidisers to metal toxicity in the PBR. These observations indicated that biomass responsible for aerobic NH_4^+ oxidation in the CSTR was diminishing due to metal toxicity whilst biomass responsible for heterotrophic or autotrophic anaerobic NH_4^+ oxidation in the PBR tolerated the metal content, as > 99 % NH_4^+-N removal efficiency was occurring. The reactor operation sequence was therefore changed to increase the biomass in the CSTR. i.e. the effluent from the PBR was fed to the CSTR to increase the active biomass (NH_4^+ oxidisers) in the CSTR. The feed was directed to the PBR. Increased NH_4^+-N removal (Figure 5.2, after day 40) was then observed in the CSTR and the MLSS increased from 1469 mg/l (37th day) to 4670 mg/l (65th day). The rapid biomass increase in the CSTR was indicated by the MLSS increasing from 1469 mg/l to 5862 mg/l in only 12 days, a three-fold increase of MLSS in the CSTR compared to the initial value of 1469 mg/l

on day 37. Average NH_4^+-N removal efficiency during this period (from days 37 to 65) was > 94 % with influent and effluent NH_4^+-N concentrations of 27.43 mg/l and 1.48 mg/l, respectively. The pH of the CSTR varied between 7.25 and 8.83. However, the optimum pH condition for NH_4^+ oxidizers is about 7.5 (Egli *et al.*, 2003).

After changing the SRT to 8 days, there was a gradual decrease (from > 94 % to > 80 %) of NH_4^+-N removal efficiency (Figure 5.2, after day 65). The influent NH_4^+-N concentration also varied between 14 mg/l on the 65th day and 1.7 mg/l on the 87th day. The average influent and effluent NH_4^+-N concentrations during this period (days 65 to 89) were 7.85 mg/l and 1.52 mg/l, respectively. Growth of NH_4^+ oxidizers could have been retarded during this time, as enough nitrogen for cellular synthesis may not have been available in the reactor.

Nitrate formation in the CSTR was observed since the beginning of the reactor operation (Figure 5.4) irrespective of poor NH_4^+-N removal. The maximum, a $\pm$7 fold increase (from 13 mg/l to 94 mg/l) of nitrate formation was observed on day 5. The average NO_3^--N formation was > 220 % during this period with average influent and effluent NO_3^--N concentrations of 10.31 mg/l and 33.18 mg/l, respectively.

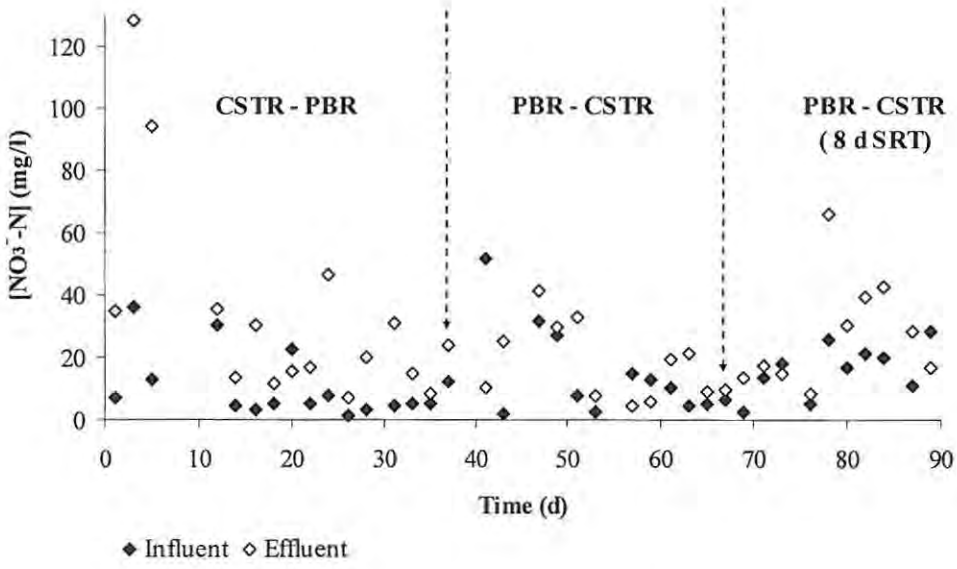

Figure 5.4: Nitrate (NO_3^--N) formation in the CSTR during the period of day 0 to 89.

Once the reactor operation sequence was swapped (from day 37) as described earlier, the NO_3^--N formation in the CSTR was reduced from > 220 % to > 26 %. During this period (day 37 to day 65), the average influent and effluent NO_3^--N concentrations in the CSTR were 15.43 mg/l and 18.76 mg/l, respectively and NH_4^+-N removal was improved (Figure 5.2, after day 40) despite the poor NO_3^--N formation.

When the SRT was set to 8 days in the CSTR, NO_3^--N formation was again improved at the expense of NH_4^+-N removal efficiency (decreased from > 94 % to > 80 %). However, NO_3^--N formation was increased from > 26 % to > 69 % with average influent and effluent NO_3^--N concentrations of 14.43 mg/l and 24.51 mg/l, respectively, during the period between days 65 and 89 (Figure 5.4).

5.3.2 Packed bed reactor (PBR) Operation

Figure 5.5 shows the NH_4^+-N removal in the PBR. During the first 12 days, there was no significant NH_4^+-N removal in the PBR. This could have been due to the time taken by the microbes for acclimatisation to high metal concentration (30 mg/l). However, after 12 days of operation, a high amount of NH_4^+-N removal was observed, with > 99 % removal efficiency. Average influent and effluent NH_4^+-N concentrations of the PBR were 107.63 mg/l and 0.55 mg/l respectively (for further details see Appendix C, Table C.2).

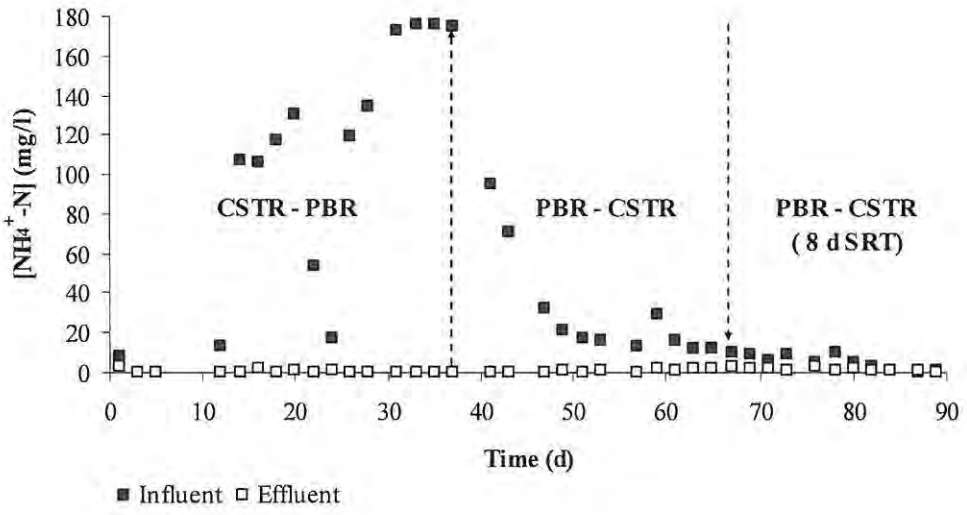

Figure 5.5: Ammonium removal in the PBR during the period of day 0 to 89.

Over 95 % of NH_4^+-N removal was attained in the PBR, even after changing the reactor operation sequence (from day 37 to 65). The average influent and effluent NH_4^+-N concentrations were 24.91 mg/l and 1.04 mg/l, respectively during this period. However, a dramatic reduction of NH_4^+-N removal efficiency was observed from day 47 to 65. This could have been due to a lack of enough nitrogen in the PBR for cellular synthesis of NH_4^+ oxidizers as a result of low NH_4^+-N content in the feed. This situation was overcome by introducing NH_4Cl as a nitrogen source and the data showed the dramatic improvement in NH_4^+-N removal (refer Chapter 4, Reactor comparison study - Airlift suspension reactor).

During the period from days 0 to 37, the PBR showed > 73 % of NO_3^--N formation with influent and effluent concentrations of 95.74 mg/l and 166.54 mg/l, respectively (Figure 5.6). Despite the unsuccessful denitrification in the PBR, autotrophic or heterotrophic anaerobic ammonium oxidation (HAAO) performed well during this period with > 99 % NH_4^+-N removal efficiency as mentioned earlier. The feed (Claus salt) consists of Rh, N, H, and Cl^-. Apart from the feed, 10 % of the volumetric feed rate consisted of nutrient (Koran *et al.*, 2000) and by 3 % of sodium lactate, which was used as the carbon source (see Chapter 3: Preliminary studies of precious metal refinery wastewater).

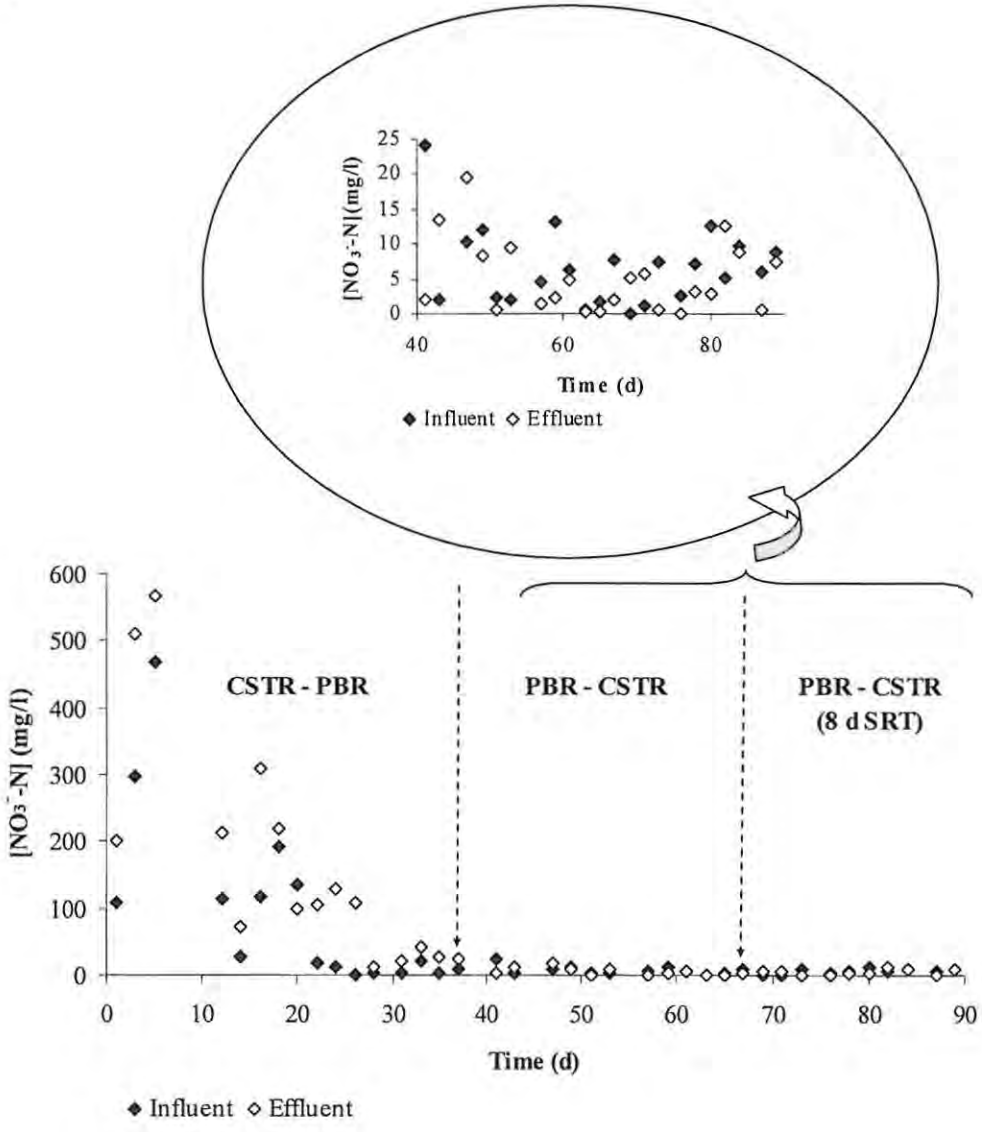

Figure 5.6: Nitrate (NO_3^--N) formation and removal in the PBR during the period of day 0 to 89.

From day 42 onwards, NO_3^--N removal was observed instead of NO_3^--N formation as experienced early (see Figure 5.5). This is what is usually expected in a denitrifying reactor operated under anoxic conditions with a carbon source and nutrients. However, an intermittent NO_3^--N formation was also

seen during this period. The overall NO_3^--N removal efficiency was > 32 % excluding the intermittent NO_3^--N formation observations with average influent and effluent NO_3^--N concentrations of 7.97 mg/l and 5.38 mg/l, respectively. Interestingly, the HAAO activity was sustained with > 95 % NH_4^+-N removal efficiency (Figure 5.5). This shows the acclimatisation of denitrifying bacteria for higher metal content after taking a longer period (89 days). The average pH values in the PBR during day 0 to day 37 and day 37 to day 89 were 6.01 and 5.35 (Figure 5.7). This is explained by the NH_4^+ oxidation in which H^+ is produced and hence, the pH is decreased.

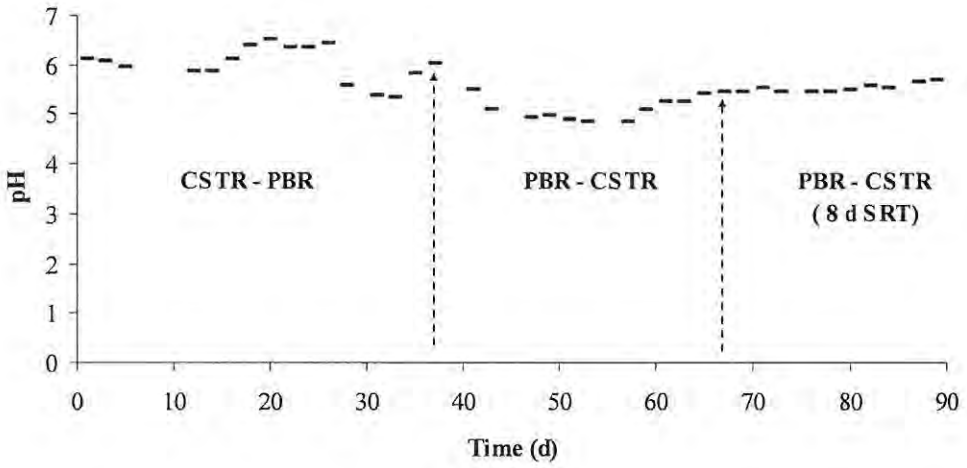

Figure 5.7: pH variation in the PBR.

5.4 Discussion

The model compound Claus salt ($[RhCl(NH_3)_5]Cl_2$) contains about 29 % of NH_3-N, ie. 100 mg of Claus salt has 24.857 mg of NH_3-N, based on stoichiometry. Therefore, no other NH_4^+ compound was introduced and hence low NH_4^+-N content was available in the feed. The high influent NH_4^+-N concentrations (e.g. 60 mg/l on day 12) in the CSTR observed from time to time were probably due to ammonification from NO_3^--N by nitrogen fixing consortia such as *Rhizobium* genera, *Azotobacter* or *Pseudomonas* (Painter, 1970).

Initially, NH_4^+-N removal in the CSTR varied significantly and hence it was not possible to determine any overall trend in the process (for primary data see Appendix C, Table C.1). Instead of NH_4^+-N removal in the process, intermittent NH_4^+-N formation was observed in the CSTR during the latter part of the 37 days. The poor NH_4^+-N removal may be due to the slow growth rate of NH_4^+ oxidisers (Sliekers *et al.*, 2003) and possible high metal toxicity (30 mg/l) impact on them. A low MLSS (< 2400 mg/l) concentration prevailed in the CSTR, which is an indication of low biomass in the reactor and hence low NH_4^+-N removal (> 5 %) was seen in the CSTR. Therefore, it could have taken a longer period than anticipated to achieve process stability (i.e. consistent NH_4^+-N removal and nitrate formation with growing biomass under metal stress).

Although there was not significant NH_4^+-N removal (> 5 %) observed in the CSTR, an effective nitrate formation (> 220 %) was observed since the beginning (Figure 5.4, day 0 to 37). This could be assumed to be due to the survival of NO_2^- oxidisers under the harsh environment (30 mg/l of metal) compared to the aerobic NH_4^+ oxidisers and quick acclimatisation to the high metal content. After changing the reactor operation sequence, the reduced NO_3^--N formation observed could have been due to higher growth of an aerobic NH_4^+ oxidising population which outcompeted the NO_2^- oxidisers for nutrient and oxygen. It has been shown that nitrite oxidising bacteria typically reside internally and adjacent to NH_4^+ oxidising bacteria aggregates, where lower oxygen conditions are detected (Kowalchuck and Stephen, 2001) and hence the NH_4^+ oxidisers have the advantage of access to more oxygen and nutrients over the NO_2^- oxidisers. Once the SRT was changed to 8 days, the growth of NO_2^- oxidisers was improved, indicated by higher nitrate formation (69 % increase, Figure 5.4) while removing the NH_4^+ oxidisers due to their slower growth rates. Therefore, a suitably manipulated SRT could be used to control the aerobic NH_4^+ oxidisers and NO_2^- oxidisers in the CSTR. This is important when partial nitrification is desired in processes like Anammox, CANON, OLAND and SHARON. Usually pH controlled aeration is the established mechanism for partial nitrification to outcompete the NO_2^- oxidisers (Verstraete and Philips, 1998).

The pH of the PBR varied between 4.84 and 6.52 during the operational period. Perhaps this could be due to the production of low molecular fatty acids (LFA) during the anaerobic carbon digestion (Barber and Stuckey, 2000) and anaerobic NH_4^+ oxidation. Ammonium oxidation is an H^+ production process. If nitrate was reduced to dinitrogen gas, then the pH in the PBR could have been increased due to bicarbonate production during denitrification. However, the opposite was observed in the reactor and therefore as described earlier, NH_4^+-N removal and pH decreases were observed.

Ammonium may have been oxidised in the PBR anaerobically either by heterotrophic or by autotrophic anaerobic NH_4^+ oxidizers, but community analysis would be required to identify the responsible microbes in the reactor precisely. Temporarily, sodium acetate was used as the carbon source instead of sodium lactate during the period of day 59 to day 76. This led to reduced NH_4^+-N removal with average influent and effluent concentrations of 12.29 mg/l and 1.85 mg/l respectively (> 84 % removal efficiency compared to overall 95 % during the period of day 37 to day 89). This illustrates the carbon source dependency of the NH_4^+ oxidisers present in the PBR. Therefore, NH_4^+ oxidation could have been carried out by heterotrophic anaerobic ammonium oxidisers (HAAO), as the carbon source led to decrease NH_4^+-N removal in the PBR. Even though the PBR was operated under anoxic condition with sodium lactate as the carbon source, no denitrification activity was observed initially (days 0 to 37). This could have been due to the sensitivity of denitrifying bacteria to the high metal concentration (30 mg/l), whereas the HAAO bacteria tolerated the high metal concentration showing > 95 % NH_4^+-N removal in the PBR during days 37 to 89.

Usually NO_3^--N is removed by heterotrophic denitrifying bacteria which need the carbon source for energy production. These heterotrophic facultative microbes use NO_3^--N as the terminal electron acceptor in the absence of oxygen. Therefore, it could be hypothesised that the HAAO bacteria have a niche to compete with denitrifying bacteria for carbon and nutrients in the presence of Rh toxicity, hence NO_3^--N removal was retarded, even though the NO_3^--N was available in abundance in the PBR (average of >166 mg/l of NO^-_3-N). The other possible reason for poor NO_3^--N removal was the effect of dissolved oxygen in the influent, because those facultative denitrifying bacteria promptly use oxygen as the terminal electron acceptor in their energy production process when the oxygen is available.

Based on this study it was shown that the identifying the fundamental steps under extreme pH conditions, high metal concentrations and high NO_3^--N concentrations are important in developing a continuous nitrogen removal process for metal refinery wastewater. Preliminary batch experiments showed that NH_4^+-N could be removed to 0.05 mg/l in 72 hours at pH 4 in a nitrification NH_4^+ oxidation step and subsequent denitrification achieved effluent NO_3^--N concentrations of as little as 3.6 mg/l (see Chapter 3: Preliminary studies of precious metal refinery wastewater). Ammonium oxidising bacteria (AOB) produce large quantities of extracellular polysaccharides (EPS) when growing in surface biofilm communities. High EPS bacteria have a greater tolerance to low pH (Hesselsoe and Sorensen, 1999). This was verified using a continuous system consisting of a CSTR and PBR. However, this biological process could be inhibited if this process configuration was applied to real PMR wastewater without pre-treatment, such as neutralisation and dilution, due to extreme pH conditions, high concentrations of nitrogen compounds (e.g. 1721 mg/l NO_3^--N was measured in one stream of wastewater, (see Chapter 3: Preliminary studies of precious metal refinery wastewater), high COD (≈16000 mg/l) and high metal concentration (≈30 mg/l total heavy metals concentration). High COD also inhibits nitrification by allowing heterotrophic organisms to outcompete the nitrifying bacteria, and hence excessive aeration is needed for effective nitrification. However, nitrification and denitrification processes could be used as a feasible approach as presented in this section (overall > 80 % of NH_4^+-N removal and < 32 % nitrate removal) with necessary modifications for metal refinery wastewaters considering nitrogen removal efficiency, operational cost, process control and optimisation. Further, tracking of nitrifying and denitrifying populations and their activities are important in bioreactor ecology. However, the organisms which are more suitable for a particular reactor design or performance are yet to be identified (Kowalchuck and Stephen, 2001). It is worthwhile to find out whether the HAAO which existed in the PBR had higher tolerance to metal toxicity compared to the autotrophic aerobic or anaerobic NH_4^+ oxidisers. If HAAO did exist, the PBR could be a better reactor type than the CSTR in terms of NH_4^+ oxidation, NO_3^--N removal (after optimising), construction and operational parameters (easy construction, low maintenance, single reactor system, low energy cost in terms of aeration and mixing, etc).

5.5 Interim conclusions

Both CSTR and PBR reactors effectively removed the NH_4^+-N from the simulated metal refinery feed with > 95 % removal efficiency. However, precious metal toxicity data for complex mixtures are not available in published literature and hence the mechanism of the enzymatic inhibition of NH_4^+-N and NO_3^--N removal occurring in the process could not be ascertained as was the case for the single-stage reactors described in the previous chapter. Though the standard procedure of nitrogen removal is based on first nitrification and then denitrification, the opposite was more effective as far as biomass retention and effective NH_4^+-N removal were concerned in the CSTR. However, these results along with a simulation study and metal toxicity data can be used to optimise the overall nitrogen removal in the PMR wastewater. It is too early to draw firm conclusions based on these results alone for deciding the best reactor type, as reactors were not run for their optimum conditions by varying related parameters such as HRT, SRT, metal concentrations, recycling ratio, dissolved oxygen in the case of the CSTR etc considering each reactor type. However, these studies showed the long acclimatisation period (approximately over 65 days) taken by denitrifying bacteria for high metal concentration (30 mg/l) and shorter acclimatisation period by heterotrophic anoxic NH_4^+ oxidising bacteria with merely 12 days for > 99 % NH_4^+-N removal. Denitrification was not effective (just > 32 % nitrate removal in the PBR after 65 days of acclimatisation), probably due to high metal toxicity for the denitrifying bacteria whereas NH_4^+-N removal in both CSTR and PBR performed well. This could be due to the tolerance capacity for metal toxicity by nitrifying consortia under both aerobic (CSTR) and anoxic (PBR) conditions, reiterating the conclusion drawn in Chapter 4, that it is necessary to determine the toxicity thresholds of the PGMs to activated sludge. This procedure is described in Chapter 6.

Further, in order to ascertain the best operational conditions (in terms of HRT – to increase the daily treatment capacity, SRT – to keep the optimum biomass content, and maximum NH_4^+-N and NO_3^--N removal rates) for each reactor type, a simulation study using a mathematical model was required. Based on the simulation study the best process condition will be tested for further improvement of the process. The model development and simulation results are presented in Chapters 7 and 8.

CHAPTER 6

To make ideas effective, we must be able to fire them off. We must put them into action.

- Virginia Woolf (1882-1941).

6.0 Determination of inhibition coefficients (K_i) for selected platinum group metals (PGMs) using activated sludge respiration (ASR)

6.1 Introduction

Metal-microorganism interaction is a twofold relationship. Trace amounts of essential metals enhance the growth of microorganisms while high concentrations can completely inhibit or retard their growth. The cations K^+ and Mg^{2+} are bulk intracellular species, while Na^+, Ca^{2+}, a number of transition metals and Zn^{2+} are all essential metals which are involved in the stabilisation of a range of biological structures, from cell walls to protein conformations (Hughes and Poole, 1989; Principi *et al.*, 2006). These relationships are important in biological processes involved in nitrogen or metal removal and metal extraction processes as one or few metals could enhance, inhibit or retard the growth of microbial communities responsible for biological nitrogen or metal removal and metal extraction processes. As found in both Chapter 4 and Chapter 5, it became clear that identification of the toxicities of the PGMs to AS was necessary, even when using a single model ammonium compound.

Ammonium (NH_4^+) forms many metal complexes with precious metals such as cis-diamminedichloroplatinate(II) ($PtCl_4(NH_3)_2$), pentaammine chlororhodium (III) dichloride ($[RhCl(NH_3)_5]Cl_2$), hexaammine ruthenium chloride ($[Ru(NH_3)_6]Cl_3$), ammonium hexachlororuthenate (IV) ($(NH_4)_2[RuCl_6]$), ammonium hexachloro iridate (IV) ($(NH_4)_2[IrCl_6]$) and ammonium hexachloroosmiate(IV) ($(NH_4)_2[OsCl_6]$) etc. Solubility of these metals is influenced by pH (Eckenfelder, 2000). Nitrogen-fixing organisms could be used to prepare metal dinitrogen complexes that allow the reduction of dinitrogen gas (N_2) under mild conditions (Hughes and Poole, 1989). Even though this is a useful way to synthesise simple metal ligands that bind metal ions selectively and strongly in inorganic chemistry, the opposite is the expected result in the nitrogen compound removal processes for metal refinery wastewaters. Nitrate (NO_3^-) also forms strong metal ligands, making recovery or removal of metals from metal refinery wastewaters difficult (Kasia *et al.*, 2005). Hence, removal of NH_4^+-N and NO_3^--N are important in metal refinery wastewater not only for nitrogen removal from wastewater for meeting the prevailing discharge standards but also for the recovery of the valuable metals contained in the wastewater.

Inhibitory effects of metal complexes on cell division but not growth has been studied in the group of *VIIIB* elements such as Pt, Rh and Ru (Hughes and Poole, 1989). However, those inhibitory effects on activated sludge processes in wastewater treatment have not been well documented. Biological nitrogen removal from municipal wastewater is a well-established practice with different processes and different process configurations such as Simultaneous Nitrification and Denitrification (SND), ANaerobic AMMonium OXidation (Anammox) (Mulder *et al.*, 1995), Completely Autotrophic Nitrogen removal Over Nitrite - CANON (Sliekers *et al.*, 2002), Single reactor High Activity

Ammonia Removal Over Nitrite - SHARON (Hellinga *et al.*, 1998), and Oxygen Limited Autotrophic Nitrification and Denitrification - OLAND (Verstraete and Philips, 1998) etc. Even though metal toxicity on nitrification and denitrification processes have been studied using commonly found heavy and base metals such as Cr, Cd, Pb, Cu and Zn etc (Beyenal *et al.*, 1997; Lewandowski., 1985; Madoni *et al.*, 1996; Pernetti *et al.*, 2003), there is a paucity of literature concerned with precious metal toxicity in these processes. The precious metal refinery wastewater contains the platinum group metals (PGMs) with numerous other metals such as heavy and base metals. Metal toxicity in micro-organisms occurs by displacing the native metals from their normal binding sites or by binding to proteins and nucleic acids and altering their conformation (Hughes and Poole, 1989). This could lead to shifts in the normal metabolic pathways to alternatives or inhibit the desired processes completely. Therefore, the influence of toxic compounds arising from metals on nitrification and denitrification needs to be evaluated in developing tailor made bioprocesses for nitrogen removal from the PMR wastewater. Short- and long-term effects of those metal compounds on the novel processes are yet to be studied. During long-term processes, some adaptation mechanisms of the bacteria involved may be expected (Lewandowski, 1985). The effect of metal toxicity on poor nitrate removal (< 15 %) in a packed-bed denitrification reactor (Kasia *et al.*, 2005) and relatively poor (< 75 %) NH_4^+-N removal in an airlift suspended reactor (Chapter 4: Reactor Comparison Study) have been reasoned as precious metal toxicity. This may be due to the toxicity of the metals (a concentration of 30 mg/l) used in the experimental studies. Lewandowski (1985) studied the short-term influence of Cr^+ on denitrification process by measuring the inhibition coefficient (K_i) in activated sludge under anoxic conditions. Further, he proposed the inhibition by Cr^{+6} to be considered as a non-competitive kind. Although the existence of metal toxicity and microbes over five decades, the mixed toxicity of metal mixtures are not widely available in scientific literature, perhaps due to the complexity and variability of various effects by different metals (Younger and Wolkersdorfer, 2004).

Oxygen uptake rate (OUR) measurement is a commonly used tool to detect toxic shocks, shock loads and monitoring the nitrification in biological wastewater systems (Kong *et al.*, 1996; Lewandowski *et al.*, 1985; Pernetti *et al.*, 2003; Surmacz-Gorska *et al.*, 1996; Vanrolleghem and Lee, 2003). Even though OUR measurements in a mixed culture environment do not distinguish the oxygen uptake (OU) by nitrifying bacteria alone, OUR measurements can be used to determine the degree of toxicity of metals on activated sludge processes (ASP) and for determination of inhibition coefficient (K_i) (Lewandowski *et al.*, 1985). Simultaneous measurements of NH_4^+-N utilisation rate (AUR) and NO_3^--N formation rate (NFR) could enhance the results that are obtained during the OU measurements to assess the metal toxicity to nitrification. Similarly, the NO_3^--N utilisation rate (NUR) measured under anoxic conditions, along with different metal concentrations, could be used as a tool to determine the effect of metal toxicity in denitrification.

This chapter presents the results obtained for the precious metal inhibition coefficients (K_i) for selected PGMs in activated sludge respiration (ASR) using a respirometric study, which was based on pressure measurements and subsequent conversion into OU using ideal gas and Henry's laws. The objectives of these experiments were to find the K_i of the selected PGMs in ASR and how different metal concentrations affect selected biochemical parameters involved during the ASR.

6.2 Materials and Methods

This section describes four main components used during the experiment, namely; general principle of the OxiTop which was the basic system used for respirometric analysis, principles used to determine the K_i for selected PGMs, sample preparation and physico-chemical analysis carried out.

6.2.1 The OxiTop® system

The OxiTop® system is based on the pressure change in a fixed volume, in which a sample is degraded within a closed system containing a known gas volume, in part consisting of oxygen (Rudrum, 2005). The OxiTop® consists of a data logger/transmitter fitted with a screw cap containing carbon dioxide absorbent (sodium hydroxide - NaOH), a pressure sensor and sealable reaction vessel. Figures 6.1a and 6.1b show the OxiTop® system and its components. During measurements, the system was kept at constant temperature of 20 °C in an incubator (Model: *TS 606/3-i*, WTW, Germany). Stirring was achieved using magnetic stirrer bars using a stirring pad. This was important for efficient oxygen transfer from gas phase to liquid phase in the reaction vessel when dissolved oxygen (DO) was consumed by the microbes and subsequent release of carbon dioxide (CO_2) into gas phase in which NaOH absorbs the CO_2.

Figure 6.1a: The OxiTop system on the stirring pad

Figure 6.1b: Components of the OxiTop reactor

6.2.2 The principle

Inhibition coefficients for different metal concentrations were evaluated based on the respirometry using OxiTop system (WTW, Germany). The measurement is based on monitoring biomass respiration in a closed volume. Carbon dioxide produced during respiration is trapped using NaOH pellets in the gas phase as described earlier. Subsequently, pressure reduction in the gas phase is solely due to OU by biomass. This is measured using a pressure sensor, which is fixed in the underside of the lid of the bottle. The obtained data are stored in the data acquisition system connected to the pressure sensor. Upon completion of the measurement, the stored data from the data logger are transferred to the controller (using infrared signal), which is then connected to a PC through an RS - 232 port for further data processing. Assuming ideal behaviour of the gas phase, pressure reduction was first converted into specific oxygen uptake (SOU), using the ideal gas law and Henry's law (Rudrum, 2005). Equations used are given below.

$$\frac{d[O_2]_g}{dt} * V_g = -OUR_l * V_l \tag{6.1}$$

$$\frac{d[O_2]_g}{dt} * V_g = \frac{V_g}{RT} * \frac{dP_{O_2}}{dt} \tag{6.2}$$

Eliminating $\frac{d[O_2]_g}{dt}$ term from equations (6.1) and (6.2), the equation (6.3) is obtained;

$$OUR_l = \left(-\frac{V_g}{V_l}\right) * \left(\frac{1}{RT}\right) * \left(\frac{dP_{O_2}}{dt}\right) \tag{6.3}$$

Where:

$[O_2]_g$	-	Oxygen concentration in the gas phase	[g/l]
V_g	-	Gas phase volume	[l]
V_l	-	Liquid phase volume	[l]
P_{O_2}	-	Partial pressure of oxygen	[Pa]
T	-	Gas temperature	[K]
t	-	Time	[s]
R	-	Universal gas constant	[Pa.l/g/K]

A detailed account of derivation equations (6.1) and (6.2) can be found in Rudrum (2005).

Then, SOU was calculated based on the unit mixed liquor volatile suspended solids (MLVSS) and expressed in $mgO_2/mgMLVSS$. The SOU values for individual time point were then plotted, and the

maximum slope of this dependence was found. This slope represents the specific oxygen uptake rate (SOUR, mg O_2/mg VSS/seconds). Reaction rate (v) was obtained by multiplying the SOUR and MLVSS. Inhibition coefficients (K_i) for individual metals were found by plotting $1/v$ *vs.* i (inhibitor concentration – metal) as described in Appendix DI, and the K_i was determined as the concentration where $1/v$ became zero.

$$\text{Specific Oxygen Uptake Rate (SOUR)} = \left(\frac{\text{OUR}}{\text{MLVSS}} \right) \tag{6.4}$$

Where OUR – Oxygen Uptake Rate (O_2-mg/mg MLVSS)

VSS – volatile suspended solids (mg/l)

$$\text{Relative Activity (RA)} = \left(\frac{\text{SOUR}_{\text{M(x)}}}{\text{SOUR}_{\text{C}}} \right) \tag{6.5}$$

Where $\text{SOUR}_{\text{M(x)}}$ = SOUR with metal concentration of x mg/l

SOUR_{C} = SOUR without metals (control)

It is assumed that substrate utilisation rate is proportional to the oxygen uptake rate during the respiration (Lewandowski et al., 1985: see Appendix EI). Then the following equation can be written:

$$v(\text{enzyme reaction rate, mgO}_2\text{/l/h}) = SOUR(mgO_2 / mgMLVSS / h) * VSS(mg / l) \tag{6.6}$$

6.2.3 Sample preparation

Schott bottles of 250 ml were used in the respirometric measurements, with total sample volumes of 100 ml. Each sample consisted of 45 ml inoculum, a spike of the particular metal stock solution (see below), and deionized water used to make up the volume to 100 ml. Samples were run in duplicate. Metal concentrations ranging from 0 to 25 mg/l for Pt, Pd, Rh, and Ru were prepared and analyses were performed as described below. Atomic absorption spectrophotometer standards (EC Lab Services Ltd., Port Elizabeth, South Africa) stock solutions were used to obtain the desired concentrations of each metal. Then, pH was adjusted to 7.5 ± 0.5 using 3M NaOH (UniLab, Merck Ltd., Johannesburg) prior to inoculation. The NH_4^+-N concentration in each sample was kept at 100 mg/l to avoid substrate deficiency during the experimental period of 10 hours using ammonium sulphate (UniLab, Merck) as the substrate. Trickling filter humus sludge obtained from the Grahamstown Municipal Wastewater Treatment Works, South Africa was used as inoculum. It was aerated without nutrient supplements for 24 hours prior to use.

6.2.4 Analysis

The total COD, soluble COD, MLSS, MLVSS and pH were measured before the start of each experiment and at the end of each experiment. The COD concentrations were measured using

colorimetric reagent kits (Merck Chemicals (Pty) Ltd, Johannesburg) based on the principles of *Standard Methods* (APHA *et al.*, 1998). *Spectroquant*® reagent test number 14538/9 (COD) were used which was analogous to *Standard Method* 5220-D. The concentration of MLSS and MLVSS were measured using the *Standard Methods* (2540-D and 2540-E respectively) (APHA *et al.*, 1998). The pH was measured using a pH electrode (CyberScan 2500, Eutech Instruments, Singapore).

6.3 Results

The results presented for the four PGMs studied are SOU variation with time, experimental parameters measured, and toxicity threshold for each metal using the best fitted curve of SOUR vs. metal concentrations. The initial adaptation period data, in which positive pressure developed, were neglected as described in BOD Primer, WTW, Germany.

6.3.1 Platinum (Pt)

Figure 6.2 shows the variations of SOU for different Pt concentrations. After about 2 hours, a slight change in toxicity stress was observed for Pt concentration of 10, 15 and 20 mg/l. The highest toxicity stress was shown by 25 mg/l of Pt. This was the generally expected trend. Compared to the control (0 mg/l), 5 mg/l of Pt showed some stimulant activity. However, after that with the increase of metal concentration there was a consistent decrease of SOU due to the metal toxicity.

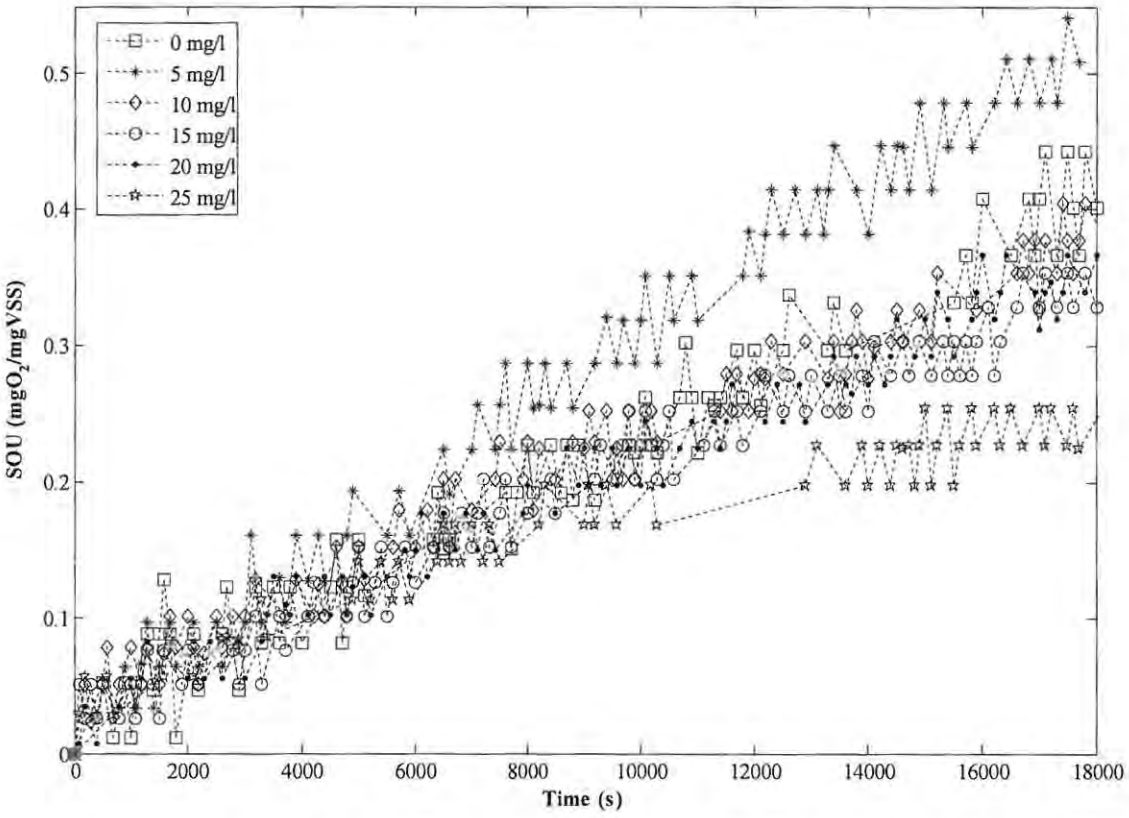

Figure 6.2: Specific oxygen uptakes for different Pt concentrations.

The maximum SOUR (d(SOU)/dt at t = 0) values were calculated by linear regression analysis (Ho, 2006) using MATLAB Version 7.0 (The Mathworks Inc., USA). The results are summarised in Table 6.1. The R^2 values are > 0.9, suggesting that assumption of linear dependency between SOU and [Pt] was reasonable. As mentioned earlier, at 5 mg/l of Pt the sludge showed ≈ 31 % increase in SOUR (Table 6.1).

Table 6.1: Enzyme reaction rate (v) for different Pt concentrations.

[Pt] (mg/l)	SOUR (mgO_2/mgMLVSS/h)	R^2	SOUR / $SOUR_0$	Mean MLVSS (mg/l)	v (mgO_2/l/h)	$1/v$ (l.h/mgO_2)
0	0.0770	0.9550	1.00	238.5	18.37	0.0544
5	0.1010	0.9772	1.31	274.0	27.66	0.0362
10	0.0683	0.9660	0.89	330.0	22.53	0.0444
15	0.0637	0.9664	0.83	325.0	20.69	0.0483
20	0.0663	0.9697	0.86	353.0	23.40	0.0427
25	0.0403	0.9008	0.52	318.5	12.84	0.0779

This could be due to stimulation of microbial activity when Pt was introduced to the system. However, SOUR values for 10, 15 and 20 mg/l Pt were almost the same. Probably at this range, the microbial population was acclimatised to the increased metal concentration by developing a buffer. Then, at 25 mg/l of Pt, an approximately 48 % decrease in maximum SOUR was observed, compared to the control.

Figure 6.3 shows the variation of $1/v$ *vs.* [Pt] and the inhibition coefficient (K_i), obtained by extrapolating to zero on the y-axis (ie. where $1/v$ = zero).

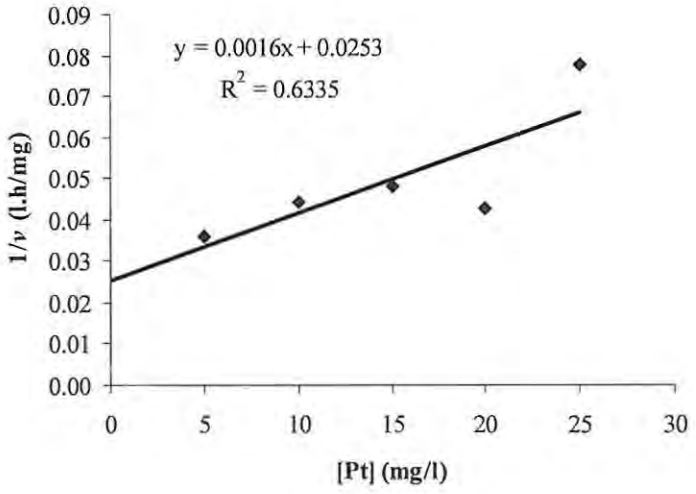

Figure 6.3: Reciprocal of v *vs.* different Pt concentrations.

The results shown in Figure 6.3 and the quality-of-fit data (0.63) suggest the validity of linear dependency of $1/v$ *vs.* [Pt]. The K_i of Pt for microbial activated sludge respiration (ASR) was observed to be obtained at a concentration of 15.81 mg/l of Pt.

Process parameters for Pt are summarised in Table 6.2. A slight growth was observed in the presence of Pt with exception of the Pt concentration for 15 mg/l. Percentages of VSS increase for metal concentrations of 0, 5, 10, 15, 20 and 25 mg/l are 19 %, 12.4 %, 3.1 %, 0 %, 4 % and 18.1 % respectively. Except in the control (in which pH reduction could be attributed to nitrification which produces H^+), there was not a significant pH variation.

Table 6.2: Parameter variation for Pt during the experiments.

State	Parameter	Metal concentration (mg/l)					
		0	**5**	**10**	**15**	**20**	**25**
Initial	COD_{TOTAL} (mg/l)	1305 ± 7	1368 ± 103	1443 ± 39	1428 ± 60	1448 ± 11	1338 ± 18
	$COD_{SOLUBLE}$ (mg/l)	< 25	18 ± 11	< 25	< 25	13 ± 4	23 ± 18
	MLSS (mg/l)	1104 ± 30	1158 ± 12	1204 ± 30	1292 ± 83	1338 ± 41	1288 ± 65
	FS (mg/l)	887 ± 53	900 ± 24	879 ± 65	967 ± 83	992 ± 35	996 ± 53
	MLVSS (mg/l)	217 ± 24	258 ± 12	325 ± 35	325 ± 0	346 ± 77	292 ± 12
	pH	7.96 ± 0.05	7.83 ± 0.18	7.79 ± 0.12	7.87 ± 0.02	7.81 ± 0.13	7.77 ± 0.04
Final	COD_{TOTAL} (mg/l)	1378 ± 46	1228 ± 4	1255 ± 28	1295 ± 57	1343 ± 53	1218 ± 11
	$COD_{SOLUBLE}$ (mg/l)	< 25	25 ± 0	45 ± 7	< 25	88 ± 4	88 ± 46
	MLSS (mg/l)	1140 ± 28	1105 ± 7	1185 ± 7	1220 ± 42	1260 ± 0	1225 ± 64
	FS (mg/l)	880 ± 85	815 ± 35	850 ± 14	895 ± 21	900 ± 0	880 ± 14
	MLVSS (mg/l)	260 ± 57	290 ± 42	335 ± 21	325 ± 21	360 ± 0	345 ± 50
	pH	7.72 ± 0.02	7.80 ± 0.01	7.82 ± 0.02	7.85 ± 0.03	7.86 ± 0.00	7.88 ± 0.09

The total COD consists of biodegradable, non-biodegradable (inert material) materials and biomass in the sample, whereas soluble COD consists of the soluble, biodegradable portion of total COD. Therefore, a lower soluble COD indicates that a higher proportion of the total COD was contributed by active biomass and inert materials. According to Table 6.2, soluble COD in all the samples had a small impact on the total COD, implying that the active biomass and inert materials contributed most of the total COD.

6.3.2 Palladium (Pd)

Figure 6.4 shows the variation of SOU with time for Pd. Compared to the other metals (except for Rh), Pd showed a typical logistic curve (an exponential growth) of microbial population growth for all metal concentrations. Similar to Pt, there was some stimulant activity at 5 mg/l. Concentrations of 10 and 20 mg/l, and 15 and 25 mg/l showed similar SOU pattern after about 60 minutes, once acute acclimatisation was achieved. However, during the first 45 minutes, except the control, all the other

metals concentrations had similar SOU until the population adjusted to each metal concentration. The SOU *vs.* time for Pd followed an exponential dependency for all concentrations. Therefore, the best fit curve (except 0 mg/l) for each concentration (Ho, 2006) was obtained using $y = A\,[1 - e^{-Bx}]$ type dependency using MATLAB 7.0. Table 6.3 presents the summary of curve fitting parameters for Pd. The type of dependency for 0 mg/l was found $y = Ae^{Bx}+Ce^{Dx}$, where A = 0.3367, B = $-3.514*10^{-5}$, C = -0.4161 and D = -0.0005 with R^2 of 0.9366 using the MATLAB Curve Fitting Toolbox.

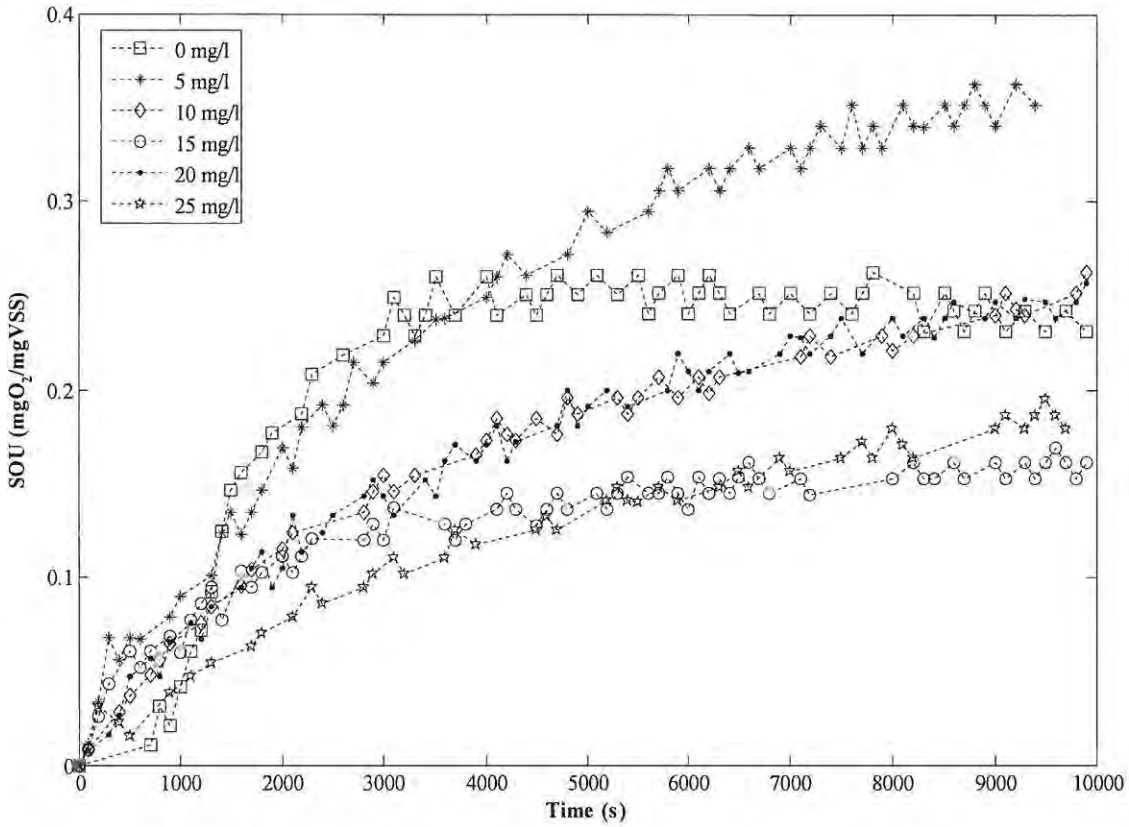

Figure 6.4: Specific oxygen uptake for different Pd concentrations.

The maximum SOUR (d(SOU)/dt at t = 0) for each Pd concentration was found to occur at t = 0, thus SOUR values were tabulated as shown in Table 6.3. The K_i for Pd was obtained by plotting $1/v$ *vs.* [i] and extrapolating to zero on the *y*-axis (ie. where $1/v$ is zero: Figure 6.5). The K_i of Pd was observed to be obtained at a concentration of 25 mg/l. It shows the positive correlation (R^2 = 0.53) in the relationship between $1/v$ *vs.* [Pd].

Table 6.4 summarises the process parameters measured for Pd during the experiments. Biomass decay can be observed for all Pd concentrations, as MLSS decreased. However, an increase in soluble COD was observed in every sample except at 5 mg/l (decrease is about 8 %). Soluble COD increase percentages are 18.6, 6.3, 22.1, 50.0, and 57.0 for metal concentrations of 0, 10, 15, 20 and 25 mg/l, respectively. Total COD decreases were observed in all samples. The percentage decreases in total COD were 28.7, 17.4, 14.2, 11.3, 17.8 and 15.8 % for 0, 5, 10, 15, 20 and 25 mg/l [Pd], respectively.

The pH decrease was observed at low metal concentrations (5, 10 and 15 mg/l). However, at 20 and 25 mg/l of Pd concentrations showed a slight pH increase, possibly due to denitrification.

Table 6.3: Enzyme reaction rate (v) for different Pd concentrations.

[Pd] (mg/l)	A	B	R^2	SOUR ($mgO_2/mgMLVSS/h$)	SOUR / $SOUR_0$	v ($mgO_2/l/h$)	$1/v$ ($l.h/mgO_2$)
0	-	-	0.9366	0.7488	1.00	614.02	0.0016
5	0.3845	0.0003	0.9923	0.4153	0.55	298.99	0.0033
10	0.2604	0.0003	0.9898	0.2812	0.38	236.23	0.0042
15	0.1533	0.0006	0.9623	0.3311	0.44	317.88	0.0031
20	0.2654	0.0003	0.9872	0.2866	0.38	246.50	0.0041
25	0.2070	0.0002	0.9860	0.1490	0.20	156.49	0.0064

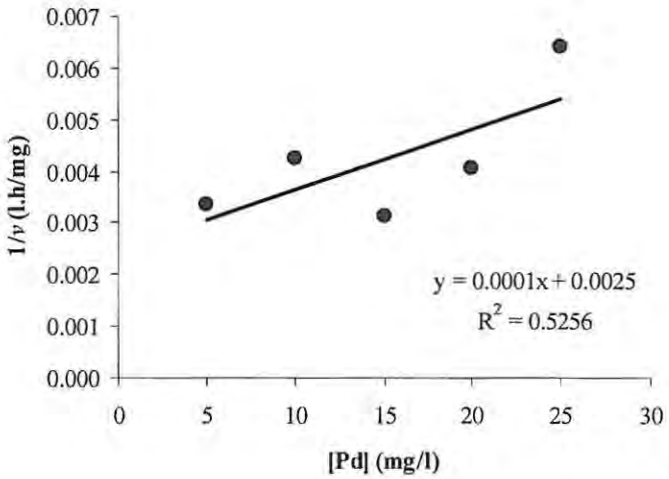

Figure 6.5: Reciprocal of *v vs.* different Pd concentrations.

Table 6.4: Parameter variation for Pd during the experiments.

State	Parameter	Metal concentration (mg/l)					
		0	5	10	15	20	25
Initial	COD_{TOTAL} (mg/l)	4440 ± 530	4058 ± 138	3840 ± 85	4013 ± 117	4253 ± 265	4785 ± 721
	$COD_{SOLUBLE}$ (mg/l)	70 ± 7	63 ± 4	80 ± 14	88 ± 25	80 ± 21	68 ± 39
	MLSS (mg/l)	3520 ± 57	3600 ± 28	3680 ± 85	3890 ± 99	4010 ± 14	3920 ± 57
	FS (mg/l)	2720 ± 85	2880 ± 0	2840 ± 255	2930 ± 127	3150 ± 99	2870 ± 184
	MLVSS (mg/l)	800 ± 28	720 ± 28	840 ± 170	960 ± 28	860 ± 85	1050 ± 127
	pH	7.80 ± 0.00	7.77 ± 0.06	7.74 ± 0.00	7.74 ± 0.02	7.82 ± 0.01	7.78 ± 0.18
Final	COD_{TOTAL} (mg/l)	3165 ± 7	3350 ± 99	3295 ± 92	3560 ± 184	3495 ± 50	4025 ± 629
	$COD_{SOLUBLE}$ (mg/l)	83 ± 11	58 ± 4	85 ± 7	113 ± 11	120 ± 21	125 ± 14
	MLSS (mg/l)	3500 ± 170	3450 ± 99	3550 ± 14	3670 ± 42	3820 ± 28	3910 ± 71
	pH	7.60 ± 0.04	7.51 ± 0.01	7.64 ± 0.04	7.75 ± 0.01	7.83 ± 0.04	7.92 ± 0.03

6.3.3 Rhodium (Rh)

The variations of SOU with time for Rh are shown in Figure 6.6. Similar to the Pd experiment, the SOU for all the concentrations showed an exponential dependence with time. In contrast to Pt and Pd, none of the Rh concentrations showed any stimulant activity. A gradual decrease in SOU with time was observed with the increase of metal concentration, as generally expected. Metal concentrations from 15 mg/l to 25 mg/l showed the highest toxicity effect on the ASR.

The maximum SOUR for each concentration was obtained by fitting a linear curve (Ho, 2006) for each metal concentration as described earlier using MATLAB 7.0. Table 6.5 shows a strong exponential dependency (> 0.97) of various Rh concentrations with time. Compared to the control, a 48 % SOU reduction could be observed at 25 mg/l Rh, which was the lowest SOU for all concentrations considered during the experiment.

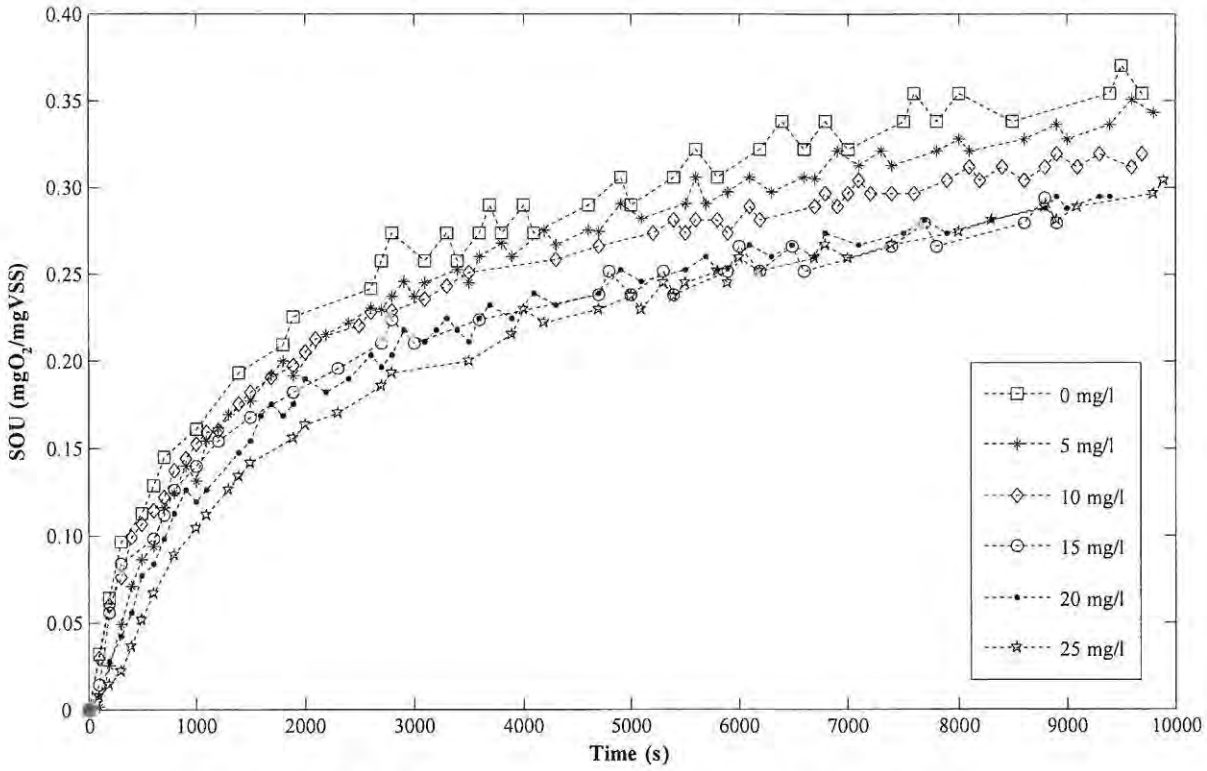

Figure 6.6 Specific oxygen uptake for different Rh concentrations.

By plotting $1/v$ vs. different Rh concentrations and fitting a linear dependency, the K_i was evaluated. Inhibition coefficient of Rh for ASR was found to be 33.34 mg/l as shown in Figure 6.7 where $1/v = 0$. The value of $1/v$ at 15 mg/l of Rh was excluded in evaluation of the K_i due to the improvement of R^2 value from 0.5904 to 0.7372.

Table 6.5: Enzyme reaction rate (v) for different Rh concentrations.

[Rh] (mg/l)	SOUR (mgO_2/mgMLVSS/h)	R^2	SOUR / $SOUR_0$	Mean MLVSS (mg/l)	v (mgO_2/l/h)	$1/v$ (l.h/mgO_2)
0	0.9286	0.9792	1.00	1025	951.80	0.0011
5	0.7174	0.9926	0.77	1080	774.84	0.0013
10	0.8178	0.9828	0.88	1085	887.29	0.0011
15	0.7640	0.9796	0.82	1175	897.69	0.0011
20	0.6207	0.9915	0.67	1170	726.19	0.0014
25	0.4855	0.9892	0.52	1110	538.86	0.0019

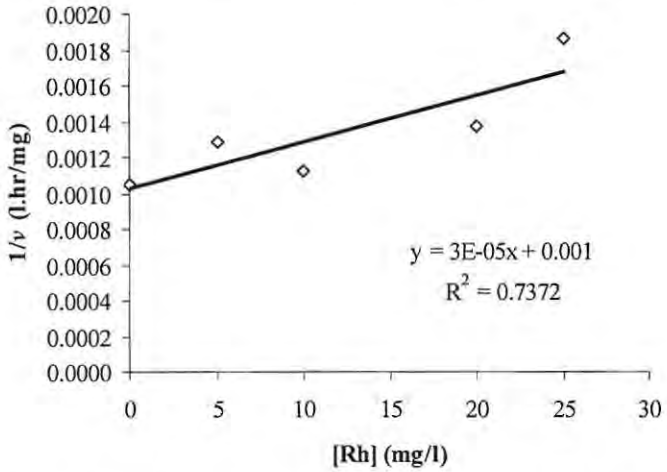

Figure 6.7: Reciprocal of v *vs.* different Rh concentrations.

According to Table 6.6, biomass decay was occurred in all samples except in the control showing a decrease of MLSS in each. Further, pH decrease was observed except at 25 mg/l of Rh. The pH decrease could be attributed to nitrification which produces $H^{\pm}$.

Table 6.6: Parameter variation for Rh during the experiment.

State	Parameter	Metal concentration (mg/l)					
		0	5	10	15	20	25
Initial	COD_{TOTAL} (mg/l)	2690 ± 191	2820 ± 14	2725 ± 85	2803 ± 18	2920 ± 148	2903 ± 32
	$COD_{SOLUBLE}$ (mg/l)	71 ± 65	134 ± 62	< 25	25 ± 0	< 25	25 ± 0
	MLSS (mg/l)	2550 ± 28	2805 ± 49	2645 ± 78	2790 ± 127	2920 ± 127	2835 ± 21
	FS (mg/l)	1525 ± 21	1725 ± 7	1560 ± 28	1615 ± 21	1750 ± 113	1725 ± 21
	MLVSS (mg/l)	1025 ± 49	1080 ± 57	1085 ± 49	1175 ± 106	1170 ± 14	1100 ± 42
	pH	7.53 ± 0.45	7.42 ± 0.52	7.17 ± 0.12	7.17 ± 0.23	7.35 ± 0.05	7.20 ± 0.28
Final	COD_{TOTAL} (mg/l)	2649 ± 815	2018 ± 32	2036 ± 146	2258 ± 49	2136 ± 110	2060 ± 74
	$COD_{SOLUBLE}$ (mg/l)	< 25	< 25	< 25	< 25	< 25	< 25
	MLSS (mg/l)	2260 ± 57	2555 ± 78	2465 ± 35	2520 ± 28	2615 ± 7	2545 ± 64
	FS (mg/l)	1285 ± 64	1440 ± 21	1565 ± 85	1525 ± 7	1410 ± 14	1460 ± 127
	MLVSS (mg/l)	975 ± 7	960 ± 57	990 ± 120	1000 ± 21	1055 ± 7	1085 ± 64
	pH	5.86 ± 0.04	5.76 ± 0.06	5.89 ± 0.06	6.00 ± 0.01	6.16 ± 0 .08	6.27 ± 0.10

In overall, total COD was decreased in all the samples while soluble COD was increased except in the control. Percentage decrease of total COD were 1.5, 28.4, 25.3, 19.4, 26.8, and 29.0 % for 0, 5, 10, 15, 20, and 25 mg/l, respectively. Based on Table 6.6, the total COD of all the samples have been mainly contributed by biomass and inert materials showing low soluble COD (< 5 % contribution). Soluble COD was decreased in all the samples during the experiments showing the utilisation of readily available organic substrates.

6.3.4 Ruthenium (Ru)

Specific oxygen uptake variation with time for Ru is shown in Figure 6.8. Ruthenium showed a gradual toxicity for increased metal concentrations by reducing the maximum SOU with time. During the first 60 minutes, it was not possible to observe a significant different of SOU, as the data points were clustered. However, a linear dependency of SOU with time was seen. Therefore, the best fit curves for each concentration were obtained using a linear dependency using MATLAB 7.0 as described earlier.

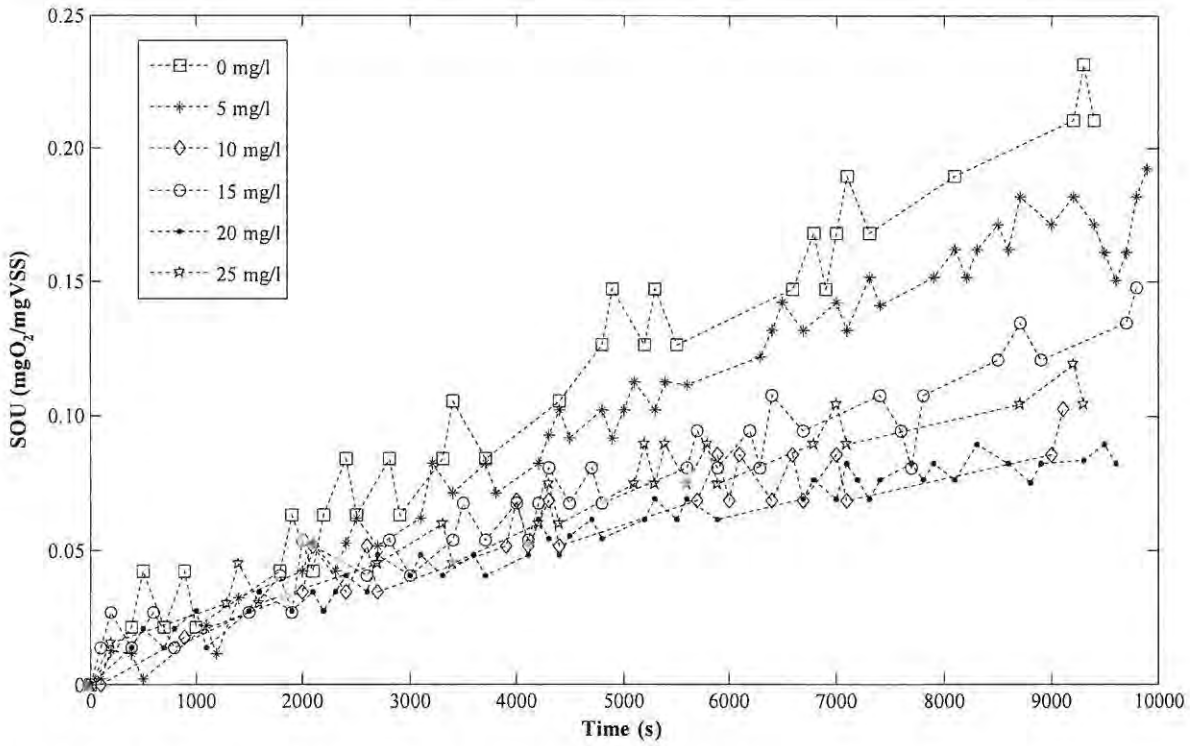

Figure 6.8: Specific oxygen uptake for different Ru concentrations.

Table 6.7 shows the SOUR, R^2 and the ratio of SOUR and $SOUR_0$ obtained for various Ru concentrations. Ruthenium also showed a strong linear dependency ($R^2 > 0.83$) of SOU with time, similar to those observed with Pt, Rh and Ir. The lowest SOU was observed at 20 mg/l of Ru, with a 64 % reduction of SOU with respect to the control.

Table 6.7: Enzyme reaction rate (v) for different Ru concentrations.

[Ru] (mg/l)	SOUR (mgO_2/mgMLVSS/h)	R^2	SOUR / $SOUR_0$	Mean MLVSS (mg/l)	v (mgO_2/l/h)	$1/v$ (l.h/mgO_2)
0	0.0799	0.9638	1.00	795	63.54	0.0157
5	0.0657	0.9708	0.82	930	61.13	0.0164
10	0.0333	0.8343	0.42	960	31.97	0.0313
15	0.0453	0.9349	0.57	1050	47.59	0.0210
20	0.0290	0.9333	0.36	1145	33.22	0.0301
25	0.0398	0.9176	0.50	1195	47.58	0.0210

Figure 6.9 shows the variation of $1/v$ with different Ru concentrations. By plotting the linear dependency as described earlier, it was observed that K_i is attained at a concentration of 39.25 mg/l of Ru. This was verified with > 0.5 of R^2 as shown in Figure 6.9.

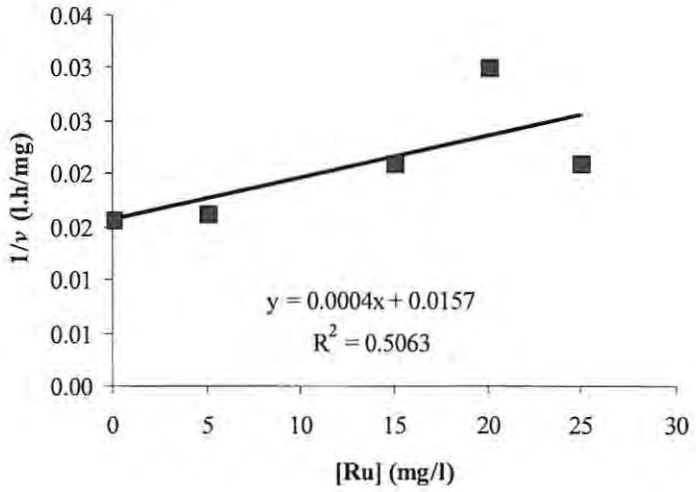

Figure 6.9: Reciprocal of *v vs.* different Ru concentrations.

Table 6.8 summarises parameter variation for different Ru concentrations. A pH decrease was observed for all Ru concentrations, which could be attributed to nitrification, as mentioned earlier. Further, significant pH reductions were observed compared to experiments with other metals (e.g. Pt, Pd, Rh), which may be due to the less toxic effect of Ru on nitrifying consortia or the subsequent pH decrease might have led to changes in metal speciation, thus forming metal species less toxic to microbial respiration. The MLSS was reduced for all the Ru concentrations except for 25 mg/l. Corresponding MLVSS was increased by percentages of 1.3, 26.8, 6.1, 0, 16.0, and 25.5 for 0, 5, 10, 15, 20, and 25 mg/l, respectively. No pattern could be observed in changing of total COD during the experiment. However, at low concentrations of Ru (5, 10, 15), decreases in soluble COD were observed, while at high concentrations (20 and 25 mg/l), increases were observed.

Table 6.8: Parameter variation for Ru during the experiments.

State	Parameter	Metal concentration (mg/l)					
		0	5	10	15	20	25
Initial	COD_{TOTAL} (mg/l)	3525 ± 106	3750 ± 191	3683 ± 11	3743±74	3848 ± 11	4118 ± 456
	$COD_{SOLUBLE}$ (mg/l)	120 ± 57	68 ± 18	< 25	78±74	18 ± 4	25 ± 0
	MLSS (mg/l)	3190 ± 42	3310 ± 99	3480 ± 0	3570±127	3600 ± 113	3590 ± 14
	FS (mg/l)	2400 ± 28	2490 ± 42	2550 ± 42	2520±113	2540 ± 0	2530 ± 72
	MLVSS (mg/l)	790 ± 14	820 ± 57	930 ± 42	1050 ± 240	1060 ± 113	1060 ± 57
	pH	7.58 ± 0.05	7.42 ± 0.00	7.38 ± 0.07	7.35±0.02	7.35 ± 0.00	7.34 ± 0.02
Final	COD_{TOTAL}	4665 ± 997	3728 ± 11	3930±191	4523 ± 1050	3698 ± 180	4110 ± 467
	$COD_{SOLUBLE}$	55 ± 21	60 ± 35	< 25	38 ± 11	38 ± 11	73 ± 4
	MLSS (mg/l)	3170 ± 71	3180 ± 283	3450 ± 42	3420 ± 85	3480 ± 57	3760 ± 170
	FS (mg/l)	2370 ± 99	2140 ± 85	2460 ± 113	2370 ± 14	2250 ± 71	2430 ± 99
	MLVSS (mg/l)	800 ± 170	1040 ± 198	990 ± 71	1050 ± 99	1230 ± 127	1330 ± 71
	pH	6.77 ± 0.06	6.80 ± 0.06	6.84 ± 0.01	6.92 ± 0.01	6.93 ± 0.01	6.93 ± 0.03

6.4 Discussion

Various metal toxicity-modifying mechanisms such as complexation, changes in speciation and competition (Heijerick *et al.*, 2002) can lead to different toxicity levels for different micro-organisms. Generally, the effect of metals on microbes is categorised based on toxicity and availability (Ford *et al.*, 1995). The toxicity categories are type I (non-critical), type II (potentially toxic and relatively available) and type III (potentially toxic and relatively unavailable due to their rarity or insolubility). Based on these categories, Pt and Pd have been categorised as type II while Rh, Ru, Ir and Os have been categorised as type III.

6.4.1 Factors influencing the metal toxicity in microbial respiration

The toxicity of metals in biological processes is mainly caused by their ability to denature proteins by blocking the functional groups, displacing essential metals or modifying the active sites of the enzymes or biomolecules responsible for cellular synthesis and energy generation reactions (Ford *et al.*, 1995). Toxicity of mono- and divalent metals is predominantly due to the free metal ion in solution and hence most toxicity studies assume soluble metal salts are completely dissolved and bioavailable (Younger and Wolkersdorfer, 2004). However, solubilities of metals depend on pH, dissolved oxygen, water hardness and other factors, leading to variable metal toxicities. According to Table 6.8, all Ru samples have shown pH decreases and Ru has a K_i of 39.25 mg/l. As the pH decreases, the solubility of the Ru in the sample could have been increased or a more toxic form (oxidation state) may have been formed, hence higher toxicity to ASR. On the other hand, Rh may have formed less toxic species at neutral pH, hence low metal toxicity compared to other PGMs. As the PMR wastewater contains a mixture of different metals in solution, it is required to weight the effects of different metals in the

solution. The simplest models assume pure summation of the toxic effects of different metals present (Younger and Wolkersdorfer, 2004).

Organic and inorganic acids produced by bioremediation microorganisms such as *Pseudomonas* spp., are able to solubilise and transport metals (Ford *et al.*, 1995).Therefore, PGMs could also be subjected to similar conditions under denitrification where volatile fatty acids are produced. Thus, toxicity of PGMs on the denitrifying consortium may be attenuated. Further, the metal complexation capacity of dissolved organic carbon (DOC) has been shown to decrease metal toxicity (Heijerick *et al.*, 2002). These conditions might have caused higher tolerance of metals such as Rh, and Ru with K_i of 33.34 mg/l and 39.25 mg/l, respectively. Hypothetically this could be attributed to the metals' oxidation states being enzymatically altered and then the metals transformed to less toxic forms under the pH conditions prevailing in the experiments (Olson *et al.*, 1982).

Ford *et al.* (1995) also stated that metals and microbes interact extracellularly (involving extracelluar polymers, proteins, acid metabolites, and changes in the localised environment due to biochemical processes), at the cell-surface (binding to microbial cell surfaces with specific functional groups) and intracellularly (accumulation of metals in microbial cells due to specific transport processes). Extracellular polymeric substances (EPS) and proteins strongly bind metals (Arican *et al.*, 2002; Ford *et al.*, 1995; Hughes and Poole, 1989). Thus EPS and metal ions are bound as a direct consequence of negatively charged functional groups of the EPS (e.g. pyruvate, succinate, urinate, hydroxyl and phosphate). Lipopolysaccharides (LPS) in Gram-negative bacteria also consist of functional groups that can bind the metals. Teichoic/teichuronic acids and peptidoglycan in Gram-positive bacteria provide carboxylate and phosphate groups as potential metal binding sites (Ford *et al.*, 1995; Hughes and Poole, 1989). Therefore, it can be assumed that different microbes can bind different metals depending on the available biochemical. However, it has been reported that even toxic metals (e.g. Cu) are necessary for several enzymes. For example, Ni is a component of hydrogenases in many micro-organisms and has been found that stimulate chemolithotrophic growth (Ford *et al.*, 1995) thus a nitrifying consortium may be benefited. Figure 6.10 shows the potential interaction of metals, microbes and different factors involved in metal toxicity in nitrification and denitrification.

The pH-dependent binding of positively charged cations can rapidly occur with stability constants in excess of those generally measured for humic substances and other naturally occurring ligands (Ford *et al.*, 1995). However, there were no detailed structural investigations on biofilm (polysaccharide) interactions on metal surfaces at a molecular level in the scientific literature, especially for salt induced gelation, thixotrophy, wettability and spreading (Paradies, 1995).

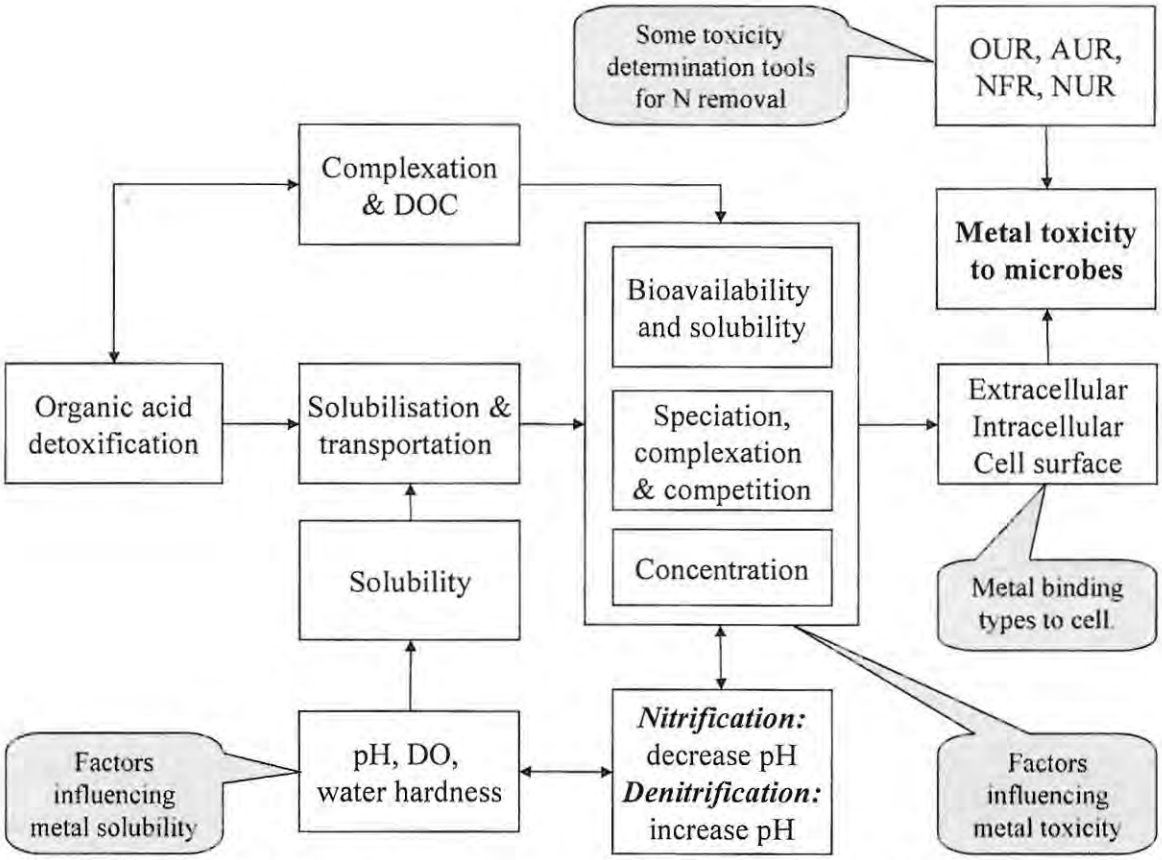

Figure 6.10: Metal toxicity and microbes interaction in nitrification and denitrification. AUR - Ammonium Uptake Rate; NUR - Nitrate Utilisation Rate; NFR - Nitrate Formation Rate and DOC - Dissolved Organic Carbon.

The pH changes can significantly affect the metal speciation and bioavailability, thus different degrees of toxicity on microbes could be imposed (Arican *et al.*, 2002; De Schamphelaere *et al.*, 2004; Hughes and Poole, 1989). Metals exist as free cationic species at acidic pH while at alkaline pH those metals precipitate as either hydroxides or oxides (Hughes and Poole, 1989). Nitrification and denitrification could occur in the sample as mentioned earlier and there was pH decrease (nitrification – more metals would be dissolved) or increase (denitrification – metals could be precipitated) in certain samples during the experiments (e.g. pH decrease – Rh, and Ru; pH increase – Pt and Pd at higher concentrations). As a result of change of oxidation state of metals, the degree of toxicity might have been changed (Madoni *et al.*, 1996) due to the change of binding sites of functional groups of different biochemicals (e.g. EPS, LPS, proteins, lipids etc). For example, the effect of metal salts concentrations (produced by metal recovery industries) on nitrification and denitrification were demonstrated by previous authors; Vredenbregt *et al.* (1997) and Yang *et al.* (1995) observed a significant decrease of nitrification (up to 3.4 wt %) and denitrification (2.3 wt %). Free ions are the most important metal species determining toxicity and it should be noted that other metal species and metal-organic

complexes (e.g. M-carbonates and M-hydroxides) may also contribute to the overall acute metal toxicity (Heijerick *et al.*, 2002).

6.4.2 Model of Metabolic activities and metal toxicity

Metal inhibitors which form insoluble salt precipitates due to heavily positively charged ions are considered as non-competitive (Lewandowski *et al.*, 1985). Models developed for single, pure enzymes have limitations when applied where mixed culture inhibitions are involved, such as in wastewater treatment. The relationship between the reaction velocity and inhibitor concentration presented by Lewandowski (1985; 1986; 1987), adapted from Aiba *et al.* (1973) is shown as Equation (6.6).

$$V = V_{Max} \times \left(\frac{S}{K_m + S} \right) \times \left(\frac{K_I}{K_I + S_I} \right) \tag{6.6}$$

V = Velocity of a reaction (mg/l/h)

V_{Max} = Maximum velocity of enzyme reaction when saturated with substrate (mg/l/h)

S = Substrate concentration (mg/l)

S_I = Inhibitor concentration (mg/l)

K_m = Michaelis constant, that concentration of substrate giving half maximum rate (mg/l)

K_I = inhibitor coefficient, that concentration of substrate giving half maximum rate (mg/l)

Equation (6.6) can be expanded for *n* number of metals, as given below:

$$V = V_{Max} \times \left(\frac{S}{K_m + S} \right) \times \prod_{n=1}^{n} \left(\frac{K_{I,n}}{K_{I,n} + S_{I,n}} \right) \tag{6.7}$$

Where n = 1, 2, 3,…., n for *n* number of metals.

Appendix DI presents a brief summary of kinetic model development for determination of K_i as described in Equations (6.6) and (6.7). Applications of this model can be found in Gumaelius *et al.*, (1996) and Lewandowski *et al.*, (1985; 1987). Table 6.9 presents a summary of PGMs K_i for ASR along with the other metals which have been reported by other researchers on different consortia.

Madoni *et al.* (1996) found that order of toxicity of metals to protozoans in activated sludge was Cd > Cu > Pb > Zn > Cr in decreasing order. However, heavy metal toxicity to bacterial communities have been reported with discrepancies such as Cd > Cu > Zn > Cr > Pb and Cd > Cr > Cu > Pb > Zn, depending the type and structure of the bacterial community (Madoni *et al.*, 1996). A toxicity study carried out using OUR and AUR of AS in the presence of heavy metals by Madoni *et al.* (1999) showed that toxic effects after 1 and 24 hours of exposure separated the metals into two distinct

groups: in the decreasing order of Cd > Cu > Zn and Pd > Cr. Further, they showed that nitrifiers had lower sensitivity to heavy metals than heterotrophic bacteria.

Table 6.9: Inhibition coefficients for different metals in wastewater treatment processes.

Metal*	K_i (mg/l)	Remarks	Reference
Pt	16	48 % inhibition at 25 mg/l (mixed culture)	In this research
Pd	25	80 % inhibition at 25 mg/l (mixed culture)	In this research
Rh	33	48 % inhibition at 25 mg/l (mixed culture)	In this research
Ru	39	64 % inhibition at 20 mg/l (mixed culture)	In this research
Cd	39	50 % inhibition of AS (mixed culture)	Kelly *et al.*, 2004
Cu^{2+}	0.9	91 % of inhibition of AS (mixed culture)	Madoni *et al.*, 1999
Cu	15	50 % of inhibition of AS (mixed culture)	Kelly *et al.*, 2004
Cr^{4+}	50	100 % inhibition	Dilek and Yetis, 1992
Cr^{6+}	87	100 % inhibition of AS (mixed culture)	Lewandowski *et al.*, 1985
Pb	17	67 % inhibition of nitrifiers	Madoni *et al.*, 1999
Ni	76	50 % inhibition of AS (mixed culture)	Kelly *et al.*, 2004
Zn^{2+}	3.	100 % inhibition of nitrifiers	Benmoussa *et al.*, 1986
Zn	41	50 % inhibition of AS (mixed culture)	Kelly *et al.*, 2004

***Note:** Zero valance status of metals (e.g. Pt, Cu, Pb, and Zn etc) does not represent the metal oxidation state used in the research. This representation is due to unavailability of information on the metal's oxidation state as reported or has not been investigated in respective researches.

However, a long term study (24 days) carried out by Principi *et al.* (2006) showed higher sensitivity of nitrifiers than heterotrophs to heavy metals, and that biomass metal accumulation was in the order of Cu > Ni > Zn. Therefore, long-term toxicity tests are vital for evaluating the toxicity to different microbes involved in nitrification and denitrification processes, in contrast to 10 hours as done in this research. Even though a community analysis was not carried out in this research, the toxicity of PGMs to the ASR based on the K_i (the higher the K_i the lower the toxicity) was found to be in the order of Pt > Pd > Rh > Ru. This verified early speculation on PGMs toxicity (Hughes and Poole, 1989) on micro-organisms generally in category II. i.e. potentially toxic and relatively available. However, a detailed and quantitave comparison could not be carried out, as there was not enough information about PGMs toxicity on the AS process (ASP). Further, for better understanding of the level of toxicity of PGMs on ASP, it is required to carry out a detailed community analysis to ascertain the different degrees of tolerance by various consortia.

Even though the optimal pH for nitrifying and denitrifying consortia without toxic conditions are in the range of 7 – 8 (Gumaelius *et al.*, 1996), it would probably be possible to improve the nitrogen

removal by varying the pH conditions within the suboptimal range so that changing metal speciation would lead to less toxic effects on the microbes. However, this needs further investigation, as pH changes would cause one metal to form less toxic species or complexes while another may form more toxic species or complexes. The toxicity differences in the same metals observed here could be due to speciation and complexation and not to competition, as these experiments were performed with single metal in solution. This could be due to the shift of metabolic pathway to the second best energy generation path when metals block the functional groups of the enzymes responsible for the principal metabolic pathways.

6.4.3 Drawbacks of the OxiTop system based OUR measurements for toxicity studies

Some of the pitfalls of the OxiTop system are the long stabilisation period required (i.e. to produce negative pressures; this is an important factor for acute toxicity studies of less than 10 hours or so) and incorrect pressure measurements when other gasses are evolved (e.g. NH_3 production due to pH change in toxicity studies where NH_4^+-N is used as the substrate). However, significant amounts of NH_3 were not produced due to pH changes considering pH status before and after the experiments (see Chapter 4: Appendix B: Table B.4 for NH_3 *vs.* NH_4^+ equilibrium under different pH and temperatures). Further, there was not a mechanism to measure N_2 which was probably produced probably due to simultaneous nitrification and denitrification while the experiment was being carried out. Reproducibility of the OxiTop and its working principle has been extensively evaluated elsewhere (Rudrum, 2005). Furthermore, the accuracy of inhibition coefficients of different metals are important only in the order of magnitude for the simulation work, as this inhibition is introduced in the form of an inhibition switching function (Henze *et al.*, 1987). However, the OxiTop system is a simple, quick and user friendly tool to determine OUR, BOD and perform toxicity studies (Veeken *et al.*, 2003). Beside the early mentioned drawbacks specific to the OxiTop system, another disadvantage of respirometric measurement-based studies is the highly variable SOU depending on the inoculum used. This is evident with different SOUR in different controls used in the experiments (e.g. 0.0799 for Ru; 0.9286 for Rh and 0.0770 for Pt; all units in $mgO_2/mgVSS/h$). In order to minimise the errors due to variable SOUR in different batches, it is vital to use high (e.g. > 2400 mg/l MLSS) biomass concentration at the start up which would minimise the long stabilisation period due to higher SOU and pH correction in the metal solution before introduction of the inoculum. Reproducibility was highly affected by site and time specific conditions leading to variations of microbial population available at the time of inoculum were collected, as reported by previous workers (Gumaelius *et al.*, 1996).

6.5 Interim conclusions

In order to incorporate the metal toxicity data in the simulation model developed in response to the conclusions drawn in Chapter 5 (see Chapter 7: Mathematical modelling and simulation of activated

sludge process for nitrogen removal in precious metal refinery wastewater), four experimental models were developed for selected PGMs (Pt, Pd, Rh, and Ru) by correlating the metal concentration and microbial maximum SOUR. These models can be used to reveal the inhibition coefficient for each metal in the trickling filter humus sludge process. Based on the experimental model developed, the toxicity of the PGMs to trickling filter humus sludge respiration was found to be in the order of Pt > Pd > Rh > Ru with inhibition coefficients of 16 mg/l, 25. mg/l, 33 mg/l and 39 mg/l, respectively.

As this toxicity test was carried out using an original trickling filter humus sludge inoculum, in order to ascertain the PGM toxicity to nitrification and denitrification, it is recommended to measure the AUR, NFR and NUR along with the OUR in the nitrification process under different metal concentrations. This would assist in distinguishing respiration by nitrifying consortia from the rest of the microbes present in the mixed liquor, and the NUR would reveal the denitrifying activity under anoxic conditions.

Further, metal speciation of those metals under different pH conditions, metal complexation and competition in actual PMR wastewater could have different effects on nitrification and denitrification processes. Therefore, the effects of metal speciation, complexation and competition of different metal mixtures in PMR wastewaters are needed for further investigation for better understanding of metal toxicity on nitrification and denitrification processes.

CHAPTER 7

Rest satisfied with doing well, and leave others to talk of you as they please.

- Pythagorus (c.580-c.500 B.C.).

7.0 Modelling of biological removal of nitrogen species from precious metal refinery (PMR) wastewater using the activated sludge process (ASP)

7.1 Introduction

Mathematical models could be defined as models within a mathematical framework where equations of various types are defined to relate inputs, outputs and characteristics of a system (Jeppsson, 1996). Further, Jeppsson (1996) stated that a mechanistic model is a model based on fundamental engineering and scientific knowledge about the physical, chemical and biological mechanisms that affect a system, and a model based on elementary principles tends to produce more reliable results when used for extrapolation. Jeppson (1996) provides a detailed discussion on different modelling techniques, types and general modelling strategy. Mathematical modelling of nitrification and denitrification processes essentially consists of two main components. i.e application of general biofilm theory and process modelling (nitrification and denitrification, completely autotrophic nitrogen removal over nitrite (CANON), oxygen limited autotrophic nitrification and denitrification (OLAND) which are based on ANaerobic AMMonium OXidation (Anammox) etc., an autotrophic nitrogen removal process (ANRP)). In developing the general biofilm theory, it is necessary to define what exactly a biofilm is, what parameters affect the formation of the biofilm and how the biofim propagates in the medium. Dynamic biological processes which take place in the reactor are influenced by the nature of the physical environment, i.e. type of reactor, enhanced mixing, improved mass (substrates and products) transfer per specific surface area of a given reactor, uniform or heterogeneous distribution of biomass (e.g. CSTR vs. packed bed reactor (PBR)), and sludge activation by recirculation of effluent in reactors etc.

Biofilms are layer-like aggregations of micro-organisms and their extracellular polymers (EPS) attached to a solid surface (Rittmann and Mccarthy, 2001). Substrate and product mass transport and biochemical conversions through the intracellular and intercellular environment of a microbial population will lead to the formation of a biofilm. However, biofilm structure formation depends on physical factors such as those governing substrate transport as well as general biological and specific biological factors such as growth yield and substrate conversion rates (van Loosdrecht *et al.*, 2002).

Mathematical modelling of biofilm processes will assist scientists and engineers who work in biotechnology applications to simulate the possible results prior to running the actual experiments in the laboratory or field. Further, the correct mathematical model can help to predict the actual behaviour of various biofilm processes under different conditions. This will cut down the analytical experiments and their running cost, while saving time. Once the actual experiments start, the processes can be run under the optimum conditions obtained under the simulation study. Hence, the cost of lab

experiments as well as time can be reduced significantly while the model can be used to simulate different reactor operations under different conditions.

Development of models is done on different bases, such as one dimensional (1-D) single species (1-S) models, one dimensional two species model, one dimensional multi species models, two dimensional multi species models, three dimensional multi species models, etc. The International Water Association (IWA) Task Group on Biofilm Modelling developed their benchmark problems for comparison and used diverse modelling techniques which included analytical, pseudo-analytical, and numerical solutions to the biofilm problems (Noguera and Morgenroth, 2004). Biofilm modelling in wastewater treatment applications have been developed considerably in recent years; especially after introducing activated sludge model number 1(ASM1), ASM2, ASM2d and ASM3 those made uniformity among different modelling methods. According to Wimpenny *et al.* (2000), the modelling technique could be either a biofilm as a continuum or as a discrete system. In continuum-based analysis, the model is described by a set of differential and partial differential equations. This is the most traditional way of mathematical modelling. Cellular automata (CA), fractals, finite element methods (FEM) etc., are used to model the discrete systems (Wimpenny *et al.*, 2000, Kreft *et al.*, 2001). Modelling of biofilms for nitrification and denitrification processes has been done in recent years by many researchers (Tsuno *et al.*, 2002; Rittmann *et al.*, 2002; Seixo *et al.*, 2004).

One-dimensional models reasonably support process engineers in biofilm reactor design, due to their intrinsic simplicity and need for small sets of data and parameters (Tsuno *et al.*, 2002). In the 1-D model the concentrations of substrates and microbial species are averaged over planes parallel to the substratum and spatial gradients are considered in the direction perpendicular to the substratum (Wanner and Morgenroth, 2004). However, neither spatial biomass nor substrate distribution over the space can be simulated accurately using 1-D models.

The objectives of this chapter are to review the current knowledge in biofilm modelling with respect to one dimensional multi species models, to identify the critical parameters in biofilm modelling with reference to nitrification and denitrification, and to propose a model for nitrification and denitrification processes in metal refinery wastewater treatment using general biofilm theory and the Activated Sludge Model number 1 (ASM1) by coupling anaerobic ammonium oxidation (Anammox) and precious metal toxicity.

7.2 General theory of biofilm development

Metabolically active microbes catalyse the pollutant-removing reactions. The active biomass is grown and sustained through the utilisation of its energy- and electron generating primary substrates, which are its electron donor and electron acceptor (Rittmann and McCarthy, 2001).

Biofilms are studied at either the macroscopic level (i.e. measuring general properties of biofilm developed in a reactor or system) or microscopically (i.e. using microscopy and micro-electrodes) (van Loosdrecht *et al.*, 2002). A detailed mathematical model for biofilm development by Wanner and Gujer (1986) considered a one-dimensional biofilm based on the gradients perpendicular to the interface of biofilm and bulk liquid. One dimensional models neither reveal how a biofilm structure develops with lateral gradients nor how e.g. pores contribute to the overall biofilm conversions (van Loosdrecht *et al.*, 2002). But these simple models are sufficient for understanding the biofilm processes in quantitative manner (Wanner, 1996). Further, this kind of model is generally adequate for describing the macroscopic conversions in a biofilm system and gives reasonable details of the layered structure of a biofilm (van Loosdrecht *et al.*, 2002). Picioreanu (1998; 2000b; 2001) developed a comprehensive quantitative model structure for biofilm growth considering convection (Navier-Stokes equations for fluid flow), diffusion (Fick's laws), reactions (substrate consumption and biomass production), biofilm growth and detachment (based on the force exerted by the liquid flow). Rittmann *et al.* (2002) developed a transient-state, multiple-species biofilm model, which experiences time-varying conditions including periodic detachment by backwashing. Table 7.1 shows a short history of development of different biofilm models by various early researchers.

The model developed by Fouad and Bhargava (2005) presented the knowledge of hydraulic retention time (θ), influent substrate concentration (S_o), stagnant liquid layer thickness (L), minimum substrate concentration (S_{min}) that can maintain the biofilm growth, the desired value of substrate concentration in the bulk phase (S) and kinetics constants those permit computation of the suspended biomass concentration (X). Knowing the value of S_{min} is important, as it indicates the point where endogenous respiration starts in the biofilm. This helps to keep the desired biomass in the reactor while supplying sufficiently the required electron donor and electron acceptor.

7.2.1 Governing laws and equations

Removal of the target substrate (pollutant: e.g. ammonium / ammonia, nitrate, nitrite or organic pollutant) can only be achieved if the biomass is provided with a suitable electron donor, electron acceptor and nutrients as required (van Hooren, 2002). Each of these components could be rate limiting in the conversion process.

Monod kinetics are frequently used for describing the growth of microbes and hence the substrate consumption by microbes as shown below (Henze *et al.*, 2002, Rittmann and McCarthy, 2001). Further, Monod-type expressions provide reasonable models to describe the growth of enriched culture sustained in wastewater treatment (WWT) reactors, with the provision that the kinetics parameters to be interpreted not as absolute values, but as average figures related to the predominant species in particular growth conditions of the reactor (Jeppsson, 1996).

Table 7.1: Summary of features of different biofilm models.

Type	Special features	References
1-D	Bacterial growth and decay factors for a steady state biofilm	Rittmann and McCarthy, 1980a, 1980b
1-D	Bacterial growth and decay factors for unsteady state biofilm with duel nutrient limitation	Rittmann and Bruner, 1984; Rittmann and Dovantzis, 1983
1-D	BIOSIM – the first detailed model of one-dimensional multi-substrate and multi-species biofilm including attachment and detachment.	Warner and Gujer, 1986
	Modification of BIOSIM model to irregular biofilm structures	Warner and Reichert, 1996
2-D	Application of cellular automata for biofilm modelling	Wimpenny and Colasanti, 1997a,b
2-D	Improved cellular automata (CA) model using mass transport	Picioreanu *et al.*, 1998
1-D	Simplified mixed culture biofilm model decoupling substrate diffusion and biochemical conversion	Rauch *et al.*, 1999
1-D	Detachment mechanisms on competitive biofilms	Morgenroth and Wilderer, 2000
3-D	3-D biofilm study - correlation of spatial structure, hydrodynamics conditions and mass transfer and conversion.	Eberl *et al.*, 2000
1-D	Hydrodynamics and correlated mass transfer with biofilm structure	Kreft *et al.*, 2001; Noguera *et al.*, 1999; Picioreanu *et al.*,2000
2-D	Cellular automata (CA) model describing single-species biofilm with a single growth-limiting nutrients	Hermanowicz, 2001
2-D	Cellular automata (CA) model describing heterogeneous structures and predicting nutrient concentration gradients, fluxes and steady state conditions	Pizarro *et al.*, 2001
2-D	Multi-nutrient, multi-species model of nitrifying biofilm to predict the structures, i.e. surface enlargement, roughness and diffusion depth in the biofilm	Kreft *et al.*, 2001
1-D	Transient-state, multi-species biofilm model for biofiltration	Rittmann *et al.*, 2002
1-D	Simple biofilm model of bacterial competition for attached surface using nitrifier biofilm – applicable for both autotrophic and heterotrophic bacteria	Tsuna *et al.*, 2002
1-D	Heterogeneous biofilm model predicting the microbial activity using stratified biofilms	Beyenal and Lewandowski, 2005
1-D	Simplified biofilm model for steady state completely mixed biofilm-activated sludge reactor	Fouad and Bhargava, 2005
1-D	Single and multi-species biofilm model for floc diffusion process based on analytical solution	Perez *et al.*, 2005

7.2.1.1 Monod kinetics

$$\mu_{syn} = \left(\frac{1}{X_a} \frac{dX_a}{dt} \right)_{syn} = \hat{\mu} \frac{S}{K + S} \tag{7.1}$$

Where μ_{syn} = specific growth rate due to synthesis (1/T)

X_a = concentration of active biomass (M_x/L^3)

t = time (T)

S = concentration of rate limiting substrate (M_s/L^3)

$\hat{\mu}$ = maximum specific growth rate (1/T)

K = concentration giving one-half the maximum rate (M_s/L^3)

Active biomass has an energy demand for maintenance, which includes cell functions such as motility, repair and resynthesis, osmotic regulation, transport and heat loss (Rittmann and McCarthy, 2001). Endogenous decay is defined as the flow of energy and electrons required to meet maintenance needs. This is shown by:

$$\mu_{decay} = \left(\frac{1}{X_a} \frac{dX_a}{dt} \right)_{decay} = -b \tag{7.2}$$

Where b = endogenous-decay coefficient (1/T)

μ_{decay} = specific growth rate due to decay (1/T)

According to Rittmann and McCarthy (2001), not all the active biomass lost by decay is actually oxidised to generate energy for maintenance needs. Though the majority of biomass is oxidised, a small fraction accumulates as inert biomass. Therefore, true respiration for energy generation is:

$$\left(\frac{1}{X_a} \frac{dX_a}{dt} \right)_{resp} = -f_d b \tag{7.3}$$

Where f_d is the fraction of the active biomass which is biodegradable.

Then, the rate of conversion of active biomass into inert biomass is the difference between the overall decay rate and the oxidation rate:

$$-\left(\frac{1}{X_a}\frac{dX_i}{dt}\right)_{resp} = \frac{1}{Xa}\left(\frac{dX_a}{dt}\right)_{inert} = -(1-f_d)b \qquad (7.4)$$

Where X_i = inert biomass concentration.

The net specific growth rate of active biomass = new biomass growth rate + decay rate:

$$\mu = \left(\frac{1}{X_a}\frac{dX_a}{dt}\right) = \mu_{syn} + \mu_{dec} = \hat{\mu}\frac{S}{K+S} - b \qquad (7.5)$$

Michaelis-Menten kinetics are used in explaining the enzyme kinetics in biochemical conversions. This is given by:

$$v = \hat{v}\frac{S}{K_M + S} \qquad (7.6)$$

Where v = Enzymatic reaction rate

$\hat{v}$ = Maximum reaction rate

K_M = Michaelis-Menten coefficient

S = Substrate concentration

7.2.1.2 Effect of temperature

The prevailing temperature has an important effect on selective inhibition of undesired biomass in ANRP such as CANON and OLAND. For example, Anammox (Anaerobic ammonium oxidation) organisms favour high temperatures with 40 ± 3 °C as the optimal temperature range (Wyffels *et al.*, 2004; Hao *et al.*, 2002; Hellinga *et al.*, 1999). At higher temperatures, ammonium oxidisers have a higher growth rate than the nitrite oxidisers. Therefore, by controlling temperature the nitrite oxidisers can be eliminated so that nitrite oxidation can be prevented (Wyffels *et al.*, 2004).

The Arrhenius relation can be used for predicting the temperature dependency of ammonium and nitrite oxidisers (Hao *et al.*, 2002):

$$r_T = r_{293} \exp[-E_{act}(293\text{-}T)/R293T] \qquad (7.7)$$

Where r_T = rate of reaction at temperature T, E_{act} = Activation energy, R = universal gas constant, T = temperature in Kelvin.

For small temperature changes, the product of 293T does not change much and hence the expression relative to standard temperature can be used (Hao *et al.*, 2002):

$$r_T = r_{293} \exp[-\theta(293-T)] \quad (7.8)$$

Where $\theta = E_{act}/R293T$

7.2.1.3 Effect of aeration

Hao *et al.* (2002) stated that ammonium surface load (ASL) was associated with an optimal dissolved oxygen (DO) level for maximum nitrogen removal efficiency in the CANON process. Further, Hao *et al.* (2002), mention that ASL needs to be stoichiometrically related to the oxygen mass transfer to the biofilm. Therefore, DO and ASL are the two key process factors governing the behaviour of CANON process (Chapter 2: Literature Review and Chapter 9: Operational Protocol). The general approach for controlling the nitrite oxidisers in ANRP is adopting the oxygen limited conditions to outcompete the nitrite oxidisers in the reactor (Wyffels *et al.*, 2004; Sleakers *et al.*, 2003; Hao *et al.*, 2002). Oxygen mass transfer coefficient, according to Campos *et al* (2000) is given by:

$$K_{La} \bullet (O_{2.sat} - O_2) = 4.57 \bullet r_{NH_4^+} \quad (7.9)$$

Where K_{La} = Oxygen mass transfer coefficient, O_{2SAT} = Saturated oxygen concentration, O_2 = Oxygen concentration.

7.2.1.4 Effect of pH

Biological conversion reactions involving proton consumption or production affect the pH of the medium in which they take place (Volcke *et al.*, 2005). Further, Volcke *et al.* (2005) stated when modelling systems for simulation purposes, it is required to model the pH effect correctly on both biological conversion reactions and chemical dissociation reactions (acid/base chemistry) which are subject to significant pH changes. As stated earlier, ammonium oxidation is an acidifying process (i.e. producing protons). The equilibrium between ammonia (NH_3) and ammonium (NH^+_4) and the equilibrium between nitrous acid (HNO_2) and nitrite (NO^-_2) are pH dependant. Further, ammonia and nitrous acid are considered as the substrate for ammonium oxidisers and nitrite oxidisers respectively whereas ammonium and nitrite are substrates for anammox bacteria. Sliekers *et al.* (2002) speculated that free ammonia may inhibit the nitrite oxidisers. As accumulation of nitrite (< 100 mg/l: Strous *et al.*, 1999) is desired in the ANRP process, pH controlled aeration could be another better option to outcompete the nitrite oxidisers in the reactor. Therefore, the pH calculation in the reactor will be modelled below, as it influences many factors (ammonia / ammonium and nitrous acid / nitrite concentrations) in ANRP operation. According to van Hulle (2005), considering the equilibrium between ammonium (NH^+_4) and ammonia (NH_3):

$$S_{NH_3} = \frac{S_{TAN}}{1 + \frac{10^{-pH}}{K_e^{NH}}} \quad (10)$$

Where $TAN = NH_3 + NH^+_4$ and $K_e^{NH} = \frac{NH_3 \bullet H^+}{NH^+_4}$

Similarly for equilibrium between HNO_2 and NO^-_2,

$$S_{HNO_2} = \frac{S_{TNO_2}}{1 + \frac{K_e^{NO}}{10^{-pH}}} \quad (7.11)$$

Where $TNO_2 = HNO_2 + NO^-_2$ and $K_e^{NO} = \frac{NO_2 \bullet H^+}{HNO_2}$

The pH calculation is modelled using the charge balance over the reactor as proposed by Hellinga *et al.* (1999). A detailed discussion on charge balance and pH calculation can be found in Hellinga *et al.* (1999), Volcke *et al.* (2005) and Van Hulle (2005).

$$pH = -\log[H^+] \quad (7.12)$$

$$K_w = [H^+]*[OH^-] \quad (7.13)$$

$$S_{HCO_3^-} = \frac{S_{IC}}{1 + \left(\frac{K_{CO_3}}{S_{H^+}}\right) + \left(\frac{S_{H^+}}{K_{CO_2}}\right)} \quad (7.14)$$

$$S_{CO_3^{2-}} = \frac{S_{IC}}{1 + \left(\frac{S_{H^+}}{K_{CO_3}}\right) + \left(\frac{S^2{}_{H^+}}{K_{CO_3} * K_{CO_2}}\right)} \quad (7.15)$$

$$S_{NO_2^-} = \frac{S_{TNO_2}}{1 + \left(\frac{S_{H^+}}{K_{HNO_2}}\right)} \quad (7.16)$$

$$S_{NH_4^+} = \frac{S_{TNH_4}}{1 + \left(\frac{K_{NH_3}}{S_{H^+}} \right)} \tag{7.17}$$

The gap in charge balance can be written as:

$$\Delta_{ch} = -S_{H^+} + \frac{K_W}{S_{H^+}} + S_{HCO^-_3} + 2S_{CO_3^{2-}} + S_{NO^-_2} - S_{NH_4^+} - S_{Z^+} \tag{7.18}$$

Where S_{Z^+} is a net concentration of additional positively charged ions present in the influent. Once the equations 13 – 17 have been solved, the charge balance should be close to zero. The iterative Newton-Raphson method is used to solve the above equations (Hellinga *et al.*, 1999; van Hulle, 2005).

7.2.1.5 Diffusion in biofilms

Substrate diffusion to the biofilm occurs through two processes, namely liquid film diffusion in the boundary layer and biofilm diffusion in the biofilm itself. The liquid film diffusion signifies the mass transfer between the turbulent flow in the bulk liquid and the surface of the biofilm (Christiansen *et al.*, 1995). The thickness of the boundary layer and liquid film diffusion coefficient depend on the hydraulic conditions of the flow and the transport of substrate in the biofilm is controlled by molecular diffusion.

The degree of substrate penetration in the biofilm is given by

$$\beta = \sqrt{\frac{2.D.S}{K_{of}.L}} \tag{7.19}$$

Where D = Diffusivity (m^2/s)

S = Substrate concentration (g/m^3)

K_{of} = zero-order intrinsic removal rate ($g/m^3.d$)

L = thickness of the biofilm (m)

Under strong diffusion-limited conditions the biofilm becomes a heterogeneous and porous structure. When the conversion is the rate-limiting step, it becomes homogeneous and compact (van Loosdrecht *et al.*, 2002). The biofilm density is defined as the amount of biomass per volume biofilm excluding the pore volume (van Loosdrecht *et al.*, 2002).

Gjaltema *et al.* (1994) found that even in a well-mixed biofilm reactor, different types of biofilms are formed due to differences in shear rates at different surface sites in the reactor. Even in hydraulically well-mixed systems, substrate gradients can occur when the characteristic time for substrate conversion is smaller than the characteristic mixing time (Gjaltema *et al.*, 1994). The dominant factor

on biofilm morphology is the ratio between detachment rate and biofilm surface loading rate (van Loosdrecht *et al.*, 2002). Further, van Loosdrecht *et al.* (2002) found that a thinner biofilm is formed by either an increase of shear rate (by changing the number of particles) or lowering substrate loading rate (by changing the surface specific loading rate to the biofilm) in an airlift suspension reactor.

Faster growing heterotrophic microbes are always located at the surface of the biofilm while the slower growing autotrophic microbes are predominantly located below the heterotrophic layer where they are better protected from detachment (Morgenroth and Wilderer, 2000). Therefore, substrate transport to the autotrophic layer through diffusion should be governed by the diffusion properties of the heterotrophic layer and substrate properties. For example, in nitrification, autotrophic microbes need oxygen. However, oxygen diffusion to the autotrophic layer does not happen if the biofilm thickness is more than 150 μm (Kowalchuck and Stephen, 2001) due to diffusion limitations of oxygen in the biofilm.

7.2.1.6 Microbial growth and decay, attachment and detachment

Morgenroth and Wilderer (2000) state that competition between the faster growing heterotrophic and slower growing autotrophic bacteria is affected by the Chemical Oxygen Demand (COD)/N ratio and the biofilm thickness dynamics, i.e. for high COD/N ratios the faster growing heterotrophic bacteria overgrow, resulting in substrate transport limiting to slower growing autotrophic bacteria and high variations of the biofilm thickness dynamics caused by long backwashing intervals providing the room for faster growing heterotrophic bacteria (Muslu, 2002). This is an important aspect of nitrification with regard to organic wastewater, as autotrophic biomass has slower growth rate compared to heterotrophic biomass under the aerobic conditions.

Once the biofilm is fully grown various processes lead to detachment (Horn and Hempel, 1997, Zhang and Bishop, 1994). These can be categorised as abrasion (caused by collision of biofilm support particles), erosion (caused by shear forces of the moving fluid in contact with the biofilm surface), sloughing (detachment of single cells) and predator grazing (Morgenroth and Wilderer, 2000). On the other hand, EPS produced by biomass keep the biofilm sticky and resistant to detachment to some extent. The EPS production rate is inversely proportional to the substrate consumption rate (Laspidou and Rittmann, 2002). Therefore, the EPS production rate could be used as an indicator of how the substrate is used in the reactor.

7.2.1.7 Metabolic activities and metal toxicity

The influence of toxic compounds arising from metals on nitrification and denitrifiction is not well understood. The situation is much worse with respect to novel nitrogen removal processes like, Anammox, CANON, Single reactor High Activity Ammonia Removal Over Nitrite (SHARON) and

OLAND. Further, the difference between the short- and long-term influences of those metal compounds on the above processes is yet to be studied. During long-term processes, some adaptation mechanisms of the bacteria involved may be expected (Lewandowski, 1985). The effect of metal toxicity on poor nitrate removal in packed bed reactor (Kasia *et al.*, 2005) and airlift suspended reactor (Chapter 4: Reactor comparison study) have been reported. This may be due to the toxicity of the metals (a concentration of 30 mg/l) used in the experimental studies. Lewandowski (1985) studied the short-term influence of Cr^{+6} on denitrification process by measuring the inhibition constant K_i in activated sludge under anoxic conditions. Further, he proposed the inhibition by Cr^{+6} to be considered as a non-competitive kind. The relationship between the reaction velocity and inhibitor concentration was presented by Lewandowski (1985; 1986; 1987) adapting from (Aiba *et al.*, 1973):

$$V = V_{Max} \times \left(\frac{S}{K_m + S} \right) \times \left(\frac{K_I}{K_I + S_I} \right) \tag{7.20}$$

V = Rate of a reaction ($mgl^{-1}h^{-1}$)

V_{Max} = Maximum Rate of enzyme reaction when saturated with substrate ($mgl^{-1}h^{-1}$)

S = Substrate concentration (mgl^{-1})

S_I = Inhibitor concentration (mgl^{-1})

K_m = Michaelis constant, that concentration of substrate giving half maximum rate (mgl^{-1})

K_I = inhibitor coefficient, that concentration of substrate giving half maximum rate (mgl^{-1})

The equation (20) can be expanded for n number of metals as given below:

$$V = V_{Max} \times \left(\frac{S}{K_m + S} \right) \times \prod_{n=1}^{n} \left(\frac{K_{I,n}}{K_{I,n} + S_{I,n}} \right) \tag{7.21}$$

Where n = 1,2,3,....,n for 'n' number of metals.

7.3 Nitrogen removal process modelling

Figure 7.1 summarises the various factors affect on mathematical modelling of nitrogen removal process for precious refinery wastewaters considering microsopic and macroscopic approach. Nitrogen balance analysis as described in Chapter 5 showed nitrogen removal from various reactors could not be explained solely by the standard nitrification and denitrification processes. Therefore, it was assumed that the anammox activity could have taken place in the inner layers of biofilm where oxygen

is limited (especially in the CSTR). Further, NH_4^+ and NO_3^- analysis in clarifiers showed that there was some ammonification activity. Therefore, the proposed model consists of autotrophic and heterotrophic nitrogen removal activities, ammonification and the metal toxicity which affect on both autotrophs and heterotrophs.

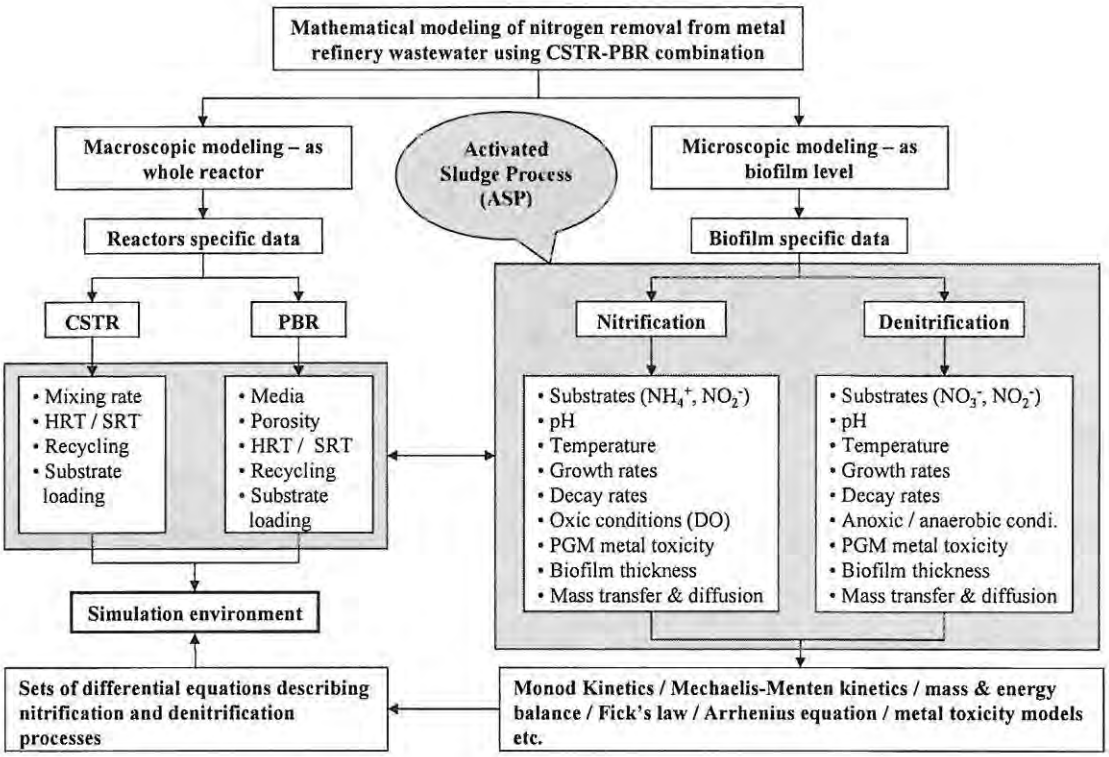

Figure 7.1: Factors affecting mathematical modelling of nitrogen removal processes

In mathematical modelling of nitrogen removal processes, it is worthwhile to look at some of the free energies of reactions which would possible in those processes. Nitrogen has different oxidation states depending on the compound formed. Table 7.2 shows some of the important nitrogen species which occurs in wastewater (aquatic phase) and their Gibbs standard free energy at neutral pH. All reactions except reaction (3) are exergonic, as the free energy is decreased during the reactions. When comparing the two reactions (5) and (6) in Table 7.2, reaction (6) has a higher free energy decrease, when NO^-_2 is used as the electron donor. Theoretically, ammonium also can be used as an inorganic electron donor in the absence of oxygen.

The great differences in reaction free energies for aerobic versus anaerobic and organic versus inorganic reactions have great effects on resulting bacterial yields (Rittmann and McCarthy, 2001). Fundamentally ammonium also could be used as an inorganic electron donor for denitrification (Jetten *et al.*, 1999). Further, Jetten *et al.* (1999) showed the free energy for this reaction is nearly favourable as for the aerobic nitrification process (Table 7.3).

Aerobic ammonium oxidising is an acidifying process (see Table 7.3; last reaction) and therefore pH control is vital for preventing the inhibition of active microbes (Khin and Annachhatre, 2004). Anammox stoichiometry (Dapena-Mora *et al.*, 2004) used in sequencing batch reactor (SBR) was applied in the modeling process assuming that the complete biomass retention in the reactor lead to an indefinite solid retention time (SRT). Aerobic and anoxic endogenous respiration was included in the model using the same kinetics as for the nitrification, as only negligible error occurred due to a tiny anoxic decay coefficient (Hao *et al.*, 2002).

Table 7.2: N-compounds half-reactions and their Gibb's standard free energy at pH = 7.

No.	Reduced-oxidised compound	Half-reaction	$\Delta G^{0'}$ kJ/e$^-$eq
1	Ammonium – nitrate	$1/8NO_3^- + 5/4H^+ + e^- \rightarrow 1/8NH_4^+ + 3/8H_2O$	-35.11
2	Ammonium – nitrite	$1/6NO_2^- + 4/3H^+ + e^- \rightarrow 1/6NH_4^+ + 1/3H_2O$	-32.93
3	Ammonium – nitrogen	$1/6N_2 + 4/3H^+ + e^- \rightarrow 1/3NH_4^+$	+26.70
4	Nitrite – nitrate	$1/2NO_3^- + H^+ + e^- \rightarrow 1/8NO_2^- + 1/2H_2O$	-41.65
5	Nitrogen – nitrate	$1/5NO_3^- + 6/5H^+ + e^- \rightarrow 1/10N_2 + 3/5H_2O$	-72.20
6	Nitrogen – nitrite	$1/3NO_2^- + 4/3H^+ + e^- \rightarrow 1/6N_2 + 2/3H_2O$	-92.56

Source: Rittmann and McCarthy, 2001.

Table 7.3: Gibbs free energy for several reactions involved in denitrification.

Reaction equation	$\Delta G^{'}$ / kJ mol$^{-1}NH_4^+$ or NO_3^-
$2NO_3^- + 5H_2 + 2H^+ \rightarrow N_2 + 6H_2O$	-560
$8NO_3^- + 5HS^- + 3H^+ \rightarrow 4N_2 + 4H_2O + 5SO_4^{2-}$	-465
$3NO_3^- + 5\ NH_4^+ \rightarrow 4N_2 + 9H_2O + 2H^+$	-297
$NO^-_2 + NH^+_4 \rightarrow N_2 + 2H_2O$	-358
$2O_2 + NH_4^+ \rightarrow NO_3- + H_2O + 2H^+$	-349
$6O_2 + 8\ NH_4^+ \rightarrow 4N_2 + 12H_2O + 8H^+$	-315

Source: Jetten *et al.*, 1999

A comparison of ammonium oxidation by aerobic ammonia oxidizers and anammox is shown in Table 7.4. According to Hao *et al.* (2002) nitrite inhibition of the Anammox process was not included in the model's rate equation, as nitrite concentration rarely reaches 100 mg/l. When the oxygen concentration is as low as 2 μM, this inhibits the Anammox activity completely but reversibly (Jetten *et al.*, 2001).

Table 7.4: Some parameters of aerobic and anaerobic ammonium oxidation.

Parameter	Nitrification $NH_4^+ + O_2 \rightarrow NO_2^-$	Anammox $NH_4^+ + NO_2^- \rightarrow N_2$	Units
ΔG	-275	-357	kJ/mol
$E_{activation}$		70	kJ/mol
μ_{max}	0.04	0.003	h^{-1}
Doubling time	0.73	10.6	D
Aerobic rate	200 – 600	0	mgN/g protein/min
Anaerobic rate	2	60	mgN/g protein/min
$K_{S\text{-}NO2}^-$	N/A	< 0.07	μM
$K_{S\text{-}TAN}$	5 – 2600	5	μM
$K_{S\text{-}O2}$	10 – 50	N/A	μM

Source: Jetten *et al.*, 2001: N/A = not applicable, K_S = affinity constant

7.3.1 The nitrogen removal process modelling for precious metal refinery wastewater

The autotrophic nitrogen removal was represented by using the combination of partial nitrification (nitritation) and Anammox pathway as modelled by van Hulle (2005). The biofilm model used in this process modelling was assumed as a one-dimensional multi-substrate and multi-species biofilm model. The heterotrophic denitrification and ammonification were incorporated as appeared in the Activated Sludge Model no. 1 (Henze *et al.*, 1987). In order to introduce precious metal toxicity into the above model, process inhibition by metals was introduced using the model used by Lewandowski (1985) and the respirometric data generated through batch experiments carried out using platinum group metals (PGMs) (see Chapter 6). This hybrid model was named ASM1_PGM for identification purposes.

Short-cut nitrogen removal processes such as CANON, OLAND and SHARON have been a key interest in recent years for removal of nitrogenous compounds from wastewater. The interesting features of these processes are less oxygen demand (hence low energy for aeration), low sludge production and no (CANON and OLAND) or less (SHARON) carbon source requirement. Therefore, these processes are more suitable for inorganic wastewaters such as metal refinery wastewater (Chapter 2: Literature Review). In recent years, mathematical modelling of autotrophic nitrogen removal processes has been done for various types of wastewaters (van Hulle, 2005; Wyffels *et al.*, 2004, Hao *et al.*, 2002). The autotrophic nitrogen removal process (CANON) can be explained by following two governing equations without considering the biomass synthesis.

$$NH^+_4 + 1.5O_2 \rightarrow NO^-_2 + H_2O + H^+ \quad (22)$$

$$NH^{+}_4 + 1.3NO^{-}_2 \rightarrow \quad 1.02N_2 + 1.3H_2O \qquad (23)$$

Table 2.2 (page 17) shows some of the possible reaction steps that could occur during the transformation of ammonium / ammonia to dinitrogen gas. Enzymes such as ammonia monooxygenase, hydroxylamine oxidoreductase and nitrite reductase may be involved (Jetten *et al.*, 1999). According to Jetten *et al.* (2001), the electron acceptor, nitrite, is reduced to hydroxylamine and later it reacts with the electron donor, ammonium, producing dinitrogen gas. Further, it is observed the hydrazine is the intermediate product in the final step and it is oxidised to dinitrogen gas, producing electrons for the initial reduction of nitrite to hydroxylamine. These intermediate products formed are not considered in the model development (van Hulle, 2005).

7.3.2 Model development procedure

The IWA task Group on Mathematical Modelling for the Design and Operation of Activated Sludge Processes (ASP) used the matrix format introduced by Petersen (1965) who used it in chemical reaction engineering applications (van Hulle, 2005; Henze *et al.*, 1987). The first step of developing the model is to identify the components related to the process model for setting up the Petersen matrix. The second step is to develop the matrix to identify the biological processes occurring in the system. The final step is to calibrate the model using corresponding stoichiometric coefficients and validation of the model.

7.3.2.1 Identification of the components of the model

Although heterotrophic activity and standard denitrification are not parts of autotrophic nitrogen removal processes (CANON and OLAND), certain studies have demonstrated the presence of heterotrophs in autotrophic reactors (Fux *et al.*, 2002). Therefore, the model used by van Hulle (2005) incorporated heterotrophs. This model is further extended by introducing PGMs as inhibitive compound to the enzymatic reactions in the processes, assuming the metal inhibition is non-competitive as described by Lewandowski (1985). Then, components in the ASM1_PGM with metal toxicity are shown in Table 7.5.

7.3.2.2 Developing the process matrix and rate equations

Usually Monod kinetics are used to describe the growth kinetics of microbial systems. However, the maximum specific growth rate (μ_{max}) is dependent on the prevailing environmental conditions such as temperature, pH, oxygen condition, nutrients and toxic substances (Henze *et al.*, 2002). Therefore, if we assumed all the environmental conditions are kept as the optimum conditions except toxic substances, this would lead to retarded growth rates. Then, the effects of metals in autotrophic nitrogen removal processes will have a multiple negative effect as autotrophic micro-organisms have rather slower growth rates compared to heterotrophs. However, how PGM toxicity affects the growth of

autotrophs and heterotrophs is not understood. According to ASM1, growth, decay and hydrolysis are the main processes. Usually hydrolysis processes are slower compared to biological growth (Henze *et al.*, 2002).

Table 7.5: Components of the Petersen matrix for ASM1_PGM (modified from van Hulle, 2005).

Component	Remarks
Readily biodegradable substrates (S_S)	Here S_S is produced from X_S
Oxygen (S_O)	Main electron acceptor
Total ammonium nitrogen (S_{TAN})	Ammonium + Ammonia
Total nitrite nitrogen (S_{TNO2})	Nitrous acid + nitrite
Nitrate (S_{NO3})	
Heterotrophic biomass including denitrifiers (X_H)	
Ammonia oxidising biomass (X_{NH})	
Nitrite oxidising biomass (X_{NO})	
Anammox biomass (X_{AN})	
Slowly biodegradable substrates (X_S)	X_S is produced due to microbial decay
Inert biomass (X_I)	
Soluble PGMs (S_{PGM})	Included for precious metal refinery wastewater

Biodegradable matter (S_S) such as Methyl-i-butylketone (MIBK), 1,2,4-Trimethylbenzene (TMB), and Dibutylamine (DBA) is used in PGM refining and is therefore found in PMR wastewater. The death-generation concept of ASM1 shows S_S could be developed as a result of decay of biomass followed by growth (of heterotrophs) on secondary substrates arising from decay (van Hulle, 2005; van Loosdrecht and Henze, 1999). Considering these factors, the modified model including the PGM interaction in the nitrogen removal process is shown in Figure 7.2.

When microbes use an electron-donor substrate for synthesis, a portion of electrons is initially transferred to the electron-acceptor to provide energy for the conversion of the other portion of electrons into microbial cells (Rittman and McCarthy, 2001). Further, during the decay of cells (due to normal maintenance or predation) a portion of electrons in cell synthesis are transferred to the acceptor to generate more energy and the remainder is converted into non-active organic cell residue (X_I). Hellinga *et al.* (1999) state that unionized ammonia (NH_3) and nitrous acid (HNO_2) are the actual substrates in ammonia oxidisation and nitrite oxidisation respectively. As it is not clear whether the ionized or unionized form of ammonia is the actual substrate for the anammox, total ammonium-nitrogen (TAN = ammonia + ammonium) and total nitrite-nitrogen (TNO_2 = nitrous acid + nitrite) were used as the actual substrate for anammox (van Hulle, 2005).

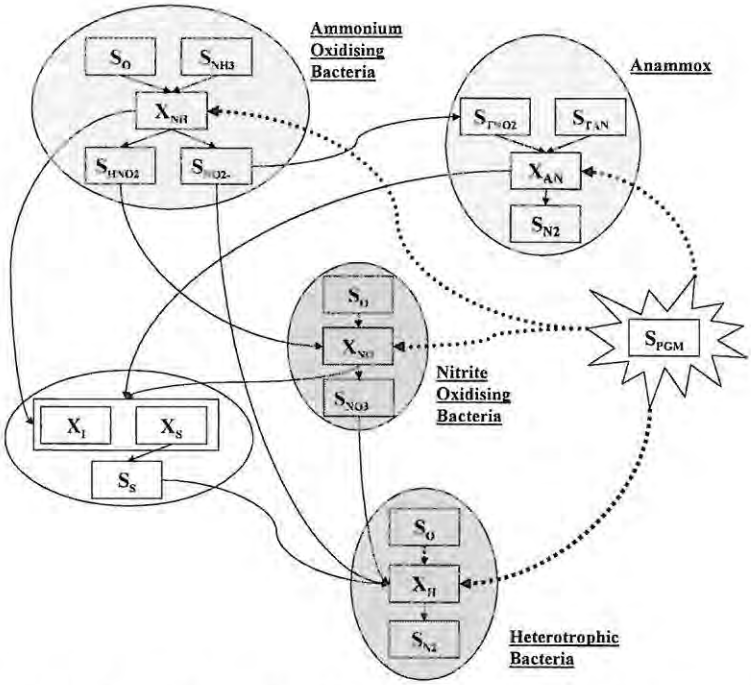

X_{NH} – Ammonia Oxidising Bacteria (AOB), X_{AN} – Anammox bacteria, X_{NO} – Nitrite Oxidising Bacteria (NOB), X_H – Other Heterotrophs (including denitrifiers)

Figure 7.2: Modified model of ASM1_PGM for precious metal refinery wastewater (modified from van Hulle, 2005; Henze *et al.*, 1987).

Nitrite-nitrogen and nitrate-nitrogen could be used as the electron-acceptor in the absence of oxygen for the heterotrophs (anoxic conditions). As oxygen concentration in the reactor is controlled in order to maintain low oxygen conditions conducive to autotrophic nitrogen removal, it can be assumed that heterotrophs use nitrite and nitrate as their terminal electron-acceptors. However, the growth rate of heterotrophs under anoxic conditions is assumed to be lower than the growth rate under oxic conditions (van Hulle, 2005). Further, it was assumed that metals are not directly involved in chemical reactions, but bind or alter the active sites of enzymes vital for nitrification and denitrification. Therefore, no stoichiometric relations were incorporated, similar to oxygen inhibition in anoxic environment (Henze *et al.*, 1987). Table 7.6 shows the kinetics equations used in ASM1.e as used by van Hulle (2005). This has been expanded to accommodate the metal toxicity in the aerobic- and anaerobic- ammonium oxidation using kinetics used by Lewandowski (1985). Table 7.7 presents the stoichiometric coefficients for each component. Table 7.8 presents stoichiometric parameters of ASM.e and yield coefficients (Van Hulle, 2005).

As shown in Figure 7.2, the nitrite (NO_2^-) and nitrate (NO_3^-) could be used as electron acceptors by the heterotrophs in the absence of oxygen. Further, in completely autotrophic nitrogen removal processes, it is intended to keep lower oxygen concentrations in reactors. Therefore, heterotrophs may use nitrite

Table 7.6: Kinetic equations for ASM1_PGM (Modified from ASM1 and van Hulle, 2005).

No. (*j*)	Process	Process rate equation, ρ_j (M/L^3/T)
1	Hydrolysis of entrapped organics	$k_H * \left(\frac{X_S / X_H}{K + X_S / X_H} \right) * X_H$
2	Hydrolysis of entrapped organic nitrogen	$k_H * \left(\frac{X_S / X_H}{K + X_S / X_H} \right) * \left(\frac{X_{ND}}{X_S} \right) * X_H$
3	Ammonification of soluble organic nitrogen	$k_a * S_{ND} * X_H$
4	Growth of heterotrophs (X_H)	$\mu_H^{\max} * e^{\theta_H^{growth} * (T - T_r)} * \left(\frac{S_O}{K_{O,H} + S_O} \right) * \left(\frac{S_S}{K_{S,H} + S_S} \right) * \prod_{n=1}^{n} \left(\frac{K_{PGM,n}}{K_{PGM,n} + S_{PGM,n}} \right) * X_H$
5	Decay of heterotrophs (X_H)	$b_H * e^{\theta_H^{decay} * (T - T_r)} * X_H$
6	Growth of X_H on X_{NO-3}	$\mu_H^{\max} * e^{\theta_H^{growth} * (T - T_r)} * \eta_{NO3} * \left(\frac{K_{O,H}}{K_{O,H} + S_O} \right) * \left(\frac{S_{NO3}}{K_{NO3,H} + S_{NO3}} \right) * \left(\frac{S_{NO3}}{S_{TNO2} + S_{NO3}} \right) * \left(\frac{S_S}{K_{S,H} + S_S} \right) * \prod_{n=1}^{n} \left(\frac{K_{PGM,n}}{K_{PGM,n} + S_{PGM,n}} \right) * X_H$
7	Growth of X_H on X_{TNO-2}	$\mu_H^{\max} * e^{\theta_H^{growth} * (T - T_r)} * \eta_{NO2} * \left(\frac{K_{O,H}}{K_{O,H} + S_O} \right) * \left(\frac{S_{TNO2}}{K_{TNO2,H} + S_{TNO2}} \right) * \left(\frac{S_{NO2}}{S_{NO2} + S_{NO3}} \right) * \left(\frac{S_S}{K_{S,H} + S_S} \right) * \prod_{n=1}^{n} \left(\frac{K_{PGM,n}}{K_{PGM,n} + S_{PGM,n}} \right) * X_H$
8	Growth of X_{NH}	$\mu_{NH}^{\max} * e^{\theta_{NH}^{growth} * (T - T_r)} * \left(\frac{S_O}{K_{O,NH} + S_O} \right) * \left(\frac{S_{NH3}}{K_{NH3,NH} + S_{NH3}} \right) * \prod_{n=1}^{n} \left(\frac{K_{PGM,n}}{K_{PGM,n} + S_{PGM,n}} \right) * X_{NH}$

Table 7.6 (cont'd): Kinetic equations for ASM1_PGM (Modified from ASM1 and van Hulle, 2005)

No. (*j*)	Process	Process rate equation, ρ_j (M/L^3/T)
9	Decay of X_{NH}	$b_{NH} * e^{\theta_{NH}^{deacy} * (T-T_r)} * X_{NH}$
10	Growth of X_{NO}	$\mu_{NO}^{\max} * e^{\theta_{NO}^{growth} * (T-T_r)} * \left(\frac{S_O}{K_{O,NO} + S_O}\right) * \left(\frac{S_{HNO2}}{K_{HNO2,NO} + S_{HNO2}}\right) * \prod_{n=1}^{n} \left(\frac{K_{PGM,n}}{K_{PGM,n} + S_{PGM,n}}\right) * X_{NO}$
11	Decay of X_{NO}	$b_{NO} * e^{\theta_{NO}^{deacy} * (T-T_r)} * X_{NO}$
12	Growth of X_{AN}	$\mu_{AN}^{\max} * e^{\theta_{AN}^{growth} * (T-T_r)} * \left(\frac{S_{TAN}}{K_{TAN,AN} + S_{TAN}}\right) * \left(\frac{S_{TNO2}}{K_{TNO2,AN} + S_{TNO2}}\right) * \left(\frac{K_{O,AN}}{K_{O,AN} + S_O}\right) * \prod_{n=1}^{n} \left(\frac{K_{PGM,n}}{K_{PGM,n} + S_{PGM,n}}\right) * X_{AN}$
13	Decay of X_{AN}	$b_{AN} * e^{\theta_{AN}^{deacy} * (T-T_r)} * X_{AN}$

Table 7.7: Stoichiometric matrix of soluble and particulate components of ASM1_PGM (modified from van Hulle, 2005).

Component No	1	2	3	4	5	6	7	8	9	10	11	12	13
Name	Oxygen	Readily Biodegradable Substrate	TAN	TNO_2	Nitrate	Nitrogen Gas	Heterotrophs	AOB	NOB	Anammox	Slowly Degradable Substrate	Inert Particulates	Metals
Symbol													
Unit	S_O mgO_2/L	S_S mgCOD/L	S_{TAN} mgN/L	S_{TNO2} mgN/L	S_{NO3} mgN/L	S_{N2} mgN/L	X_H mgCOD/L	X_{NH} mgCOD/L	X_{NO} mgCOD/L	X_{AN} mgCOD/L	X_S mgCOD/L	X_I mgCOD/L	S_{PGM} mg/L
Process No													
Hydrolysis of entrapped organics		1									-1		
Growth of heterotrophs (X_H)	$-(1-Y_H)/Y_H$	$-1/Y_H$	$-i_{nbm}$				1						
Decay of heterotrophs (X_H)			$i_{nbm}-f_p i_{nxi}$				-1				$(1-f_i)$	f_i	
Growth of X_H on X_{NO-3}		$-1/Y_{H,NO3}$	$-i_{nbm}$	$(1-Y_{H,NO3})/(1.14Y_{H,NO3})$	$-(1-Y_{H,NO3})/(1.14Y_{H,NO3})$		1						
Growth of X_H on X_{TNO-2}		$-1/Y_{H,NO2}$	$-i_{nbm}$	$-(1-Y_{H,NO2})/(1.71Y_{H,NO2})$		$(1-Y_{H,NO2})/(1.71Y_{H,NO2})$	1						
Growth of X_{NH}	$-(3.43-Y_{NH})/Y_{NH}$		$-1/Y_{NH}-i_{nbm}$	$1/Y_{NH}$				1					
Decay of X_{NH}			$i_{nbm}-f_p i_{nxi}$					-1			$(1-f_i)$	f_i	
Growth of X_{NO}	$-(1.14-Y_{NH})/Y_{NH}$		$-i_{nbm}$	$-1/Y_{NO}$	$1/Y_{NO}$				1				
Decay of X_{NO}			$i_{nbm}-f_p i_{nxi}$						-1		$(1-f_i)$	f_i	
Growth of X_{AN}			$-1/Y_{AN}-i_{nbm}$	$-1.52-1/Y_{AN}$	1.52	$2/Y_{NO}$				1			
Decay of X_{AN}			$i_{nbm}-f_p i_{nxi}$							-1	$(1-f_i)$	f_i	

and nitrate as electron acceptors. However, due to the slower growth rates of heterotrophs in inorganic wastewaters (e.g. metal refinery), there would be a close competition over the oxygen between autotrophs and heterotrophs. But, autotrophs have the advantage of having necessary inorganic electrons donors such as ammonium / ammonia and hence under these conditions will have better growth rates compared to heterotrophs.

Autotrophic decay rates have a major impact on nitrification in WWTP design and operation due to wash-out (by varying HRT and SRT) or overload (substrate inhibition) depending on the bio-kinetics parameters selected for plant performance (Manser *et al.,* 2006). Further, modelling of nitrification process as a single step is a major drawback in ASM as bio-kinetics of AOBs and NOBs can not be distinguished. Therefore, van Hulle (2005) model gives insight into the nitrification process as it has separated the nitrification as two step processes. A detailed discussion on modelling of nitrification, heterotrophic growth and predation in ASP can be found in Moussa *et al.*(2005). Table 7.9 shows parameters related to nitrification and denitrification processes.

Table 7.8: Stoichiometric parameters of ASM.e and Yield coefficients (Van Hulle, 2005).

Symbol	Definition	Value	Units
$Y_{H,O}$	Heterotrophic yield on oxygen	0.67	gCOD/gCOD
$Y_{H,NO3}$	Heterotrophic yield on nitrate	0.54	gCOD/gCOD
$Y_{H,TNO2}$	Heterotrophic yield on TNO2	0.54	gCOD/gCOD
$Y_{NH,O}$	Autotrophic yield of X_{NH}	0.15	gN/gCOD
$Y_{NO,O}$	Autotrophic yield of X_{NO}	0.041	gN/gCOD
Y_{AN}	Autotrophic yield of X_{AN}	0.159	gN/gCOD
f_P	Production of X_I from decay	0.1	gCOD/gCOD
i_{nxi}	N content of X_I	0.02	gN/gCOD
i_{nbm}	N content of biomass	0.0583	gN/gCOD

7.3.2.3 Mass balance over reactor and clarifier

In order to find the effects of HRT, SRT and recycle ratio on the removal of nitrogenous compounds from the proposed model, general mass balance based equations were obtained considering Figure 7.3 as described by Fouad and Bhargava (2005). For modelling the nitrogen compounds from a given reactor, we can consider the mass balance over the reactor and clarifier in case of recirculation of the effluent back to the reactor inlet for improved biomass retention (activated sludge). Figure 7.3 shows a schematic diagram of a reactor and a clarifier whose two control volumes could be used to balance the mass of incoming to each compartment. Volumetric flow rates are indicated in Q, substrates are indicated in S and biomass is represented as X. Subscript "i" and "o" indicate inlet and outlet of each compartment. Subscript "j" indicates different substrates (j = 1,2,....)

Table 7.9: Parameters related to nitrification and denitrification processes (updated from van Hulle, 2005)

Symbol	Definition	Value (at 20°C)	Units
k_h	Maximum specific hydrolysis rate	3	gCOD/gCOD/d
K_x	Saturation constant for slowly biodegradable substrates	0.03	gCOD/gCOD/d
μ^{max}_H	Maximum growth rate of X_H	6	1/d
$K_{O,H}$	Saturation constant for S_O of X_H	0.2	mgO_2/L
$K_{S,H}$	Saturation constant for S_S of X_H	20	mgCOD/L
b_H	Decay rate of X_H	0.62	1/d
η_{NO3}	Anoxic reduction factor for NO^-_3	0.6	-
η_{TNO2}	Anoxic reduction factor for TNO_2	0.6	-
$K_{NO3,H}$	Saturation constant for S_{NO3} of X_H	1	$mgNO^-_3 - N/L$
$K_{TNO2,H}$	Saturation constant for S_{TNO2} of X_H	1	$mgTNO^-_2 - N/L$
μ^{max}_{NH}	Maximum growth rate of X_{NH}	0.8	1/d
$K_{O,NH}$	Saturation constant for S_O of X_{NH}	0.6	mgO_2/L
$K_{NH3,NH}$	Saturation constant for S_{NH3} of X_{NH}	0.75	$mgNH_3 - N/L$
b_{NH}	Decay rate of X_{NH}	0.05	1/d
μ^{max}_{NO}	Maximum growth rate of X_{NO}	0.79	1/d
$K_{O,NO}$	Saturation constant for S_O of X_{NO}	1.5	mgO_2/L
$K_{HNO2,NO}$	Saturation constant for S_{HNO2} of X_{NO}	8.723×10^{-4}	$mgHNO^-_2 - N/L$
b_{NO}	Decay rate of X_{NO}	0.033	1/d
μ^{max}_{AN}	Maximum growth rate of X_{AN}	0.019	1/d
$K_{O,AN}$	Inhibition constant for S_O of X_{AN}	0.01	mgO_2/L
$K_{TNO2,AN}$	Saturation constant for S_{TNO2} of X_{AN}	0.05	$mgTNO^-_2 - N/L$
$K_{TAN,NH}$	Saturation constant for S_{TAN} of X_{AN}	0.07	mgTAN – N/L
b_{AN}	Decay rate of X_{AN}	0.0025	1/d
K_{Pt}	Half-saturation inhibition coefficient for Pt	15.81	mg/L
K_{Pd}	Half-saturation inhibition coefficient for Pd	25.00	mg/L
K_{Rh}	Half-saturation inhibition coefficient for Rh	33.34	mg/L
K_{Ru}	Half-saturation inhibition coefficient for Ru	39.25	mg/L

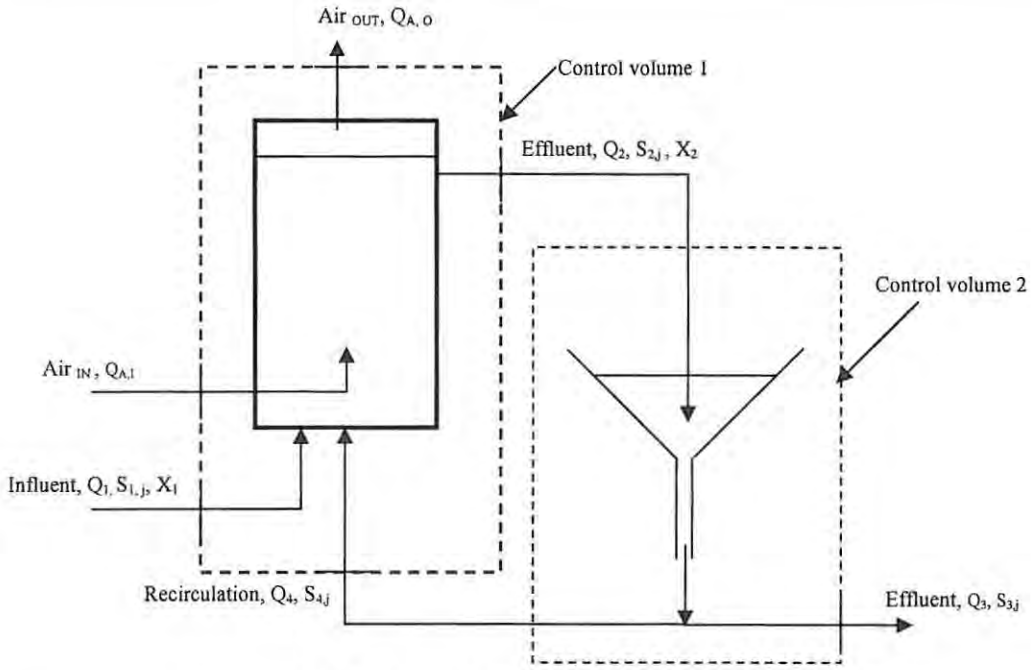

Figure 7.3: Mass transport in reactor and clarifier.

Considering the control volume 1, substrate balance, rate of accumulation of substrate j in the reactor are described by:

$$\frac{dS_{2,j}}{dt} = Q_1 S_{1,j} + Q_4 S_{4,j} - Q_2 S_{2,j} - aVJ - \left(VX_2 \frac{KS_{2,j}}{K_s + S_{2,j}} \right) \tag{7.24}$$

Where Q = flow rate, a = specific surface area of the biofilm, V = volume of the reactor, J = substrate flux into the biofilm, K_s = Monod half saturation coefficient, and K = maximum specific rate of substrate utilization.

Biomass balance, rate of biomass growth in the reactor can be written as:

$$\frac{dX_2}{dt} = VX\left[\frac{YKS_{2,j}}{K_s + S_{2,j}} - K_d \right] + YaVJ\frac{b_s}{b_t} - (Q_2 X_2) \tag{7.25}$$

Where Y = yield coefficient, b_S = specific shear loss rates, b_t = sum of specific decay and shear loss rates, K_d = specific decay rate.

Similarly, for control volume 2, substrate balance, rate of accumulation of substrate j in the reactor:

$$\frac{dS_{\bar{2},j}}{dt} = Q_1 S_{1,j} + Q_4 S_{4,j} - Q_2 S_{2,j} - aVJ - \left(VX \frac{KS_{\bar{2},j}}{K_s + S_{\bar{2},j}} \right) \tag{7.26}$$

and biomass balance for clarifier (control volume 2):

$$\frac{dX_{\bar{2}}}{dt} = V_c X_{\bar{2}} \left[\frac{YKS_{\bar{2},j}}{K_s + S_{\bar{2},j}} - K_d \right] + YaV_c J \frac{b_s}{b_t} - Q_3 X_{\bar{2}} - Q_4 X_{\bar{2}} \qquad (7.27)$$

Where Y = Yield coefficient, b_S = specific shear loss rates, b_t = sum of specific decay and shear loss rates, K_d = specific decay rate, V_c = clarifier volume, subscript $\bar{2}$ denotes the average properties in the clarifier.

7.3.3 Model calibration

The selection of values for the kinetics and stoichiometric coefficients (see Tables 7.7, 7.8 and 7.9) of a mathematical model is known as model calibration (Jeppsson, 1996). Usually this is done by specific and well-controlled experiments carried out at pilot and bench-scale experiments. According to Jeppsson (1996), values obtained through this type of approach may not be totally reliable. The first reason for this is the difficulty of configuring and operating a small-scale plant exactly the same way as a full-scale plant and thereby introducing a risk of changing the behaviour of microorganism population and also the conditions that influence the values of the parameters which should be determined. Secondly, the experiments and calculations are based on the fact that the coefficients are constant during the experimental period which can take from minutes to weeks, depending on the parameters to be determined. Petersen *et al.* (2003) presented a simplified method to assess structurally identifiable parameters in Monod-based ASP models. They used the Taylor series expansion approach and the output (measured variable) vector, $\underline{y}$ and its derivatives with respect to time were assumed to be known. Petersen (2000) presented a detailed discussion on calibration and identification of model parameters in activated sludge models. Viotti *et al.* (2002) presented a mathematical model and a calibration procedure for biofiltration process.

7.3.4 Model validation

In this model, experimental data and data from a literature survey are used to compare the values simulated or estimated in the model. Some of the parameters which can be used during the simulation study are shown in Tables 7.4, 7.7 and 7.11. Figure 7.4 shows the solving algorithm for the proposed model (ASM1_PGM) for metal refinery wastewater. A sensitivity analysis was carried out to find the effect model parameter variations in the calibration process. This was done using the simulation environment and most appropriate model parameter values were selected from the literature. These are presented in Chapter 8.

7.3.5 Limitations of the model

Simplifying assumptions (one-dimensional multi-substrate and multi-species) of biofilm modelling was used here. The most significant restriction of this program is the one-dimensional in space

assumption which is not valid for biofilms consisting of three dimensional, mushrooms like structures (Wanner and Morgenroth, 2004).

7.4 Simulation and scenario analysis

The simulation study was performed using MATLAB 7.0 / Simulink 6.0 (The Mathworks Inc. USA). One-dimensional multi-substrate and multi-species biofilm model was assumed for biofilm simulation (Wanner and Morgenroth, 2004; Reichert *et al.*, 1995).

7.5 Interim conclusions

A model for nitrogen removal in precious metal refinery wastewaters (ASM1_PGM) was developed based on ASM1, autotrophic nitrogen removal process modelled by van Hulle (2005) based on ASM1 and incorporating metal toxicity inhibition used by Lewandowski (1985). In ASM1_PGM, identifying the respective parameters for the given process was the most important aspect of the validation of the model. Initially, values for each unknown parameter were adopted from the literature. However, it should be noted that those values could be significantly different from the actual values under different sets of reactor operating conditions. Therefore, it is necessary to run batch tests to find out more reliable values for the proposed model. Chapter 8 presents the approximate model calibration and simulation results.

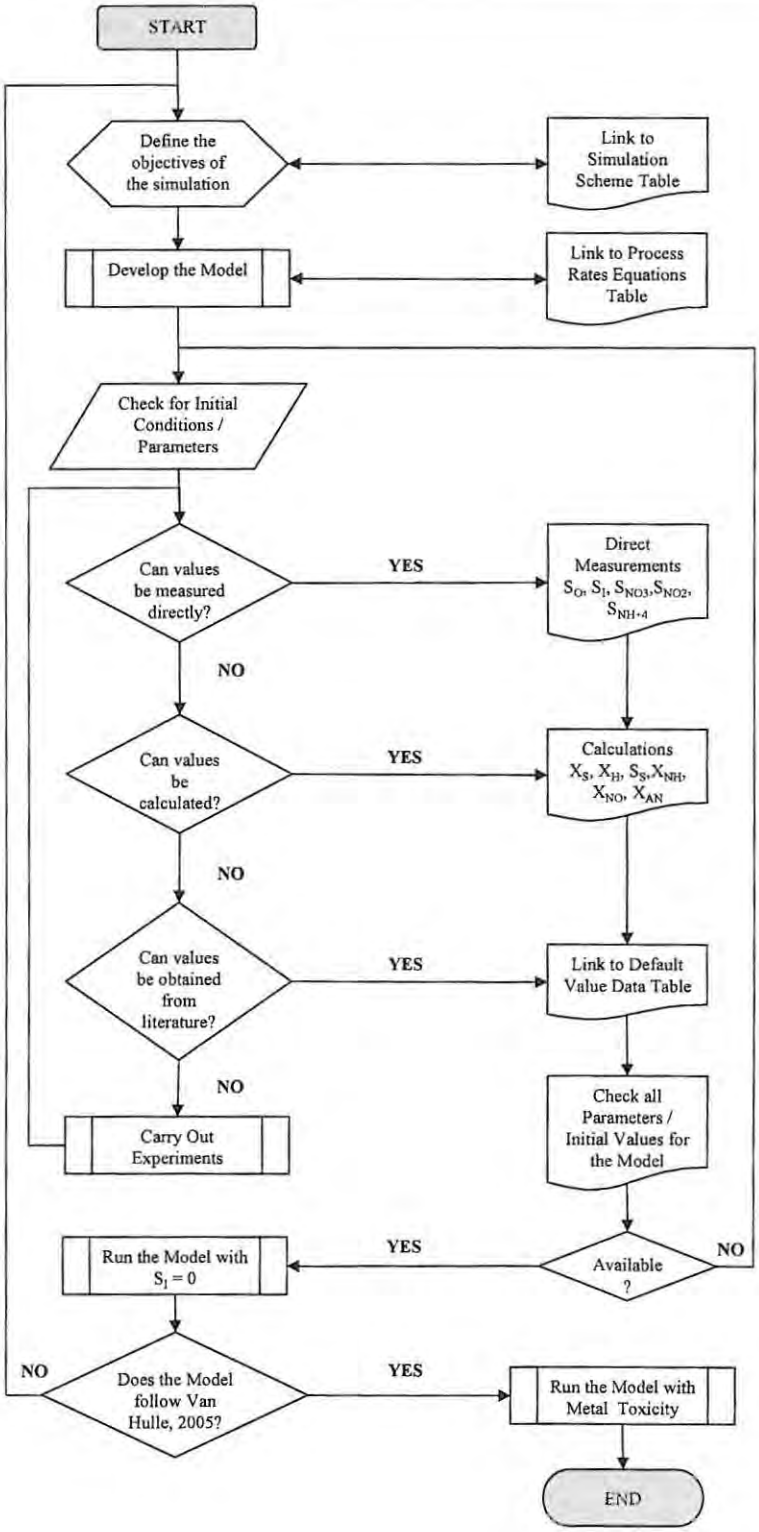

Figure 7.4: Equation solving algorithm for the model of nitrogen removal in metal refinery wastewater.

CHAPTER 8

You seldom accomplish very much by yourself. You must get the assistance of others.

- Henry Kaiser (1882-1967).

8.0 Simulation and approximate calibration of ASM1_PGM for nitrogenous compounds removal from precious metal refinery (PMR) wastewater

8.1 Introduction

During the last decade, the dynamic simulation of wastewater treatment processes has achieved a significant improvement and popularity not only among academics but also among industrial practitioners (Bury *et al.*, 2001). This is mainly due to the development of unifying biokinetics models such as Activated Sludge Model 1 (ASM1), ASM2, ASM2d and ASM3 as well as increasing affordability of personal computers (PCs) with a considerable amount of processing power (Bury *et al.*, 2001; Henze *et al.*, 1987). Apart from the unified ASMs and PCs, dedicated software tools have been developed in the recent past by many software vendors (Morgenroth *et al.*, 2002; Vanhooren *et al.*, 2003). Therefore, process modelling and simulation can be carried out using traditional high level programming languages like C, C++, and Pascal, general purpose simulators like MATLAB/Simulink, closed dedicated (built-in models) simulators like BioWin, EFOR, and STOAT, and open dedicated simulators (built-in models and user defined models) like Aquasim, SIMBA and WEST (Van Hulle, 2005; Vanhooren *et al.*, 2003; Olsson and Newell, 2001). Usually, a general purpose simulation environment such as MATLAB/Simulink gives a greater flexibility to the modeller with sound programming skills than the open dedicated software such as WEST and Aquasim due to wide spread use in academics and industrial establishments, abundance of literature on application developments, extensive built-in on-line and off-line documentation, readily available in-house assistance in most places (e.g. universities and R & D institutions) and public access through internet forums etc (Alex *et al.*, 2001).

Simulation of mathematical models enables the designer to predict, evaluate and control the detailed design processes prior to construction under different conditions. However, modelling of ill-defined systems such as biological wastewater treatment processes compared to well-defined systems based on fundamental mass and energy balance principles (e.g. electrical and mechanical systems) are more complex and challenging to the designer (Vanhooren *et al.*, 2003). Therefore, careful modelling, system identification and calibration of mathematical models developed for biological processes are vital for predicting the process performance correctly (Olsson and Newell, 2001).

Model-based evaluations of wastewater treatment processes have been done for different applications in the recent past (Hao and van Loosdrecht, 2004; Spanjers *et al.*, 2001). Most of these model-based evaluations have been focussed mainly on municipal wastewaters and they have rarely been used for high strength industrial wastewaters as a result of the complexity of biological inhibitions effected by the presence of numerous compounds (Bury *et al.*, 2001). Biological treatment of high strength

industrial wastewaters has a greater potential in attenuating the environmental stress exerted by those industries. However, long acclimatisation periods required by responsible microbes, lack of detailed knowledge on microbial toxicity of industrial wastewaters (e.g. mining industry and PGM metal toxicity to biological wastewater treatment), significant time taken to investigate various parameters affecting the processes (e.g. usually it is preferred to have 6-8 sludge ages to evaluate the effect of change of a particular variable such as metal toxicity in ASP) have hindered progress. Therefore, model based evaluation of potential of biological treatment of industrial wastewaters is a favourable course of action due to possible significant cost reduction, time saving and fast dynamic results prior to lab / pilot scale experiments. The objectives of this chapter are to present the results of simulation, sensitivity analysis, verification and calibration of the model developed (ASM1_PGM) for nitrogenous compounds removal from precious metal refinery (PMR) wastewater as described in Chapter 7.

8.2 Materials and methods

This section explains how the model was implemented in the MATLAB environment, simulation and approximate model calibration using a sensitivity analysis.

8.2.1 Model implementation and simulation

The model developed in Chapter 7 was implemented in MATLAB 7.0 / Simulink 6.0 (The Mathworks Inc., USA). First the ASM1_PGM was implemented in the MATLAB Script Editor (scripts are given in Appendix E). The model was simplified by neglecting the terms for ammonification and entrapped organic nitrogen hydrolysis. Table 8.1 shows the initial conditions used for the steady state simulation of the model described above under aerobic and anoxic conditions. As experimental work was carried out at mean room temperature of 20 °C, the default values for parameters in ASM1 were chosen. No temperature corrections were considered during the simulation as proposed in the model (see Chapter 7).

It is noted that the biomass fractions such as heterotrophs, AOB, NOB, etc. could not be established by experimental work in this research. This information is required to implement the model described in Chapter 7 (see Table 7.7 of Chapter 7). Based on the experimental work, the MLVSS was 38 % of the MLSS (mean value, data shown in Appendix E, Table E1). Therefore, it was assumed that 50, 25, 15, and 5 % of the MLVSS were contributed by heterotrophs (X_H), AOB (X_{AOB}), NOB (X_{NOB}) and Anammox bacteria (X_{ANX}), respectively for simulation purposes. Therefore, the simulation work presented here is a guide but does not exactly represent all the real conditions that prevailed in the reactors, as many of the state variables and parameters were not determined experimentally.

Table 8.1: Initial conditions used to find the steady state states.

Component	Notation (x)	Concentrations (mg/l)	
		Aerobic	Anoxic
Dissolved oxygen (S_O)	-	2.5	0.0
Soluble organic compounds (S_S)	x(1)	10	15
Total ammonium (TAN)	x(2)	69	35
Total nitrite (TNO_2)	x(3)	0.03	0.02
Nitrate (NO_3^-)	x(4)	68	111
Heterotrophic biomass (X_H)	x(5)	523	523
Ammonium oxidisers (X_AOB)	x(6)	262	262
Nitrite oxidisers (X_NOB)	x(7)	157	157
Anammox biomass (X_ANX)	x(8)	5	52
Slowly degradable organics (X_S)	x(9)	52	52

8.2.2 Sensitivity analysis:

A sensitivity analysis using the simulation was carried out to identify the model parameters which were highly sensitive in predicting the model behaviour. This was done by varying the values in different percentages in the model parameters and evaluating the final output in comparison with the experimental results. It should be noted that the sensitivity analysis was carried out as a *short-cut* method to calibrate the model, but it should not be considered as a replacement for experimental parameter estimation, which is vital under the given wastewater conditions. Four parameters were selected as initial estimates: Yield coefficients for heterotrophic (Y_H) and ammonium oxidising biomass (Y_{AOB}), ammonium (K_{NH3}) and oxygen (K_{OA}) half-saturation constant for AOB (X_{AOB}). Each parameter was changed by different percentages and the fitness of the model prediction with the measured output was observed. The best fitting value (which is the value least error occurred between simulation and measured values) was used in searching the next parameter and similarly this was altered by different percentages to find the best fitting values. This was repeated for all the selected parameters and for simplification purposes only the NH_4^+-N and NO_3^--N model outputs were considered.

8.3 Results

The results are presented in the different sections: steady state, dynamic simulations of the model described in Chapter 7 using the CSTR and PBR, and sensitivity analysis for approximate model calibration.

8.3.1 Steady state analysis of process performance in the CSTR and PBR

Steady state analysis carried out for NH_4^+-N removal and NO_3^--N formation in the CSTR using the initial conditions presented in Table 8.1 is shown in Figure 8.1, which summarises the effect of

different [Rh] on NH_4^+-N removal and NO_3^--N formation in the CSTR. Figure 8.1a shows that an increase in [Rh] causes a dramatic increase in the time taken to reach steady state in NH^+_4-N removal. Accordingly, Figure 8.1b followed a similar trend for NO^-_3-N formation with the increase of [Rh]. Figure 8.1c presents how AOB responded to the increased [Rh]. It clearly showed at lower [Rh] < 10 mg/l, there was a growth of AOB, whereas at higher [Rh] (> 15 mg/l) no clear growth could be observed. According to Figure 8.1d, NOB were more sensitive to increased [Rh] as there was no growth at all for all the Rh concentrations. Similar results to those were observed as shown in Figure 8.1b with respect to SOU under the metal toxicity studies described in Chapter 6 (see Figures 6.2, 6.4, 6.6 and 6.8; Figure 6.6 exclusively showed the effect of different [Rh] on SOU, page numbers 83, 86, 88 and 90, respectively). This is due to the fact that the SOU is proportional to NH_4^+ oxidation and NO_3^- formation and thus both studies showed similar trends. Figure 8.1 presents the effect of metal toxicity on nitrification as expected under the theoretical framework and corroborates the findings in Chapter 6.

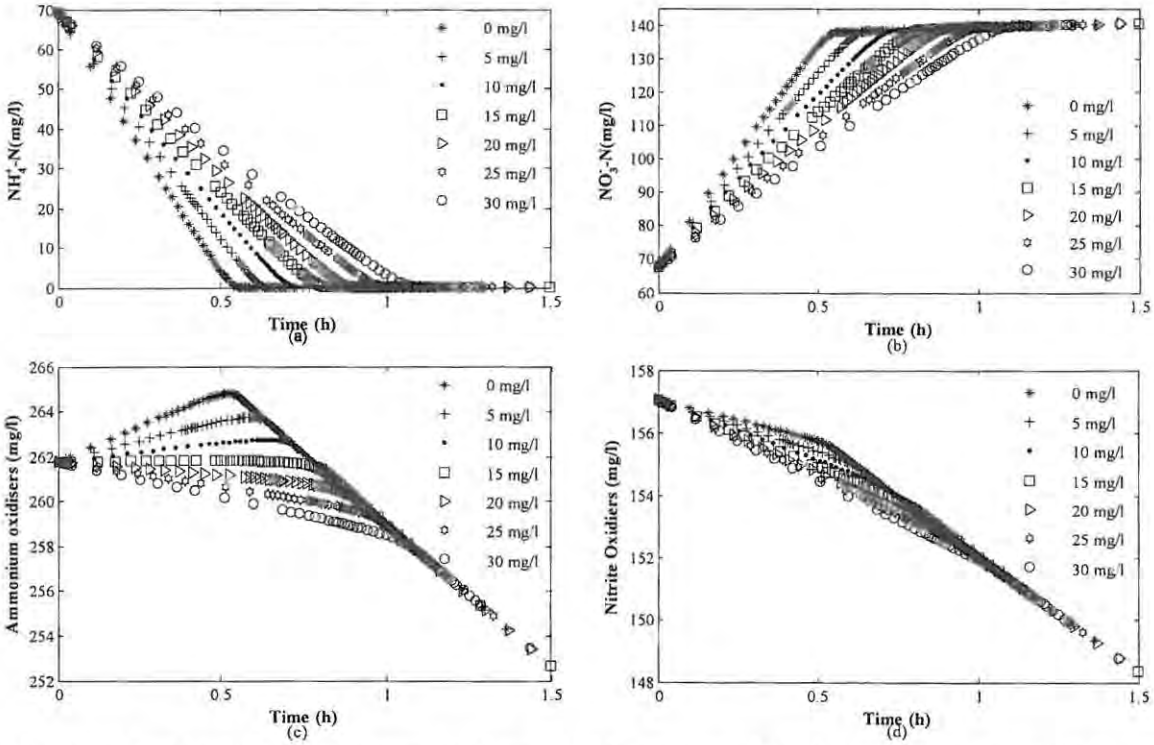

Figure 8.1: The effect of different [Rh] on NH_4^+-N removal, NO_3^--N formation, growth / decay of ammonium oxidisers (AOB) and nitrite oxidisers (NOB) under aerobic conditions.

Figure 8.2 summarises the effect of different [Rh] on denitrification in the PBR. Similar to the above description, the toxicity effect on microbial growth for different [Rh] determined in Chapter 6 could be observed again here. Even though a toxicity study similar to the one described above was not carried out under anoxic conditions, the effect of increased [Rh] on the final steady state [NO_3^--N] was evident in Figure 8.2b. This is complemented by Figure 8.2c, as increased [Rh] had led to the lowest final

heterotrophic biomass concentration. However, according to Figure 8.2d, Anammox biomass showed robust behaviour with respect to different [Rh]. This could be because the default parameter values used for Anammox organisms did not adequately represent the metal toxicity effects on them. Therefore, further research would be highly recommended when the Anammox process is adapted to PMR wastewaters.

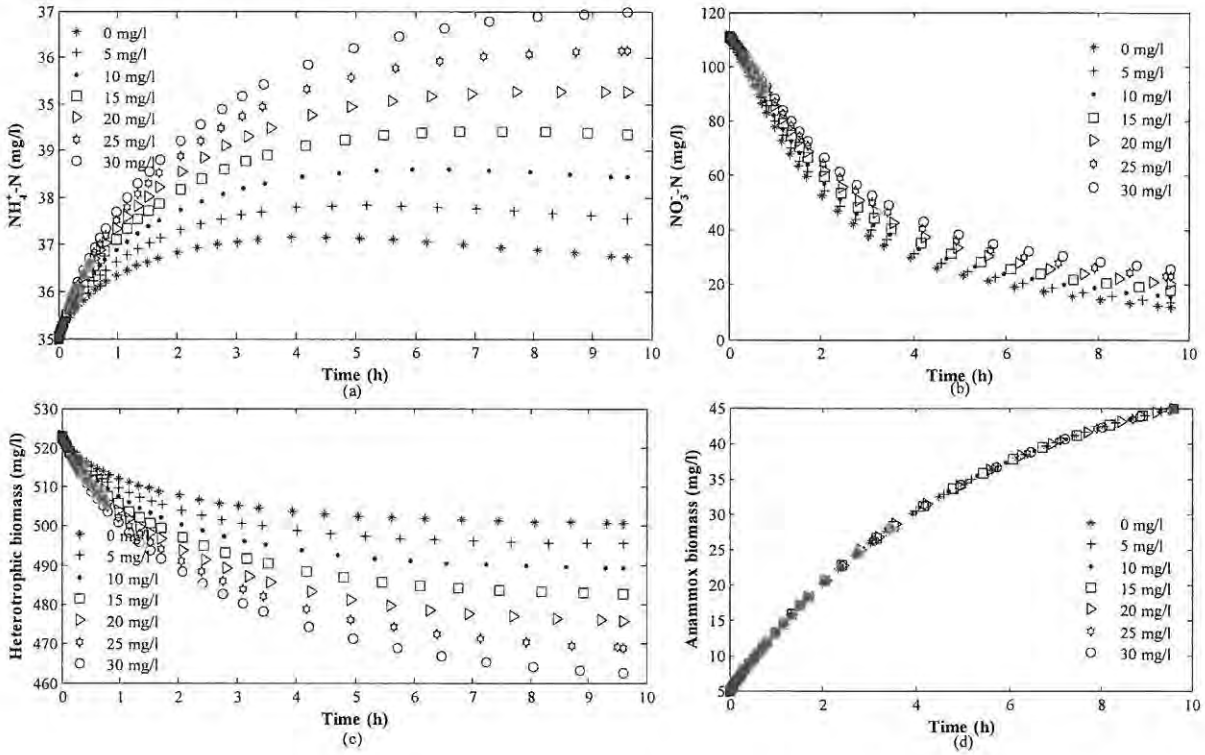

Figure 8.2: The effect of different [Rh] on NH_4^+-N formation, NO_3^--N removal, growth / decay of heterotrophic denitrifiers (X_H) and Anammox (X_{ANX}) under anoxic conditions.

8.3.2 Dynamic simulation of the CSTR performance

Dynamic simulation of performance of the CSTR was carried out using the experimental data collected over > 80 days. As shown in Figure 8.3, the model under performed compared to the measured state variables. The predicted final concentration of NH_4^+-N reached almost complete removal, whereas the measured values greatly differed from the model prediction. Further, no similarities in the trends in the two respective values (i.e. correlation between model and measured values) were observed. However, the predicted final concentration of NO_3^--N in the CSTR has followed a similar trend as the corresponding measured values (Figure 8.3b). A similar trend could also be observed in the final COD concentration (Figure 8.3d). This strongly suggests the need for parameter calibration to correct the model prediction. It was noted that the default parameter values used for the simulation work did not accurately represent the simulated wastewater. They have been proposed for or determined based predominantly on municipal wastewater. The wastewater used in this experiment was simulated metal refinery wastewater, which contained more toxic concentrations of metal those normally found in the municipal wastewaters.

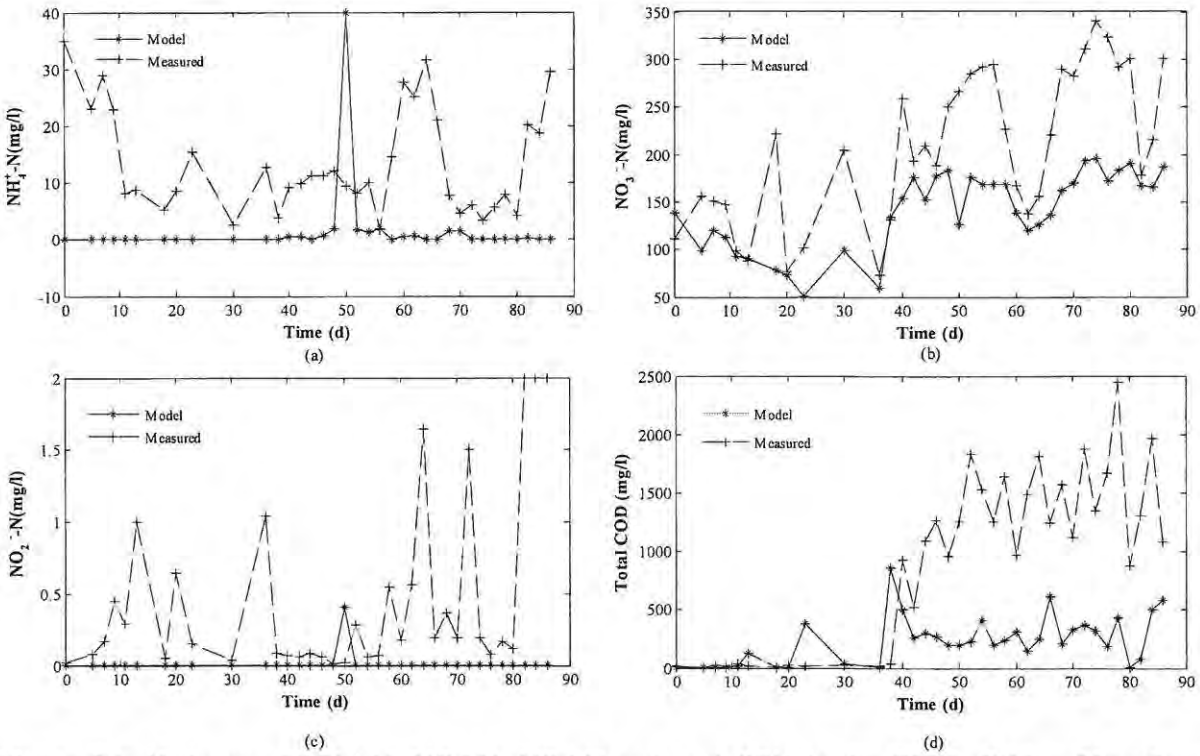

Figure 8.3: Variation of NH_4^+-N, NO_3^--N, NO_2^--N and total COD in the CSTR. [Rh] = 20 mg/l and dissolved oxygen [DO] = 2.5 mg/l.

8.3.3 Dynamic simulation of the PBR performance

Figure 8.4 shows the dynamic simulation performance of the PBR. The model predicted final NH_4^+-N in the PBR had an approximate similar trend to the measured value (Figure 8.4a).

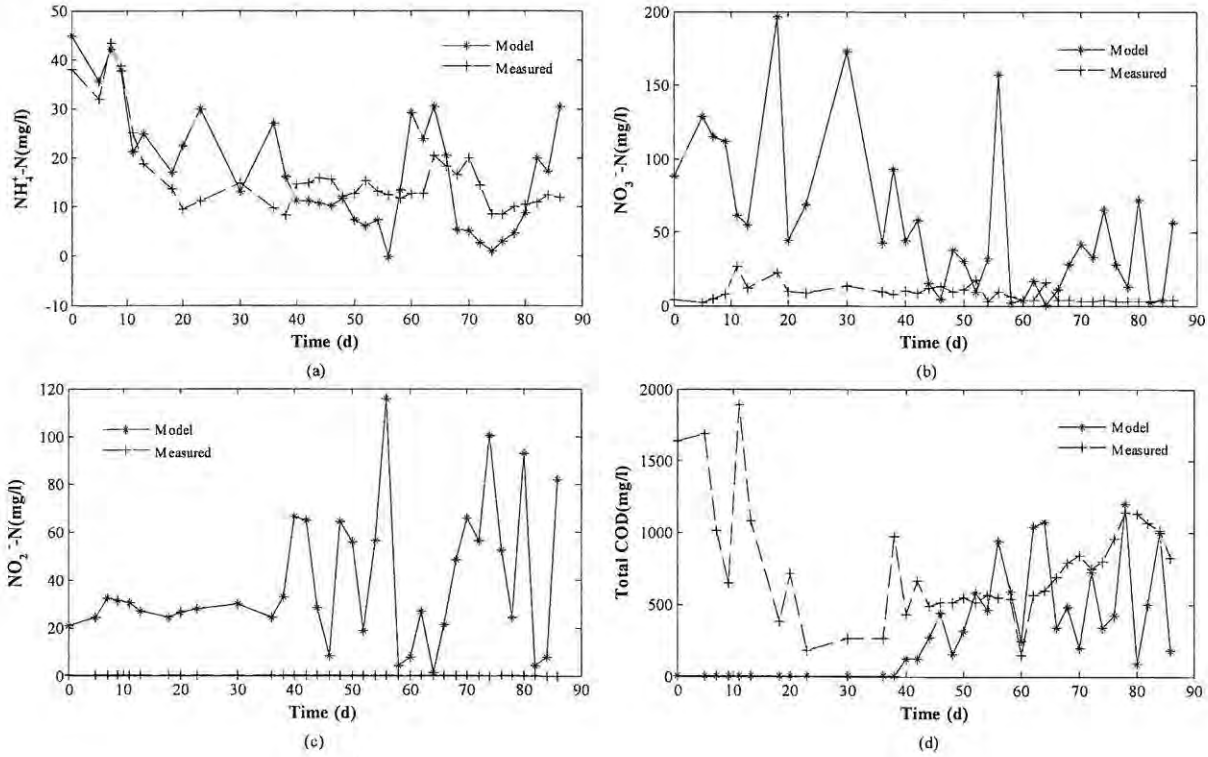

Figure 8.4: Variation of NH_4^+-N, NO_3^--N, NO_2^--N and total COD in the PBR. [Rh] = 20 mg/l and dissolved oxygen [O_2] = 0 mg/l.

A similar trend could be observed for final COD, even though the prediction during the initial period (day 0 to 40 in Figure 8.4d) did not follow the measured values. The model has over performed compared to the measured state variables in the PBR. This could be due to the assumption made during the mass balance calculation, as the completely mixed conditions assumed in the PBR were not a true description. Therefore, Figure 8.4 clearly shows the need for proper hydraulic modelling of the PBR as well as the parameter calibration required for the given wastewater conditions.

8.3.4 Sensitivity analysis of critical parameters identified in the model

During the model simulation the default parameters shown in Table 8.2 were used. However, dynamic simulation showed a difference between the model prediction and the measured values, as is generally expected. In order to calibrate the model some parameters were selected, as suggested by Henze *et al.* (1987). The values presented in Table 8.2 represent domestic wastewater at neutral pH and 20 °C. This was a major issue as those parameter values were not perfectly suitable for the PMR wastewater type in this simulation. Therefore, the desirability of empirically determining the parameters to be used in a model can not be overemphasised, as those values are strongly dependant on specific factors in the wastewater and on environmental conditions such as pH and temperature (Henze *et al.*, 1987).

Figure 8.5 demonstrates the influence of Y_H and Y_{AOB} on model fitting. As shown in Figure 8.5a, Y_H had a significant effect on the final NH_4^+-N concentration. The best Y_H was found to lie in the range between 10 % and 15 % of the value used originally (0.52 gCOD/gCOD) during the simulation. This value is considerably lower than that proposed for municipal wastewater. This could be due to the metal toxicity and thus low yield of heterotrophs. However, Y_H was not observed to have a similar influence on final NO_3^--N concentration (Figure 8.5b), even though there was an observable change in the output [NO_3^--N]. Similar to Y_H, Y_{AOB} had a greater effect on final [NH_4^+-N] (Figure 8.5c) even though the change was 5 % of the originally assumed value. The best range of Y_{AOB} was found to lie between 95 % and 105 % of 0.19 gCOD/gCOD. However, Y_{AOB} changes had little impact on output [NO_3^--N] (Figure 8.5b *cf* Figure 8.5d). Simulation data relevant to Figure 8.5 are given in Appendix E: Tables E2 to E5.

Figure 8.6 presents the effects of half-saturation coefficients of ammonium (K_{NH3}) and oxygen (K_{OA}) on final [NH_4^+-N] and [NO_3^--N]. The smallest difference between the model prediction and the measured value of [NH_4^+-N] was found to lie between 50 % and 85 % of the K_{NH3} (0.52 gNH_4^+-N/m^3, Table 8.2). Similarly, K_{OA} was found at 125 % of the original assumed value (0.235 gO_2/m^3, Table 8.2). However, the effect of both K_{NH3} and K_{OA} on final [NO_3^--N] was insignificant as shown in Figures 8.6b and 8.6d. The primary simulation data relevant to Figure 8.6 are presented in Appendix E: Tables E6 to E9.

Table 8.2: Parameter selection for simulation of ASM1_PGM.

Parameter	Symbol	Units	Value used (ASM1_PGM)	Default range (Henze *et al.*, 1987)
Stoichiometric parameters				
Yield coefficient for heterotrophs	Y_H	gCOD/gCOD	0.52	0.46 – 0.69
Yield coefficient for autotrophs	Y_A	gCOD/gCOD	0.041 – 0.150	0.07 – 0.28
Particulate biomass fraction	f_P	-		0.08
Nitrogen fraction in biomass	i_{XB}	gN/gCOD	0.02	0.086
Nitrogen fraction in particulate	i_{XP}	gN/gCOD	0.0583	0.06
Kinetic parameters				
Maximum specific growth of heterotrophs	μ_H	1/d	8.72	3 – 13.2
Maximum specific growth of autotrophs	μ_A	1/d	1.36 – 2.02*	0.34 – 0.65
Decay coefficient of heterotrophs	b_H	1/d	2.32*	0.09 – 4.38
Decay coefficient of autotrophs	b_A	1/d	0.092 – 0.190	0.05 – 0.15
Half-saturation coefficient for heterotrophs	K_S	$gCOD/m^3$	50	10 – 180
Half-saturation coefficient of oxygen for heterotrophs	$K_{O,H}$	gO_2/m^3	0.2*	0.01 – 0.15
Half-saturation coefficient of oxygen for autotrophs	$K_{O,A}$	gO_2/m^3	0.235	0.5 – 2.0
Half-saturation coefficient of nitrate	K_{NO}	gNO_3^--N/m^3	1*	0.1 – 0.2
Half-saturation coefficient of ammonium	K_{NH3}	gNH_3-N/m^3	0.52**	0.6 – 3.6
Half-saturation coefficient of hydrolysis	K_X	gCOD/gCOD	0.03**	0.15
Ammonification constant	k_a	m^3/(gCOD.d)	0.016	0.016
Maximum hydrolysis rate	k_h	gCOD/(gCOD.d)	3*	2.2
Correction factor for anoxic X_H	η_g	-		0.6 – 1.0
Correction factor for hydrolysis under anoxic conditions	η_h	-		0.4

*Wyffels *et al.*, 2004; **van Hulle, 2005.

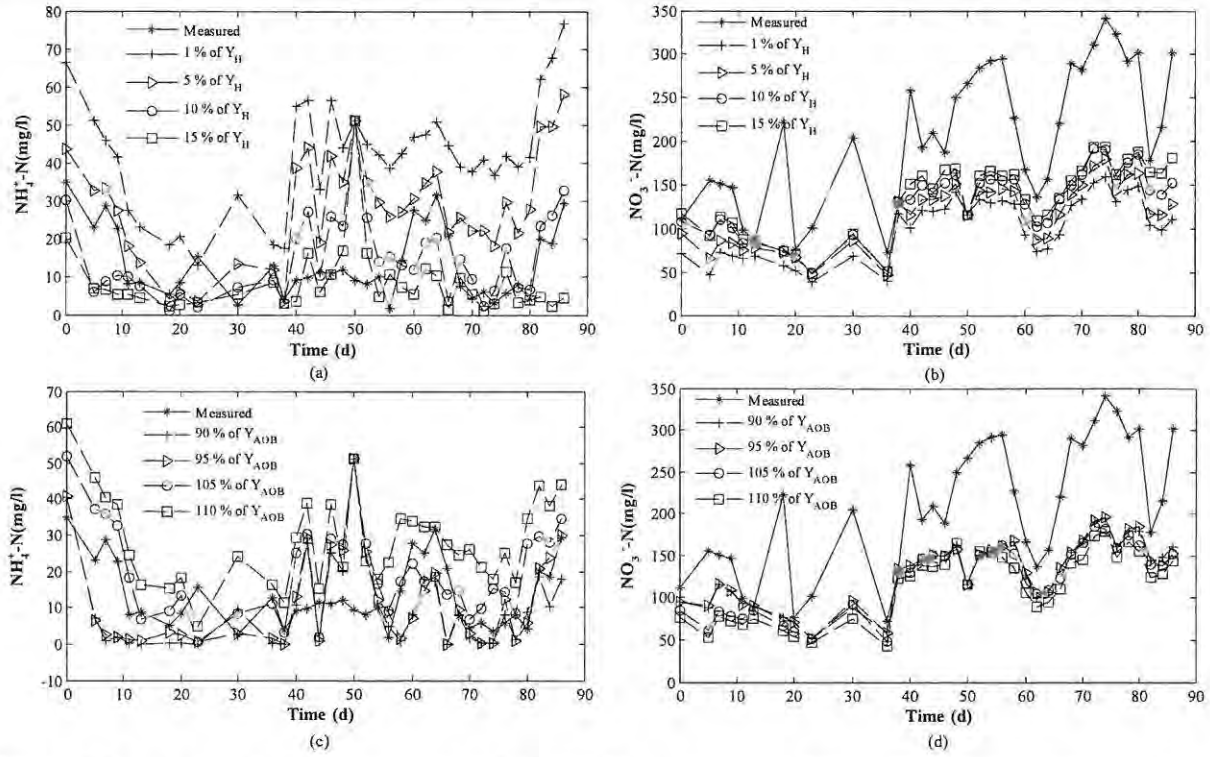

Figure 8.5: Effect of different values of Y_H and Y_{AOB} on model fitting. Values are expressed as a percentage of the original value assumed (0.44 gCOD/gCOD and 0.19 gCOD/gCOD).

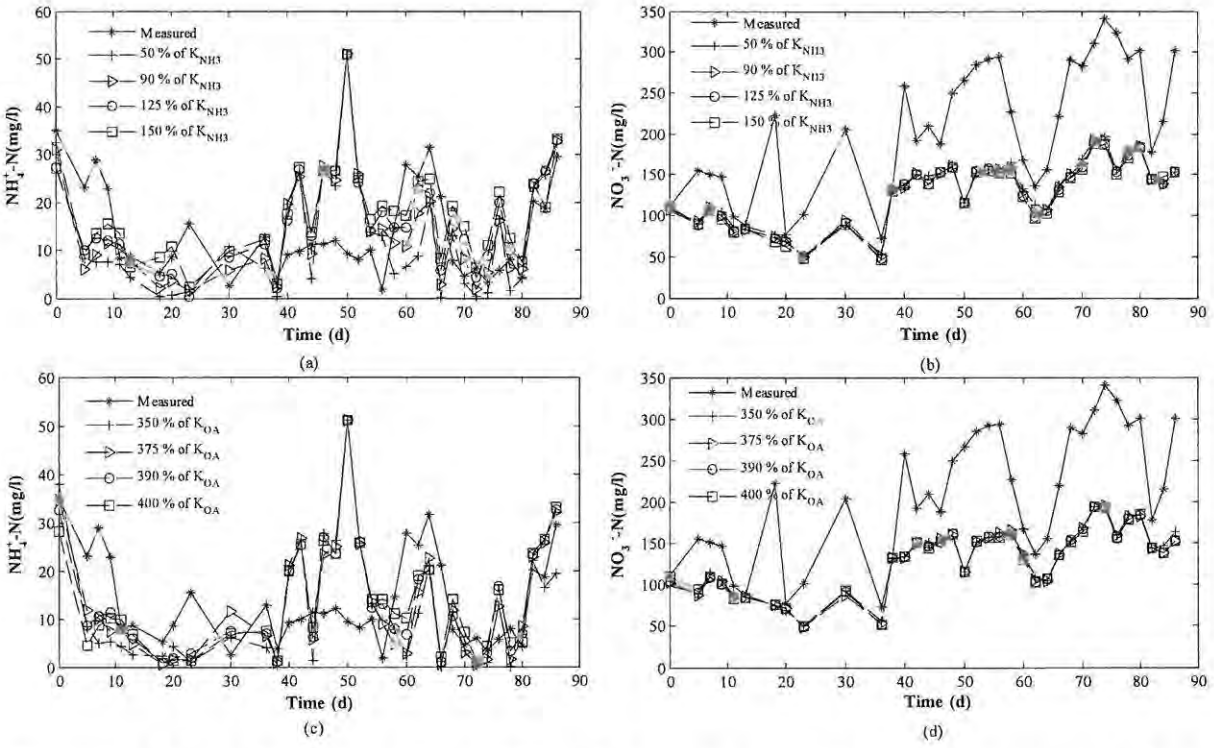

Figure 8.6: Effect of different values of K_H and K_{OA} on model fitting. Values are expressed as a percentage of the original value assumed (0.85 gNH_3-N/m^3 and 0.235 gO_2/m^3).

8.4 Discussion

Figure 8.1 presented the theoretical performance of NH_4^+-N formation and NO_3^--N removal under different [Rh]. The discrepancy between Figures in this simulation and the metal toxicity studies (Chapter 6) could be attributed to many factors. First, substrate limitation in the toxicity study was not represented in the simulation as the model assumed that the substrate was not limited. Second, nutrient use, competition and its limitation to different biomass fractions have not been incorporated into the model (Chapter 7: Tables 7.6 and 7.7, pages 118 and 120). Further, NH_4^+-N formation due to ammonification and hydrolysis of entrapped organics has not been accounted for during the simulation of the model, for simplification purposes. Thus we could expect an under performance of the model with respect to the final NH_4^+-N in reactors. However, the final NO_3^--N concentration under steady state simulation reached the same value (e.g. 140 mg/l of NO_3^--N) irrespective of the [Rh] concentration compared to the trend showed in SOU under different [Rh] (Figure 8.1b *vs.* Figure 6.6 of Chapter 6, page 88). These could be reasons for the model not showing different final NO_3^--N concentrations at different [Rh] under the steady state simulation.

Monod type expressions provide reasonable models to describe the growth of enriched cultures sustained in WWTP provided that the kinetics parameters are interpreted not as absolute values, but as average figures related to predominant species in the particular growth conditions prevailing in the reactor (Jeppsson, 1996). Half-saturation coefficients for oxygen and nitrate are not critical as long as they are in the order of appropriate order of magnitude, since their functions are switching different environmental conditions in the reactors (Henze *et al.*, 1987).

8.4.1 Metal toxicity and nitrate removal

Chloramines penetrate biofilms more efficiently than traditional chlorites, but chloramine degradation results in the release of free ammonia (NH_3), inducing growth of AOB (Kowalchuk and Stephen, 2001). Therefore, it was expected that Claus salt (pentaaminechlororhodium dichloride) would lead to better growth of AOB. However, due to the bound Rh chloramine compound may have inhibited growth. Proper performance of nitrogen removal systems is affected by biomass wash-out or overload depending on the decay rates of nitrifying bacteria (Manser *et al.*, 2006). Therefore, knowledge of autotrophic decay is important for reliable modelling of nitrification using activated sludge systems. However, those kinetics were not experimentally determined in this study and this might have lead to incorrect model fitting. Further research on autotrophic decay rates under PGM toxicity is required for proper calibration of the ASM1_PGM model. Further, the effect of pH on Rh speciation and hence the degree of toxicity to microbial respiration was not evaluated, as those have not been incorporated into the model described in Chapter 7.

The CSTR, PBR and ALSR were initially run with a Rhl concentration of 30 mg/l (Chapters 4 and 5). Even though effective NH_4^+-N removal and NO_3^--N formation were observed, complete nitrogen removal was not achieved in any of the reactors (especially in the PBR, with < 32 % NO_3^--N removal). However, with incremental metal concentration increase from 10 mg/l to 15 mg/l with 100 mg/l of NH_4^+-N in the feed showed a dramatic improvement in NO_3^--N removal in the PBR (Chapter 9). The incremental metal toxicity to heterotrophic biomass were simulated in Figure 8.2 and showed how the increased metal concentration affected NO_3^--N removal.

Based on the simulation results and the experimental results, the NH_4^+-N and NO_3^--N removal did not occur as expected through the standard nitrification and denitrification processes. It can therefore be hypothesised that a certain quantity of NH_4^+-N may have been removed by the Anammox process, leading to an acceptable nitrogen balance in the system. This is explained when the model's nitrification step is disintegrated into two steps as nitritation (i.e. NH_4^+-N to NO_2^--N by *Nitrosomonas* spp.) and nitratation (i.e. NO_2^- to NO_3^- by *Nitrobacter* spp.). The nitritation step leads to the Anammox process by consuming NH_4^+-N in the absence of a nitratation step. Further, the reactor system used in Chapter 9 consumed lower amounts of carbon (sodium lactate) and metal (Rh) compared to what was used in the early PBR (Chapters 4 and 5: 3 % of volumetric flow rate of feed solution and 30 mg/l of Rh). However, improved NH_4^+-N and NO_3^--N removal (> 90 %) were observed. This implies the existence of heterotrophic anoxic ammonium oxidisers (HAAO) which are sensitive to metal concentration and carbon source. The HAAO probably outcompete the usual denitrifying bacteria for the carbon source and they are more tolerable to metal toxicity than the nitrate oxidisers.

8.4.2 Experimental model calibration

Model calibration was defined as adaptation of the model to fit a certain set of information obtained from the wastewater system being studied (Petersen, 2000). Therefore, calibration of the proposed model was one of the critical stages of the simulation study. Even though sensitivity analysis could be used as a guide or reference to which parameters should be found empirically, the experimental determination of parameters is the most important stage of model calibration. By measuring simultaneous oxygen uptake, ammonium oxidation and nitrate formation rates in the aerobic CSTR, the growth, substrate utilization and oxygen consumption by ammonium and nitrite oxidisers could be found (Bernet *et al.*, 2005; Fux *et al.*, 2006; Vanrolleghem and Coen, 1995). For this DO, NH_4^+-N and NO_3^--N electrodes would be the most feasible measuring approach, as the fate of each component can be monitored on a real-time basis thus improving the quality of data (Olsson and Newell, 2001; Rieger *et al.*, 2005; Vanrolleghem and Coen, 1995). Similarly, by monitoring the nitrate removal in the PBR, denitrification rates could be measured using a nitrate electrode coupled with a data acquisition system. The approximate calibration also showed the importance of correct identification of responsible biomass types and the fraction of them in each reactor (or nitrification and denitrification).

It is especially worthwhile to estimate the contribution of heterotrophic denitrifiers and Anammox under the denitrifying conditions so that environmental conditions can be improved for the main contributor to N removal.

8.4.3 Hydraulic modelling of reactors

Hydraulic modelling of each reactor type and its clarifier is also an important aspect of model simulation, in addition to proper calibration of parameters. The ASM1_PGM generally assumed well-mixed conditions in most of wastewater reactors (e.g. CSTR) which was not practically true, due to various reasons such as dead zones, different flow characteristics (e.g. uneven flow through porous media in PBR), and different flow types (turbulent in CSTR *vs.* plug flow in plug flow reactors). These influence the effectiveness or inefficiency of oxygen transfer; creation of anoxic zones within aerobic reactors or aerobic zones in anoxic reactors. This situation was apparent in the dynamic simulation of the PBR. Further, incorrect flow rate representations due to flow path blockages (e.g. biomass growth on inner surfaces of flow tubes) in laboratory scale reactors are not noticed in many instances. These led to incorrect feed and recirculation rates thus producing undetectable errors. Therefore, selecting the correct hydraulic model for the chosen reactor type also plays an important role in model verification.

8.5 Interim conclusions

A mathematical model (ASM1_PGM) developed for the bioprocess of nitrogenous compounds removal from precious metal refinery wastewater was simulated and approximately calibrated using a sensitivity analysis. Through a scenario analysis, the most sensitive parameters affecting the validity of the model were identified for further refinement of the proposed model. Approximate validity of the model was supported by the experimental results presented in Chapter 6 using toxicity studies and the CSTR-PBR configuration discussed in Chapter 9.

Simulation results showed that nitrogen removal occurred not only through the standard nitrification and denitrification process, but also some sort of Anammox activity. The simulation results also showed the ability to control the process under different conditions such as differing metal concentrations. The next chapter presents the proposed control strategy based on the experimental work (Chapters 4, 5 and 6) and simulation results obtained in this chapter.

CHAPTER 9

I'm not the smartest fellow in the world, but I can sure pick smart colleagues.

- Franklin Roosevelt (1882-1945).

9.0 Potential process configuration and operational protocol for the nitrogenous compounds removal from the precious metal refinery (PMR) wastewater

9.1 Introduction

Process control with respect to wastewater treatment can be viewed as manipulating process parameters (such as pH and dissolved oxygen) to achieve the desired effluent quality through different biochemical process paths (e.g. ammonium removal through nitrite or simultaneous nitrification and denitrification), meeting of designed discharge levels of the contaminants found in the influent and optimum use of plant resources such as pumps, chemicals, and energy (Jeppsson and Pons, 2004; Olsson and Newell, 2001). This enhances the decision making process and forecasting the performance of the wastewater treatment plant. Meeting the ever-increasing controls over minimum discharge standards set by regulating authorities and the cost of potable water have led many industries to treat their wastewaters within their industrial facilities, so that discharge of wastewater to external environments can be done without any additional burden to the environment.

Process control in wastewater treatment is a daunting task as there is no or little control over the raw material or the various process parameters available to the plant operator. Attenuating of disturbances by appropriate control actions (pre-treatment, neutralization, dilution, etc.) is therefore the main objective of process control. For example, variations of influent contaminant concentrations, shock loads, seasonal variations and / or process modifications, minimum discharge standards set by regulating authorities, availability of appropriate sensors and actuators, capital and operational cost are the main factors affecting wastewater treatment process control (Vanrolleghem and Lee, 2003). In addition, selecting of appropriate on-line sensors / electrodes is crucial for monitoring and controlling of wastewater treatment plants. However, reliability, consistency, accuracy, response time, durability and cost are to be considered when selecting suitable sensors and electrodes for a particular process (Rieger *et al.*, 2005). Currently there are many options such as affordable high performance PCs, advanced software tools such as LabVIEW, MATLAB, and WEST for model based and real-time control of processes. Progressively improving knowledge on the activated sludge process (ASP) and appropriate mathematical models to describe it are two key aspects of ASP process control. Thus evolving knowledge can be embedded into process control modules in the form of knowledgebased expert system (KBES) for better process control and decision making (Keller *et al.*, 2002).

Gradual increases in metal concentration and thus NH_4^+-N and NO_3^--N removal were studied in this experiment. Intermittent aeration and mixing, an anoxic-aerobic-anoxic reactor configuration, and integrated process parameter monitoring and control to improve the process in terms of reduced cost of aeration, removal of pH adjustment requirement and immediate decision making (in the event of

sudden changes of process influent qualities which affect the smooth operation of the removal process) were included in the investigation. Further, intermittent aeration and mixing were used to attempt to build the anoxic regions within the aerobic reactor, where simultaneous nitrification and denitrification (SND) or Anammox processes may occur.

The objective of this chapter was to present a potential operation protocol for the removal of nitrogenous compounds from precious metal refinery wastewater, using literature based knowledge screening, experimental work carried out and model simulation-based information.

9.2 Materials and methods

In developing a control strategy for nitrogenous compounds removal from PMR wastewaters, the following approach was adopted. First literature-based parameter screening was carried out for identification of optimum conditions by various researchers (see Chapter 2: Literature Review). Then, using those values simulation studies and experimental work were carried out.

9.2.1 Literature based screening

Critical parameters affecting nitrification and denitrification were screened for the proposed control strategy. Some of the key parameters identified during the literature review are presented in the analysis section (9.3.1).

9.2.2 Experimental setups and different reactor configurations

Three experimental configurations (Figures 9.1, 9.2 and 9.3) were compared in developing the proposed control strategy for removal of nitrogenous compounds from PMR wastewaters. Configurations shown in Figures 9.1 and 9.2 were tested and the relevant results were presented in Chapter 5. A primary denitrification reactor was introduced in Figure 9.3 in order to control the pH and improved biomass retention in the CSTR. This was described in Materials and Methods in Chapter 5. The main parameters considered were pH, biomass retention in the CSTR, NH_4^+-N and NO_3^--N removal. As described in Chapter 5, CSTR-PBR (Figure 9.1) and PBR-CSTR (Figure 9.2) configurations were considered in developing the PBR-CSTR-PBR (Figure 9.3) configuration. The feed composition, sampling interval, chemical analysis and hydraulic retention time (HRT) used for the PBR-CSTR-PBR configuration were the same as these described in Chapter 5: Materials and methods. However, the working volumes of $PBR_{Primary}$, CSTR and $PBR_{Secondary}$ were 0.75 l, 12 l and 6 l, respectively.

9.2.3 Model simulations

The model described in Chapter 7 was implemented in the MATLAB 7.0 / Simulink 6.0 (Mathworks Inc., USA) environment. The model was then simulated for evaluating the behaviour in the time space

for various parameters such as substrate utilisation (NH_4^+-N and NO_3^--N), biomass growth, effect of different HRTs, recirculation ratios in reactors and intermittent aeration etc.

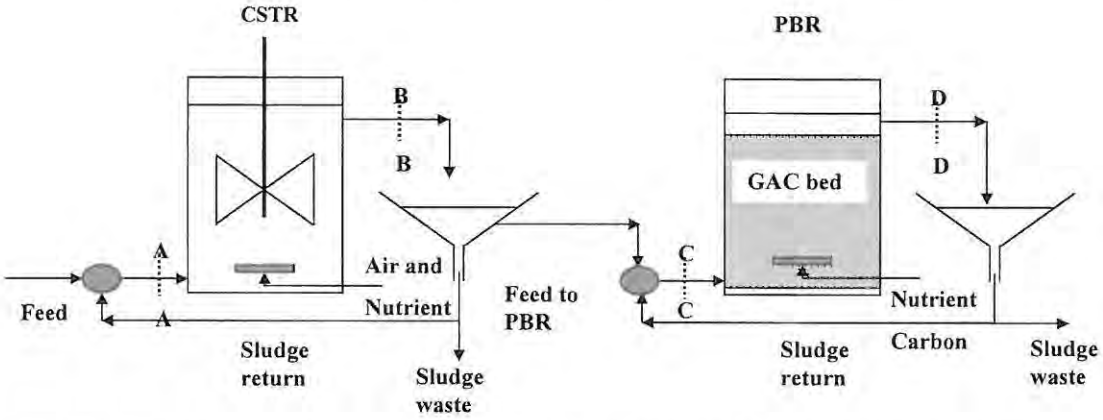

Figure 9.1: CSTR-PBR configuration. A-A, B-B, C-C and D-D indicate sampling points.

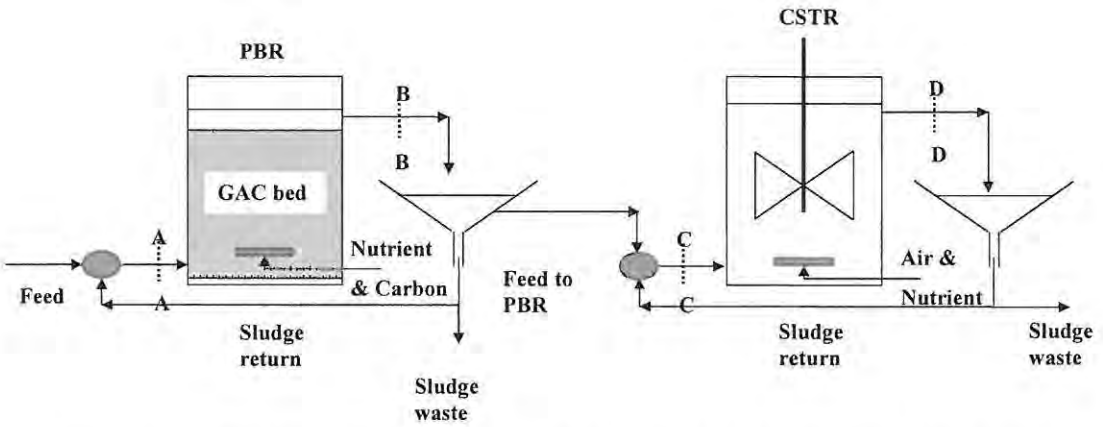

Figure 9.2: CSTR-PBR configuration. A-A, B-B, C-C and D-D indicate sampling points.

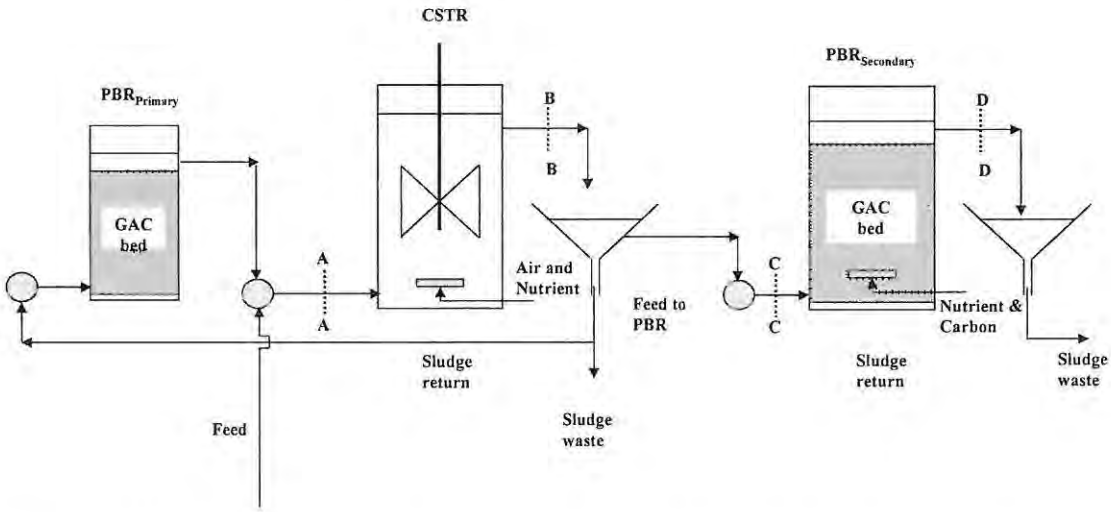

Figure 9.3: PBR-CSTR-PBR configuration. A-A, B-B, C-C and D-D indicate sampling points.

9.3 Analysis

Analysis was carried out under the three sections described in Materials and methods.

9.3.1 Literature based screening

Under the literature based knowledge screening, mainly nitrification, denitrification, factors affecting on those, different processes (such as SND, anammox) and their respective control conditions were evaluated. Even though novel processes (such as CANON, OLAND and SHARON) were not tested in this research, attention was paid to explore the possibility of use of those processes and their control aspects in nitrogenous compounds removal from PMR wastewater.

9.3.1.1 Nitrification

Nitrification is the oxidization of ammonium into nitrate in two steps by different microbial consortia, as described in Chapter 2. Oxidisation of NH_4^+ into NO_2^- is termed as nitritation while oxidation of NO_2^- to NO_3^- is termed as nitratation. Nitrifiers grow optimally at slightly alkaline pH (7.2-8.2) and temperatures between 25 and 35 °C (Carrera *et al.*, 2003). At pH below 6.5, no growth of AOB was observed by previous researchers (Burton and Prosser, 2001), but the preliminary investigations reported in Chapter 3 showed that nitrification occurred even at pH 4. This could be due to nitrification carried out by acidophiles which can tolerate low pH. Similar results have been reported in a biofilm grown on chalk particles (Gieseke *et al.*, 2006; De Boer and Kowalchuk, 2001). At higher pH, the equilibrium of ammonia-ammonium shifts to ammonia, thus inhibiting the nitrification process (Carrera *et al.*, 2003).

Nitrite oxidizers can be restricted by free ammonia (FA) where mixed cultures are presents such as in activated sludge. The FA concentration of 1 – 5 mg NH_3 /l were shown to inhibit the NOB with minor effects on AOB (Abeling and Seyfried, 1992). According to Zhu and Chen (2002), temperature impacts on the fixed film nitrification rate were not significant as predicted in the van't Hoff-Arrhenius equation, while diffusion mass transport played an important role in nitrification in fixed films.

9.3.1.2 Denitrification

Denitrification is the conversion of NO_3^- into $N_{2(g)}$ by heterotrophic anoxic bacteria as described in Chapter 2. Transient formation of NO during denitrification has been cited as an indication of growth of filamentous organisms in activated sludge (Verstraete and Philips, 1998).

Oxygen entering the anoxic reactors affects the denitrifying metabolic activities and kinetics due to the inhibitory effect of increased DO on denitrification rates (Plosz *et al.*, 2003). Zero head space reactors provide an effective means of excluding oxygen penetration (Jobbagy *et al.*, 2000). The oxidation-reduction potential (ORP) could be used as a tool to monitor the DO in the denitrification reactors

where DO suppresses the denitrifying activity (Fuerhacker *et al.*, 2000). An ORP of 100-125 mV promotes optimal denitrifying activity. However, ORP should be adjusted to each specific wastewater appropriately.

9.3.1.3 Different process configurations

The optimum DO levels for AOB and NOB have been found to be 3 – 4 mg/l (van Hulle, 2005). The saturation DO concentration ($S_{O2,\ sat}$) in fresh water between 0 and 40 °C temperatures can be expressed as (Zhu and Chen, 2002):

$$S_{O_2,sat} = \frac{468}{31.6 + T} \qquad (9.1)$$

Where T = temperature of water.

Implementing mathematical equation 9.1 control algorithms and real-time temperature monitoring in the reactor can easily calculate the saturated oxygen concentration at different operating temperatures. This enhances the oxygen mass transfer calculations in the liquid phase so that control action can be taken accurately, based on the real-time values.

Nitrite accumulation decreases with increasing DO and pH (Gapes *et al.*, 2003). Bernet *et al.* (2005) controlled the [DO]/[NH_4^+-N] ratio in the range of 0.05 to 0.1, and found that 80 % of influent NH_4^+-N was oxidised to nitrite using online control in an inverse turbulent bed reactor. They used a synthetic mineral wastewater containing 250 to 500 mg/l of NH_4^+-N and stated the keys for developing their short-cut process were pH, HRT and DO control. Thus this strategy may be used for partial nitratation of PMR wastewater by short-cut processes such as CANON, OLAND and SHARON. During partial nitritation, ammonium (NH_4^+) is oxidised only to nitrite (NO_2^-). The SHARON process operates without biomass retention and at relatively high temperatures (30 – 35 °C) by controlling the dilution rate (SRT = HRT, approximately 24 hours). At higher temperatures AOB have higher growth rates than nitrite oxidizers (NOB). Therefore, by careful control of dilution and temperature, nitrite oxidation is prevented by washing out the NOB (Wyffels *et al.*, 2004). Imposing oxygen-limited conditions is the most feasible and practical approach allowing AOB to outcompete the NOB in mixed systems with sludge retention (Wyffels *et al.*, 2004).

A study by Arrojo *et al.* (2006) illustrated the effects of mechanical stress on anammox biofilm granules. This experiment was carried out at constant nitrogen loading rate of 0.3 gN/(l.d) with varying stirring speeds between 60 and 250 rpm. Up to 180 rpm no negative effect on anammox activity was not observed, but at 250 rpm, anammox activity was reduced by 60 %. Mass transfer effects play an important role within the large flocs prevailing in conventional activated sludge systems (Manser *et al.*, 2005). Mass transfer effects depend strongly on variable parameters such as floc size and floc density, which may vary significantly from wastewater treatment plant to plant.

9.3.2 Experimental work and different reactor configurations

Previous results obtained from the CSTR, PBR and ALSR led to exploring the possibilities of different reactor configurations for removal of nitrogenous compounds, as it was not clear whether there is a specific type bioreactor which would suit a particular organism or wastewater type (Kowalchuk and Stephen, 2001). Therefore, three reactor configurations were analysed with a view to developing a control strategy.

9.3.2.1 Ammonium and nitrate removal

Ammonium removal in the CSTR-PBR and PBR-CSTR configuration were reported in Chapter 5. Figure 9.4 shows the NH_4^+-N removal in the PBR-CSTR-PBR configuration. Compared to CSTR-PBR and PBR-CSTR configurations, a gradual increase in NH_4^+-N removal efficiency was observed in the PBR-CSTR-PBR, with a mean removal efficiency of 90.7 ± 5.7 % during 75 days of operation. Primary data are given in Appendix F: Tables F.1, F.2 and F.3.

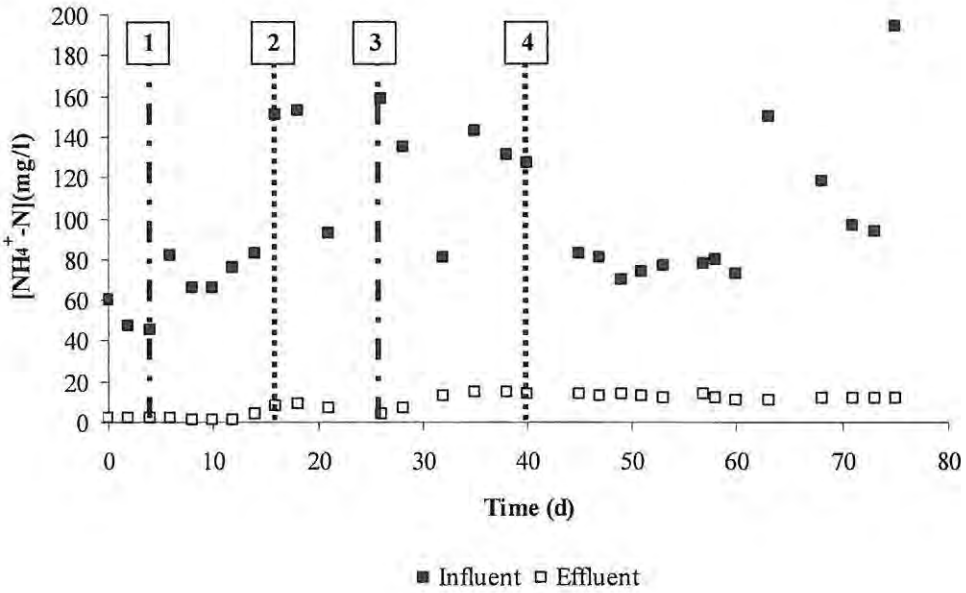

Figure 9.4: Ammonium removal in PBR-CSTR-PBR configuration. The influent changed at four points in time: 1 – [NH_4^+-N] was increased from 75 mg/l to 150 mg/l, 2 – [Rh] was increased from 20 mg/l to 25 mg/l, 3 – [NH_4^+-N] was decreased from 150 mg/l to 100 mg/l, and 4 – [Rh] was decreased from 25 mg/l to 20 mg/l.

Figure 9.5 shows that the NO_3^--N removal decreased once the NO_3^--N influent concentration was increased, as a result of the increased NH_4^+-N influent concentration in the CSTR. Inhibition of denitrification due to high concentrations of NO_3^- has been reported previously (Glass and Silverstein, 1998). This is due to the toxicity of accumulated NO_2^--N and unionised nitrous acid species. The equilibrium between NO_2^- and HNO_2 is pH dependant. Even though denitrification is an HCO_3^- production process in which pH is increased, Figure 9.6 shows slightly acidic conditions in the PBR. It

can be hypothesised that the denitrifying bacteria which were already under metal toxicity stress could have been further inhibited by substrate inhibition, due to the increased NO_3^--N concentration in the reactor. Therefore, it is important to determine the maximum influent NO_3^- concentration in the denitrifying reactor under the maximum tolerable metal and influent NH_4^+-N content which would produce the maximum tolerable NO_3^--N concentration to avoid substrate inhibition.

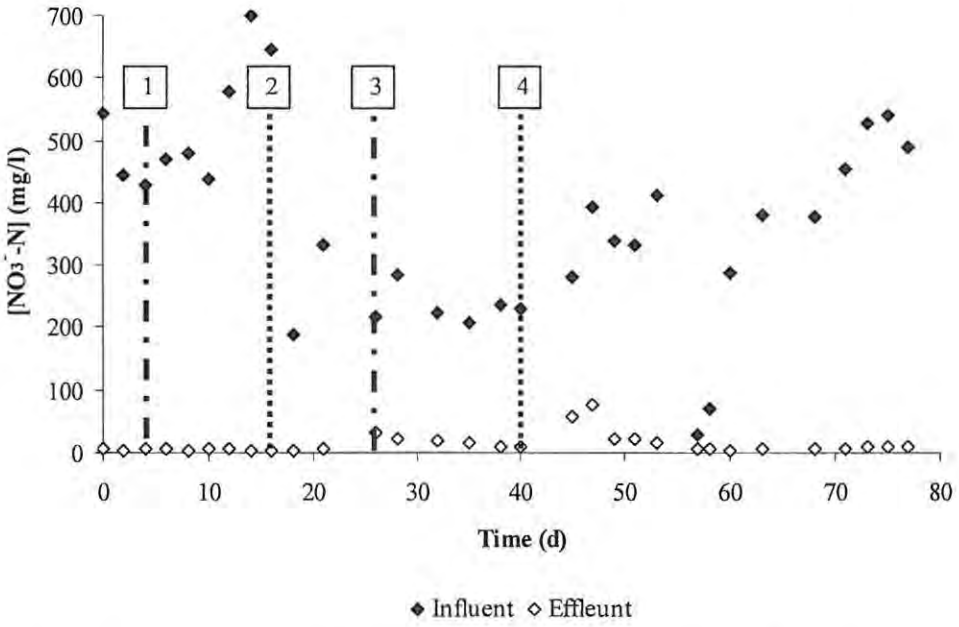

Figure 9.5: Nitrate removal in PBR-CSTR-PBR configuration. The influent changed at four points in time: 1 – [NH_4^+-N] was increased from 75 mg/l to 150 mg/l, 2 – [Rh] was increased from 20 mg/l to 25 mg/l, 3 – [NH_4^+-N] was decreased from 150 mg/l to 100 mg/l, and 4 – [Rh] was decreased from 25 mg/l to 20 mg/l.

9.3.2.2 pH and mixed liquor suspended solids (MLSS)

Maintaining suitable pH and sufficient biomass in nitrification and denitrification processes is vital for maximum removal of nitrogen compounds, as metal toxicity hinders the growth of responsible biomass for the above processes. Therefore, precise control of pH and metal concentrations should lead to optimum biomass retention in each reactor, provided that self-substrate inhibition (high NH_4^+-N and/or NO_3^--N) is avoided with sufficient nutrients available in the reactor.

According to Figure 9.6, more stable pH variations were observed in both the CSTR and the PBR in the PBR-CSTR configuration than in the CSTR-PBR configuration (i.e. from day 37 to day 89). A rapid biomass increase was also observed in the CSTR under the PBR-CSTR configuration (see Chapter 5). The main advantage of the PBR-CSTR configuration was that no biomass introduction was necessary to the CSTR after initial inoculation. Overall NH_4^+-N and NO_3^--N removal under the CSTR-PBR and PBR-CSTR were > 90 % and > 95 %, respectively.

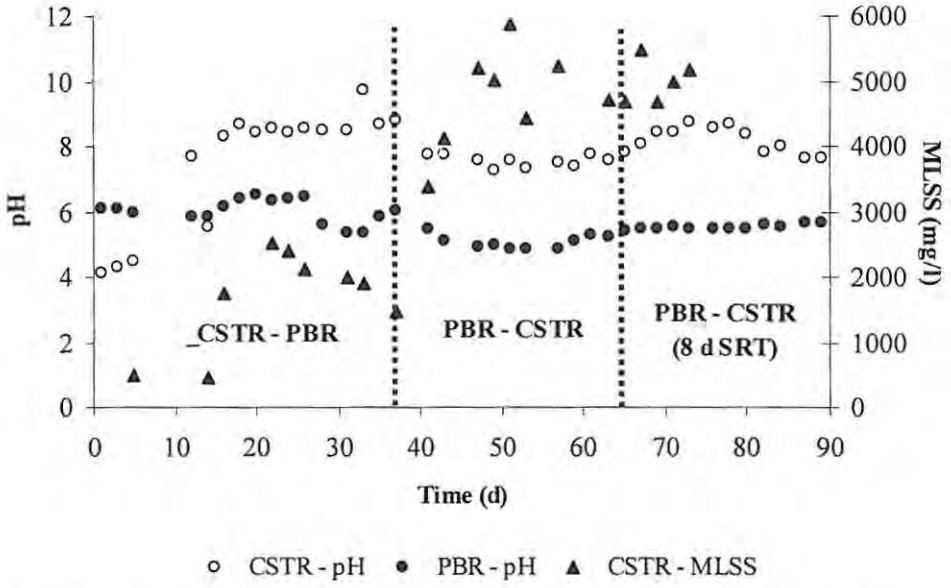

Figure 9.6: pH and MLSS variation in CSTR-PBR and PBR-CSTR configuration (Chapter 5). Vertical lines indicate the days on which configuration and SRT were changed.

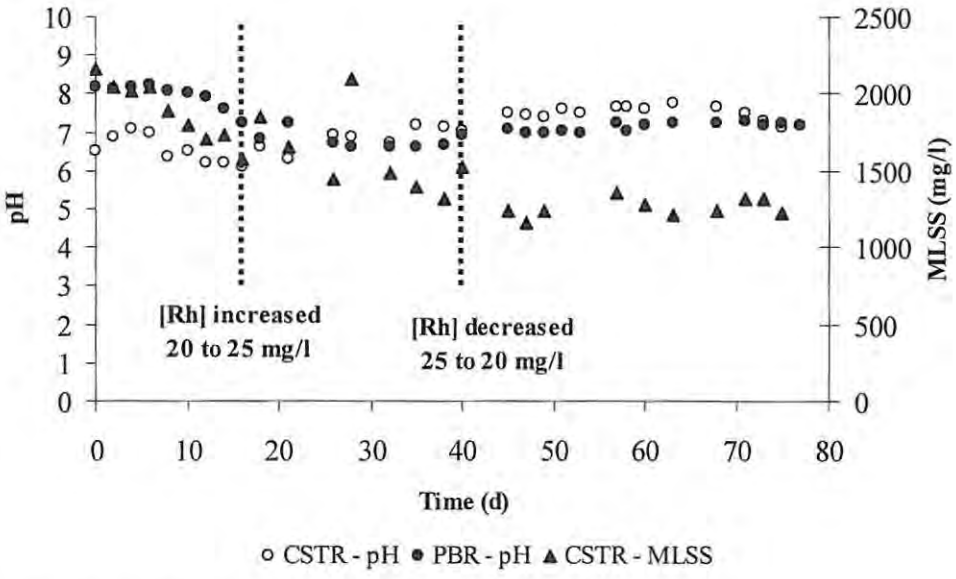

Figure 9.7: pH and MLSS variation in PBR-CSTR-PBR configuration.

Increased influent metal content led to a decrease in the biomass. However, once the metal concentration was returned to the original value stable biomass concentrations prevailed, even though the MLSS was below 1500 mg/l. The PBR-CSTR-PBR configuration showed a more consistent pH compared to the CSTR-PBR or PBR-CSTR configurations described earlier (Figure 9.6 *cf.* Figure 9.7). Table 9.1 compares the summary of three reactor configurations in terms of nitrogen removal and other process parameters.

Table 9.1: Parameter analysis under different reactor configurations.

Process parameter	Process configuration*		
(units)	CSTR-PBR	PBR-CSTR	PBR-CSTR-PBR**
[NH_4^+-N] removal in CSTR (%)	49.0 ± 29.6	67.8 ± 22.9	90.7 ± 5.7
[NH_4^+-N] removal in PBR (%)	99.4 ± 1.10	70.9 ± 16.7	-
[NO_3^--N] removal in PBR (%)	-	62.5 ± 29.5	95.2 ± 6.8
pH :			
CSTR	7.59 ± 1.83	7.89 ± 0.45	7.05 ± 0.50
$PBR_{Secondary}$	6.01 ± 0.36	5.32 ± 0.28	7.28 ± 0.51
MLSS in CSTR (mg/l)	1619 ± 745	5023 ± 428	1567 ± 323
Combined reactor volume (l)	11.40	11.40	18.75

* All values except reactor volumes are given in MEAN ± STANDARD DEVIATION format.

** Under the PBR-CSTR-PBR configuration overall NH_4^+ and NO_3^- removals were calculated instead of individual reactor removal efficiencies as opposed to the CSTR-PBR configuration.

9.3.2.3 Metal toxicity

Control of the influent metal concentration entering the biological nitrogen removal system plays an important role, as shown by the respirometric analysis in Chapter 6. Table 9.2 shows the saturation inhibition coefficients for selected PGMs determined in Chapter 6. In contrast to the municipal wastewater plant, *in situ* metal refinery wastewater plants within an industrial facility have more control over their influent concentrations, as they are process specific. High metal concentrations inhibit biological removal processes, hence a suitable dilution mechanism needs to be adopted prior to biological treatment. Even though the model explained in Chapter 7 can predict the effect of metal mixtures it does not distinguish the differences due to metal speciation and/or complexation. This is one of the main drawbacks of the model presented in Chapter 7. However, the simulation of the model could show what metal concentrations should be maintained for optimum biological nitrogen removal. The model could be improved by introducing metal speciation under different pH conditions at the expense of model simplification. However, a detailed study on the degree of toxicity by different metal species under different pH conditions would have to be evaluated carefully.

Table 9.2: Saturation inhibition coefficients for selected PGMs.

Metal	Saturation inhibition coefficient (K_i) (mg/l)
Pt	16
Pd	25
Rh	33
Ru	39

9.3.3 Model simulation for DO dynamics

The model developed in Chapter 7 was simulated to find out the time dependant behaviour of different state variables such as NH_4^+-N, NO_3^--N, NO_3^--N, COD and different biomass types under various DO concentrations. Figure 9.8 presents the effect of different DO concentrations on the removal / formation of NH_4^+-N, NO_3^--N, NO_2^--N and total COD with a set [Rh] of 20 mg/l, as used in the experimental work used in this chapter. According to Figure 9.8a, there was a rapid NH_4^+-N removal activity by AOB for > 1 mg/l of DO. This was supported by Figure 9.9b. Higher AOB affinities to DO have led to rapid response of NH_4^+-N removal. The AOB were clearly inhibited at low DO. A similar trend was observed in attaining the steady state of NO_3^--N formation, as shown in Figure 9.8b. The highest DO allowed steady state to be reached quickest (0 mg/l *vs.* 3 mg/l of DO). This phenomenon can easily be described using Figure 9.8c, in which NO_2^--N accumulation could be observed at lower DO as would be expected from the theory.

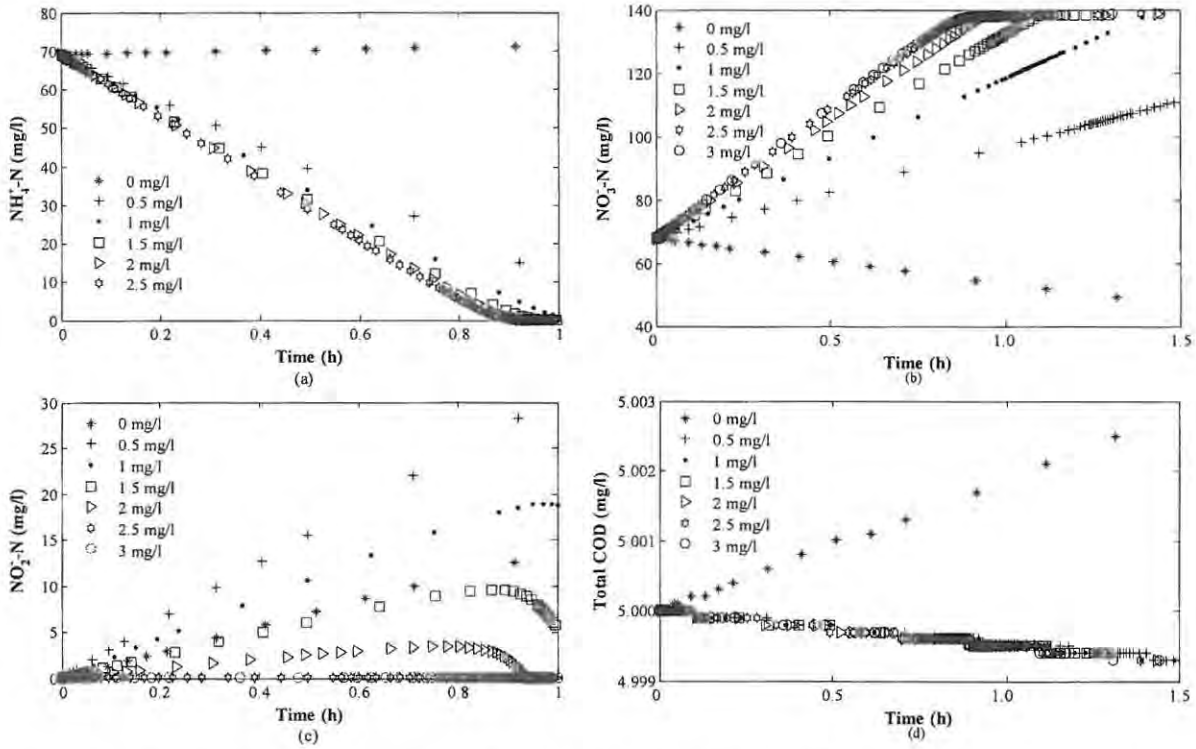

Figure 9.8: The effect of different [DO] on NH_4^+-N, NO_3^--N, NO_2^--N and COD.

Relatively low sensitivity to different DO levels by heterotrophs, as shown in Figure 9.9a, could be attributed to their ability to switch between oxygen and NO_2^- or NO_3^- as a terminal electron acceptor. According to Figure 9.9c, growth of NOB could be observed at DO concentrations > 1 mg/l, opposed to rapid response of AOB to DO (Figure 9.9b *vs.* 9.9c). This reiterates the importance of DO control for deciding the type of nitrogen removal process (e.g. anammox *vs.* standard nitrification denitrification). Figure 9.9d illustrates the inhibition of anammox biomass at DO > 0 mg/l.

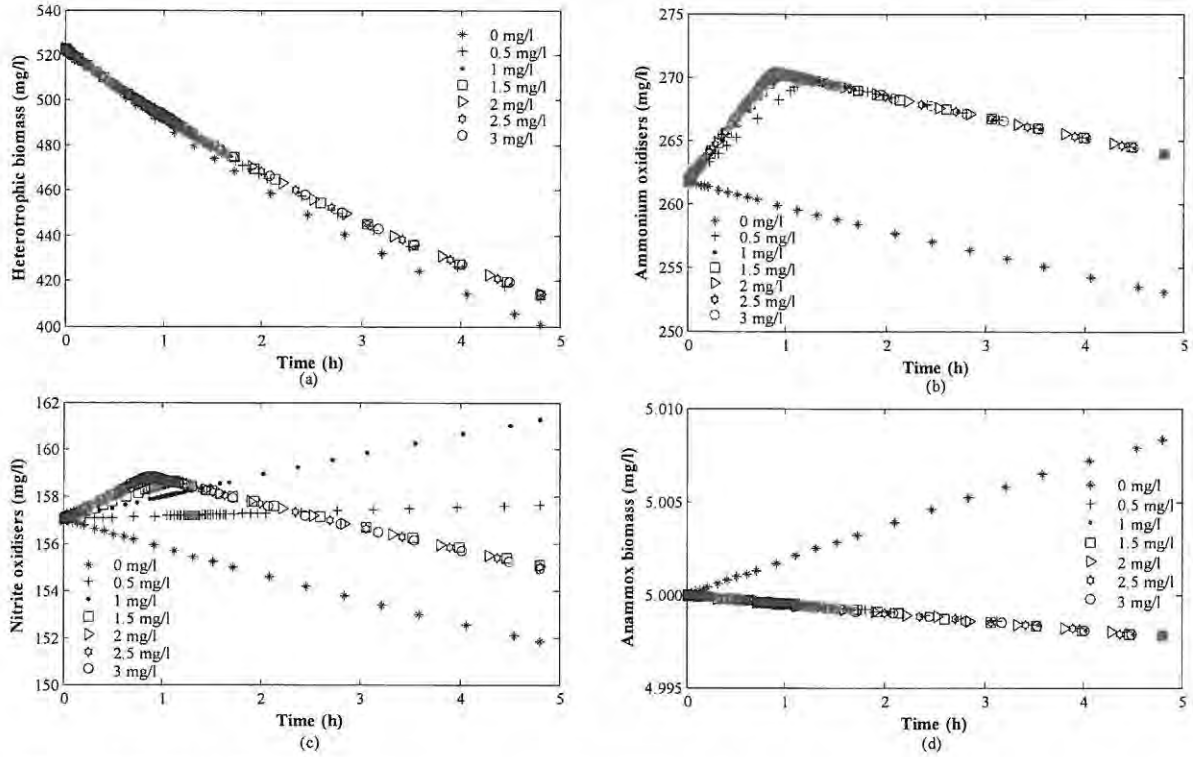

Figure 9.9: The effect of different [DO] on different biomass types.

9.4 General discussion and process control protocol

In the event of biological removal of nitrogenous compounds from PMR wastewater, not only the nitrogen species removal efficiency but also the final concentrations of each nitrogen species in the final treated effluent are important, as these impact on downstream metal recovery as well as on opportunities for the water to be reused within the processing plant or discharged to appropriate water receiving bodies under the relevant regulations.

Pollice *et al.* (2002) showed that at given temperature and pH, the sludge age (SRT) is the critical parameter for partial nitrification under an unlimited oxygen supply. Conversely, under oxygen limitation (i.e. intermittent aeration), complete and stable conversion of NH_4^+-N into NO_3^--N is independent of the SRT. The main advantages of aeration control instead of SRT control in biological nitrogen removal processes are potential energy saving (less aeration), better flexibility of aeration control in plant operation, reduced risks of biomass washout at low SRT and limited ammonia oxidation to nitrite, thus favouring autotrophic simultaneous ammonia and nitrite removal (Pollice *et al.*, 2002).

Even though it is generally assumed that no conversion processes take place in the clarifier, Figure 9.10 shows that NO_3^--N changed in the CSTR and PBR clarifiers. However, the mean percentage conversions of NO_3^--N concentrations in the CSTR and PBR clarifiers were only 2.9 % and 0.07 %, respectively. Therefore, the NO_3^--N conversions in the clarifiers can be neglected. Mass

transfer within the free flocs of organisms in stirred tanks reactors is not well understood, and its significance to biological reaction rates is a matter of speculation (Olsson and Newell, 2001). According to Figure 9.8, increased HRT could have been used for complete conversion at each stage instead of the operated HRT value.

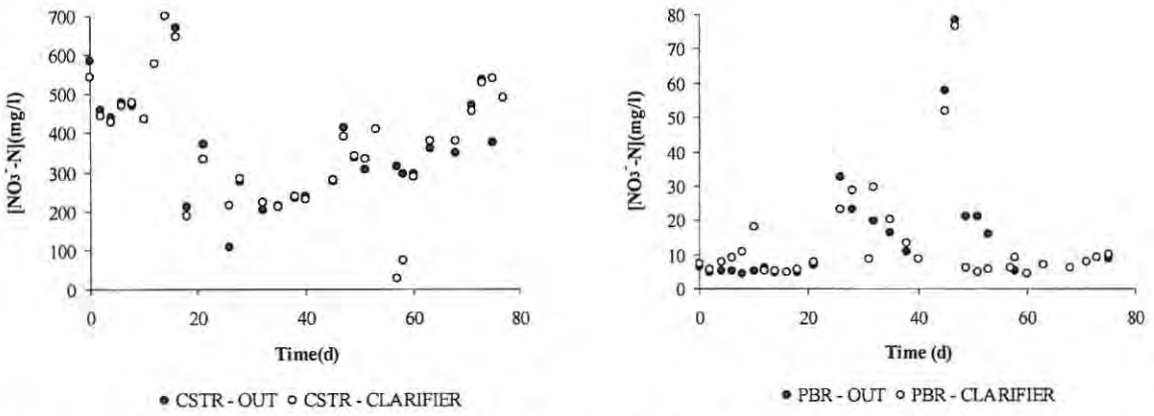

Figure 9.10: Nitrate concentrations in reactor effluents (i.e. clarifier influents) and clarifier effluents (CSTR and $PBR_{Secondary}$).

Coexistence of Anammox and heterotrophic bacteria and hence competition between them for the nutrient supply is not well understood. However, under anoxic conditions (*e.g.* in the PBR) the coexistence and competition would play an important role in deciding which denitrifying path will dominate in the reactor (standard denitrification *vs.* Anammox).

Main parameters such as pH can be controlled using an ON/OFF algorithm, while DO can be controlled through a PID control algorithm which could be easily implemented through LabVIEW / MATLAB / Simulink environments (Nuruzzaman, 2004; Seixo *et al.*, 2004; Travis and Kring, 2006). The desired DO concentration can be implemented by manipulating the air flow into the reactor and monitoring the existing DO in the reactor. The control action is taken through a PID controller embedded in the control software (e.g. PID VI in LabVIEW). Integrated sensors could be used effectively to monitor the nitrogen removal from the metal refinery wastewater (Sin *et al.*, 2003). This integrated sensor can monitor nitrification, denitrification and carbon source degradation simultaneously. Titration techniques have also been studied for monitoring the activated sludge process (Gapes et al., 2003; Gernaey *et al.*, 1998a; 1998b; Vanrolleghem and Lee, 2003). The linear relationship between autotrophic biomass fraction and C_{org}/N ratio described by Seixo *et al.* (2004) simplifies the determination of various biomass fractions found in ASP. Usually it is difficult to determine the autotrophic and heterotrophic biomass separately but both types are lumped together as VSS.

Physical / chemical sensors (DO, pH, NH_4^+-N, NO_3^--N) are the most commonly used sensors in controlling wastewater treatment plants. Real-time analysis of wastewater samples using image analysis capabilities contained in modern software tools such as LabVIEW and MATLAB/Simulink (Hahn, 2004; Travis and Kring, 2006; Nuruzzaman, 2004) could be used for knowledge-based control systems for enhanced decision making. This area would be important in sludge settling problems occurring in activated sludge plants. However, detailed mechanisms to get samples, image capturing, analysis and comparison with the knowledgebase are needed for further study. Possibly developing an advanced algorithm for online image analysis and coupling it with a suitable representative sample capturing mechanism would achieve this. Further, simple rule based KBES could be implemented in the control algorithm for enhanced process control. Figure 9.11 shows a sample of such simple rules based on the literature based knowledge screening and experimental work described earlier.

Implementing a KBES based on simple rules such as shown in Figure 9.11 eliminates the requirement for the service of a technical expert in the event of diagnosis or process optimisation. This is applicable not only for small to medium scale WWTPs but also large scale WWTPs. Figure 9.12 shows the potential operational protocol for biological removal of nitrogenous compounds from the PMR wastewater. Based on the above descriptions, batch model treatment plant control may assist in better process operation. For example, increase metal concentration or NH_4^+-N hinders the removal process. Therefore, batch-wise pre-treated wastewater can be sent to the main nitrogen removal plant appropriately.

Rule 1:
WHEN "MLSS is very small"
AND
"sludge wastage rate is small"
DO "make a small increment change in return sludge set-point"

Rule 2:
WHEN "effluent suspended solids concentration is medium"
AND
"denitrification is indicated"
DO "make a small increment change in sludge wastage rate"

Rule 3:
WHEN "influent [metal] concentration is > 10 mg/l"
AND
"nitrification is not indicated"
DO "make a small increment change in influent sludge dilution rate"

Figure 9.11: Simple rule base for wastewater treatment plant control (Olsson and Newell, 2001).

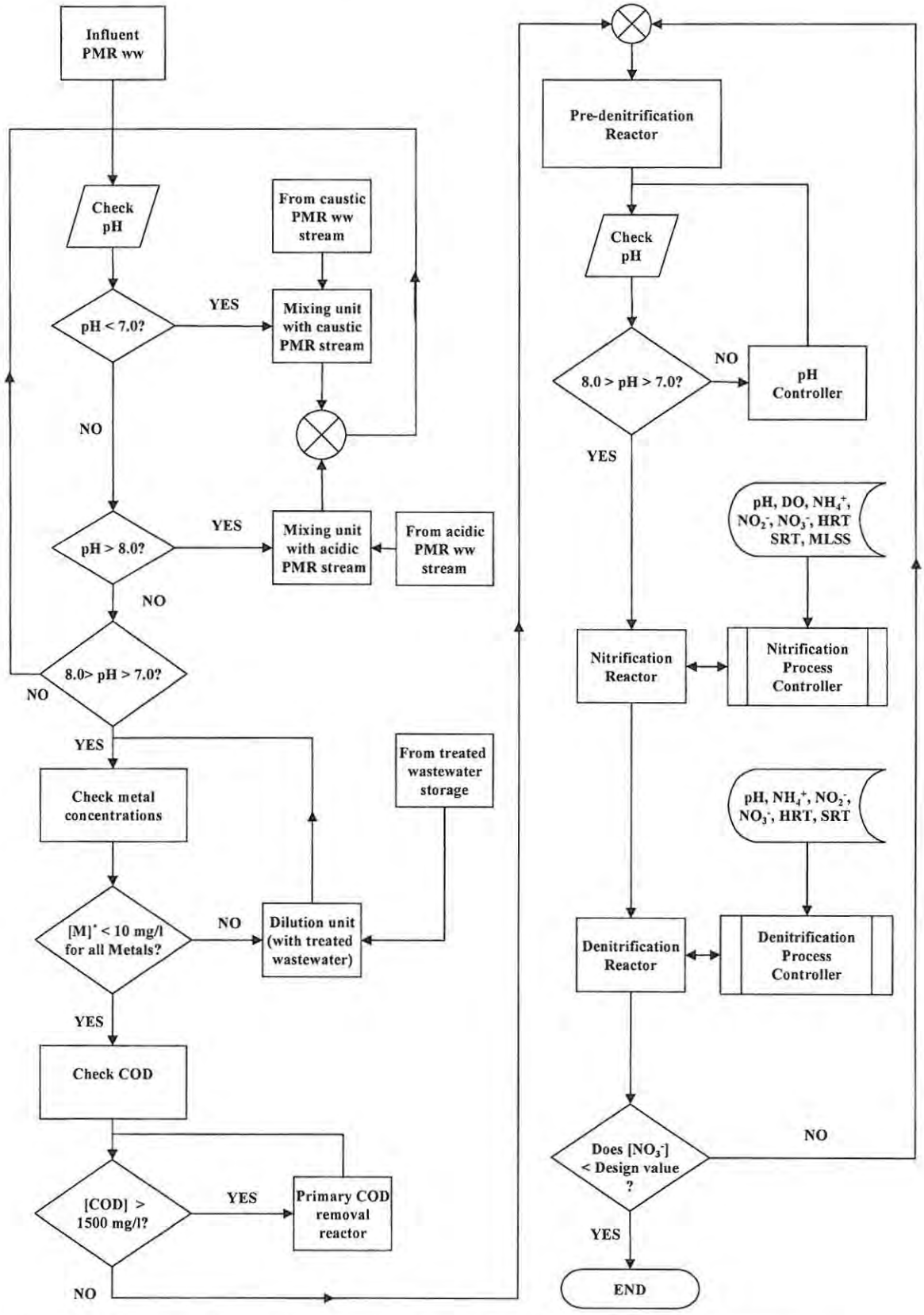

Figure 9.12: Proposed control strategy for nitrogen removal from the PMR wastewater.

9.5 Interim conclusions

A control strategy for removal of nitrogenous compounds from PMR wastewater was proposed based on the literature screening, experiments and simulation work. Of all the different reactor configurations investigated, the PBR-CSTR-PBR showed higher overall removal efficiencies of nitrogenous compounds, compared to the CSTR-PBR and PBR-CSTR configurations described in Chapter 5. Neither pH control nor continuous biomass introduction to the CSTR was needed in this configuration. The simulation showed that how different [DO] lead to NO_2^--N accumulation and effect on anammox biomass. Therefore, it is vital to control the DO dynamics in selection of the desired process path such as standard nitrification denitrification or anammox and its different process configurations (e.g. CANON).

However, detailed experimental procedures are required for further refinement of the proposed control strategy using actual refinery wastewater. For example, the optimum floc size for simultaneous SND or anammox activity needs to be found using different stirring speeds which do not break the microbial flocs excessively, as described earlier. Nitrogen removal capacity per unit reactor volume under different HRTs and PGM concentrations need to be evaluated experimentally to determine the optimum HRT and maximum tolerable metal toxicity. To enhance this greater understanding of the process it becomes necessary to move away from the 'black box' approach and try to create, at least, a 'grey box' in which some of the micro-organisms might be identified, the better to design an environment in which they might work to our advantage the best. To this end the author took the first steps into microbiology in the form of some identification tests for microbial groups, as described in the following chapter.

CHAPTER 10

In soloing – as in other activities – it is easier to start something than it is to finish it.

- Amelia Earhart (1898-1937).

10.0 Preliminary investigations of microbial analysis in a reactor system removing nitrogenous compounds from simulated metal refinery (PMR) wastewaters

10.1 Introduction

The identification of the micro-organisms which are responsible for the biological reactions which underpin the process is an important aspect in developing a bioprocess to remove nitrogenous compounds from precious metal refinery (PMR) wastewater. There is a niche for certain microbes which can survive in the harsh environment imposed by industrial wastewaters such as PMR wastewater (Johnson and Hallberg, 2003; Logan *et al.*, 2005). Extreme pH conditions and high chemical oxygen demand (COD) concentrations are two of the main characteristics of PMR wastewater, apart from a number of toxic metals contained in the wastewater (see Chapter 3). It has been observed that prokaryotic microbes that are metabolically active in extremely acidic environments are widely distributed in the domains of *bacteria* and *archaea* (Johnson and Hallberg, 2003). Usually nitrification is carried out by two distinct autotrophic microbial consortia, i.e. ammonium oxidation by *Nitrosomonas*-like species and nitrite oxidation by *Nitrobacter* species. Denitrification is carried out by a wide range of facultative microbes which converts NO_3^- into $N_{2(g)}$.

Microbial characterisations of municipal wastewaters have been reported by many researchers (Daims *et al.*, 2001; Egli *et al.*, 2003a, 2003b; Ginige *et al.*, 2005; You *et al.*, 2002). However, identification of microbial communities responsible for specific wastewater types such as PMR wastewater is hardly ever reported. Therefore, it is necessary to identify the species or strains which can tolerate extreme pH conditions as well as the various toxic metals found in the PMR wastewaters. This would enable customised process control, optimisation and specific reactor designs for pilot or full scale operation of biological nitrogen removal systems for PMR wastewaters. Preliminary biochemical and physiological studies are vital prior to further studies at molecular level, such as DNA and RNA sequencing (Wilderer *et al.*, 2002). Molecular ecology and microbial community analysis using molecular biology are wide areas of research in which several entire doctoral theses have been written. The discovery of a phylogenetic tree for the reactor types used here would fall beyond the scope of this project in terms of both subject area and time. Therefore, selected biochemical and physiological studies were carried out for preliminary broad classification of the microbial communities in two reactors which were used for nitrification and denitrification using carefully simulated PMR wastewater. Chapters 8 and 9 describe reactor systems from which samples were taken for initial microbial characterisation. The objectives of this chapter were to present the preliminary results of microbial characterisation and their relevance to the said wastewater type for maximum removal of nitrogenous compounds under high metal concentrations.

10.2 Materials and methods

Ten biochemical and physiological tests were carried out during the preliminary investigation. The two reactors were running over a period of 75 days fed with carefully simulated PMR wastewater containing rhodium (Rh) as the precious metal, bound with an NH_4^+ compound (Claus salt: pentaaminechlororhodium dichloride) provided by Anglo Platinum Ltd., Rustenburg, South Africa. The feed contained 20 mg/l of Rh and 100 mg/l of NH_4^+-N. The reactor system consisted of a serially connected primary packed-bed reactor ($PBR_{primary}$), continuously stirred tank reactor (CSTR) and secondary packed-bed reactor ($PBR_{secondary}$) as described in Chapters 8 and 9. The biomass samples were taken from the CSTR (nitrification reactor) which achieved > 90 % NH_4^+ removal and $PBR_{secondary}$ (main denitrification reactor) which showed > 95 % NO_3^- removal. A summary of reactor performance was presented in Chapter 9: Table 9.1.

10.2.1 Motility determination and flagella staining

Subsamples were taken from the CSTR and PBR, and decimal dilutions were conducted using physiological saline. This was prepared by dissolving 8.5 g of NaCl (Saarchem, Merck Ltd) in 1000 ml of deionised water, and autoclaved at 121 °C for 15 minutes (AD-530RD laboratory autoclave, Relax Industries, Johannesburg, RSA). Subsamples from dilutions of up to 10^4 from both reactor cultures were pipetted onto microscope slides, cover slips were put on them and they were examined with 100 × magnification using an Olympus CH20 light microscope (Olympus Optics Ltd., Tokyo, Japan).

After 5 to 15 minutes, staining for the presence of flagella was conducted using the method described by Heimbrook *et al.* (1989). The dye was prepared as follows: saturated aqueous solution of $KAl(SO_4)_2.12H_2O$ (Sigma-Aldrich, Johannesburg) was prepared by dissolving 1 g of the compound in 20 ml of deionised water. A mass of 5 g of phenol (Sigma-Aldrich, Johannesburg) was dissolved in 100 ml of deionised water, and 2 g of tannic acid (Sigma-Aldrich, Johannesburg) was weighed into a 100 ml Erlenmeyer flask. Ten millilitres of the solution of $KAl(SO_4)_2.12H_2O$ and phenol were added, and the mixture was stirred until complete dissolution of tannic acid.

A mass of 12 g of crystal violet (Sigma-Aldrich, Johannesburg) was dissolved in 100 ml of 95 % ethanol (Merck Chemicals Pty Ltd., Johannesburg, RSA). A volume of 2 ml of this solution was added to the mixture of tannic acid, phenol and $KAl(SO_4)_2.12H_2O$. This was filtered through a 0.22 μm pore size nylon membrane syringe filter (Microsep, Port Elizabeth, RSA) attached to a 5 ml plastic syringe (Wallace Pharmacy, Grahamtown, RSA). After staining, the individual slides were incubated at room temperature to allow for the dye to diffuse through the preparation and stain the possibly present flagella. This was conducted on the dilution that provided the best resolution in motility determinations. The flagella were stained by applying drops of a dye to the edge of the cover slip of the particular slide studied.

10.2.2 Gram staining

The Hücker method of Gram staining was used (Gerhardt *et al.*, 1981). Solution A for the staining reagent was prepared by dissolving 2 g of crystal violet in 20 ml of 95 % ethanol. Solution B was prepared by dissolving 0.8 g $(NH_4)_2(COO)$ (Sigma-Aldrich, Johannesburg, RSA) in 80 ml of deionised water. Solutions A and B were mixed, allowed to stand at room temperature for 24 hours, and filtered through a 0.22 μm nylon membrane filter, just before application. The mordant solution was prepared by mixing 1.0 g of iodine and 2.0 g of KI (Merck Chemicals Ltd.), grinding them using a mortar and a pestle, and slowly adding 300 ml of deionised water.

Ethanol (95 % v/v) was used as the decolourising agent, while safranin solution was used as the counterstain, prepared by dissolving 2.5 g of safranin (Fluka, Sigma-Aldrich) in 10 ml of 95 % ethanol, and adding 100 ml of deionised water. Subsamples of both reactor cultures were taken, and decimal dilutions were performed just as with the motility determination and flagella staining (see above). Cultures were heat-fixed, and submerged into the staining agent with crystal violet for about 60 s. The slides were then rinsed under tap water, and immersed into the iodine mordant for 10 s. The slides were rinsed briefly under tap water, blot dried with filter paper, and immersed into 95 % ethanol for a period of 30 s. After successive filter paper blotting, the slides were submerged into the counterstain solution for 10 s. After rinsing with tap water, the slides where blotted with filter paper, and examined under 100 × magnification using oil immersion filters. Images were captured using an Olympus digital camera (Camedia C4040, Tokyo, Japan) fitted to an Olympus light microscope (BX50, Tokyo, Japan).

10.2.3 Lactose utilisation

The ability of bacteria to utilise lactose as the source of energy and carbon was tested by the ability of the bacteria to grow on Mackonkey agar with salt and crystal violet (Merck Ltd., Johannesburg, RSA). A mass of 51.5 g of Mackonkey agar was weighed into a 2000 ml Erlenmeyer flask, and dissolved in 1000 ml of deionised water. The mixture was autoclaved at 121 °C for 15 minutes to sterilise. After autoclaving and cooling to approximately 50 °C, the medium was poured into aseptic 90 mm plastic Petri dishes (EC Lab Services, Port Elizabeth, RSA), and allowed to solidify at room temperature. Samples were taken from both reactors using the appropriate sampling ports and collected in sterilised test tubes. The subsamples were plated onto Mackonkey agar plates, which were allowed to dry at room temperature and incubated upside down at 37 °C.

10.2.4 Growth at 37 °C and addition of NaCl

Nutrient broth medium was purchased from Biolab (Merck Ltd., Johannesburg, RSA), prepared and sterilised according to the specifications by the manufacturer in 500 ml Erlenmeyer flasks. Samples from the CSTR and PBR were inoculated into the nutrient broth medium, as well as replicates

prepared with 10 % addition of NaCl, to test for halotolerance. The cultures were incubated at 37 °C for 24 hours.

10.2.5 Acidification of carbohydrates

A medium was prepared by dissolving 10 g of yeast extract (Merck Ltd., Johannesburg, RSA), 10 g of glucose, maltose, lactose or sucrose (Merck Ltd., Johannesburg, RSA) in 1000 ml of MilliQ water and the pH values were adjusted to 7.2 with 6 M HCl (Merck Chemicals Ltd). The media were autoclaved at 121 °C for 15 minutes, and individual flasks were inoculated with 10 ml of the reactor media. The samples and aseptic controls were incubated at the reactor temperatures for 24 hours, after which the pH drop between the control and samples for a particular reactor.

10.2 6 Catalase test

Hydrogen peroxide (H_2O_2) in 3 % solution was prepared by diluting saturated aqueous solution of H_2O_2 with the fraction of 30 % (Sigma-Aldrich, Johannesburg, RSA). Samples were taken out of both reactors, and 0.5 ml of each sample was aseptically transferred into a sterile test tube. A volume of 0.5 ml of the 3 % solution of H_2O_2 was added, and bubbling was observed if the test for catalase activity was positive.

10.2.7 Indole production test

A mass of 10 g of tryptone was weighed into a 2000 ml Erlenmeyer flask, and dissolved in 1000 ml of deionised water. A volume of 5 ml of the solution was pipetted into each individual test tube, and the tubes' content was autoclaved at 121 °C for 15 minutes. After autoclaving, the test tubes were inoculated with 0.5 ml of cultures from both reactors, giving 10 % inoculum concentration. Both cultures were incubated at 25 °C for different periods of time, and 1 ml samples were withdrawn and tested for indole presence. The methods, based on the Kovacs and the Erlich reagents (Sigma-Aldrich), were combined. Both reagents contain *p*-dimethylaminobenzaldehyde as the active ingredient. Detection of indole is based on the formation of a Schiff's base, which is formed by the reaction of the amine group of the indole ring, and the aldehyde group of *p*-dimethylaminobenzaldehyde. These compounds have been shown to be highly hydrophobic (Hoshika, 1975), and that is why extraction with xylene occurs in the Erlich method of indole production detection.

The remaining components of the Erlich reagent are ethanol and concentrated HCl, while pentanol, butanol and concentrated HCl are the remaining components in the Kovacs reagent. The alcohols present are responsible for phase separation, and/or formation of a single phase with the Kovacs reagent. Based on the above mentioned facts, it is likely that the Schiff's base will be concentrated close to the interface between the aqueous and the organic layer. As a result, the substitution of the Erlich reagent for the Kovacs reagent in the extraction with xylene should produce comparable results.

Samples were taken from both reactor cultures after 32 and 37 hours of incubation. A volume of 1 ml of xylene (Sigma-Aldrich) was added to 1 ml of the respective sample from the test tube. The mixture was vortexed for 30 s and allowed to stand at room temperature for 10 minutes to achieve phase separation. A volume of 0.5 ml of Kovacs reagent was added to the mixture by pipetting it down the wall of the of the test tube, and the mixture was allowed to react at room temperature for 5 minutes. Positive reaction is given by the formation of a red colour on the organic side of the interface between the xylene and the reactor sample.

10.2.8 Methyl red test

A solution of methyl red was prepared by weighing 0.1 g of the dye (Merck Chemicals Ltd), and dissolving it in 300 ml of 95 % ethanol in a 500 ml Erlenmeyer flask. The solution was transferred into a 500 ml volumetric flask and made up to the volume mark with deionised water. Methyl red Vogesky-Proskauer (MRVP) broth was prepared by weighing 7.0 g of polypeptone (Merck Ltd., Johannesburg, RSA) into a 2000 ml Erlenmeyer flask. 5.0 g of K_2HPO_4 was added together with 5.0 g of glucose (Merck Ltd., Johannesburg, RSA), and the mixture was dissolved in 1000 ml of deionised water. The solution was autoclaved at 121 °C for 15 minutes, along with test tubes covered with aluminium foil. A volume of 5 ml of the MRVP broth was pipetted into nine test tubes. Three of the test tubes were used as negative controls, while three were inoculated with the culture from the CSTR, and the remaining three with the culture from the PBR. The cultures were incubated at 37 °C for 48 hours, and then 5 drops of the methyl red solution was added to each test tube. If the test was positive, then the pH of the broth would drop to 4.2, yielding a red colour upon addition of the methyl red solution. Negative reaction is indicated by a yellow or orange colour.

10.2.9 Vogesky-Proskauer test

A solution of α-naphthol was prepared by weighing 5 g of the compound (Merck Chemicals Ltd) into a 500 ml Erlenmeyer flask, and dissolving it in 100 ml of 95 % ethanol. The solution was transferred into a 500 ml volumetric flask, and made up to the volume mark with deionised water. A solution of KOH was prepared by weighing 40 g of the compound (Merck Chemicals Ltd) into a 500 ml Erlenmeyer flask and dissolving it in 60 ml of deionised water. Both solutions were stored at 4 °C in the dark until use. The MRVP broth was prepared by weighing 7.0 g of polypeptone (Merck Chemicals Ltd) into a 2000 ml Erlenmeyer flask. 5.0 g of K_2HPO_4 was added together with 5.0 g of glucose (Merck Chemicals Ltd), and the mixture was dissolved in 1000 ml of deionised water. The solution was autoclaved at 121 °C for 15 minutes, along with test tubes covered with aluminium foil.

A 5 ml aliquot of the MRVP broth was pipetted into six test tubes. Two of the test tubes were used as negative controls, while two were inoculated with the culture from the CSTR, and the remaining two with the culture from the PBR. One test tube of each culture and one control were incubated at 37 °C for 48 hours, while the rest of the samples were incubated at 25 °C for the same period of time.

Subsequently, 1 ml of each sample was removed, 0.6 ml of the solution of α-naphthol was added, and the mixture was thoroughly mixed for 30 s. The same procedure was repeated with 0.2 ml of the solution of KOH, the samples were then incubated in slanted positions for 15 and 60 minutes. If the test was positive, a strong red colour would be observed from the top of the liquid layer down to the bottom of each sample.

10.2.10 Starch hydrolysis test

A mass of 10 g of tryptone was weighed into a 2000 ml Erlenmeyer flask and 15 g of Biolab bacteriological agar (Merck Ltd.) was added along with 1000 ml of deionised water. The pH of the mixture was adjusted to 7.2 using 6 M HCl, and it was brought to boiling point on a hotplate. After reaching 95 °C and achieving dissolution of the agar, 2 g of soluble starch was added into the mixture and it was sealed with aluminium foil. The content of the Erlenmeyer flask was autoclaved at 121 °C for 10 minutes. After autoclaving and reaching approximately 50 °C, the medium was poured into 90 mm aseptic plastic Petri dishes, and allowed to solidify at room temperature. Samples from both reactors were taken into sterilized test tubes using the appropriate sampling ports, streaked onto the solidified plates and incubated upside down at 37 °C for 24 hours. Iodine solution was prepared as with Gram staining, and the plates were flooded after the end of the incubation period. Cleared zones on the agar surface indicated starch hydrolysing activity of the organism.

10.2.11 Scanning electron microscopy (SEM) study

Two sub samples were taken and air dried on the slide cover and glued to the metallic holder. Then, samples were gold-coated using a sputtering system (Balzers 10 NION, Switzerland). Then each sample was placed in the holder of a scanning electron microscope (Vega, Tescan, TS5136 LM, Czech Republic) and examined under different magnifications after setting according to the manufacturer's instructions.

10.3 Results

Table 10.1 summarises the results obtained from the selected biochemical and physiological tests. Both sub samples from the CSTR and PBR showed Gram negative staining. Interestingly, the PBR had only Gram negative rods visible under optical microscopy whereas the CSTR consisted of both rods and cocci. Both cultures provided a positive indole reaction after 37 hours of incubation. The cultures from the PBR grew under aerobic conditions, indicating that the bacteria present were probably facultative anaerobes. Positive growth of both cultures showed they were capable of using lactose as a carbon source. The Methyl red test was negative for both cultures, indicated by the presence of orange colour. The Vogesky-Proskauer test was negative for both cultures due to the appearance of a strong brown colour. During the morphological studies using light microscopy and scanning electron microscopy (SEM), single flagella were observed on some rods (Figure 10.3).

Further rods dominated in both reactors (Figures 10.1 to 10.4). Figures 10.2 to 10.4 show the scanning electron micrographs of samples from the CSTR and PBR.

Table 10.1: Summary of results from the microbial characterisation tests.

Test	Results	
	CSTR	**PBR**
Motility determination and flagella staining	Non-motile cocci and non-motile rods without flagella	Non-motile rods with no flagella present and slight yellow pigmentation
Gram staining	Gram negative: rods and cocci (Figure 10.1a)	Gram negative: only rods (Figure 10.1b)
Lactose utilisation	Positive growth	Positive growth
Growth at 37 °C and addition of NaCl	Positive growth with and without NaCl	Positive growth with and without NaCl
Acidification of carbohydrates	pH drops with glucose and lactose only	pH drops with all carbohydrates
Catalase	Weak bubbling	Negative
Indole production	Positive indole reaction	Positive indole reaction
Methyl red	Negative	Negative
Vogesky-Proskauer	Negative with strong brown colour	Negative with strong brown colour
Starch hydrolysis	No starch hydrolysis occurred.	Starch hydrolysis occurred.

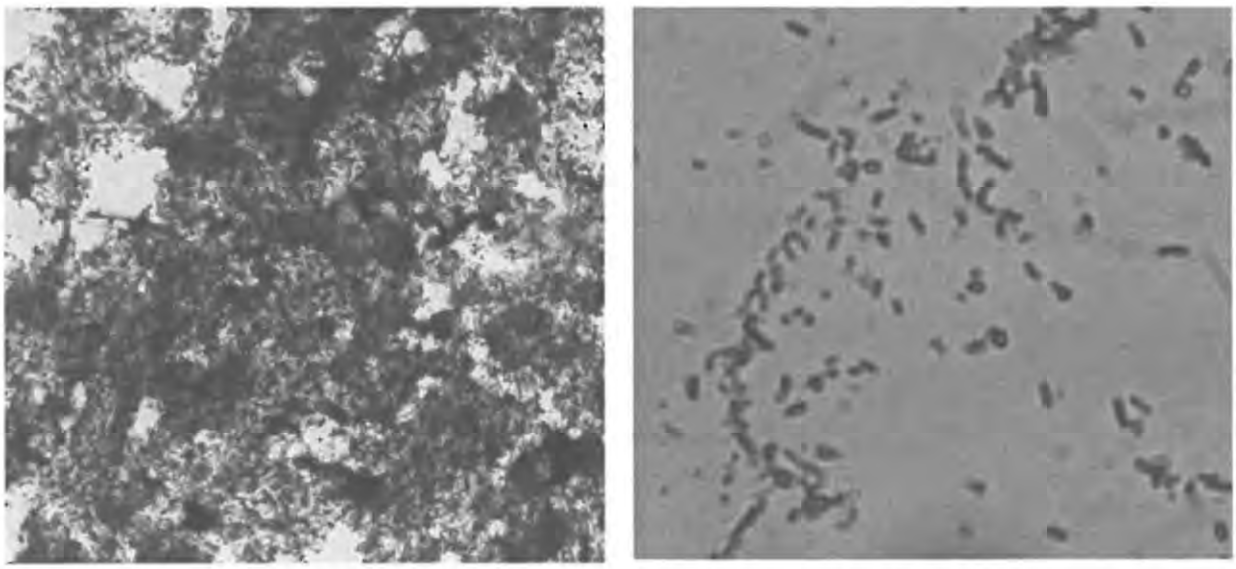

a: CSTR (40 ×) b: PBR (100 ×)

Figure 10.1: Gram stained microbial flocs as appeared in samples (Olympus Camedia digital camera).

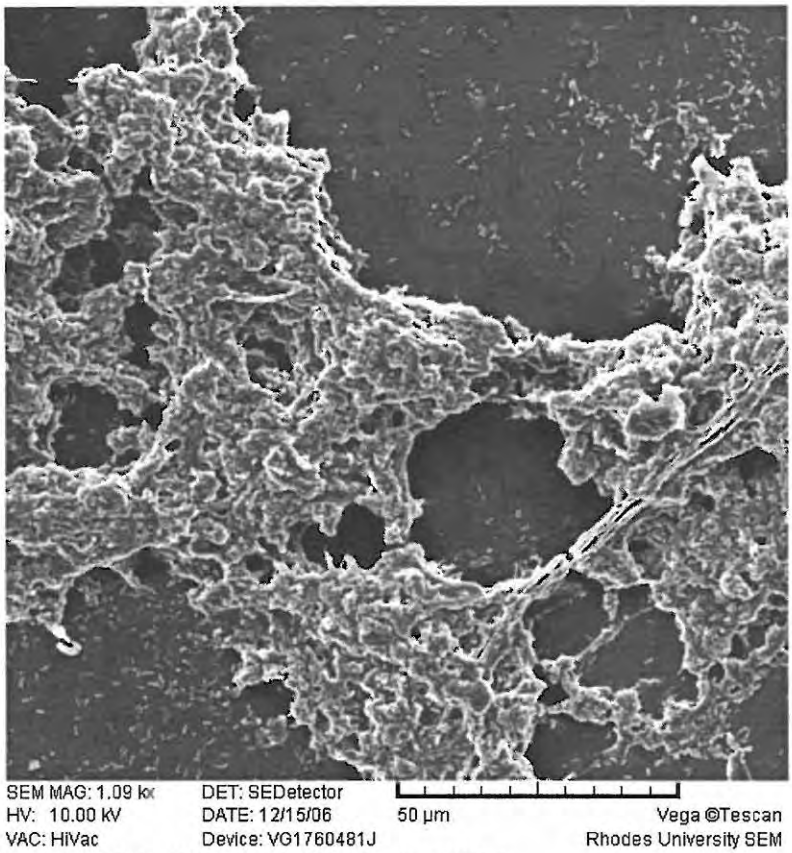

Figure 10.2: Microbial flocs in the CSTR.

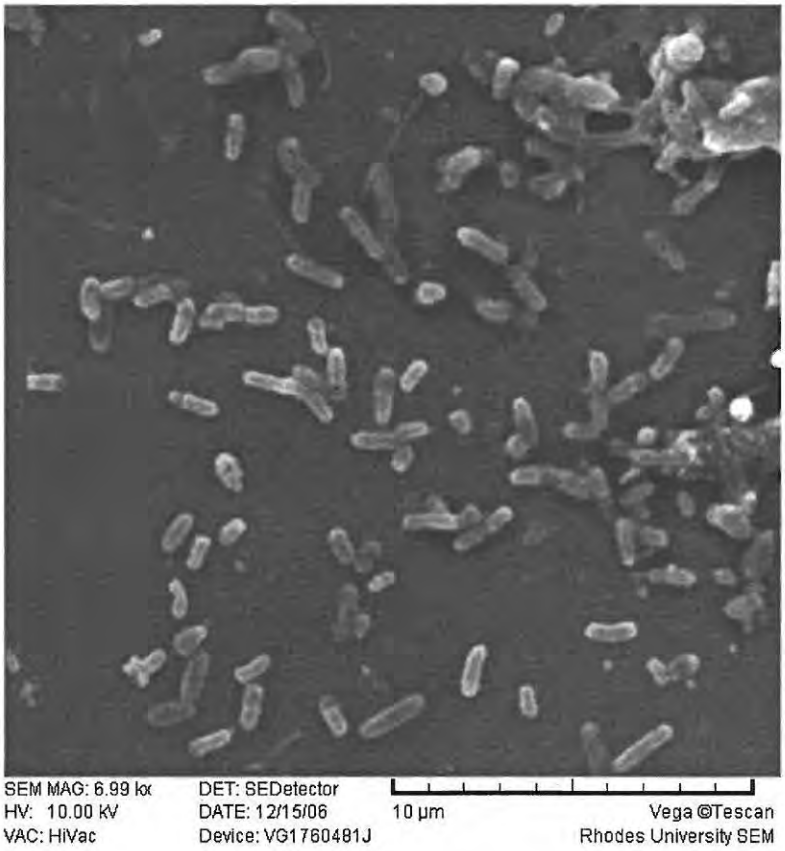

Figure 10.3: Rods and some flagella, consortium in the CSTR.

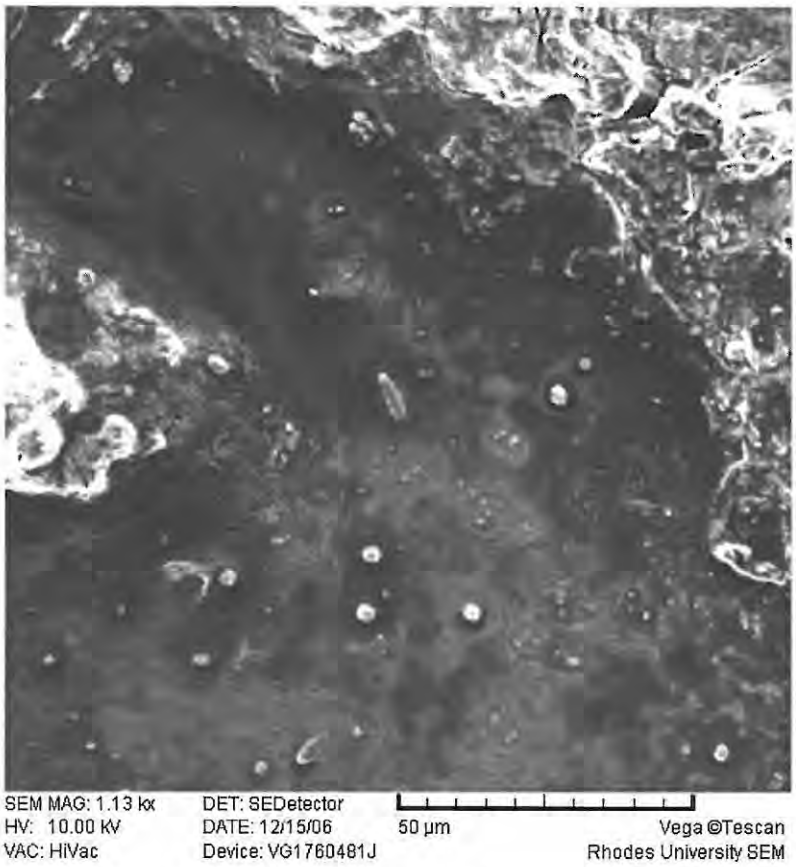

Figure 10.4: Microbial flocs in the PBR.

10.4 Discussion

Identification of genera and/or species in nitrification and denitrification is vital in designing an optimised nitrogenous compound removal process for PMR wastewater, as stressed earlier. Based on the preliminary biochemical and physiological studies carried out and considering the physico-chemical parameters (pH, NH_4^+, NO_2^-, NO_3^-, and MLSS etc) prevailing in the CSTR and PBR, the organisms were compared with the most probable genera found in soil or wastewater as reported by earlier researchers.

Based on the selected biochemical studies and cell morphology (Figures 10.1 to 10.4) of the microbial flocs in sub samples, attention was paid to a few genera as described below. According to Buchanan and Gibbons (1974), the genus of *Nitrosomonas* contains motile or non-motile organisms which are found singly, in pairs or as short chains and which are Gram negative. These microbes oxidise NH_4^+ to NO_2^- for fixing CO_2 for energy generation and as their carbon source. The pH range for growth is 6.5 to 8.5. The genus of *Nitrosococcus* contains spherical, motile or non-motile cells which convert NH_4^+ to NO_2^- for fixing CO_2, also for energy generation and as a carbon source. The optimum pH range is 6 to 8. According to Table 10.1, Figures 10.1 and 10.3, *Nitrosomonas* and *Nitrosococcus* genera can be suggested to exist in the CSTR.

Nitrobacter spp. are non-motile, Gram negative, rods, which are strictly aerobic and oxidise NO_2^- to NO_3^- for fixing CO_2 for energy generation and as a carbon source (Buchanan and Gibbons, 1974). The pH range for their growth is 6.5 to 8.5. The CSTR was operated in a pH range of 7.05 ± 0.50 showing the pH that prevailed in the reactor was within the optimum range for *Nitrobacter*.

The CSTR showed > 90 % NH_4^+-N removal with a mean MLSS of 1567 ± 323 mg/l and pH of 7.05 ± 0.50 (see Chapter 9: Table 9.1). Therefore it could be assumed that an effective NH_4^+-N removal occurred in the CSTR, even at 20 mg/l of Rh. Based on the preliminary microbial study the most probable genera could be *Nitrosomonas* and *Nitrosococcus*. However, phylogenetic study would be required for confirmation or to identify more accurate genera or species. Usually NOB reside in the inner layers of the AOB and nitrification is limited to the top 100 – 150 μm of the biofilm (Kowalchuck and Stephen, 2001). The observations of microbial flocs of > 100 μm (Figure 10.2) and previously reported total nitrogen loss (simultaneous nitrification and denitrification) in the CSTR (Chapter 4 and 5) suggest that there could be some microbial consortia which can denitrify in the inner layers of the microbial flocs of the CSTR.

The genus of *Pseudomonas* contains straight or curved Gram negative rods which are catalase positive, but not helical. Some species can denitrify under anoxic conditions. These species grow well under neutral or alkaline pH between 7.0 and 8.5 (Buchanan and Gibbons, 1974). *Pseudomonas mallei* is capable of denitrification with positive starch hydrolysis and does not have flagella (refer Table 10.1). *Flavobacterium* spp. vary from coccobacilli to slender rods, are motile or non-motile, grow on yellow, orange, red or brown and are Gram negative. Some of these species grow at 37 °C and are widely distributed in soil, fresh and marine waters (Buchanan and Gibbons, 1974). They have also been reported in activated sludge (You *et al.*, 2002). They are indole positive organisms with denitrifying capability and may have occurred in the CSTR (refer to Table 10.1).

Denitrification is positively correlated to pH and it may occur in waste up to about pH 11 (Knowles, 1982). At low pH (< 4), the nitrogen oxireductases which reduce N_2O are progressively inhibited, decreasing the overall denitrification rate. The pH of the denitrification reactor from which samples were analysed for microbial characterisation was 7.28 ± 0.51. Therefore, the pH in the reactor was within the optimum range for denitrification, thus metal toxicity could be the major inhibitor for denitrification activities. However, during the experimental period > 95 % NO_3^- was removed in the PBR with 20 mg/l of Rh. This shows that the denitrification may have been carried out effectively by some denitrifying consortia, even under high metal concentrations.

An NH_4^+-N increase was observed in the PBR after day 30 in the PBR-CSTR-PBR configuration described in Chapters 8 and 9 (Figure 10.5). This may have been due to NO_3^- reduction to NH_3.

Anaerobic metabolism of *Bacillus subtilis* including dissimilatory reduction of NO_3^- to NH_3 via NO_2^- has been reported previously (Ye and Thomas, 2001). However, since Gram negative staining was observed in the PBR subcultures, it can not be deduced that *B. subtilis* was the responsible microbe for dissimilatory NO_3^- reduction to NH_3 as *B. subtilis* is Gram positive (Voskuil and Chamblis, 1998). However, *Enterobacteriaceae* (Gram negative, motile or non-motile facultative anaerobes), bacilli, and clostridia can also reduce NO_3^- and NO_2^- to NH_4^+ (Knowles, 1982).

According to Egli *et al.* (2003a), AOB with different composition and complexity may form in reactor systems without obvious differences in performance measured by chemical parameters such as the rates of NO_2^- formation or NH_4^+ oxidation. Further, Egli *et al.* suggest choosing conditions favouring complex communities of AOB from the perspective of performance stability. Microbial species diversity in an activated sludge plant or a biofilm reactor is governed by the composition of the influent wastewater, environmental conditions such as pH, DO and temperature and process conditions prevailing in the plant or reactor (Wilderer *et al.* 2002).

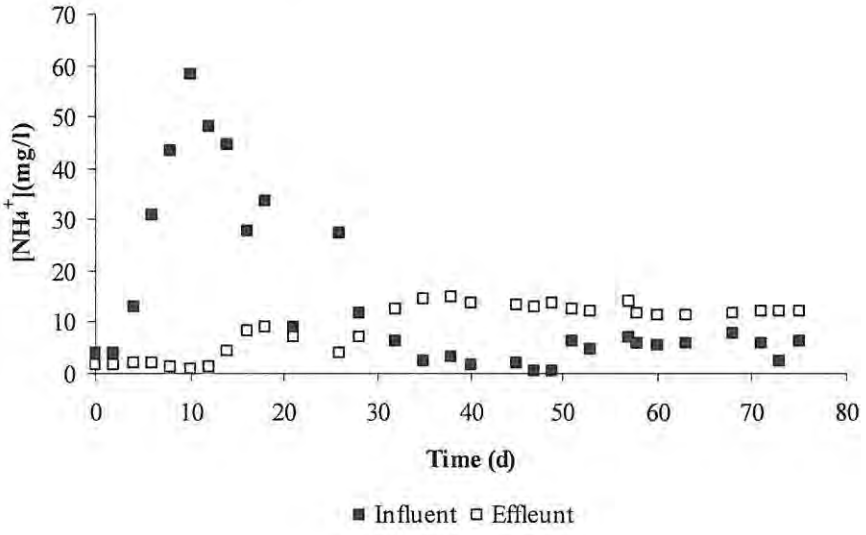

Figure 10.5: Ammonium formation in the PBR.

10.5 Interim conclusions

Gram negative, non-motile rods and cocci were detected in the aerobic part of the experimental system, indicating that, as expected, more than one species was present in the CSTR. The other physiological tests provided inconclusive results, probably originating from the mixed nature of the bacterial consortia present. In the PBR, the dominating micro-organism was a Gram negative, non-motile rod with slight yellow pigmentation. The organism had the ability to grow in liquid media with low and high concentration of chlorides, under both aerobic and anaerobic conditions. Based on these attributes as well on the acid production in carbohydrate media and the ability to hydrolyse starch, it was concluded that the dominant bacteria in the supernatant of the PBR were probably members of the

Flavobacterium genus. The probable species was *F. ferrugineum.* No conclusive species assignment is possible at this time, but it can be inferred that the CSTR and the PBR contained different microbial communities. The differences in community structure could only have arisen from short and medium term community acclimatisation, since both reactors received their initial inocula from the same source.

Based on this very preliminary investigation, it is recommended that DNA sequencing for better understanding of the microbial ecology prevailing in both reactors under high NH_4^+-N (> 50 mg/l), NO_3^--N (> 150 mg/l) and metal concentrations (> 15 mg/l) should be carried out. This information would assist in the optimisation of reactor environment (control of pH, DO, COD, metal concentration etc) to suit particular species or strains which can tolerate the high metal toxicity prevailing in PMR wastewater, while removing the highest amount of nitrogenous compounds from the wastewater.

CHAPTER 11

A problem well stated is a problem half solved.

- Charles Kettering (1876-1958).

11.0 Metal recovery from untreated and biologically treated simulated precious metal refinery wastewater

11.1 Introduction

Recovery of residual metals from precious metal refinery (PMR) wastewater is vital in terms of avoiding the loss of valuable metals which would otherwise be discarded in the wastewater, the potential toxic effects to the receiving ecosystem (Lenz *et al.*, 2005) and taking advantage of the lower capital intensive process of extracting metals from wastewater than the actual mining process. Precious metal refinery wastewater contains metals bound to nitrogenous compounds as a result of use of ammonium based blasting agents and solvents in metal extraction process (Kasia *et al.*, 2005). Therefore, removal of nitrogenous compounds from PMR wastewater may assist in recovery of metal in the wastewaters.

Heavy metals have conventionally been removed from industrial wastewaters by means of range of abiotic processes, such as ion-exchange, electrolytic techniques, adsorption and hydroxide precipitation (Naeem *et al.*, 2006; Eckenfelder, 2000). However, these processes are less economical for low metal concentrated wastewaters, produce toxic sludge which needs to be treated further, and are capital and technology intensive (Ray *et al.*, 2005). However, the phenomenon of metal accumulation by dead biomass (biosorption) is well documented (Barba *et al.*, 2001; Zhao *et al.*, 1999). The main advantages of these accumulation bioprocesses are the relatively low expense, non-hazardous reagents and potential regeneration of biosorbent after recovery. Hence those processes have been focused on in recent years. Bacteria, algae and fungi accumulate high concentrations of metal cations through passive cell wall adsorption reactions and fungi have a number of advantages compared to bacteria and algae, such as resistance to harsh environmental conditions (low pH and water activity) (Naeem *et al.*, 2006). The sorption process consists of a solid phase (sorbent: e.g. biomass) and a liquid phase (solvent: e.g. wastewater), containing dissolved species to be sorbed (sorbate: e.g. metal ion) and due to the affinity of the sorbent for the sorbate, the latter is attracted into the solid and bound there by different mechanisms (Volesky, 2001).

The three sorbents used were the yeast *Saccharomyces cerevisiae*, the water fern *Azolla filiculoides* and granular activated carbon (GAC). *Saccharomyces cerevisiae* is an inexpensive, readily available fungal biomass source which has shown > 35 % Rh recovery using a pure Rh solution (Mack, 2005). *Azolla filiculoides*, an aquatic weed, was selected as this biomass showed high affinity for both platinum and gold in previous studies (Antunes, 2002; Antunes *et al.*, 2001). Further, *A. filiculoides* is found in abundance throughout the RSA and has posed an environmental threat, as it depletes the dissolved oxygen in reservoirs (Zhao and Duncan, 1998). Granular activated carbon (GAC) was

selected for comparison purposes and to study the effect of GAC on metal toxicity in the PBR in which GAC was used as the biofilm carrier. The GAC has widely been used for detoxification of heavy metals in municipal and industrial wastewater (Eckenfelder, 2001; Manktelow *et al.*, 1984; Metcalf and Eddy, 2004). In this research, the effectiveness of metal recovery by bio/sorption was evaluated after removal of nitrogenous compounds from simulated PMR wastewater. The objective of this chapter was to compare the results of metal recovery effectiveness before and after the removal of nitrogenous compounds from simulated PMR wastewater had taken place.

11.2 Materials and methods

The experiment was carried out as a batch study using the untreated simulated PMR wastewater (feed solution used in nitrification and denitrification studies, Chapters 4 and 5: Materials) and the treated wastewater (process effluent). First the two wastewater types were analysed for NH^+_4-N, NO_2^--N and NO_3^--N concentrations using spectrophotometric kits (Merck Chemicals Ltd.) based on the principles of *Standard Methods* (APHA *et al.*, 1998). Spectroquant® test numbers 14752 (NH^+_4-N), 14776 (NO^-_2-N) and 14773 (NO^-_3-N) were used (analogous to *Standard Methods* 4500-NH_3-F, 4500-NO_2-B and 4500-NO_3-E, respectively). pH was measured using an electrode (CyberScan 2500, Eutech Instruments, Singapore).

Yeast biomass (*S. cerevisiae*) was obtained from a bakery supplied by Anchor Yeast Inc. and it was oven-dried overnight at 80 °C prior to use. *Azolla filiculoides* was prepared as described by Zhao *et al.* (1999). Fresh *A. filiculoides* was collected from a local dam near Grahamstown, South Africa. It was then washed with distilled water and oven-dried for 6 hours at 60 °C. The dry biomass was milled and sieved to select particles between $2-3$ mm in size for use. Granular activated carbon with approximate particle size of $1-2$ mm was obtained from a pet shop at Grahamstown, South Africa. The GAC was oven-dried at 80 °C overnight prior to use.

A mass concentration of 1 g/l of each sorbent was mixed with 100 ml of treated and untreated wastewater in 150 ml Erlenmeyer flasks. All samples were triplicated and continuously mixed on a benchtop shaker (Labcon, Lab Design Engineering, Maraisburg, South Africa) at 180 rpm for 24 hours at room temperature of 22 °C and atmospheric pressure of 961.1 mbar. Samples were then centrifuged at 5000 rpm for 5 minutes using a bench top centrifuge (Labfuge Ae, Heraeus Sepatech, Germany) to separate the sorbents from the bulk solution. After adjusting the pH to < 2 using 55 % HNO_3 (UniLab, Merck Chemicals Ltd.), each sample was filtered using a cellulose acetate membrane of 45 μm pore size (Whatman, England). Each acidified supernatant sample was then analysed for residual metals using an atomic absorption spectrophotometer (GBC 909C, Australia). All glassware was acid washed in 5 % HNO_3 and rinsed in deionised water before use.

11.3 Results

Table 11.1 presents the characterisation of nitrogenous compounds in the untreated and treated wastewaters used for the metal recovery batch study. Total nitrogen and NH_4^+-N removal efficiencies of the system from which the effluent was taken (Chapter 9: PBR-CSTR-PBR) were > 88 % and > 90 %, respectively. Table 11.2 shows the comparison of metal recovery from untreated wastewater and denitrified effluent. According to Table 11.2, there was a clear demonstration of improvement in metal recovery after removal of nitrogenous compounds from the raw wastewater. Recovery efficiency of the three sorbents were in the order of *A. filiculoides* > *S .cerevisiae* > GAC for untreated wastewater and GAC > *S. cerevisiae* > *A. filiculoides* for denitrified effluent (treated wastewater).

Table 11.1: Characteristics of untreated wastewater and denitrified effluent.

Parameter	Untreated wastewater (mg/l)			Denitrified effluent (mg/l)		
	NH_4^+-N	NO_2^--N	NO_3^--N	NH_4^+-N	NO_2^--N	NO_3^--N
Sample 1	130.8	0	0.6	12.1	0.41	1.8
Sample 2	116.8	0	0.5	11.2	0.42	4.4
Sample 3	130.0	0	0.4	11.3	0	3.6
Mean	125.9	0	0.5	11.5	0.28	3.3
Standard deviation	7.9	0	0.1	0.5	0.24	1.3
Rhodium (Rh)		18.902			N/A	
pH		5.39			7.72	

Table 11.2: Residual [Rh] in solution after bio/sorpion of metal in treated (denitrified effluent) and untreated wastewater.

Sample	Biosorption (SC and AF) / adsorption (GAC) (mg/l)					
	Untreated wastewater			Denitrified effluent		
	SC	AF	GAC	SC	AF	GAC
Sample 1	13.423	13.134	13.313	9.268	9.324	7.410
Sample 2	14.393	14.610	14.923	9.136	8.429	6.192
Sample 3	15.876	-	17.760	9.351	8.016	5.561
Mean	14.564	13.872	15.332	9.252	8.590	6.388
Standard deviation	1.235	1.0437	2.252	0.108	0.669	0.940
Recovery efficiency (%)	23.0	26.6	18.9	51.1	54.6	66.2

Saccharomyces cerevisiae – SC; *Azolla filiculoides* – AF; Granular activated carbon - GAC

Figure 11.1 shows the metal recovery per unit mass of each sorbent. Two distinct behaviours can be observed in metal recovery improvement with and without treatment of the simulated wastewater. The GAC showed the lowest metal capacity per unit mass before treatment of the wastewater and the

highest capacity for metals per unit mass after treatment of the wastewater for removal of the nitrogenous compounds.

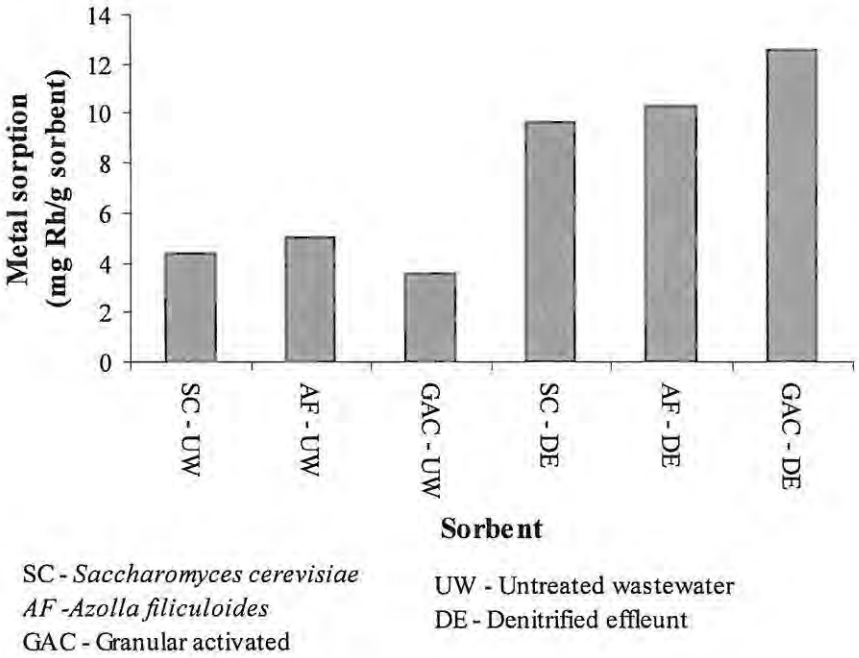

Figure 11.1: Metal recovery per unit mass of different sorbents with treated and untreated wastewater.

11.4 Discussion

Ionic binding of sorbent to metals can be described by various mechanisms such as ion-exchange, complexation, adsorption of simple ionic species and hydrolysis products of metal ions (Santos *et al.*, 2004). Although many biological materials bind heavy metals, only those with sufficiently high metal-binding capacity and selectivity for heavy metals are suitable for use in a full-scale biosorption process (Kratochivil and Volesky, 1998). The results from Tables 11.1 and 11.2 illustrated the importance of nitrogenous compounds removal from the PMR wastewater, showing that not only does it protect the environment, but it also significantly improves efficiency of metal recovery, enabling more active sites for the sorbent for metal binding. *Saccharomyces cerevisiae* showed > 28 % metal recovery improvement in denitrified effluent compared to the raw wastewater. *Azolla filiculoides* and GAC showed > 27.5 % and > 47 % improvements in metal recovery efficiency with the denitrified effluent compared to the untreated wastewater.

Out of the two biosorbents used, *S. cerevisiae* has been widely used for recovery or detoxification of heavy metals in municipal and industrial wastewaters (Dostalek *et al.*, 2004; Naeem *et al.*, 2006). Complete and rapid reversibility of the sorption process has led researchers to assume that the uptake of the metal cations is a passive reaction (non-metabolic) with metals, most likely bound exclusively

onto the functional groups present on the fungal cell wall (Naeem *et al.*, 2006). Further, at low pH, the majority of functional groups are protonated and minimal adsorption occurs. On the other hand, at high pH such as that which prevailed in the denitrified effluent (7.72), functional groups on the cell wall deprotonate sequentially and the extent of cation adsorption increases correspondingly. The results shown in Table 11.2 and Figure 11.1 partly corroborate this explanation: at low pH (untreated wastewater, pH 5.39), *S. cerevisiae* showed a lower metal uptake than at high pH (treated denitrified effleunt, pH 7.72) by a factor of two or more. Removal of nitrogenous compounds from the raw wastewater might have helped to bind the metal as more active sites are now available. A previous rhodium recovery study using *S. cerevisiae,* by Mack (2005), showed > 50 % metal uptake reduction in actual metal refinery wastewater compared to a pure solution of Rh, attributed to different compounds binding to the sites available to Rh and the existence of strong metal ligands in the actual metal refinery wastewater. Further, Mack (2005) reported > 40 % of metal recovery using Rh(III) pure solution with heat treated *S. cerevisiae*, compared to this study (23 % Rh recovery in the simulated untreated wastewater which had pH of 5.39). The significant difference in metal recovery efficiencies (40 % *vs.* 23 %) can be attributed to factors such as different Rh sources used (pure solution of Rh (III) *vs.* simulated wastewater with nitrogenous compounds) and different Rh oxidation state due to the pH prevailing in respective experiments, even though both Rh sources had the same Rh (III) oxidation state (in this study Rh was sourced as pentaaminechlororhodium (III) dichloride). Further, the metal recovery efficiency improvement from 23 % to 51 % after removal of nitrogenous compounds from the simulated wastewater showed that nitrogenous compounds competed for the binding sites available to *S. cerevisiae.*

Azolla filiculoides has been used as a biosorbent for adsorption of gold (III) and platinum (IV) from simulated and mining wastewaters (Antunes *et al.*, 2003). A batch study by Antunes *et al.* (2003) found that at a 1 g/l of biomass concentration, an initial platinum concentration of 20 mg/l and a pH of 2 were the optimal conditions for adsorption of Pt by *A. filiculoides.* In the current batch study, 20 mg/l of Rh and 1 g/l of *A. filiculoides* were used at pH 5.39 and 7.72. Thus the high pH may have led low Rh recovery. Therefore, Rh speciation at different pH needs to be investigated so that the number of binding sites available to the sorbent can be increased to obtain the maximum possible recovery of Rh from the PMR wastewater. A batch study using pure Pt (IV) solution by Antunes *et al.* (2003) with *A. filiculoides* at 1 g/l demonstrated > 80 % metal recovery efficiency at pH 2. However, Rh recovery efficiencies using *A. filiculoides* (1 g/l biomass concentration) achieved with treated and untreated simulated wastewater were > 54 % and > 26 %, at pH of 5.39 and 7.72, respectively. Even though two metals (i.e. Pt and Rh) can not be compared on similar basis, it shows the some common characteristics, such as pH dependency and similarities among PGMs with respect to biosorption. Reduced Rh recovery efficiency compared to two earlier studies (Mack, 2005, Rh and Antunes *et al.*, 2003, Pt) suggested that functional groups in the biomass might not have had adequate access to bind

the metal due to strong metal ligands such as NH_4^+-N and NO_3^--N present in the simulated wastewater. This was clearly demonstrated; once the nitrogenous compounds were removed from the simulated wastewater, the recovery efficiency improved from 26.6 % to 54.6 % without pH optimisation.

Granular activated carbon has hardly been reported for PGM recovery. Therefore, direct comparison to other research could not be carried out, but the promising potential of GAC was demonstrated with > 66 % metal recovery after treating the simulated wastewater. The dual role of GAC as a biofilm carrier and as the best sorbent for metal recovery in the PBR was highlighted. This suggests that GAC has the ability to attenuate the metal toxicity by absorbing the metals ions. This is supported by the > 99 % NH_4^+-N removal observed in the PBR in which GAC was used as the biofilm carrier (Chapters 4 and 5). Further, better biomass growth was observed in the PBR (Chapter 5). As pointed out in Chapter 2, micropores in GAC act as temporary micronutrient storage for better microbial growth in the reactor. Higher resilience to varying metal concentration with high NH_4^+-N removal was also demonstrated in the PBR. All these positive trends in the PBR have been at least partly caused by the use of GAC as a biofilm carrier. However, the cost of GAC has to be considered in developing a nitrogen removal and metal recovery system using GAC. In addition, non-destructive metal recovery is vital for regeneration of the sorbent for reuse in multiple sorption-desorption cycles for better process economy (Ray *et al.*, 2005).

The activated sludge (AS) process itself removes some heavy metals from wastewater, as it contains suitable sorbents. Its application has been reported for Cd, Cu and Ni (Al-Qodah, 2006). Different factors affect the removal of heavy metals in AS, such as the form of the heavy metal, its oxidation state, the mixed liquor, dissolved oxygen concentration, pH and presence of complexing agents (Özbelge *et al.*, 2004). The enhancement of the bioadsorption capacity of AS by alkali pretreatment could be attributed to the removal of the impurities, rupture of the cell membrane and the exposure of new binding sites to the ions by removing the lipids and proteins that mask them (Al-Qodah, 2006). Further, the toxic effects of heavy metals have been shown to decrease as the concentrations of complexing agencies increase, due to the decrease in free metal ions and their reactions with complexing agents. Özbelge *et al.* (2004) stated that the toxicity characteristics of a certain metal can be greatly modified by the other heavy metals present in solution because they compete for available organic ligands in sludge and wastewater. The effect of different metal concentrations of PGMs on specific oxygen uptake was demonstrated in Chapter 6.

It could be worthwhile to carry out a metal recovery comparison study using the nitrified wastewater (i.e. NH_4^+-N removed) from the outlet of the CSTR, where the highest [NO_3^--N] is available and the denitrified wastewater (NO_3^--N removed) from the outlet of the PBR to asses which nitrogen compounds has a greater influence on metal recovery by sorption.

Kratochvil and Volesky (1998) reported that packed-bed sorption columns were the most efficient recovery system for continuous removal of heavy metals. The operation cycle of these columns consisted of loading, regeneration and rinsing. Once the metal-sorption capacity of the column was exhausted, the sorbent was removed for regeneration with solutions of acids or hydroxides and the cycle ended with rinsing and / or back-washing. Therefore, when we look closely at the denitrification and metal recovery in the same column, a packed-bed column has some interesting features in point of view of process design, which could eventually lead to development of a robust system for both denitrification and metal recovery as a single stage process. Backwashing helps to remove excess biomass in the PBR while attenuating the degree of toxicity on denitrifying consortia depending on the type of sorbent. Thus it is the mutual benefit of each activity. However, careful and in-depth studies are required for optimising the two processes without compromising the nitrogen removal in the PBR.

11.5 Interim conclusions

The importance of nitrogenous compounds removal from PMR wastewater for effective metal recovery was demonstrated by final [Rh] in wastewater treated by sorption. Sorption of Rh by *S. cerevisiae* and *A. filiculoides* from wastewater after treatment was 40 % better than sorption of Rh from untreated wastewater, and with GAC as the sorbent the improvement was 60%. Metal ligation by nitrogenous compounds such as NH_4^+-N, NO_2^--N and NO_3^--N has hindered the recovery of metals in the simulated PMR wastewater by occupying the active sites available for the sorbent or by preferentially binding to the metal. Out of three sorbents used, the GAC achieved the highest efficiency of metal recovery from the denitrified effluent. The potential suitability of the PBR as a denitrification and metal recovery dual process unit was indicated. The results in Chapters 4, 5 and 6 and this chapter show the strong possibility of integration of nitrogen removal and metal recovery of PMR wastewaters.

CHAPTER 12

There is no mistake so great as the mistake of not going on.

- William Blake (1757-1827).

12.0 Conclusions and recommendations

The hypothesis was made that nitrogenous compounds in the PMR wastewater could be removed biologically, assisting the downstream recovery of precious metals contained in the wastewater was tested and proved through a series of experimental and theoretical modelling works. Hence, a preliminary bioprocess for removal of nitrogenous compounds from PMR wastewaters was developed using a model compound. Important process configurations, toxicity thresholds for selected PGMs and a model predicting the behaviour of the bioprocess using ASM1 and metal toxicity were developed.

12.1 Development of a nitrogen removal system for PMR wastewater

12.1.1 Preliminary investigations

According to the preliminary investigations, nitrogenous compounds removal in the PMR wastewater can be achieved either in a single-stage, where low ammonium (< 1 mg/l) and high nitrate (> 1000 mg/l) exist using the denitrification only option, or in a dual-stage system, where ammonium and nitrate concentrations are significant, using the nitrification-denitrification option. However, a study on long term variations of influent concentrations has to be done for decision making and detailed design processes. Further, treatment of a single wastewater stream would be more feasible than treating two separate acidic and caustic wastewaters, after evaluating the safety aspects of mixing highly acidic and caustic wastewater streams.

Based on the batch experiments, nitrification of acidic wastewater could be carried out even at pH 4, indicating that there was no need for pH adjustment, as the nitrifying microbes were able to acclimatise to low pH conditions. However, it was not clear which microbial species were responsible for removal of ammonium at low pH. Forty-eight hours was a suitable hydraulic retention time (HRT) for nitrification at pH 4 using the acidic wastewater, attaining > 85 % NH_4^+-N removal.

For denitrification, there was no statistically significant difference between sodium lactate and sodium acetate as a carbon source. Sodium lactate could be used as the carbon source based on the value recovery of PGM and denitrification process efficiency. Therefore, sodium lactate was used as the carbon source for denitrification. An appropriate HRT can be taken as 24 hours, based on the nitrate conversion, as there was an increase - decrease pattern after a certain time. This could be due to the hydrolysis of entrapped organic nitrogen and its subsequent release to the bulk solution. For a 1:1 a ratio of wastewater and inoculum, addition of 3 % (18 g/l) carbon source by volume gave the best nitrate conversion under the conditions used here. There was no significant pH change in the denitrification process, unlike in the nitrification process.

12.1.2 Reactor comparison study

All the reactors studied removed NH_4^+-N effectively from the simulated metal refinery wastewater with >85 % removal efficiency under the set conditions. The overall total nitrogen (TN) removal efficiencies in the CSTR, PBR and ALSR were > 68 %, > 79 % and 45 % respectively. Either autotrophic or heterotrophic nitrogen removal was observed in the three reactors studied. However, metal toxicity data for nitrification and denitrification for complex metal mixtures are not yet published, hence the mechanism of the enzymatic inhibition of NH_4^+-N and TN removal occurring in the process could not be ascertained. Robust behaviour of the PBR with consistent pH conditions and high anoxic NH_4^+-N and TN removal, compared to the CSTR and ALSR, suggested the PBR as a good candidate for wastewater treatment where pH is low and heavy metal concentrations high. The presence of metal inhibitor at a concentration of 30 mg/l did not significantly alter the NH_4^+-N removal in any of the reactors. However, based on the results of the comparison study, it became necessary to determine the metal toxicity threshold for the microbial consortium without compromising NH_4^+-N, NO_2^--N and NO_3^--N removal. Therefore, it is necessary to investigate the long term acclimatisation of nitrifying and denitrifying consortia to high metal concentrations by running reactors for a longer period than these used here. Further, it is too early draw conclusions based on these results for deciding the best reactor, as the system was not run for process optimisation considering each reactor type. Therefore, in order to confirm the effectiveness of each reactor type, each system needs to run under the optimum conditions.

12.1.3 CSTR-PBR operation

Both CSTR and PBR reactors effectively removed the NH_4^+-N from the simulated metal refinery wastewater with > 95 % removal efficiency. However, precious metal toxicity data for complex mixtures are not available in published literature and again the mechanism of the enzymatic inhibition of NH_4^+-N and NO_3^--N removal occurring in the process could not be ascertained. Though the standard procedure of nitrogen removal is based on first nitrification and then denitrification, the opposite was more effective as far as biomass retention and effective NH_4^+-N removal were concerned in the CSTR. However, these results along with a simulation study and metal toxicity data, can be used to optimise the overall nitrogen removal in the PMR wastewater. Therefore, it is still not possible to draw conclusions based on these results alone for deciding the best reactor type, as reactors were not run for their optimum conditions by varying related parameters such as HRT, SRT, metal concentrations, recycling ratio, dissolved oxygen (in the case of the CSTR), etc, considering each reactor type. However, these studies showed the long acclimatisation period (approximately over 65 days) needed by denitrifying bacteria for high metal concentration (30 mg/l) and the shorter acclimatisation period of heterotrophic anoxic NH_4^+ oxidising bacteria with merely 12 days for > 99 % NH_4^+-N removal. Further, denitrification was not effective (just > 32 % nitrate removal in the PBR after 65 days of acclimatisation), probably due to high metal toxicity for the denitrifying bacteria

whereas NH_4^+-N removal in both CSTR and PBR performed well. This could be due to the tolerance capacity for metal toxicity by nitrifying consortia under both aerobic (CSTR) and anoxic (PBR) conditions.

12.2 Development of a mathematical model

12.2.1 Metal toxicity studies for ASP respiration

In order to incorporate the metal toxicity data in the simulation, four experimental models were developed for PGMs (Pt, Pd, Rh, and Ru) by correlating the metal concentration and microbial maximum SOUR. These models can be used to reveal the complete inhibition concentration for each metal in the activated sludge process. Based on the experimental model developed, the toxicity of the PGMs to activated sludge respiration was found to be in the order of Pt > Pd > Rh > Ru with inhibition coefficients of 16 mg/l, 25 mg/l, 33 mg/l, 39 mg/l, respectively. Higher inhibition coefficients indicate lower metal toxicity.

As this toxicity test was carried out using activated sludge cultured from trickling filter humus sludge, in order to ascertain the PGM toxicity on nitrification and denitrification, it is recommended that the AUR, NFR and NUR be measured along with the OUR in the nitrification process under different metal concentrations. This would assist in distinguishing the respiration by nitrifying consortia from respiration by the rest of the microbes present in the mixed liquor, and the NUR would reveal the denitrifying activity under anoxic conditions.

Further, metal speciation of those metals under different pH conditions, metal complexation and competition in actual PMR wastewater could have different effects on nitrification and denitrification processes. Therefore, the effect of metal speciation, complexation and competition of different metal mixtures in PMR wastewaters should be further investigated for better understanding of metal toxicity on nitrification and denitrification processes.

12.2.2 Mathematical modelling of nitrogen removal in PMR wastewater

A model for nitrogen removal in PMR wastewaters was developed based on the ASM1, the autotrophic nitrogen removal process modelled by van Hulle (2005) based on ASM1 and incorporating metal toxicity inhibition used by Lewandowski (1985). In the current ASM1- PGM model, identifying the respective parameters for the given process was the most important aspect of validation of the model. Initially, values for each unknown parameter were adopted from the literature. However, it should be noted that those values could be significantly different from the actual values under different sets of reactor operating conditions.

The model developed was approximately calibrated using a sensitivity analysis and verified to characterise the operation of removal of nitrogen from metal refinery wastewater considering the metal toxicity. Based on the metal toxicity threshold for rhodium, a test run was carried out for complete nitrogen removal from the PMR wastewater. Further optimisation is needed for other metals (Pt, Pd, Ir, Ru, and Os) which can be predicted using the developed model and metal toxicity threshold for each metal. Once this model was calibrated experimentally, it can be used for both process optimisation and control of nitrogen removal process in PMR wastewater.

12.2.3 Simulation and calibration of ASM1_PGM for PMR wastewater

A mathematical model (ASM1_PGM) developed for the bioprocess of nitrogenous compounds removal from precious metal refinery wastewater was simulated and approximately calibrated using a sensitivity analysis. Through a scenario analysis, the most sensitive parameters affecting the validity of the model were identified for further refinement of the proposed model. Approximate validity of the model was supported by the experimental results presented in Chapter 6 using toxicity studies and the CSTR-PBR configuration discussed in Chapter 9.

Simulation results showed that nitrogen removal occurred not only through the standard nitrification and denitrification process, but also some sort of anammox activity. The simulation results also showed the ability to control the process under different conditions such as differing metal concentrations. The model can be used as an effective tool for model based optimisation of the experimental work / the bioprocesse after proper calibration using empirically.

12.3 Potential process control protocol for nitrogenous compounds removal from PMR wastewater

A control strategy for removal of nitrogenous compounds from PMR wastewater was proposed based on the literature screening, experiments and simulation work. Of the different reactor configurations the PBR-CSTR-PBR showed higher overall removal efficiencies of nitrogenous compounds compared to the CSTR-PBR and PBR-CSTR configurations. Neither pH control nor biomass introduction to CSTR was needed under this configuration, as automatic pH control and MLSS maintenance was observed.

However, detailed experimental procedures are required for further refinement of the proposed control strategy. For example, the optimum floc size for simultaneous SND or anammox activity needs to be found using different stirring speeds which do not break the microbial flocs excessively, as described earlier. Nitrogen removal capacity per unit reactor volume under different HRTs and PGM concentrations need to be evaluated experimentally to determine the optimum HRT and maximum tolerable metal toxicity.

12.4 Metal recovery batch test

The importance of nitrogenous compounds removal from PMR wastewater for effective metal recovery was demonstrated by final [Rh] in wastewater treated by sorption. Sorption of Rh by *S. cerevisiae* and *A. filiculoides* from wastewater after treatment was 40 % better than sorption of Rh from untreated wastewater, and with GAC as the sorbent the improvement was 60%. Metal ligation by nitrogenous compounds such as NH_4^+-N, NO_2^--N and NO_3^--N has hindered the recovery of metals in the simulated PMR wastewater by occupying the active sites available for the sorbent or by preferentially binding to the metal. Out of three sorbents used, the GAC achieved the highest efficiency of metal recovery from the denitrified effluent. The potential suitability of the PBR as a denitrification and metal recovery dual process unit was indicated. The results in Chapters 4, 5 and 6 and this chapter show the strong possibility of integration of nitrogen removal and metal recovery of PMR wastewaters.

12.5 Microbial identification in the CSTR and PBR

This work was performed in addition to the original objectives stated in section 1.2 (page 4). Gram negative, non-motile rods and cocci were detected in the aerobic part of the experimental system, indicating that more than one species was present in the CSTR. The results of the other physiological tests provided inconclusive results, probably originating from the mixed nature of the consortia present. No species assignment is possible at this time. In the PBR, the dominating microorganims was a Gram negative, non-motile rod with slight yellow pigmentation. The organism had the ability to grow in liquid media with low and high concentration of chlorides, under both aerobic and anaerobic conditions. Based on these attributes as well on the acid production in carbohydrate media and the ability to hydrolyse starch, it was concluded that the dominant bacteria in the supernatant of the PBR were probably members of *Flavobacterium* genus, possibly *F. ferrugineum.*

Based on this very preliminary investigation, it is recommended that DNA sequencing for better understanding of the microbial ecology prevailing in both reactors under high NH_4^+-N (> 50 mg/l), NO_3^--N (> 150 mg/l) and metal concentrations (> 15 mg/l) should be carried out. This information would assist in the optimisation of reactor environment (control of pH, DO, COD, metal concentration etc) to suit particular species or strains which can tolerate the high metal toxicity prevailing in PMR wastewater, while removing the highest amount of nitrogenous compounds from the wastewater.

12.6 General recommendations

This holistic approach of bioprocess development paved the way to investigate the whole process at once considering significant number of aspects such as wastewater characterisation, different reactors and process configurations, metal toxicity, process modelling and microbial community analysis. However, it is necessary to conduct specific experimental work in detailed to optimise the developed

bioprocess. As much of this research was carried out using a simulated refinery wastewater, testing the proposed mathematical model and verifying the bioprocess using actual refinery wastewater is still required. This study showed that the longer the period of operation the better the process stability. Therefore, a mini-scale (20 to 50 litres of reactor capacity) should be run for determination of the process stability and robustness using the actual PMR wastewaters. The model parameters were mainly taken from the literature. However, in order to asses the model accurately, the specific model parameters using actual refinery wastewaters should be found.

For scaling up of the CSTR, a computational fluid dynamics (CFD) study would be useful to investigate the optimum stirring speed and mixing while the optimum floc size can be maintained for maximum removal of nitrogen from the wastewater. It is important to keep the optimum floc size in suspension to achieve the both ammonium oxidation and nitrite oxidation, as excessive mixing (or stirring) will lead mechanical floc breakage and consequent poor ammonium and nitrite removal in the CSTR. On the other hand, poor mixing would lead to settling of biomass in the tank, heterogeneous dissolution of oxygen, substrate and nutrients in the bulk fluid and hence poor ammonium and nitrite removal in the CSTR. Similarly biofilm and hydraulic modelling of PBR is necessary for proper simulation work. During the current simulation work the assumption made as completely mixing condition is not true in PBR. Possibly modelling of the hydraulics of the PBR as serially connected plug flow reactors would enhance the simulation. Further, flow through porous media could be used as the hydraulic modelling basis in the PBR.

13.0 References

Abeling, U., Seyfried, C.F., 1992. Anaerobic–aerobic treatment of high – strength ammonium wastewater – nitrogen removal via nitrite. Water Science and Technology, 26(5-6):1–12.

Aesøy, A., Ødegaard, H., Bach, K., Pujol, R., Hamon, M., 1998. Denitrification in a Packed Bed Biofilm Reactor (BIOFOR) – Experiments with different carbon sources. Water Research, 32:1463–1470.

Akunna, J.C., Bizeau, C., Moletta, R., 1993. Nitrate and nitrite reductions with anaerobic sludge using various carbon sources: Glucose, glycerol, acetic acid, lactic acid and methanol. Water Research, 27:1303–1312.

Al–Qodah, Z., 2006. Biosorption of heavy metal ions from aqueous solutions by activated sludge. Desalination, 196:164–176.

American Public Health Association (APHA), the American Water Works Association (AWWA), and the Water Environment Federation (WEF), *Standard Methods for the Examination of Water & Wastewater*. Lenore S. Clescerl, Arnold E. Greenberg, Andrew D. Eaton (Editors). 1998. ISBN 0–87553–235–7.

Antunes, A.P.M., Sanyahumbi, D., Nightingale, L., Payne, R., Maclear, A., Duncan, J.R., 2003. Development of bioreactor systems for the treatment of heavy metal containing effleunts. WRC Report No. 845/1/03. Water Research Commission, Gezina, 0031, Republic of South Africa.

Antunes, A.P.M., 2002. Removal and recovery of gold and platinum from aqueous solutions utilizing the non–viable biomass *Azolla filiculoides*. PhD Thesis. Department of Biochemistry, Microbiology and Biotechnology, Rhodes University, Grahamstown, South Africa.

Antunes, A.P.M., Watkins, G.M., Duncan, J.R., 2001. Batch studies on the removal of gold (III) from aqueous solution by *Azolla filiculoides*. Biotechnology Letters, 23:249–251.

Arican, B., Gokcay, C.F., Yetis. U., 2002. Mechanistics of nickel sorption by activated sludge. Process Biochemistry, 37(11):1307–1315.

Arrojo, B., Mosquera–Corral, A., Campos, J.L., Mendez, R., 2006. Effects of mechanical stress on Anammox granules in a sequencing bacth reactor (SBR). Journal of Biotechnology, 123:453–463.

Baeza, J.A., Gabriel, D., Lafuente, J., 2002. Improving the nitrogen removal efficiency of an A^2/O based WWTP by using an on–line Knowledge Based Expert System. Water Research, 36:2109 – 2123.

Bagay, M.M., Sherrard, J.H., 1981. Combined effects of cadmium and nickel on the activated sludge process. Journal of the Water Pollution Control Federation, 53:1609–1619.

Barba, D., Beolchini, F. and Veglió, F., 2001. A simulation study on biosorption of heavy metals by confined biomass in UF/MF membrane reactors. Hydrometallurgy, 59:89–99.

Barber, W.P., Stuckey, D.C., 2000a. Nitrogen removal in a modified Anaerobic Baffled Reactor (ABR): 1, Denitrification. Water Research, 34:2413–2422.

Barber, W.P., Stuckey, D.C., 2000b. Nitrogen removal in a modified Anaerobic Baffled Reactor (ABR): 2, Nitrification. Water Research, 34:2423–2432.

Battistoni, P., Fava, G., Ruello, M.L., 1993. Heavy metal shock load in activated sludge uptake and toxic effects. Water Research, 27:821–827.

Beg, S.A., Hassan, M.M., Chaudhry, M.A.S., 1998. Chromium (IV) inhibition in multi–substrate carbon oxidation and nitrification process in an upflow packed bed biofilm reactor. Biochemical Engineering Journal, 143–152.

Bernet, N., Sanchez, O., Cesbron, D., Steyer, J.P., Delegès, J.P., 2005. Modelling and control of nitrite accumulation in a nitrifying biofilm reactor. Biochemical Engineering Journal, 24:173–183.

Beyenal, H., Lewandowsky, Z., 2005. Modelling mass transport and microbial activity in stratified biofilms. Chemical Engineering Science, 60:4337–4348.

Beyenal, N.Y., Ozbelge, T.A., Ozbelge, H.O., 1997. Combined effects of Cu^{2+} and Zn^{2+} on activated sludge process. Water Research, 31:699–704.

Bilanovic, D., Battistoni, P., Cecchi, F., Pavan, P., Mata–Alvarez, J., 1999. Denitrification under high nitrate concentration and alternating anoxic conditions. Water Research, 33:3311–3320.

BOD Primer, 2004. Determination of biochemical oxygen demand (BOD). WTW,Germany.

Bothe, H., Jost, G., Schloter, M., Ward, B.B., Witzel, K.P., 2000. Molecular analysis of ammonia oxidation and denitrification in natural environments. FEMS Microbiology Reviews, 24:673–690.

Bott, C.B., Love, N.G., 2001. The immunochemical detection of stress proteins in activated sludge exposed to toxic chemicals. Water Research, 35:91–100.

Bourrel, S., Dochain, D., Babary, J.P., Queinnec, I., 2000. Modeling, identification and control of a denitrifying biofilter. Journal of Process Control, 10:73–91.

Brombacher, C., Bachofen, R., Brandl, H., 1997. Biohydrometallurgical processing of solids: a patent review. Applied Microbiology and Biotechnology, 48:577–587.

Brindle, K., Stephenson, T., Semmens, M.J, 1998. Nitrification and oxygen utilization in a membrane aeration reactor, Journal of Membrane Science, 144:197– 209.

Brun, R., Kuhni, M., Siegrist, H., Gujer, W., Reichert, P., 2002. Practical identifiability of ASM2d parameters – systamatic selection and tuning of parameters subsets. Water Research, 36:4113–4127.

Buchanan, R.E. Gibbons, N.E., 1975. Bergey's manual of determinative bacteriology, 8th Edition, The Williams and Wilkins Company, Baltimore.

Burerell, P.C., Keller, J., Blackall, L.L, 1998. Microbiology of a nitrite–oxidising bioreactor. Applied and Environmental Microbiology, 64:1878–1883.

Burgess, J.E., Stuetz, R.M., Morton, S., Stephenson, T., 2002. Dinitrogen oxide detection for process failure early warning systems. Water Science and Technology, 45(4–5): 247–254.

Burton, S.A.Q., Prosser, J.I., 2001. Autotrophic Ammonia Oxidation at Low pH through Urea Hydrolysis. Applied and Environmental Microbiology, 67(7): 2952–2957.

Bury, S.J., Groot, C.K., Huth, C., Hardt, N., 2002. Dynamic simulation of chemical industry wastewater treatment plants. Water Science and Technology, 45(4-5):355-363.

Campos, J.L., Mendez, R., Lema, J.M., 2000. Operation of a nitrifying activated sludge airlift (NASA) reactor without biomass carrier. Water Science and Technology 41(4–5):113–120.

Casasus, A., Hamilton, R.K., Svoronos, S.A., Koopman, B., 2005. A simple model for diauxic growth of denitrifying bacteria. Water Research, 39:1914–1920.

Carrera, J., Baeza, J.A., Vicent, T., Lafuente, J., 2003. Biological nitrogen removal of high–strength ammonium industrial wastewater with two–sludge system. Water Research, 37: 4211– 4221.

Chandran, K., Smets, B.F., 2000. Single–step nitrification models erroneously describe batch ammonia oxidation profiles when nitrite oxidation becomes rate limiting. Biotechnology and Bioengineering, 68:396–406.

Checchi, N., Marsili–Libelli, S., 2005. Reliability of parameter estimation in respirometric models. Water Research, 39:3686–3696.

Chen, J.–H., Hsu, Y.–C., Chen, Y.–F., Lin, C.–C., 2003. Application of gas–inducing reactor to obtain high oxygen dissolution in aeration processes. Water Research, 37:2929–2928.

Cho, D.H., Kim, E.Y., 2003. Characterization of Pb^{2+} biosorption from aqueous solution by *Rhodotorula glutini.* Bioprocess and Biosystem Engineering, 25: 271–277.

Christiansen, P., Hollesen, L., Harremoes, P., 1995. Liquid film diffusion on reaction rate in submerged biofilters. Water Research, 29:947–952.

Coakley, G.J., 2000. The Mineral Industry of South Africa: In U.S. geological survey minerals yearbook – 2000:25.5–15.15.

Dahl, C., Sund, C., Kristensen, G.H., Redenbregt, L., 1997. Combined biological nitrification and denitrification of high–salinity wastewater. Water Science and Technology, 36 (2–3):345–352.

Daims, H., Nielsen, J.L., Nielsen, P.H., Schleifer, K–H., Wagner, M., 2001. In situ characterisation of *Nitrospira*–like nitrite–oxidising bacteria active in wastewater treatment plants. Applied and Environmental Microbiology, 67(11):5273–5284.

Dapena–Mora, A., Campos, J.L., Mosquera–Corral, A., Jetten, M.S.M., Mendez, R., 2004a. Stability of the ANAMMOX process in a gas–lift reactor and a SBR. Journal of Biotechnology, 110:159–170.

Dapena–Mora, A., Van Hulle, S.W.H., Campos, J.L., Mendez, R., Vanrolleghem, P.A., Jetten, M.S.M., 2004b. Enrichment of Anammox biomass from municipal activated sludge: experimental and modeling results. Journal of Chemical Technology and Biotechnology, 79:1421–1428.

De Boer, W., Kowalchuk, G.A., 2001. Nitrification in acid soils: micro–organisms and mechanisms. Soil Biology and Biochemistry, 33:853–866.

De Carlo, E.H., Thomas, D.M., 1985. Removal of arsenic from geothermal fluids by adsorptive bubble flotation with colloidal ferric hydroxide. Environmental Science and Technology, 19:538–544.

De Schamphelaere, K.A., Heijerick, D.G., Janssen, C.R., 2004. Comparison of the effect of different pH buffering techniques on the toxicity of copper and zinc to Daphnia magna and Pseudokirchneriella subcapitata. Ecotoxicology, 13(7):697–705.

Dilek, F. B., Yetis, U., 1992. Effects of heavy metals on activated–sludge process. Water Science and Technology, 26: 801–813.

Dostalek, P., Patzak, M., Matejka, P., 2004. Influence of specific growth limitation on biosorption of heavy metals by Saccharomyces cerevisiae. International Biodeterioration & Biodegradation 54:203 – 207.

Dobson, R.S., Burgess, J. E., 2007. Biological treatment of precious metal refinery wastewater: A review. Minerals Engineering, 20:519–532.

Dobson, R.S., 2006. Honours thesis, Dept. of Biochemsitry, Microbiology and Biotechnology, Rhodes University, Grahamstown, South Africa.

DWAF, 1996. South African water quality guidelines, Volume 7: Aquatic Ecosystems, First edition 1996. Department of Water Affairs and Forestry, Private Bag X313, Pretoria 0001.

Eberl, H.J., Picioreanu, C., Heijnen, J.J., van Loosdrecht, M.C.M., 2000. A three–dimensional numerical study on the correlation of spatial structure, hydrodynamic conditions, and mass transfer and conversion in biofilms. Chemical Engineering Science, 55:6209–6222.

Eckenfelder, W.W., 2000. Industrial Water Pollution Control, Third Edition, McGraw–Hill Book Co. Singapore, pp. 138 – 140.

Egli, K., Langer, C., Siegrist, H.R., Zehnder, A.J.B., Wagner, M., van der Meer, J.R., 2003a. Community Analysis of Ammonia and Nitrite Oxidisers during Start–Up of Nitritation Reactors. Applied Environmental Microbiology, 69:3213–3222.

Egli, K., Bosshard, F., Werlen, C., Lais, P., Siegrist, H., Zehnder, A.J.B., Wagner, M., van der Meer, J.R., 2003b. Microbial composition and structure of a rotating biological contactor biofilm treating ammonium–rich wastewater without organic carbon. Microbial Ecology, 45:419–432.

Ekama, G.A., Wentzel, M.C., 2004. Modelling inorganic material in activated sludge systems, Water SA, 30(2):153–174.

Etchebehere, C., Errazquin, I., Barrendeguy, E., Dabert, P., Moletta, R., Muxi, L., 2001. Evaluation of the denitrifying microbiota of anoxic reactors. FEMS Microbiology Ecology, 35:259–265.

Eysenbach, E., 1994. Pretreatment of Industrial Wastes, Water Environment Federation, USA. 252.

Farabegoli, G., Chiavola, A., Rolle, E., Stracquadanio, S., 2004. Experimental study on nitrification in a submerged aerated biofilter. Water Science and Technology, 49(11–12):107–113.

Ford, T., Maki, J., Mitchell, R., 1995. Metal–microbe interactions, In Bioextraction and biodeterioration of metals. Editors: Gaylarde, C.C., Videla, H.A., Cambridge University Press, Cambridge. 1–23.

Fouad, M., Bhargava, R., 2005. A simplified model for the steady–state biofilm–activated sludge reactor. Journal of Environmental Management, 74:245–253.

Fuerhacker, M., Bauer, H., Ellinger, R., Sree, U., Schmid, H., Zibuschka, F., Puxbaum, H., 2000. Approach for a novel control strategy for simultaneous nitrification/denitrification in activated sludge reactors. Water Research, 34:2499–2506.

Fujii, T., Sugino, H., Rouse, J.D., Furukawa, K., 2002. Characterisation of microbial community in an anaerobic ammonium – Oxidizing biofilm cultured on a nonwoven biomass carrier. Journal of Bioscience and Bioengineering, 94:412–418.

Fux, C., Velten, S., Carozzi, V., Solley, D., Kéller, J., 2006. Efficient and stable nitritation and denitritation of ammonium–rich sludge dewatering liquor using an SBR with continuos loading. Water Research, 40:2765–2775.

Fux, C., Huang, D., Monti, A., Siegrist, H., 2004a. Difficulties in maintaining long–term partial nitritaion of ammonium–rich sludge digester liquids in a moving–bed biofilm reactor (MBBR). Water Science and Technology, 49(11):53–60.

Fux, C., Marchest, V., Brunner, I., Siegrist, H., 2004b. Anaerobic ammonium oxidation of ammonium–rich waste streams in fixed–bed reactors. Water Science and Technology, 49(11–12):77–82.

Fux, C., Boehler, M., Huber, P., Brunner, I., Siegrist, H., 2002. Biological treatment of ammonium–rich wastewater by partial nitritation and subsequent anaerobic ammonium oxidation (anammox) in a pilot plant. Journal of Biotechnology, 99:295–306.

Francis, A.J., Dodge, C.J., 1990. Anaerobic microbial remobilization of toxic metals coprecipitated with iron oxide. Environmental Science and Technology, 24:373–378.

Gallert, C., Winter, J., 2005. Bacterial metabolism in wastewater treatment systems. In: Environmental Biotechnology, Concepts and applications, edited by H–J. Jordening and J. Winter. Wiley–VCH Verlag GmBH & Co. KGaA., Weinheim.

Gapes, D., Pratt, S., Yuan, Z., Keller, J., 2003. Online titrimetric and off–gas analysis for examining nitrification processes in wastewater treatment. Water Research, 37:2678–2690.

Garcia–Calvo, E., Rodriguez, A., Prados, A., Klein, J., 1999. A fluid dynamic model for three–phase airlift reactors. Chemical Engineering Science, 54: 2359–2370

Gerhardt, P., Murray, R. G. E., Costilow, R. N., Nester, E. W., Wood, W. A., Krieg, N. R. and Briggs–Phillips, G., 1981. Manual of Methods of General Bacteriology. *American Society for Microbiology*, Washigton DC.

Gernaey, K.V., van Loosdrecht, M.C.M., Henze, M., Lind, M., Jorgensen, S.B., 2004. Activated sludge wastewater treatment plant modeling and simulation: state of art. Environmental Modelling and Software, 19:763–783.

Gernaey, K., Bogaert, H., Vanrolleghem, P., Massone, A., Rozzi, A., Verstreate, W., 1998a. A titration technique for on–line nitrification monitoring in activated sludge. Water Science and Technology, 37(12):103–110.

Gernaey, K., Vanderhasselt, A., Bogaert, H., Vanrolleghem, P., Verstreate, W., 1998b. Sensors to monitor biological nitrogen removal and activated sludge settling. Journal of Microbiological Methods, 32:193–204.

Gernaey, K., Verschuere, L., Luyten, L., Verstraete, W., 1997. Fast and sensitive acute toxicity detection with an enrichment nitrifying culture. Water Environmental Research, 69:1163–1169.

Gieseke, A., Tarre, S., Green, M., de Beer, D., 2006. Nitrification in a Biofilm at Low pH Values: Role of In Situ Microenvironments and Acid Tolerance. Applied and Environmental Microbiology, 72(6):4283–4292.

Ginige, M.P., Keller, J., Blackall, L.L., 2005. Investigation of an acetate–fed denitrifying microbial community by stable isotope probing, full–cycle rRNA analysis, and Fluorescent In Situ Hybridization–Microautoradiography. Applied and Environmental Microbiology, 71(12): 8683–8691.

Gjaltema, A., Arts, P.A.M., van Loosdrecht, M.C.M., Kuenen, J.G., Heijnen, J.J., 1994. Heterogeneity of biofilms in rotating annular reactors: Occurrence, structure and consequences. Biotechnology and Bioengineering, 44: 194.204.

Glass, C., Silverstein, J., 1998. Denitrification kinetics of high nitrate concentration water: pH effect on inhibition and nitrite accumulation. Water Research, 32:831–839.

Goel, R.K., Flora, J.R.V., 2005. Sequential nitrification and denitrification in a divided cell attached growth bioelectrochemical reactor. Environmental Engineering Science, 22(4):440–449.

Grunditz, C., Dalhammar, G., 2001. Development of nitrification inhibition assays using pure cultures of Nitrosomonas and Nitrobacter. Water Research, 35:433–440.

Gumaelius, L., Smith, E.H., Dalhammer, G., 1996. Potential biomarker for denitrification of wastewaters: Effects of process variables and Cadmium toxicity. Water Research, 30:3025–3031.

Hahn, B.D., 2004. Essential MATLAB for scientists and engineers. 3rd edition, Pearson education, South Africa.

Hallin, S., Rothman, M., Pell, M., 1996. Adaptation of denitrifying bacteria to acetate and methanol in activated sludge. Water Research, 30:1445–1450.

Hao, X–D., van Loosdrecht, M.C.M., 2004. Model–based evaluation of COD influence on a partial nitrification–Anammox biofilm (CANON) process, Water Science and Technology, 49(11–12):83–90.

Hao, X., Heijnen, J.J., van Loosdrecht, M.C.M., 2002. Model–based evaluation of temperature and inflow variations on a partial nitrification – ANAMMOX Biofilm process. Water Research, 36:4839 – 4849.

Hao, X., van Loosdrecht, M.C.M., Heijnen, J.J., Qian, Y., 2001. Model–based evaluation of kinetics, biofilm and process parameters in a one–reactor ammonium removal (CANON) process. Biotechnology and Bioengineering, 77:266–277.

Heijerick, D.G., De Schamphelaere, K.A.C., Janssen, C.R., 2002. Biotic ligand model development predicting Zn toxicity to the alga *Pseudokirchneriella subcapitata*: possibilities and limitations. Comparative Biochemistry and Physiology Part C: Toxicology & Pharmacology, 133(1–2):207–218.

Heimbrook, M.E., Wang, W.L.L., Campbell, G., 1989. Staining bacterial flagella easily. Journal of Clinical Microbiology, 27(11):2612–2615.

Hellinga, C., van Loosdrecht, M.C.M., Heijnen, J.J., 1999. Model based design of a novel process for nitrogen removal from concentrated flows. Mathematical and Computer Modelling of Dynamical Systems, 5(4):351–371.

Hellinga, C., Schellen, A.A.J.C., Mulder, J.W., van Loosdrecht, M.C.M., and Heijnen, J.J., 1998. The SHARON Process: an innovative method for nitrogen removal from ammonium–rich wastewater. Water Science and Technology, 37(9): 135–142.

Hermanowicz, S.W., 2001. A Simple 2D Biofilm model yields a variety of morphological features. Mathematical Biosciences, 169 (1): 1–14

Henze, M., Harremoës, P., Jansen, J.L.C., Arvin, E., 2002. Wastewater Treatment: Biological and Chemical Processes. Springer–Verlag Berlin Heidelberg, 1–430.

Henze, M., Grady, C.P.L., Gujer, W., Marias, G.V.R., Matsuo, T., 1987. A general model for single sludge wastewater treatment systems. Water Research, 21:505–515.

Hesselsoe, M., Sorensen, J., 1999. Microcolony formation as a viability index for ammonia–oxidising bacteria: *Nitrosomonas europaea* and *Nitrosispira* sp. FEMS Microbiology Ecology 28:383 – 391.

Hughes, M. N., Poole, R.K., 1989. Metals and Micro–organisms, Chapman and Hall, London.

Ho, Y–S., Second order kinetics model for the sorption of cadmium onto tree fern: A comparision of linear and non–linear methods. Water Research, 40:119–125.

Horsch, P., Leve, J., and Frimmel, F.H., Effect of an industrial wastewater on the nitrification in fixed–bed biofilm reactors – use of fluorosence in–situ hybridisation (FISH). Water Science and Technology, 49(11–12):91–97.

Horn, H., Hempel, D.C., 1997. Growth and decay in an auto–/heterotrophic biofilm. Water Research, 31:2243–2252.

Hoshika, Y., 1975. Chromatography Journal, 115–596.

Jeong, J., Hidaka, T., Tsuno, H., Oda, T., 2006. Development of biological filter as tertiary treatment for effective nitrogen removal: Biological filter for tertiary treatment. Water Research, 40:1127–1136.

Jetten, M.S.M., Cirpus, I., Kartal, B., van Niftrik, L., van de Pas–Schoonen, K.T., Sliekers, O., Haaijer, S., van der Start, W., Schmid, M., van de Vossenberg, J., Schmid, I., Harhangi, H., van Loosdrecht, M., Kuenen, J.G., Op den Camp, H., Strous, M., 2004. 1994–2004: 10 years of research on the anaerobic oxidation of ammonium. Biochemical Society Transactions, 33(I):119–123.

Jetten, M.S.M., Schmid, M., Schmidt, I., Wubben, M., van Dongen, U., Abma, W., Sliekers, O., Revsbech, N.P., Beaumont, H.J.E., Ottosen, L., Volcke, E., Laanbroek, H.J., Campos–Gomez, J.L., Cole, J., van Loosdrecht, M., Mulder, J.W., Fuerst, J., Richardson, D., van de Pas, K., Mendez–Pampin, R., Katie Third, K., Cirpus, I., van Spanning, R., Bollmann, A., Nielsen, L.P., den Camp, H.O., Schultz, C., Gundersen, J., Vanrolleghem, P., Strous, M., Wagner, M., and Kuenen, J.G., 2002. Improved nitrogen removal by application of new nitrogen–cycle bacteria. Re/View Environmental Science and Bio/Technology, 1:51–63.

Jetten, M.S.M., Wagner, M., Fuerst, J., van Loosdrecht, M.C.M., Kuenen, G., Strous, M., 2001. Microbiology and applications of the anaerobic ammonium oxidation ('anammox') process. Current Opinions in Biotechnology, 12:283–288.

Jetten, M.S.M., Strous, M., van de Pas–Schoonen, K.T., Schalk, J., van Dongen, U.G.J.M., van de Graaf, A.A., Logemann, S., Muyzer, G., van Loosdrecht, M.C.M., Kuenen, J.G., 1999. The anaerobic oxidation of ammonium. FEMS Microbiology Reviews, 22:421–437.

Jeppsson, U., Pons, M.–N., 2004. Editorial: The COST benchmark simulation model–current state and future perspective. Control Engineering Practice, 12(3):299–304.

Jeppsson, U., Alex, J., Pons, M.N., Spanjers, H., Vanrolleghem, P.A., 2002. Status and future trends of ICA in wastewater treatment – European perspective. Water Science and Technology, 45(4–5):485–494.

Jeppsson, U., 1996. Modelling aspects of wastewater treatment processes. PhD thesis, Department of Industrial Electrical Engineering and Automation (IEA), Lund Institute of Technology, Lund, Sweden.

Juliastuti, S.R., Baeyens, J., Creemers, C., Bixio, D., Lodewyckx, E., 2003. The inhibitory effects of heavy metals and organic compounds on the net maximum specific growth rate of the autotrophic biomass in activated sludge. Journal of Hazardous Materials, B100:271–283

Jobbagy, A., Simon, J., Ploz, B., 2000. The impact of oxygen penetration on the estimation of denitrification rates in anoxic processes. Water Research, 34:2606–2609.

Johnson, D.B., Hallberg, K.B., 2003. The microbiology of acidic mine waters. Research in Microbiology, 154:466–473.

Kasia, J.M., Duncan, J.R., Burgess, J.E., 2005. Biological removal of nitrogen species from metal–processing wastewater. Water SA, 31(3):407–412.

Keller, J., Yuan, Z., Blackall, L.L., 2002. Integrating process engineering and microbiology tools to advance activated sludge wastewater treatment research and development. Re/Views in Environmental Science and Bio/Technology, 1:83–97.

Kelly, C.J., Tumsaroj, N., Lajoie, C.A., 2004. Assessing wastewater metal toxicity with bacterial bioluminescence in a bench–scale wastewater treatment system. Water Research 38:423–431.

Kim, J.S., Lee, C.H., Chang, I.S., 2001. Effect of pump shear on the performance of a crossflow membrane reactor. Water Research, 35:2137–2144.

Khin, T., Annachhatre, A.P., 2004. Novel microbial nitrogen removal processes. Biotechnology Advances, 22:519–532.

Knowles, R., 1982. Denitrification. Microbial Reviews, 46(1):43–70.

Kratochvil, D., Volesky, B., 1998. Advances in the biosorption of heavy metals. TIBTECH, 16:291–300.

Kreft, J.U., Picioreanu, C., Wimpenny, J.W.T., van Loosdrecht, M.C.M., 2001. Individual–based modelling of biofilms. Microbiology, 147:2897–2912.

Kuai, L., Verstraete, W., 1998. Ammonium Removal by the Oxygen–Limited Autotrophic Nitrification–Denitrification System. Applied and Environmental Microbiology, 64:4500 – 4506.

Kong, Z., Vanrolleghem, P.V., Willems, P. and Verstraete, W., 1996. Simultaneous determination of inhibition kinetics of carbon oxidation and nitrification with a respirometer. Water Research, 30(4):825–836.

Koren, D.W., Gould, W.D., Bedard, P., 2000. Biological removal of ammonia and nitrate from simulated mine and mill effluents. Hydrometallurgy, 56:127 – 144.

Kowalchuck, G.A., Stephen, J.R., 2001. Ammonia–Oxidising Bacteria: A Model for Molecular Ecology. Annual Reviews in Microbiology, 55:485–529.

Lane, G.L., Schwarz, M.P., Evans, G.M., 2005. Numerical modelling of gas–liquid flow in stirred tanks. Chemical Engineering Science, 60: 2203 – 2214

Laspidou, C.S., Rittmann, B.E., 2001. Non–steady state modelling of extracellular polymeric substances, soluble microbial products, and active and inert biomass. Water Research, 36:1983–1992.

Lenz, K., Hann, S., Koellensperger, G., Stefanka, Z., Stingeder, G., Weissenbacher, N., Mahnik, S.N., Fuerhacker, M., 2005. Presence of cancerostatic platinum compounds in hospital wastewater and possible elimination by adsorption to activated sludge. Science of the Total Environment 345:141–152.

Lewandowski, Z., 1987. Behaviour of biological reactors in the presence of toxic compounds. Water Research 21:147–153.

Lewandowski, Z., 1986. Biological Reactor Resistance to Inhibition. Water Research 20:847 – 850.

Lewandowski, Z., Janta, K., Mazierski, J., 1985. Inhibition coefficient (K_i) determination activated sludge. Water Research, 19:671 – 674.

Lewandowski, Z., 1985. Denitrification by Packed Bed Reactors in the presence of Chromium (VI): Resistance to Inhibition. Water Research 19:589 – 596.

Lim, P.E., Tay, M.G., Mak, K.Y., Mohamed, N., 2003. The effect of heavy metals on nitrogen and oxygen demand removal in constructed wetlands. The Science of the Total Environment, 301:13–21.

Logan, M.V., Reardon, K.F., Figueroa, L.A., McLain, J.E.T., Ahmann, D.M., 2005. Microbial community activities during establishment, performance, and decline of bench–scale passive treatment systems for mine drainage. Water Research, 39:4537–4551.

Lubbert, A., Jorgensen, S.B., 2001. Bioreactor performance: a more scientific approach for practice. Journal of Biotechnology, 85:187–212.

Lucas, A. De., Rodríguez, L., Villaseñor, J., Fernández, F.J., 2005. Denitrification potential of industrial wastewaters. Water Research, 39:3715–3726.

Mack, C–L., 2005. Screening of technologies for the recovery of rhodium(iii) metal ions from a precious metal refinery wastewater, MSc Thesis. Department of Biochemistry, Microbiology and Biotechnology, Rhodes University, Grahamstown 6140, South Africa.

Madoni, P., Davoli, D., Guglielmi, L., 1999. Response of SOUR and AUR to heavy metal contamination in activated sludge. Water Research, 33: 2459–2464.

Madoni, P., Davoli, D., Gorbu,G., Vescovi, L., 1996. Toxic effect of heavy metals on the activated sludge protozoan community. Water Research, 30:135–141.

Maier, R.M., Pepper, I.L., Gerba, C.P., 2000. Environmental Microbiology. Academic Press, San Diego, 147 – 174, 331 – 336, 403 – 423, 505 – 533.

Manktelow, S.A., Paterson, J.G., Meech, J.A., 1984.Removal of copper and cyanide from solution using activated carbon. Environmental Geochemistry and Health, 6(1):5–9.

Manser, R., Gujer, W., Siegrist, H., 2006. Decay processes of nitrifying bacteria in biological wastewater treatment systems. Water Research, 40:2416–2426.

Manser, R., Gujer, W., Siegrist, H., 2005a. Consequences of mass transfer effects on the kinetics of nitrifiers. Water Research, 39:4633–4642.

Manser, R., Gujer, W., Siegrist, H., 2005b. A rapid method to quantify nitrifiers in activated sludge. Water Research, 39:1585–1593.

Martienssen, M., Schöps, R., 1999. Population dynamics of denitrifying bacteria in a model biocommunity. Water Research, 33:639–646.

Metcalf and Eddy Inc., 2004. Wastewater Engineering: Treatment and reuse, 4th ed. McGrew–Hill, New York.

Milbourne, J., Tomlinson, M., Gormely, L., 2003. Use of hydrometallurgy in direct processing of base metals/PGM concentrates, In: Hydrometallurgy 2003 – Fifth International Conference in Honour of Professor Ian Ritchie – Volume 1: Leaching and Solution Purification, Edited by C. A. Young, A. M. Alfantazi, C.G. Anderson, D.B. Dreinsinger, B. Harris and A. James, TMS (The Minerals, Metals & Materials Society), 617 – 630.

Monti-bragadin, C., Giacca, M., Dolzani. L., Tamaro, M., 1987. Mutagenic effects of rhodium (I) and ruthenium (I1) organometallic complexes in bacteria. Inorganica Chimica Acta, 137: 31-34.

Moo–Young, M., Chisti, Y., 1994. Biochemical Engineering in Biotechnology. Pure and Applied Chemistry, 66(1):117–136.

Morgenroth, E., Arvin, E., Vanrolleghem, P., 2002. The use of mathematical models in teaching wastewater treatment engineering. Water Science and Technology, 45(6):229-233.

Morgenroth, E., Wilderer, P.A., 2000. Influence of detachment mechanisms on competition in biofilms. Water Research, 34:417–426.

Moussa, M.S., Hooijmans, C.M., Lubberding, H.J., Gijzen, H.J., van Loosdrecht, M.C.M., 2005. Modelling nitrification, heterotrophic growth and predation in activated sludge. Water Research, 39:5080–5098.

Mulder, A., 2003. The quest for sustainable nitrogen removal technologies. Water Science and Technology, 48(1): 67 – 75.

Mulder, A., van de Graaf, A.A., Robertson, L. A., Kuenen, J.G., 1995. Anaerobic ammonium oxidation discovered in a denitrifying fluidized bed reactor. FEMS Microbiology Ecology, 16:177–184.

Muslu, Y., 2002. Kinetics characteristics of biofilm reactors. Water, Air and Soil Pollution, 140:1–20.

Naeem, A., Woertz, J.R., Fein, J.B., 2006. Experimental measurements of proton, Cd, Pb, Sr and Zn adsorption onto the fungal species *Saccharomyces cerevisiae*. Environmental Science and Technology, 40:5724–5729.

Nielsen, M., Bollmann, A., Sliekers, O., Jetten, M., Schmid, M., Strous, M., Schmidt, I., Larsen, L.H., Nielsen, L.P., Revsbech, N.P., 2005. Kinetics, diffusional limitation and microscale distribution of chemistry and organisms in a CANON reactor. FEMS Microbial Ecology, 51:247–256.

Neufeld, R.D., Hermann, E.R., 1975. Heavy metal removal by acclimated activated sludge. Journal of the Water Pollution Control Federation, 47:762–770.

Noguera, D.R., Morgenroth, E., 2004. Introduction to the IWA Task Group on biofilm modelling. Water Science and Technology, 49 (11–12), 131–136.

Nogueira, R., Melo, L.F., Purkhold, U., Wuertz, S., Wagner, M., 2002. Nitrifying and heterotrophic population dynamics in biofilm reactors: effects of hydraulic retention time and the presence of organic carbon. Water Research, 36:469–481.

Noguera, D.R., Pizzaro, G., Stahl, D.A., Rittmann, B.E., 1999. Simulation of multispecies biofilm development in three dimensions. Water Science and Technology, 39(7):123–130.

Nuruzzaman, M., 2004. Modeling and simulation in SIMULINK for engineers and scientists. 1st edition, Authorhouse publishers, Bloomington, Indiana.

Oguz, M.T., Robinson, K.G., Layton, A.C., Sayler, G.S., 2006. Volatile fatty acid impacts on nitrite oxidation and carbon dioxide fixation in activated sludge. Water Research, 40:665–674.

Olsson, G., Newell, B., 2001. Wastewater treatment systems: Modelling, diagnosis and control. 1st edition, IWA Publishing. London.

Olson, G.J., Porter, F.D., Rubinstein, J., Silver, S., 1982. Mercuric reductatse enzyme from a mercury–volatilising strain of *Thiobacillus ferooxidans*. Journal of Biotechnology, 15:1230–1236.

Özbelge, T.A., H. Önder Özbelge, H. Ö., Tursun, M., 2005. Effects of hydraulic residence time on metal uptake by activated sludge. Chemical Engineering and Processing, 44:23-32.

Painter, H.A., 1970. A review of literature on inorganic nitrogen metabolism in microorganisms, Water Research 4:393–450.

Park, S.J., Oh, J.W., Yoon, T.I., 2003. The role of powdered zeolite and activated carbon carriers on nitrification in activated sludge with inhibitory materials. Process Biochemistry, 39:211–219.

Paradies, H.H., Chemical and physicohemical aspects of metal biofilms, In Bioextraction and biodeterioration of metals. Editors: Gaylarde, C.C., Videla, H.A., Cambridge University Press, Cambridge. 197–269.

Pearce, P., 2004. Trickling filters for upgrading low technology wastewater plant for nitrogen removal. Water Science and Technology, 49(11):47–52.

Pedersen, F., Petersen, G.I., 1996. Variability of species sensitivity to complex mixtures. Water Science and Technology, 33(6): 109–119.

Perez, J., Picioreanu, C., van Loosdrecht, M.C.M., 2005. Modeling biofilm and floc diffusion processes based on analytical solution of reaction–diffusion equations. Water Research, 39:1311–1323.

Pernetti, M., Palma, L.D., Merli, C., 2003. A real time toxicity bioassay for activated sludge reactor. International Journal of Chemical Reaction Engineering, 1:A1–A11.

Petersen, B., Gernaey, K., Devisscher, M., Dochain, D., Vanrolleghem, P.A., 2003. A simplified method to asses structurally identifiable parameters in Monod–based activated sludge models. Water Research, 37:2893–2904.

Petersen, B., 2000. Calibration, identifiability and optimal experimental design of activated sludge models. PhD thesis, Department of Applied Mathematics, Biometrics and Process Control (BIOMATH), University of Gent, Belgium.

Picioreanu, C., van Loosdrecht, M.C.M., Heijnen, J.J., 2001. Two–dimensional model of biofilm detachment caused by internal stress from liquid flow. Biotechnology and Bioengineering, 72(2): 205–218.

Picioreanu, C., van Loosdrecht, M.C.M., Heijnen, J.J., 2000. Effect of diffusive and convective substrate transport on biofilm structure formation: a 2–D modeling study. Biotechnology and Bioengineering, 69(5):504–515.

Picioreanu, C., van Loosdrecht, M.C.M., Heijnen, J.J., 1998. Mathematical modeling of biofilm structure with a hybrid differential discrete cellular automaton approach. Biotechnology and Bioengineering, 58(1):101–116.

Pizarro, G., Griffeath, D., Daniel, R., Noguera, D.R., 2001. Quantitative cellular automaton model for biofilms. Journal of Environmental Engineering, 127(9):782–789.

Plósz, B.G., Jobbágy, A., Grady, Jr., C.P.L., 2003. Factors influencing deterioration of denitrification by oxygen entering an anoxic reactor through the surface. Water Research, 37:853–863.

Pollice, A., Tandoi, V., Lestingi, C., 2001. Influence of aeration and sludge retention time on ammonium oxidation to nitrite and nitrate. Water Research, 36:2541 – 2546.

Principi, P., Villa, F., Bernasconi, M., Zanardini, E., 2006. Metal toxicity in municipal wastewater activated sludge investigated by multivariate analysis and in situ hybridization, Water Research. 40:99–106.

Pulles, W., Howie, D., Otto, D., Easton, J., 1996. A manual on mine water treatment and management practices in South Africa Mine. Volume 1-5. Water Research Commission, Pretoria.

Rauch, W., Vanhooren, H., Vanrolleghem, P.A., 1999. A simplified mixed–culture biofilm model. Water Research, 33:2148–2162.

Ray, L., Paul, S., Bera, D., Chattopadhyay, P., 2005. Bioaccumulation of Pb(II) from aqueous solutions by *Bacillus Cereus* M. Journal of Hazardous Substance Research, 5:1–21.

Reichert, P., 1995. Design techniques of a computer program for the identification of processes and simulation of water quality in aquatic systems. Environmental Software, 10(3):199–210.

Reichert, P., von Schulthess, R., Wild, D., 1995. The use of AQUASIM for estimating parameters of activated sludge models. Water Science and Technology, 31(2):135–147.

Rieger, L., Thomann, M., Gujer, W., Siegrist, H., 2005. Quantifying the uncertainity of on–line sensors at WWTPs during field operation. Water Research, 39:5162–5174.

Rittmann, B.E., Stilwell, D., Ohashi, A., 2002. The transient–state, multiple–species, biofilm model for biofiltration processes. Water Research, 36:2342–2356.

Rittmann, B.E., McCarthy, P.L., 2001. Environmental Biotechnology: Principles and applications, McGrew–Hill Publishers, New York.

Rittmann, B.E., Brunner, C.W., 1984. The nonsteady–state–biofilm process for advanced organics removal. Journal of the Water Pollution Control Federation, 56: 874–880.

Rittmann, B.E., Dovantzis, K., 1983. Dual limitation of biofilm kinetics. Water Research, 17:1727–1734.

Rittmann, B.E., McCarthy, P.L., 1980a. Model of steady–state–biofilm kinetics. Biotechnology and Bioengineering, 22: 2343–2357.

Rittmann, B.E., McCarthy, P.L., 1980b. Evaluation of steady–state–biofilm kinetics. Biotechnology and Bioengineering, 22: 2359–2373.

Rossi, G., 2001. The design of bioreactor. Hydrometallurgy, 59:217–231.

Rosso, D., Stenstrom, M.K., 2005. Comparative economic analysis of the impacts of mean cell retention time and denitrification on aeration systems. Water Research, 39:3773–3780.

Rožić, M., Cerjan–Stefanović, Š., Kurajica, S., Vančina, V., Hodžić, E., 2000. Ammonical nitrogen removal by water treatment with clays and zeolites. Water Research, 34:3675–3681.

Rudrum, D.P., 2005. Innovations in composting pig manure, MSc thesis, Wageningen University, Wageningen, Netherlands, ISBN 90–8504–337–9.

Ruiz, G., Jeison, D., Rubilar, O., Ciudad, G., Chamy, R., 2006. Nitrification–denitrification via nitrite accumulation for nitrogen removal from wastewaters. Bioresource Technology, 97:330–335.

Saglam, N., Say, R., Denizli, A., Patýr, S., Aryca, M.Y., 1999. Biosorption of inorganic mercury and alkylmercury species on to *Phanerochaete chrysosporium* mycelium. Process Biochemistry, 34:725–730.

Sanchez, M., Mosquere–Corral, A., Mendez, R., Lema, J.M., 2000. Simple methods for determination of the denitrification activity of sludges. Bioresource Technology, 75:1–6.

Santos, S., Machado, R., Correia, M.J.N., Carvalho, J.R., 2004.Treatment of acid mining waters. Minerals Engineering, 17:225–232.

Sawyer, C.N., McCarthy, P.L., Parkin G.F., 1994. Chemistry for environmental engineering, Fourth Edition, MacGrew–Hill Publishers, Singapore.

Schmidt, J.E., Batstone, D.J., Angelidaki, I., 2002. Improved nitrogen removal in upflow anaerobic sludge blanket (UASB) reactors by incorporation of Anammox bacteria into the granular sludge. Water Science and Technology, 49(11–12):69–76.

Schmidt, I., Sliekers, O., Schmid, M., Cirpus, I., Strous, M., Bock, E., Kuenen, J.G., Jetten, M.S.M., 2002. Aerobic and anaerobic ammonia oxidizing bacteria – competitors or natural partners? FEMS Microbiology Ecology, 39:175–181.

Schramm, A., Beer, D.D., Wagner, M., Amann, R., 1998. Identification and Activities In Situ of *Nitrosospira* and *Nitrospira* spp. as Dominant populations in a nitrifying fluidized bed reactor. Applied Environmental Microbiology, 64 :3480–3485.

Siegrist, H., Reithaar, S., Koch, G., Lais, P., 1998. Nitrogen loss in a nitrifying rotating contactor treating ammonium–rich wastewaters without adding organic carbon. Water Science and Technology, 38(8–9):241–248.

Siegrist, H., Gujer, W., 1987. Demonstration of mass transfer and pH effects in a nitrifying biofilm. Water Research, 21:1481–1487.

Seixo, J., Varela, M.H., Coutinho, J.A.P., Coelho, M.A.Z., 2004. Influence of C/N ratio on autotrophic biomass development in a sequencing batch reactor. Biochemical Engineering Journal, 21:131–139.

Shivaraman, N., Shivaraman, G., 2003. Anammox – A novel microbial process for ammonium removal. Current Science, 84:1507 – 1508.

Sillanpaa, M., Oikari, A., 1996. Assessing the impact of complexation by EDTA and DTPA on heavy metal toxicity using microtox bioassay. Chemosphere, 32:1485–1497.

Sin, G., Van Hulle, S.W.H., De Pauw, D.J.W., van Griensven, A., Vanrolleghem, P., 2005. A critical comparison of systematic calibration protocols for activated sludge models: A SWOT analysis. Water Research, 39:2459–2474.

Sin, G., Malisse, K., Vanrolleghem, P.A., 2003. An integrated sensor for the monitoring of aerobic and anoxic activated sludge activities in biological nitrogen removal plants. Water Science and Technology, 47(2):141–148.

Sison, N.F., Hanaki, K., Matsuo, T., 1996. Denitrification with external Carbon source utilizing adsorption and desorption capability of Activated Carbon. Water Research, 30:217 – 227.

Sliekers, A.O., Third, K.A., Abma, W., Kuenen, J.G. and Jetten, M.S.M., 2003. CANON and Anammox in a gas–lift reactor. FEMS Microbiology Letters, 218:339–344.

Sliekers, A.O., Derwort, N., Gomez, J.L.C., Strous, M., Kuenen, J.G., Jetten, M.S.M., 2002. Completely autotrophic nitrogen removal over nitrite in one single reactor. Water Research, 36:2475 – 2482.

Stephen, J.R., Chang, Y–J., MacNaughton, S.J., Kowalchuck, G.A., Leung, K.T., Flemming, C.A., White, D.C., 1999. Effect of toxic metals on indigenous soil β–subgroup Proteobacterium ammonia oxidiser community structure and protection against toxicity by inoculated metal–resistant bacteria. Applied and Environmental Microbiology, 65(1):95–101.

Stilwell, L.C., Minnitt, R.C.A., Monson, T.D., Kuhn, G., 2000. An input–output analysis of the impact of mining on the South African economy. Resources Policy, 26:17–30.

Strous, M., Pelletier, E., Mangenot, S., Rattei, T., Lehner, A., Taylor, M.W., Horn, M., Daims, H., Bartol–Mavel, D., Wincker, P., Barbe, V., Fonknechten, N., Vallenet, D., Segurens, B., Schenowitz–Truong, C., Me´digue, C., Collingro, A., Snel, B., Dutilh, B.E., Op den Campl, H. J. M., van der Drift, C., Cirpus, I., van de Pas–Schoonen, K.T., Harhangi, H.R., van Niftrik, L., Schmid, M., Keltjens, J., van de Vossenberg, J., Kartal, B., Meier, H., Frishman, D., Huynen, M.A., Mewes, H–W., Weissenbach, J., Jetten, M.S.M., Wagner, M., Paslier, D.L., 2006. Deciphering the evolution and metabolism of an anammox bacterium from a community genome. Nature, 440:790–794.

Strous, M., Kuenen, J.G., Fuerst, J.A., Wagner, M., Jetten, M.S.M., 2002. The anammox case – A new experimental manifesto for microbiological eco–physiology. Antonie van Leeuwenhoek, 81:693–702.

Strous, M., Kuenen, J.G. and Jetten, M.S.M., 1999. Key Physiology of anaerobic ammonium oxidation. Applied and Environmental Microbiology, 65:3248 – 3250.

Strous, M., Heijnen, J.J., Kuenen, J.G., Jetten, M.S.M., 1998. The sequencing batch reactor as a powerful tool for the study of slowly growing anaerobic ammonium–oxidising microorganisms. Applied and Environmental Microbiology, 50:589–596.

Strous, M., van Gervan, E., Zheng, P., Kuenen, J.G., Jetten, M.S.M., 1997. Ammonium removal from concentrated waste streams with the anaerobic ammonium oxidation (anammox) process in different reactor configurations. Water Research, 31:1955–1952.

Su, M.C., Cha, D.K., Anderson, P.R., 1995. Influence of selector technology on heavy metal removal by activated sludge: secondary effects of selector technology. Water Research, 29: 971–976.

Suhasini, I.P., Sriram, G., Asolekar, S.R., Sureshkumar, G.K., 1999. Biosorptive removal and recovery of cobalt from aqueous systems. Process Biochemistry, 34:239–247.

Sucoski, G., Osorio, D.F., Brown, J.B., Neitzel, G.P., 2004. Fluid mechanics of spinner–flask bioreactor. Biotechnology and Bioengineering, 85(1):34–46.

Surmacz–Gorska, J., Gernaey, K., Demuynck, C., Vanrolleghem, P., Verstraete, W., 1996. Nitrification monitoring in activated sludge by oxygen uptake rate (OUR) measurements. Water Research, 30:1228–1236.

Szekeres, S., Kiss, I., Kalman, M., Soares, M.I.M., 2002. Microbial population in a hydrogen–dependent denitrification reactor. Water Research, 36: 4088 – 4094.

Tallec, G., Garnier, J., Billen, G., Gousailles, M., 2006. Nitrous oxide emissions from secondary activated sludge in nitrifying conditions of urban wastewater treatments plants: Effect of oxygenation level. Water Research, 40:2972–2980.

Terada, A., Hibiya, K., Nagai, J., Tsuneda, S., Hirata, A., 2003. Nitrogen removal characteristics and biofilm analysis of a membrane – aerated biofilm reactor applicable to high–strength nitrogenous wastewater treatment. Journal of Bioscience and Bioengineering, 95:170–178.

Third, K.A., Sliekers, A.O., Kuenen, J.G., Jetten, M.S.M., 2001. The CANON System (Completely Autotrophic Nitrogen–removal Over Nitrite) under ammonium limitation: Interaction and competition between three groups of bacteria. Systematic and Applied Microbiology, 24:588–596.

Tien, C.J., 2002. Biosorption of metal ions by freshwater algae with different surface characteristics. Process Biochemistry, 38:605– 613.

Travis, J., Kring, J., 2006. LabVIEW For Everyone: Graphical programming made easy and fun. 3rd Edition, Prentice Hall PTR, New Jersey.

Tsuneda, S., Nagano, T., Hoshino, T., Ejiri, Y., Noda, N., Hirata, A., 2003. Characterization of nitrifying granules produced in an aerobic upflow fluidized bed reactor. Water Research, 37:4965–4973.

Tsuno, H., Hidaka, T., Nishimura, F., 2002. A simple biofilm model of bacterial competition for attached surface. Water Research, 36:996–1006.

Tülay A. Özbelge, T.A., Özbelge, H.O., Tursun, M., 2005. Effects of hydraulic residence time on metal uptake by activated sludge. Chemical Engineering and Processing, 44:23–32.

van Benthum, W.A.J., Derissen, B.P., van Loosdrecht, M.C.M., Heijnen, J.J., 1998. Nitrogen removal using nitrifying biofilm growth and denitrifying suspended growth in a biofilm airlift suspension reactor coupled with a chemostat. Water Research 32:2009–2018.

van De Graaf, A.A., Mulder, A., de Bruijn, P., Jetten, M.S.M., Robertson, L.A., Kuenen, J.G., 1995. Anaerobic oxidation of ammonium is a biologically mediated process. Applied and Environmental Microbiology, 61:1246–1251.

van Hulle, S., 2005. Modelling, simulation and optimization of autotrophic nitrogen removal processes. PhD Thesis, Department of Applied Mathematics, Biometrics and Process Control (BIOMATH), Gent University, Gent, Belgium.

Vanhooren, H., Meirlaen, J., Amerlinck, Y.,Claeys, F., Vangheluwe, H., Vanrolleghem, P.A., 2003. WEST: modelling biological wastewater treatment. Journal of Hydroinformatics, 5(1):27-50.

van Hooren, H., 2002. Modelling for optimisation of biofilm wastewater treatment processes: A complexity compromise. PhD Thesis, Department of Applied Mathematics, Biometrics and Process Control (BIOMATH), University of Gent, Belgium.

van Loosdrecht, M.C.M., Heijnen, J.J., Ebert, H., Kreft, J., Picioreanu, C., 2002. Mathematical modelling of biofilm structures. Antonie van Leeuwenhoek 81:245–256.

van Loosdrecht, M.C.M., Henze, M., 1999. Maintenance endogeneous respiration, lysis, decay and predation. Water Science and Technology, 39(1):107–117.

Vandevivere, P., Ficara, E., Terras, C., Julies, E., Verstraete, W., 1998. Copper–mediated selective removal of nitrification inhibitors from industrial wastewaters. Environmental Science and Technology, 32: 1000–1006.

Vanrolleghem, P.A., Lee, D.S., 2003. On–line monitoring equipment for wastewater treatment processes: state of art. Water Science and Technology, 47(2):1–34.

Vanrolleghem P.A., Coen F., 1995. Optimal design of In-Sensor-Experiments for on-line modelling of nitrogen removal processes. Water Science and Technology, 31(2):149-160.

Verstraete, W., Philips, S., 1998. Nitrification–denitrification processes and technologies in new contexts. Environmental Pollution, 102(S1):717 – 726.

Viotti, P., Eramo, B., Boni, M.R., Carucci, A., Leccese, M., 2002. Development and calibration of a mathematical model for the simulation of the biofiltration process. Advances in Environmental Research, 7:11–33.

Volcke, E.I.P., Van Hulle, S., Dekissa, T., Zaher, U., Vanrolleghem, P., 2005. Calculation of pH and concentration of equilibrium components during dynamic simulation by means of a charge balance. BIOMATH technical report, Gent University, Belgium.

Volesky, B., 2001. Detoxification of metal–bearing effluents: biosorption for the next century. Hydrometallurgy, 59:203–216.

Voskuil, M.I., Chambliss, G.H., 1998. The –16 region of *Bacillus subtilis* and other gram–positive bacterial promoters. Nucleic Acids Research, 26(15): 3584–3590.

Vredenbregt, L.H.J., Nielsen, K., Potma, A.A., Kristensen, G.H., Sund, C., 1997. Fluid bed biological nitrification and denitrification in high salinity wastewater. Water Science and Technology, 36(1):93–100.

Walker, M.I., Minnitt, R.C.A., 2006. Understanding the dynamics and competitiveness of the South African minerals inputs cluster. Resources Policy, 31:12–26.

Wang, J., Huang, C.P., Allen, H.E., 2006. Predicting metals partitioning in wastewater treatment plant influents. Water Research, 40:1333–1340.

Wanner, O., Morgenorth, E., 2004. Biofilm modelling with AQUASIM. Water Science and Technology, 49(11–12):137–144.

Wanner, O., Reichert, P., 1996. Mathematical modeling of mixed–culture biofilms. Biotechnology and Bioengineering, 49: 172–184.

Wanner, O., 1996. Modelling of biofilms. Biofouling, 10: 31–41.

Wanner, O., Gujer, W., 1986. A multispecies biofilm model. Biotechnology and Bioengineering, 28:314–328.

Werther, J., Hartge, E–U., 2003. Modelling of Fluidized Bed Reactors, Chemical Reaction Engineering IX, June 29 – July 4, 2003, Quebec City, Canada.

White, C., Sayer, J.A., Gadd, G.M., 1997. Microbial solubilisation and immobilisation of toxic metals: key biochemical processes for treatment of contamination. FEMS Microbiology Reviews, 20:503–516.

WHO, 2006. Guideline for drinking water quality: Volume 1 – Recommendations, World Health Organisation. ISBN 92 4 154696 4

Wilderer, P.A., Bungartz, H.–J., Lemmer, H., Wagner, M., Keller, J., Wuertz, S., 2002. Modern scientific methods and their potential in wastewater science and technology. Water Research 36:370–393.

Wimpenny, J., Manz, W., Szewzyk, U., 2000. Heterogeneity in biofilms. FEMS Microbiology Reviews, 24:661–671.

Wimpenny, J.W.T., Colasanti, R., 1997. A unifying hypothesis for the structure of microbial biofilms, FEMS Microbial Ecology, 22, 1–16.

Windey, K., De Bo, I., Verstraete, W., 2005. Oxygen–limited autotrophic nitrification–denitrification (OLAND) in a rotating biological contactor treating high–salinity wastewater. Water Research, 39:4512–4520.

Winde, F., van der Walt, I.J., 2004. The significance of groundwater–stream interactions and fluctuating stream chemistry on waterborne uranium contamination of streams—a case study from a gold mining site in South Africa. Journal of Hydrology, 287:178–196.

Winkler, M.A., 1983. Application of the principles of fermentation engineering to biotechnology, In: Wiseman A, editor. Principles of Biotechnology. Surrey University Press, 94–143.

Worms, I., Simon, D.F., Hassler, C.S., Wilkinson, K.J., 2006. Bioavailability of trace metals to aquatic microorganisms: importance of chemical, biological and physical processes on biouptake. Biochimie, 88:1721–1731.

Woodbury, B.L., Dahab, M.F., 2001. Comparison of conventional and two–stage reversible flow, static–bed biodenitrification reactors. Water Research, 35:1563–1571.

WRC, 2005a. Research seeks answers for century–old problem. The Water Wheel, April–March:16–21.

WRC, 2005b. What a lot we got: but cautions care on how we use it. The Water Wheel, November–December:14–17.

WRC, 2005c. When water turns deadly: Investigating nitrate in SA ground water. The Water Wheel, November–December:24–27.

Wu, W., Huang, M.–Y., 2003. Output regulation of a class of unstructured models of continuous bioreactors: steady state approaches. Bioprocess and Biosystems Engineering, 25:323–329.

Wyffels, S., van Hulle, S.W.H., Boeckx, P., Volcke, E.I.P., van Cleemput, O., Vanrolleghem, P.A., Verstraete, W., 2004. Modeling and simulation of Oxygen–Limited Partial Nitritation in a Membrane–Assisted Bioreactor (MBR). Biotechnology and Bioengineering, 86(5):531–542.

Yang, P.Y., Nitisoravut, S., Wu, J.S., 1995. Nitrate removal using mixed–culture entrapped microbial cell immobilisation process under high salt concentration. Water Research, 29:1525–1532.

You, S.J., Hsu, C.L., Ouyang, C.F., 2002. Identification of the microbial diversity of wastewater nutrient removal processes using molecular biotechnology. Biotechnology Letters, 24: 1361–1366.

Younger, P.L., Wolkersdorfer, C., 2004. Mining impacts on the fresh water environment: Technical and managerial guidelines or catchment scale management. Mine Water and the Environment, 23:S2–S80.

Zhang, T.C., Bishop, P.L., 1994. Density, porosity and pore structure of biofilms. Water Research, 28:2267–2277.

Zhao, M., Duncan, J.R., Van Hille, R.P., 1999. Removal and recovery of zinc from solution and electroplating effluents using *Azolla Filiculoids*. Water Research, 33(6):1516–1522.

Zhao, M., Duncan, J.R., 1998. Removal and recovery of nickel from aqueous solution and electroplating rinse effluents using *Azolla Filiculoids*. Process Biochemistry, 33(3):249–255.

Zhu, S., Chen, S., The impact of temperature on nitrification rate in the fixed film biofilters. Aquacultural Engineering, 26:221–237.

Internet references

Anglo Platinum Inc., 2003. (http://www.angloamerican.co.uk/static/uploads/AA–REVIEW2003.pdf, accessed on 31 October 2006).

Statistics South Africa, 2004. Mining industry, www.statssa.gov.za (accessed 26 October 2006).

Appendix A: Primary Data Sheets – Chapter 3.0

Table A.1: Ammonium removal under different pH conditions

Time / hours	Ammonium (NH_4^+ - N) concentration / mg/l											
	pH = 4			pH = 5			pH = 6			pH = 7		
	1	2	3	1	2	3	1	2	3	1	2	3
0	0.52	0.62	0.48	0.12	0.20	0.20	0.07	0.06	0.07	0.01	0.02	0.03
12	0.33	0.21	0.34	0.05	0.03	0.08	0.06	0.06	0.07	0.00	0.01	0.01
24	0.28	0.28	0.20	0.05	0.03	0.04	0.08	0.10	0.07	0.05	0.03	0.01
36	0.18	0.13	0.26	0.07	0.02	0.04	0.07	0.08	0.06	0.01	0.02	0.00
48	0.06	0.09	0.07	0.07	0.04	0.08	0.09	0.10	0.08	0.03	0.03	0.02
72	0.05	0.05	0.02	0.06	0.05	0.09	0.07	0.11	0.07	0.02	0.02	0.02
Final pH	5.98	6.16	4.79	5.90	3.57	5.96	3.67	3.80	6.45	6.83	5.64	5.46

Table A.2: Denitrification of acidic PMR wastewater with different carbon sources

Time / hours	NO_3^- - N concentration in mg/l								
	Sodium Acetate			Sodium Lactate			Ethanol		
	1	2	3	1	2	3	1	2	3
0	19.3	20.0	20.7	12.0	12.5	10.3	16.6	14.4	19.3
48	25.5	18.3	17.3	11.7	11.0	9.9	15.3	16.0	11.4
72	7.7	8.4	17.4	5.4	4.6	-	9.2	7.8	11.8
96	7.9	5.2	9.6	5.2	12.7	7.3	8.8	9.3	11.0
144	10.3	3.8	5.6	5.9	4.0	5.9	6.5	5.8	6.5
168	6.4	3.5	6.0	5.8	5.6	6.3	8.4	9.1	9.8
216	4.7	7.8	4.5	6.7	3.3	7.1	6.5	7.5	8.3
240	7.2	5.6	9.2	5.4	5.9	6.7	9.3	8.2	11.2
264	3.3	9.4	8.2	10.2	11.5	9.2	8.4	4.7	10.7
384	10.5	7.0	10.2	5.4	3.6	3.7	8.4	8.1	9.6

Table A.3: Nitrate removal using nitrified effluent from nitrification batch test.

Time / hours	NO_3^-- N concentration in mg/l														
	pH = 4				pH = 5				pH = 6				pH = 7		
	1	2	3	Mean	1	2	3	Mean	1	2	3	Mean	1	2	Mean
0	8.7	6.5	9.7	8.30	5.3	4.3	7.9	5.83	7.3	3.2	6.2	5.57	8.1	5.30	6.70
24	7.1	5.7	6.8	6.53	5.1	9.9	10.9	8.63	4.1	6.4	6.7	5.73	10.1	7.00	8.55
48	5.2	6.1	8.5	6.60	4.9	4.5	5.5	4.97	4.9	5.3	7.2	5.80	5.2	6.30	5.75
72	7.4	6.9	9.5	7.93	8.1	8.9	8.9	8.63	5.1	6.1	5.9	5.70	6.5	6.20	6.35
96	5.9	5.2	11.2	7.43	4.2	8.8	6.8	6.60	6.3	7.6	6.9	6.93	9.9	8.50	9.20
144	7.4	6.9	6.1	6.80	4.8	4.8	7.7	5.77	5.6	5.0	5.8	5.47	5.5	8.70	7.10
312	6.4	6.1	6.3	6.27	3.2	6.4	7.8	5.80	5.0	7.5	7.7	6.73	2.0	5.60	3.80
360	6.7	5.0	5.4	5.70	4.2	5.9	5.9	5.33	5.9	8.0	7.0	6.97	6.2	4.10	5.15

Note: The labelling of pH 4, 5, 6 and 7 does not represent the actual pH conditions in each sample. This is the original pH condition used for nitrification of the effluent.

Table A.4: Nitrate removal using different percentages of sodium lactate.

Time / hours	Sodium lactate percentage by volume (%)											
	1.5		2.0		2.5		3.0		3.5		4.0	
	NO_3^--N	pH	NO_3^--N	pH	NO_3^--N	pH	NO_3^--N	pH	NO_3^--N	pH	NO_3^--N	pH
0	4.5	4.10	4.3	4.15	5.5	4.20	6.1	4.37	2.5	4.21	4.3	4.22
24	3.6	4.03	4.1	4.11	2.9	4.17	3.5	4.34	4.0	4.18	3.2	4.18
48	4.2	3.99	2.4	4.08	3.3	4.14	5.0	4.32	4.8	4.16	4.3	4.17
72	6.7	4.00	3.2	4.08	3.4	4.15	1.9	4.31	2.6	4.17	4.5	4.17
96	3.7	3.99	3.1	4.08	5.1	4.14	3.1	4.30	3.0	4.15	3.5	4.17
120	6.6	3.95	4.4	4.03	4.8	4.10	3.3	4.27	3.3	4.12	3.2	4.14

[NO_3^--N] is in mg/l

Appendix B – Primary Data Sheets – Chapter 4.0

Table B.1: Continuously Stirring Tank Reactor – parameter variation with time

Day	pH	CSTR - IN				CSTR - OUT			
		NH_4^+-N	NO_2^--N	NO_3^--N	COD	NH_4^+-N	NO_2^--N	NO_3^--N	COD
		mg/l	mg/l	mg/l	mg/l	mg/l	mg/l	mg/l	mg/l
1	8.64	7.8	0.17	2.6	12100	1.1	0.39	5.4	23450
3	8.46	7.7	0.21	10.3	7600	1.3	0.35	23.2	15750
5	8.52	8.4	0.19	4.0	12000	1.8	0.45	12.5	16350
7	8.94	8.1	0.22	6.4	6500	2.3	0.43	19.3	11750
9	8.60	8.4	0.28	3.7	5900	1.6	0.55	8.7	13400
11	8.97	8.9	0.16	1.9	9250	1.7	0.50	16.7	18700
13	8.98	9.4	0.15	10.1	9550	1.8	0.48	24.7	18000
16	8.55	6.8	0.20	1.1	6700	1.3	0.43	21.7	10450
18	8.70	5.8	0.19	4.0	-	1.2	0.44	19.5	-
21	8.35	7.0	0.16	7.0	-	1.4	0.47	16.3	-
24	8.44	9.2	0.23	8.3	2060	1.6	0.46	10.8	3360
26	7.99	8.3	0.28	10.8	3060	1.8	0.44	10.8	9080
32	8.51	29.0	0.15	0.5	2060	0.7	0.47	12.7	5460
37	7.73	27.8	0.02	0.6	2020	2.0	0.39	15.5	5700
41	8.21	25.6	0.29	2.9	1480	1.4	0.45	0.8	3600
45	8.24	22.9	0.25	2.5	1320	1.6	0.40	3.0	2320
47	8.23	29.0	0.20	1.0	900	1.4	0.38	0.8	1660
49	8.18	33.1	0.02	0.6	-	1.9	0.26	3.6	360
52	8.13	19.0	0.02	0.6	500	8.2	0.02	0.6	290
55	7.32	41.7	0.02	6.0	-	1.3	0.21	12.1	-

Table B.2: Packed-Bed Reactor – parameter variation with time

Day	pH	PBR - IN				PBR - OUT			
		NH_4^+-N	NO_2^--N	NO_3^--N	COD	NH_4^+-N	NO_2^--N	NO_3^--N	COD
		mg/l	mg/l	mg/l	mg/l	mg/l	mg/l	mg/l	mg/l
1	5.71	19.6	0.02	0.5	14150	3.74	0.02	0.5	17250
3	5.71	8.6	0.02	3.8	9400	2.24	0.02	12.5	13750
5	5.58	12.2	0.02	5.4	14850	3.03	0.02	15.9	15650
7	5.81	11.9	0.02	2.1	7300	3.45	0.02	3.2	14950
9	5.73	12.1	0.02	0.7	12200	3.57	0.02	9.5	14650
11	5.65	12.2	0.02	1.8	15500	3.45	0.02	10.0	16800
13	5.74	9.9	0.02	0.5	15300	3.27	0.02	19.3	13600
16	5.77	9.5	0.02	4.0	11250	1.95	0.02	19.2	12950
18	5.70	16.5	0.02	14.4	-	2.20	0.02	13.3	-
21	5.71	9.4	0.02	4.4	-	1.92	0.02	3.8	-
24	5.72	10.1	0.03	1.6	5200	2.91	0.02	10.4	17040
26	5.59	9.1	0.00	2.2	16540	1.55	0.02	2.2	28240
32	5.61	25.6	0.02	1.5	6800	2.57	0.02	0.5	22380
37	5.94	21.8	0.02	0.6	9640	0.24	0.02	2.9	25220
41	5.76	27.8	0.01	0.8	8440	1.38	0.02	6.7	23480
45	5.86	36.5	0.01	0.1	11560	1.55	0.02	0.1	20000
47	5.81	28.9	0.03	0.8	12000	1.17	0.02	0.8	20000
49	5.86	34.9	0.02	0.6	12560	1.86	0.02	0.6	20000
52	5.99	35.5	0.02	0.6	5380	0.89	0.02	1.4	11170
55	5.83	38.7	0.02	2.2	-	0.33	0.02	5.2	-

Table B.3: Airlift Suspension Reactor – parameter variation with time

Day	pH	ALSR – IN				ALSR – OUT			
		NH_4^+-N	NO_2^--N	NO_3^--N	COD	NH_4^+-N	NO_2^--N	NO_3^--N	COD
		mg/l	mg/l	mg/l	mg/l	mg/l	mg/l	mg/l	mg/l
0	8.34	27.2	0.90	11.1	100	14.6	1.16	28.8	280
3	8.06	55.8	1.98	27.0	220	27.6	2.20	42.1	440
5	8.60	31.3	0.16	5.4	220	17.1	1.40	28.2	80
7	8.65	28.5	0.02	2.2	70	20.9	1.50	41.2	40
9	8.29	20.8	1.54	25.4	-	19.3	3.00	30.0	-
11	8.38	27.0	1.68	64.6	-	26.6	9.50	61.5	-
13	7.64	22.3	6.60	74.1	80	24.1	11.20	124.4	90
15	7.76	12.6	12.00	94.8	40	6.1	8.40	115.4	170
18	7.94	1.6	8.80	100.6	20	0.3	9.40	20.5	10
21	7.63	8.8	3.50	54.9	190	1.3	3.20	78.5	130
23	7.50	0.39	0.02	37.5	240	0.05	72.30	0.02	190
25	7.82	48.0	0.02	2	50	0.5	0.02	91.7	220
27	8.08	37.5	0.02	2.2	50	26.2	0.02	74.4	20
29	8.03	32.7	0	3.9	130	7.1	0.04	70.9	3.5
31	8.16	27.1	0.21	5	70	2.7	0.58	23.7	40
33	7.92	38.0	0.35	7.8	65	3.9	1.56	67.0	15
35	7.65	31.4	0.02	0.8	980	2.6	0.05	25.0	180
37	7.43	32.7	0.11	1.5	240	3.2	0.05	19.9	25
39	7.33	31.5	0.03	0.7	300	0.5	0.02	29.0	320
42	7.43	33.2	0.03	0.4	250	2.6	0.04	23.2	300
43	7.29	12.5	0.06	10.8	330	0.8	0.02	22.9	310
44	7.34	17.3	0.19	17.8	300	1.8	0.05	28.2	300
45	7.34	12.1	0.02	39.7	250	0.4	0.01	81.6	340
46	7.36	16.0	0.07	41.5	440	0.8	0.01	72.8	390
48	7.41	13.6	0.06	34.3	310	0.8	0.01	87.5	290
49	7.49	19.5	0.08	57.7	-	2.4	0.04	211.6	-
50	7.42	27.6	0.17	117.5	-	2.0	0.04	211.6	-

Table B.4: The pH and temperature dependant $NH_4^+{}_{(aq)} \leftrightarrow NH_{3\,(g)}$ equilibrium

pH	Amount of $NH_{3\,(g)}$ per 100 mg of NH_4^+ at different temperatures (mg)					
	16 °C	18 °C	20 °C	22 °C	24 °C	26 °C
5.5	0.01	0.01	0.01	0.01	0.02	0.02
6.0	0.03	0.03	0.04	0.05	0.05	0.06
6.5	0.09	0.12	0.13	0.15	0.17	0.19
7.0	0.29	0.34	0.40	0.46	0.53	0.61
7.5	0.92	1.07	1.24	1.40	1.65	1.89
8.0	2.87	3.31	3.82	4.39	5.03	5.75
8.5	8.54	9.78	11.15	12.67	14.35	16.17
9.0	22.79	25.52	28.42	31.46	34.63	37.90

Source: http://cobweb.ecn.purdue.edu/~piwc/w3-research/free-ammonia/nh3.html, 21 – 08 – 2006.

Appendix C: Primary Data Sheets - Chapter 5.0

Table C.1: Continuously Stirring Tank Reactor – parameter variation with time

Day	pH	MLSS	CSTR - IN				CSTR - OUT			
			NH_4^+-N	NO_2^--N	NO_3^--N	COD_{total}	NH_4^+-N	NO_2^--N	NO_3^--N	COD_{total}
		mg/l	mg/l	mg/l	mg/l	mg/l	mg/l	mg/l	mg/l	mg/l
1	4.15	-	4.92	0.02	7.0	705	2.76	0.12	35.0	1125
3	4.29	-	18.90	0.02	36.0	450	1.45	0.02	128.0	1290
5	4.51	480	14.05	0.02	13.0	285	0.95	0.02	94.0	4530
12	7.68	1037	60.00	0.12	30.0	135	37.80	0.12	35.5	75
14	5.56	450	1.21	0.02	4.3	20	3.55	0.14	13.4	35
16	8.32	1769	17.80	0.05	3.5	210	3.00	0.13	30.0	495
18	8.70	-	11.35	0.17	5.0	100	56.50	0.15	11.5	100
20	8.43	-	14.00	0.10	22.5	145	12.50	0.13	15.5	100
22	8.56	2531	10.00	0.01	5.0	100	21.50	0.01	16.5	100
24	8.43	2400	6.00	0.01	7.5	100	17.50	0.04	46.5	100
26	8.57	2138	12.00	0.01	1.0	100	9.50	0.01	7.0	100
28	8.52	-	8.50	0.01	3.5	100	3.50	0.01	20.0	100
31	8.48	2000	1.00	0.02	4.5	60	0.50	0.02	31.0	50
33	8.71	1912	1.40	0.02	5.1	100	1.70	0.02	15.0	100
35	8.66	-	3.50	0.03	5.0	100	2.50	0.02	8.5	5
37	8.83	1469	2.50	0.00	12.0	100	2.00	0.01	23.5	45
41	7.75	3388	85.20	0.47	51.5	-	2.80	0.14	10.0	5415
43	7.73	4131	43.20	0.23	2.0	-	1.00	0.16	25.0	2315
47	7.55	5188	26.40	0.26	31.4	4140	0.20	0.28	41.0	8415
49	7.25	5019	30.00	0.31	27.0	16350	0.20	0.28	29.9	11700
51	7.57	5862	14.20	0.31	7.5	9425	0.20	0.35	32.7	9350
53	7.32	4440	12.40	0.21	2.6	10725	0.60	0.37	8.0	7575
57	7.53	5240	21.00	0.19	14.8	-	1.80	0.38	4.6	19225
59	7.38	-	56.20	0.06	12.7	15350	3.80	0.29	5.9	14100
61	7.75	-	12.80	0.20	10.60	15150	2.80	0.41	19.2	14650
63	7.60	4720	11.20	0.20	4.60	7075	1.60	0.36	21.3	7650
65	7.80	4670	14.00	0.24	5.00	12075	0.80	0.39	8.80	11725
67	8.05	5470	10.0	0.12	6.2	14100	0.6	0.24	9.5	19050
69	8.45	4670	17.8	0.04	2.7	16500	0.0	0.27	13.2	13700
71	8.43	4980	8.4	0.13	13.2	16700	1.4	0.31	17.1	15650
73	8.71	5160	8.6	0.23	17.7	21500	1.2	0.37	14.7	13750
76	8.55	-	9.8	0.27	5.4	10125	2.2	0.43	8.4	9475
78	8.69	-	8.2	0.33	25.5	-	3.4	0.58	65.9	-
80	8.37	-	4.8	0.33	16.6	23850	1.8	0.54	30.1	15700
82	7.79	-	4.0	0.26	21.5	13850	2.7	0.52	39.4	18600
84	7.99	-	3.1	0.22	20.2	15550	2.0	0.52	42.2	14400
87	7.65	-	1.7	0.28	10.7	15000	0.9	0.51	28.2	18600
89	7.66	-	3.8	0.42	28.4	23350	1.2	0.47	16.6	14850

Table C.2: Packed-Bed Reactor – parameter variation with time

Day	pH	PBR – IN				PBR – OUT			
		NH_4^+-N mg/l	NO_2^--N mg/l	NO_3^--N mg/l	COD_{total} mg/l	NH_4^+-N mg/l	NO_2^--N mg/l	NO_3^--N mg/l	COD_{total} mg/l
1	6.09	8.36	42.00	109.5	5145	3.52	75.00	201.5	2355
3	6.07	-	18.00	297.0	2655	0.50	53.00	509.5	1950
5	5.94	-	42.00	468.0	4800	0.05	60.00	568.0	10560
12	5.86	13.40	3.50	115.5	1035	0.34	9.50	214.0	1110
14	5.85	107.00	70.02	26.2	90	0.20	0.24	72.6	580
16	6.13	106.00	2.50	118.0	405	1.55	7.00	309.0	1485
18	6.38	117.50	8.00	192.5	2505	0.13	3.50	219.0	4785
20	6.52	130.50	21.00	136.0	5235	1.29	5.00	99.5	3825
22	6.35	54.00	9.00	19.5	2580	0.05	20.50	105.0	9675
24	6.37	17.50	0.01	11.0	450	0.64	32.00	130.5	5955
26	6.45	119.00	2.00	1.0	4590	0.03	19.50	108.5	6150
28	5.60	135.00	0.50	4.5	4590	0.12	1.50	12.5	6150
31	5.37	172.50	0.02	3.0	765	0.22	0.02	20.0	7290
33	5.36	176.00	1.00	19.7	4965	0.02	1.00	43.5	4815
35	5.82	175.50	0.22	2.0	7065	0.05	0.15	27.5	5925
37	6.01	174.50	0.23	8.5	-	0.03	0.15	24.0	-
41	5.49	95.40	0.20	24.0	3765	0.05	0.20	2.0	4020
43	5.10	70.80	0.01	2.0	4320	0.05	0.20	13.5	3870
47	4.93	32.40	0.08	10.3	13905	0.03	0.02	19.5	4470
49	4.96	21.20	0.04	12.0	5985	0.53	0.02	8.3	11595
51	4.89	17.20	0.12	2.4	9450	0.23	0.02	0.6	-
53	4.85	15.80	0.02	2.0	9250	0.90	0.02	9.4	9425
57	4.84	13.60	0.09	4.7	11325	0.07	0.02	1.5	22375
59	5.09	29.40	0.01	13.3	15850	1.71	0.01	2.2	21550
61	5.28	16.20	0.01	6.4	19850	0.88	0.01	4.9	22900
63	5.24	12.60	0.02	0.5	9525	1.54	0.02	0.3	7700
65	5.42	12.20	0.02	1.6	7675	1.71	0.02	0.4	7625
67	5.48	10.60	0.02	7.8	18750	2.91	0.02	2.1	14850
69	5.48	9.2	0.02	0.1	23450	2.21	0.02	5.1	16400
71	5.55	6.2	0.02	1.1	12000	1.97	0.02	5.8	15050
73	5.46	8.8	0.03	7.6	17850	1.14	0.02	0.7	16450
76	5.48	5.4	0.02	2.5	6800	2.57	0.02	0.0	10325
78	5.45	9.8	0.02	7.1	-	0.61	0.02	3.2	-
80	5.49	5.2	0.02	12.6	20700	1.93	0.02	3.0	14850
82	5.60	3.4	0	5.2	13350	1.09	0.02	12.7	13550
84	5.56	1.2	0.04	9.9	14400	0.78	0.02	8.8	14300
87	5.66	0.5	0.02	6.1	15800	0.61	0.02	0.5	26250
89	5.69	1.4	0.26	8.9	31400	0.31	0.02	7.6	27350

Appendix D: Supporting theory and primary data sheets - Chapter 6.0

I. *Determination of K_i for PGMs using reaction velocity (adapted from Lewandowski et al., 1985)*

Reaction rate (υ) and inhibitive compound concentration [i] can be represented as shown in the Figure E1 (Lewandowski *et al.*, 1985).

Kinetics equation of non-competitive inhibition is given by (Lewandowski *et al.*, 1985 adapted from Aiba *et al.*, 1973):

$$v = \frac{v_{max} * S * K_i}{(K_m + S) * (K_i + i)} \qquad \text{(D1)}$$

Where:

υ	-	Enzyme reaction rate	[mg/l/hr]
υ_{max}	-	Maximum rate of enzyme reaction when saturated with substrate	[mg/l/hr]
S	-	Substrate concentration	[mg/l]
i	-	Inhibitive compound concentration (metal)	[mg/l]
K_m	-	Michaelis constant that concentration of substrate giving half maximum reaction rate	[mg/l]
K_i	-	Michaelis constant that concentration of inhibitor giving half maximum reaction rate	[mg/l]

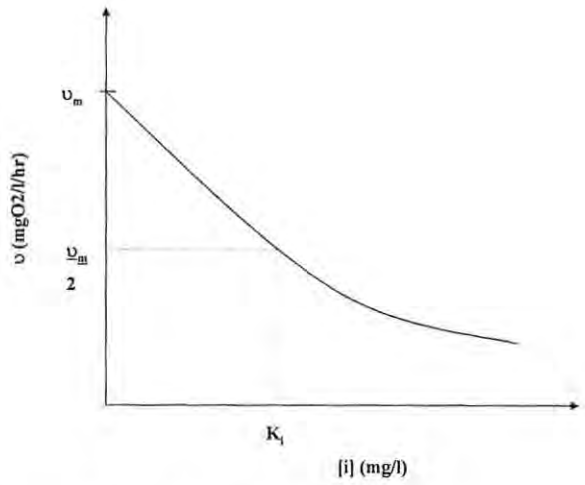

Figure D.1: Influence of the [i] on the υ

As O_2 is reduced in respiration reaction proportional to the substrate utilisation, the following relationship could be obtained.

$$v = -\frac{dS}{dt} = -\frac{d(O_2)}{dt} \tag{D2}$$

Oxygen uptake rate in a closed reactor is obtained using OxiTop system which is proportional to the substrate utilisation rate.

$$v = -\frac{dS}{dt} = \frac{v_{max} * S}{K_m + S} \tag{D3}$$

When O_2 is considered as the substrate, the Michaelis constant for is about 0.1 mg/l (Lewandowski *et al.*, 1985). As DO in AS can be approximated to saturation, $S >> K_m$, then equation (E3) is reduced to:

$$v = -\frac{d(O_2)}{dt} = v_{max} \tag{D4}$$

Similarly for non-competitive inhibitor,

$$v = \frac{v_{max} * K_i}{K_i + i} \tag{D5}$$

In order to obtain Ki, equation (E5) will be rearranged in the form of y = mx + C.

$$\frac{1}{v} = \left(\frac{1}{v_{max} * K_i}\right) * i + \frac{1}{v_{max}} \tag{D6}$$

By plotting $\frac{1}{v}$ *vs.* i, K_i can be obtained as shown Figure E2.

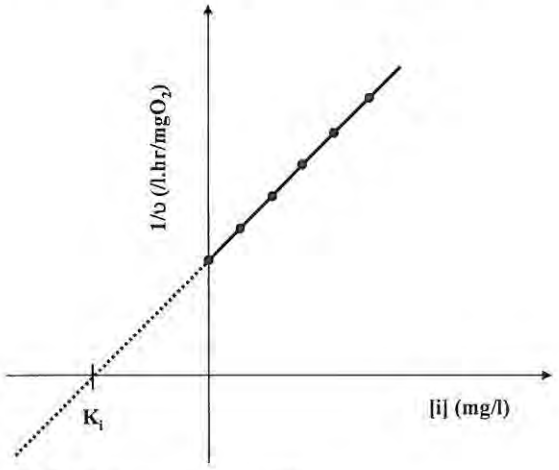

Figure D.2: Determination of K_i

II. Primary datasheets (Specific Oxygen Uptake vs. time for different metals)

Table D.1: SOU *vs.* time for different concentrations of Pt.

Time	Specific Oxygen Uptake ($mgO_2/mgVSS$)					
(s)	0 mg/l	0 mg/l	0 mg/l	0 mg/l	0 mg/l	0 mg/l
0	0.0	0.0	0.0	0.0	0.0	0.0
100	0.0522	0.0329	0.0505	0.0505	0.0074	0.0289
200	0.0522	0.0329	0.0505	0.0253	0.0348	0.0562
300	0.0522	0.0329	0.0233	0.0505	0.0074	0.0273
400	0.0522	0.0329	0.0272	0.0253	0.0074	0.0273
500	0.0522	0.0329	0.0505	0.0505	0.0549	0.0562
600	0.0115	0.0329	0.0777	0.0253	0.0348	0.0562
700	0.0115	0.0329	0.0272	0.0253	0.0348	0.0273
800	0.0522	0.0329	0.0505	0.0253	0.0348	0.0562
900	0.0522	0.0636	0.0777	0.0505	0.0549	0.0562
1000	0.0115	0.0329	0.0777	0.0505	0.0549	0.0562
1100	0.0522	0.0329	0.0505	0.0253	0.0348	0.0562
1200	0.0872	0.0657	0.0505	0.0505	0.0549	0.0562
1300	0.0872	0.0965	0.0777	0.0758	0.0823	0.0562
1400	0.0465	0.0329	0.0505	0.0505	0.0549	0.0562
1500	0.0872	0.0636	0.0505	0.0253	0.0549	0.0562
1600	0.1279	0.0965	0.0738	0.0758	0.0549	0.0562
1700	0.0872	0.0965	0.1010	0.0505	0.0549	0.0835
1800	0.0115	0.0636	0.0777	0.0505	0.0549	0.0562
1900	0.0872	0.0965	0.1010	0.0505	0.0549	0.0562
2000	0.0872	0.0965	0.1010	0.0758	0.0549	0.0562
2100	0.0872	0.0965	0.0777	0.0505	0.0823	0.0562
2200	0.0465	0.0636	0.0505	0.0505	0.0549	0.0835
2300	0.0872	0.0965	0.0738	0.0758	0.0549	0.0835
2400	0.0872	0.0965	0.1010	0.0758	0.0823	0.0835
2500	0.0872	0.0965	0.1010	0.0758	0.0549	0.0835
2600	0.0872	0.0636	0.0777	0.0758	0.0549	0.0835
2700	0.1221	0.0965	0.1010	0.0758	0.0823	0.0852
2800	0.0814	0.0965	0.1010	0.0758	0.0823	0.0835
2900	0.0465	0.0965	0.0777	0.0505	0.0823	0.0835
3000	0.1221	0.0965	0.1010	0.0758	0.0549	0.1125
3100	0.1221	0.1602	0.1282	0.1010	0.0823	0.1125
3200	0.1221	0.1294	0.1282	0.1010	0.0823	0.1125
3300	0.0814	0.0965	0.1010	0.0505	0.0823	0.1125
3400	0.1221	0.1294	0.1010	0.1010	0.1023	0.0852
3500	0.1221	0.1294	0.1010	0.1010	0.1297	0.1125
3600	0.0814	0.1294	0.1010	0.1010	0.1097	0.1125
3700	0.1221	0.0965	0.1010	0.0758	0.1097	0.1125
3800	0.1221	0.1602	0.1282	0.1010	0.1023	0.1125
3900	0.0814	0.1602	0.1282	0.1010	0.1297	0.1125
4000	0.0814	0.1273	0.1010	0.1010	0.1023	0.1125
4100	0.1221	0.1273	0.1010	0.1010	0.1023	0.1125
4200	0.1221	0.1602	0.1010	0.1263	0.1297	0.1125
4300	0.1221	0.1602	0.1244	0.1010	0.1297	0.1125
4400	0.1221	0.1273	0.1010	0.1010	0.1297	0.1125
4500	0.1221	0.1602	0.1516	0.1263	0.1023	0.1125
4600	0.1571	0.1602	0.1516	0.1263	0.1297	0.1125
4700	0.0814	0.1602	0.1244	0.1263	0.1297	0.1125
4800	0.1221	0.1602	0.1010	0.1010	0.1023	0.1125

Table D.1 (cont'd): SOU *vs.* time for different concentrations of Pt.

Time	Specific Oxygen Uptake ($mgO_2/mgVSS$)					
(s)	0 mg/l	5 mg/l	10 mg/l	15 mg/l	20 mg/l	25 mg
5000	0.1571	0.1602	0.1516	0.1516	0.1297	0.1414
5100	0.1164	0.1602	0.1282	0.1010	0.1297	0.1125
5200	0.1571	0.1602	0.1516	0.1263	0.1023	0.1125
5300	0.1571	0.1602	0.1516	0.1263	0.1297	0.1414
5400	0.1571	0.1602	0.1516	0.1516	0.1297	0.1414
5500	0.1571	0.1602	0.1516	0.1010	0.1297	0.1125
5600	0.1571	0.1930	0.1516	0.1263	0.1498	0.1125
5700	0.1571	0.1930	0.1788	0.1516	0.1498	0.1414
5800	0.1571	0.1602	0.1516	0.1516	0.1498	0.1125
5900	0.1571	0.1602	0.1516	0.1263	0.1297	0.1125
6000	0.1571	0.2238	0.1516	0.1263	0.1498	0.1414
6100	0.1571	0.2238	0.1788	0.1516	0.1772	0.1414
6200	0.1571	0.2238	0.1788	0.1516	0.1297	0.1414
6300	0.1571	0.2238	0.1516	0.1516	0.1498	0.1414
6400	0.1920	0.2238	0.2021	0.1768	0.1498	0.1414
6500	0.1513	0.2238	0.2021	0.1768	0.1772	0.1687
6600	0.1571	0.1909	0.1516	0.1516	0.1498	0.1414
6700	0.1920	0.2238	0.2021	0.1768	0.1498	0.1687
6800	0.1920	0.2238	0.1788	0.1768	0.1772	0.1414
6900	0.1920	0.2238	0.1788	0.1516	0.1772	0.1687
7000	0.1920	0.2238	0.1788	0.1516	0.1498	0.1687
7100	0.1920	0.2567	0.2021	0.1768	0.1498	0.1414
7200	0.1920	0.2238	0.2021	0.2021	0.1772	0.1414
7300	0.1920	0.2238	0.2021	0.1516	0.1498	0.1687
7400	0.1920	0.2238	0.2021	0.1768	0.1498	0.1414
7500	0.1920	0.2567	0.2293	0.1768	0.1772	0.1414
7600	0.1920	0.2874	0.2021	0.2021	0.1772	0.1687
7700	0.1513	0.2238	0.2021	0.1516	0.1772	0.1687
7800	0.1920	0.2874	0.2021	0.1768	0.1772	0.1687
7900	0.2270	0.2874	0.2021	0.1768	0.1772	0.1687
8000	0.2270	0.2874	0.2293	0.1768	0.1972	0.1687
8100	0.1920	0.2546	0.1788	0.2021	0.1772	0.1687
8200	0.2270	0.2567	0.2254	0.2021	0.1772	0.1687
8300	0.2270	0.2874	0.2021	0.2021	0.1772	0.1976
8400	0.2270	0.2546	0.2021	0.2021	0.1772	0.1687
8500	0.1920	0.2874	0.2021	0.1768	0.1772	0.1687
8600	0.1920	0.2874	0.2293	0.2021	0.2247	0.1687
8700	0.2270	0.2874	0.2293	0.2021	0.2247	0.1687
8800	0.1863	0.2546	0.2293	0.2021	0.1972	0.1687
8900	0.2270	0.2874	0.2254	0.2021	0.1972	0.1687
9000	0.1863	0.2874	0.2254	0.2021	0.2247	0.1687
9100	0.1863	0.2874	0.2526	0.2021	0.1972	0.1976
9200	0.1863	0.2874	0.2293	0.2021	0.2247	0.1687
9300	0.2270	0.3203	0.2526	0.2273	0.1972	0.1976
9400	0.2270	0.3203	0.2526	0.2021	0.2247	0.1976
9500	0.2270	0.2874	0.2021	0.2021	0.2247	0.1687
9600	0.2270	0.2874	0.2254	0.2021	0.1972	0.1687
9700	0.2270	0.3182	0.2021	0.2273	0.2247	0.1976
9800	0.2270	0.2874	0.2526	0.2526	0.2247	0.1976
9900	0.2212	0.2874	0.2021	0.2021	0.1972	0.1976
10000	0.2619	0.3182	0.2526	0.2273	0.1972	0.1976

Table D.2: SOU *vs.* time for different concentrations of Pd.

Time	Specific Oxygen Uptake ($mgO_2/mgVSS$)					
(s)	0 mg/l	5 mg/l	10 mg/l	15 mg/l	20 mg/l	25 mg
0	0.0	0.0	0.0	0.0	0.0	0.0
100	0.0108	0.0111	0.0084	0.0080	0.0075	0.0071
200	0.0108	0.0333	0.0279	0.0255	0.0164	0.0313
300	0.0108	0.0671	0.0279	0.0429	0.0164	0.0228
400	0.0108	0.0554	0.0279	0.0600	0.0266	0.0228
500	0.0108	0.0671	0.0363	0.0600	0.0471	0.0156
600	0.0108	0.0665	0.0475	0.0513	0.0559	0.0384
700	0.0108	0.0782	0.0475	0.0600	0.0559	0.0384
800	0.0313	0.0782	0.0558	0.0684	0.0471	0.0384
900	0.0205	0.0782	0.0642	0.0684	0.0648	0.0384
1000	0.0410	0.0893	0.0754	0.0597	0.0750	0.0469
1100	0.0605	0.1004	0.0754	0.0771	0.0750	0.0469
1200	0.0713	0.1004	0.0754	0.0855	0.0662	0.0541
1300	0.0918	0.1004	0.0838	0.0939	0.0839	0.0541
1400	0.1242	0.1232	0.0949	0.0768	0.0941	0.0626
1500	0.1458	0.1343	0.0949	0.1026	0.0941	0.0626
1600	0.1556	0.1226	0.0949	0.1026	0.0941	0.0626
1700	0.1664	0.1343	0.1033	0.0939	0.1043	0.0626
1800	0.1664	0.1460	0.1145	0.1023	0.1132	0.0697
1900	0.1772	0.1688	0.1145	0.1110	0.0941	0.0782
2000	0.1869	0.1688	0.1145	0.1110	0.1043	0.0782
2100	0.1869	0.1577	0.1229	0.1023	0.1323	0.0782
2200	0.1869	0.1799	0.1340	0.1110	0.1132	0.0938
2300	0.2085	0.1916	0.1340	0.1197	0.1234	0.0938
2400	0.2182	0.1916	0.1340	0.1194	0.1234	0.0853
2500	0.2182	0.1805	0.1340	0.1194	0.1323	0.0938
2600	0.2182	0.1916	0.1340	0.1194	0.1425	0.0938
2700	0.2290	0.2144	0.1340	0.1194	0.1425	0.0938
2800	0.2290	0.2033	0.1340	0.1194	0.1425	0.0938
2900	0.2290	0.2033	0.1452	0.1277	0.1514	0.1010
3000	0.2290	0.2144	0.1536	0.1194	0.1425	0.1095
3100	0.2495	0.2261	0.1452	0.1365	0.1323	0.1095
3200	0.2398	0.2261	0.1536	0.1277	0.1514	0.1010
3300	0.2290	0.2261	0.1536	0.1277	0.1514	0.1095
3400	0.2398	0.2372	0.1648	0.1277	0.1514	0.1095
3500	0.2603	0.2372	0.1648	0.1277	0.1425	0.1095
3600	0.2398	0.2379	0.1648	0.1277	0.1616	0.1095
3700	0.2398	0.2490	0.1648	0.1190	0.1705	0.1251
3800	0.2603	0.2490	0.1648	0.1277	0.1616	0.1166
3900	0.2603	0.2490	0.1648	0.1361	0.1616	0.1166
4000	0.2603	0.2490	0.1731	0.1361	0.1705	0.1251
4100	0.2398	0.2600	0.1843	0.1361	0.1807	0.1251
4200	0.2506	0.2718	0.1759	0.1448	0.1616	0.1251
4300	0.2506	0.2607	0.1731	0.1361	0.1718	0.1251
4400	0.2506	0.2607	0.1843	0.1274	0.1807	0.1251
4500	0.2398	0.2718	0.1843	0.1274	0.1807	0.1251
4600	0.2506	0.2718	0.1759	0.1361	0.1807	0.1323
4700	0.2614	0.2718	0.1759	0.1445	0.1807	0.1251
4800	0.2506	0.2718	0.1955	0.1358	0.1998	0.1407
4900	0.2506	0.2946	0.1871	0.1445	0.1807	0.1407
5000	0.2614	0.2946	0.1955	0.1445	0.1909	0.1407

Table D.2 (cont'd): SOU *vs.* time for different concentrations of Pd.

Time	Specific Oxygen Uptake ($mgO_2/mgVSS$)					
(s)	0 mg/l	5 mg/l	10 mg/l	15 mg/l	20 mg/l	25 mg
5100	0.2614	0.2835	0.1955	0.1445	0.1998	0.1407
5200	0.2506	0.2835	0.1955	0.1358	0.1998	0.1407
5300	0.2506	0.2946	0.1955	0.1445	0.1909	0.1479
5400	0.2614	0.2946	0.1871	0.1529	0.1909	0.1407
5500	0.2614	0.2946	0.1955	0.1441	0.1998	0.1394
5600	0.2409	0.2946	0.2066	0.1441	0.1998	0.1479
5700	0.2517	0.3056	0.2066	0.1445	0.1998	0.1479
5800	0.2614	0.3174	0.1955	0.1529	0.1998	0.1407
5900	0.2614	0.3063	0.1955	0.1441	0.2189	0.1407
6000	0.2409	0.3174	0.2066	0.1358	0.2100	0.1479
6100	0.2517	0.3174	0.2066	0.1529	0.1998	0.1479
6200	0.2614	0.3174	0.1983	0.1441	0.2100	0.1479
6300	0.2517	0.3063	0.2066	0.1525	0.2189	0.1479
6400	0.2409	0.3174	0.2178	0.1441	0.2189	0.1564
6500	0.2517	0.3285	0.2178	0.1529	0.2087	0.1564
6600	0.2517	0.3285	0.2178	0.1612	0.2100	0.1479
6700	0.2517	0.3174	0.2178	0.1525	0.2189	0.1635
6800	0.2409	0.3285	0.2178	0.1441	0.2189	0.1635
6900	0.2517	0.3285	0.2178	0.1525	0.2189	0.1635
7000	0.2517	0.3285	0.2178	0.1525	0.2291	0.1564
7100	0.2409	0.3174	0.2178	0.1525	0.2278	0.1635
7200	0.2409	0.3285	0.2290	0.1438	0.2189	0.1635
7300	0.2517	0.3402	0.2178	0.1525	0.2291	0.1635
7400	0.2517	0.3285	0.2178	0.1525	0.2291	0.1635
7500	0.2409	0.3285	0.2290	0.1525	0.2380	0.1635
7600	0.2409	0.3513	0.2290	0.1525	0.2189	0.1720
7700	0.2517	0.3285	0.2290	0.1525	0.2189	0.1720
7800	0.2625	0.3402	0.2290	0.1525	0.2380	0.1635
7900	0.2517	0.3285	0.2290	0.1525	0.2380	0.1792
8000	0.2517	0.3513	0.2206	0.1525	0.2380	0.1792
8100	0.2517	0.3513	0.2290	0.1609	0.2291	0.1707
8200	0.2517	0.3402	0.2290	0.1609	0.2380	0.1635
8300	0.2312	0.3395	0.2401	0.1522	0.2380	0.1792
8400	0.2517	0.3513	0.2401	0.1525	0.2278	0.1792
8500	0.2517	0.3513	0.2401	0.1609	0.2380	0.1792
8600	0.2420	0.3402	0.2401	0.1609	0.2469	0.1792
8700	0.2312	0.3513	0.2401	0.1522	0.2380	0.1792
8800	0.2420	0.3623	0.2401	0.1609	0.2380	0.1792
8900	0.2517	0.3513	0.2401	0.1609	0.2380	0.1792
9000	0.2312	0.3402	0.2401	0.1609	0.2469	0.1792
9100	0.2312	0.3623	0.2513	0.1522	0.2380	0.1863
9200	0.2420	0.3623	0.2429	0.1609	0.2380	0.1792
9300	0.2420	0.3513	0.2401	0.1609	0.2482	0.1792
9400	0.2312	0.3513	0.2513	0.1522	0.2469	0.1863
9500	0.2312	0.3623	0.2513	0.1609	0.2469	0.1948
9600	0.2420	0.3623	0.2513	0.1693	0.2380	0.1863
9700	0.2420	0.3623	0.2513	0.1609	0.2469	0.1792
9800	0.2312	0.3623	0.2513	0.1522	0.2469	0.1948
9900	0.2312	0.3623	0.2625	0.1609	0.2571	0.1948
10000	0.2420	0.3623	0.2429	0.1693	0.2380	0.1948

Table D.3: SOU *vs.* time for different concentrations of Rh.

Time	Specific Oxygen Uptake ($mgO_2/mgVSS$)					
(s)	0 mg/l	5 mg/l	10 mg/l	15 mg/l	20 mg/l	25 mg
0	0.0	0.0	0.0	0.0	0.0	0.0
100	0.03	0.00	0.03	0.01	0.01	0.01
200	0.06	0.02	0.06	0.06	0.03	0.01
300	0.10	0.05	0.08	0.08	0.04	0.02
400	0.11	0.07	0.10	0.10	0.06	0.04
500	0.11	0.09	0.11	0.10	0.08	0.05
600	0.13	0.09	0.11	0.10	0.08	0.07
700	0.14	0.12	0.12	0.11	0.10	0.09
800	0.16	0.12	0.14	0.13	0.11	0.09
900	0.16	0.14	0.14	0.14	0.13	0.10
1000	0.16	0.13	0.15	0.14	0.12	0.10
1100	0.19	0.15	0.16	0.15	0.13	0.11
1200	0.19	0.16	0.16	0.15	0.15	0.13
1300	0.19	0.17	0.17	0.17	0.15	0.13
1400	0.19	0.18	0.17	0.17	0.15	0.13
1500	0.21	0.18	0.18	0.17	0.15	0.14
1600	0.21	0.19	0.19	0.18	0.17	0.16
1700	0.21	0.19	0.19	0.18	0.18	0.16
1800	0.21	0.20	0.20	0.18	0.17	0.16
1900	0.23	0.19	0.20	0.18	0.18	0.16
2000	0.24	0.21	0.21	0.20	0.19	0.16
2100	0.24	0.21	0.21	0.20	0.18	0.17
2200	0.24	0.21	0.22	0.20	0.18	0.17
2300	0.24	0.22	0.22	0.20	0.19	0.17
2400	0.24	0.22	0.22	0.21	0.19	0.19
2500	0.24	0.23	0.22	0.21	0.20	0.19
2600	0.24	0.23	0.23	0.21	0.20	0.19
2700	0.26	0.23	0.23	0.21	0.20	0.19
2800	0.27	0.24	0.23	0.22	0.20	0.19
2900	0.26	0.24	0.24	0.21	0.22	0.20
3000	0.26	0.24	0.24	0.21	0.21	0.20
3100	0.26	0.24	0.24	0.22	0.21	0.20
3200	0.27	0.25	0.24	0.22	0.22	0.20
3300	0.27	0.25	0.24	0.22	0.22	0.20
3400	0.26	0.25	0.25	0.22	0.22	0.20
3500	0.27	0.24	0.25	0.22	0.21	0.20
3600	0.27	0.26	0.26	0.22	0.22	0.21
3700	0.29	0.27	0.26	0.24	0.23	0.21
3800	0.27	0.27	0.26	0.24	0.22	0.21
3900	0.29	0.26	0.26	0.24	0.22	0.21
4000	0.29	0.27	0.26	0.24	0.24	0.23
4100	0.27	0.27	0.26	0.24	0.24	0.22
4200	0.29	0.27	0.26	0.24	0.23	0.22
4300	0.29	0.27	0.26	0.24	0.23	0.23
4400	0.29	0.27	0.27	0.24	0.24	0.23
4500	0.29	0.27	0.27	0.24	0.24	0.23
4600	0.29	0.27	0.27	0.24	0.24	0.23
4700	0.31	0.27	0.27	0.24	0.24	0.23
4800	0.31	0.29	0.27	0.25	0.25	0.24
4900	0.31	0.29	0.27	0.24	0.25	0.24
5000	0.29	0.28	0.27	0.24	0.25	0.24

Table D.3 (cont'd): SOU *vs.* time for different concentrations of Rh.

Time	Specific Oxygen Uptake ($mgO_2/mgVSS$)					
(s)	0 mg/l	5 mg/l	10 mg/l	15 mg/l	20 mg/l	25 mg
5100	0.31	0.28	0.27	0.25	0.25	0.23
5200	0.31	0.29	0.27	0.25	0.25	0.24
5300	0.31	0.29	0.28	0.25	0.25	0.24
5400	0.31	0.29	0.28	0.24	0.25	0.24
5500	0.32	0.29	0.27	0.25	0.25	0.24
5600	0.32	0.31	0.28	0.25	0.26	0.25
5700	0.31	0.29	0.28	0.25	0.26	0.25
5800	0.31	0.30	0.28	0.25	0.25	0.25
5900	0.32	0.30	0.27	0.25	0.25	0.24
6000	0.32	0.31	0.29	0.27	0.27	0.26
6100	0.32	0.31	0.29	0.25	0.27	0.25
6200	0.32	0.30	0.28	0.25	0.26	0.25
6300	0.34	0.30	0.29	0.27	0.26	0.26
6400	0.34	0.31	0.29	0.27	0.27	0.26
6500	0.32	0.31	0.29	0.27	0.27	0.26
6600	0.32	0.31	0.29	0.25	0.26	0.26
6700	0.34	0.30	0.29	0.27	0.26	0.26
6800	0.34	0.32	0.30	0.27	0.27	0.27
6900	0.32	0.32	0.29	0.27	0.27	0.26
7000	0.32	0.31	0.30	0.27	0.27	0.26
7100	0.34	0.31	0.30	0.27	0.27	0.27
7200	0.34	0.32	0.30	0.27	0.27	0.27
7300	0.34	0.32	0.30	0.27	0.27	0.27
7400	0.34	0.31	0.30	0.27	0.27	0.27
7500	0.34	0.32	0.30	0.28	0.27	0.27
7600	0.35	0.32	0.30	0.28	0.28	0.27
7700	0.34	0.32	0.30	0.28	0.28	0.27
7800	0.34	0.32	0.30	0.27	0.27	0.27
7900	0.35	0.33	0.30	0.28	0.27	0.27
8000	0.35	0.33	0.31	0.28	0.28	0.27
8100	0.34	0.32	0.31	0.28	0.28	0.28
8200	0.34	0.33	0.30	0.28	0.28	0.28
8300	0.34	0.33	0.31	0.28	0.28	0.28
8400	0.34	0.33	0.31	0.28	0.29	0.29
8500	0.34	0.33	0.30	0.28	0.29	0.29
8600	0.35	0.33	0.30	0.28	0.29	0.29
8700	0.35	0.34	0.31	0.29	0.29	0.29
8800	0.35	0.34	0.31	0.29	0.29	0.29
8900	0.35	0.34	0.32	0.28	0.29	0.28
9000	0.35	0.33	0.31	0.29	0.29	0.29
9100	0.35	0.34	0.31	0.29	0.29	0.29
9200	0.35	0.34	0.32	0.29	0.29	0.30
9300	0.35	0.34	0.32	0.29	0.29	0.30
9400	0.35	0.34	0.31	0.29	0.29	0.30
9500	0.37	0.35	0.31	0.29	0.30	0.30
9600	0.35	0.35	0.31	0.29	0.30	0.30
9700	0.35	0.34	0.32	0.29	0.30	0.30
9800	0.37	0.34	0.33	0.29	0.30	0.30
9900	0.37	0.35	0.33	0.29	0.30	0.30
10000	0.37	0.35	0.33	0.29	0.30	0.30

Table D.4: SOU *vs.* time for different concentrations of Ru.

Time	Specific Oxygen Uptake ($mgO_2/mgVSS$)					
(s)	0 mg/l	5 mg/l	10 mg/l	15 mg/l	20 mg/l	25 mg
0	0.000	0.000	0.000	0.000	0.000	0.000
100	0.021	0.002	0.000	0.013	0.014	0.015
200	0.021	0.012	0.017	0.027	0.014	0.015
300	0.021	0.011	0.017	0.013	0.014	0.030
400	0.021	0.011	0.017	0.013	0.014	0.030
500	0.042	0.002	0.017	0.027	0.021	0.030
600	0.021	0.022	0.017	0.027	0.014	0.030
700	0.021	0.022	0.017	0.013	0.014	0.030
800	0.042	0.022	0.017	0.013	0.021	0.030
900	0.042	0.022	0.017	0.027	0.027	0.030
1000	0.021	0.022	0.034	0.027	0.027	0.030
1100	0.042	0.022	0.034	0.027	0.014	0.030
1200	0.042	0.011	0.034	0.027	0.027	0.030
1300	0.042	0.032	0.034	0.027	0.027	0.030
1400	0.042	0.032	0.034	0.027	0.027	0.045
1500	0.042	0.042	0.034	0.027	0.027	0.030
1600	0.042	0.042	0.034	0.040	0.034	0.030
1700	0.042	0.042	0.034	0.040	0.027	0.045
1800	0.042	0.042	0.034	0.040	0.027	0.045
1900	0.063	0.042	0.034	0.027	0.027	0.045
2000	0.042	0.042	0.034	0.054	0.034	0.045
2100	0.042	0.053	0.051	0.040	0.034	0.045
2200	0.063	0.042	0.034	0.040	0.027	0.045
2300	0.084	0.042	0.034	0.040	0.034	0.045
2400	0.084	0.053	0.034	0.040	0.041	0.045
2500	0.063	0.062	0.051	0.040	0.034	0.045
2600	0.084	0.052	0.051	0.040	0.034	0.045
2700	0.084	0.052	0.034	0.054	0.048	0.045
2800	0.084	0.062	0.051	0.054	0.041	0.060
2900	0.063	0.062	0.051	0.040	0.041	0.060
3000	0.084	0.062	0.051	0.040	0.041	0.060
3100	0.084	0.062	0.051	0.054	0.048	0.060
3200	0.084	0.082	0.051	0.054	0.041	0.060
3300	0.084	0.072	0.051	0.054	0.041	0.060
3400	0.105	0.072	0.051	0.054	0.048	0.045
3500	0.084	0.082	0.051	0.067	0.048	0.060
3600	0.084	0.082	0.051	0.054	0.048	0.060
3700	0.084	0.082	0.051	0.054	0.041	0.060
3800	0.105	0.072	0.051	0.067	0.048	0.060
3900	0.105	0.082	0.051	0.067	0.048	0.060
4000	0.105	0.082	0.068	0.067	0.048	0.060
4100	0.105	0.082	0.051	0.054	0.048	0.060
4200	0.105	0.082	0.068	0.067	0.062	0.060
4300	0.105	0.093	0.068	0.081	0.054	0.075
4400	0.105	0.102	0.051	0.067	0.048	0.060
4500	0.126	0.092	0.068	0.067	0.055	0.075
4600	0.126	0.102	0.068	0.081	0.062	0.075
4700	0.126	0.102	0.068	0.081	0.062	0.075
4800	0.126	0.102	0.068	0.067	0.054	0.075
4900	0.147	0.092	0.068	0.081	0.062	0.075
5000	0.126	0.102	0.068	0.081	0.062	0.075

Table D.4 (cont'd): SOU *vs.* time for different concentrations of Ru.

Time	Specific Oxygen Uptake ($mgO_2/mgVSS$)					
(s)	0 mg/l	5 mg/l	10 mg/l	15 mg/l	20 mg/l	25 mg
5100	0.126	0.113	0.068	0.081	0.062	0.075
5200	0.126	0.102	0.068	0.081	0.062	0.090
5300	0.147	0.102	0.068	0.081	0.069	0.075
5400	0.126	0.113	0.068	0.081	0.062	0.090
5500	0.126	0.112	0.068	0.081	0.062	0.075
5600	0.147	0.112	0.068	0.081	0.069	0.075
5700	0.147	0.122	0.068	0.094	0.062	0.090
5800	0.147	0.122	0.086	0.081	0.062	0.090
5900	0.147	0.122	0.086	0.081	0.062	0.075
6000	0.147	0.122	0.068	0.094	0.069	0.090
6100	0.147	0.122	0.086	0.094	0.069	0.090
6200	0.147	0.122	0.068	0.094	0.069	0.090
6300	0.147	0.122	0.068	0.081	0.069	0.090
6400	0.147	0.132	0.068	0.108	0.069	0.090
6500	0.147	0.142	0.086	0.094	0.069	0.090
6600	0.147	0.132	0.086	0.094	0.069	0.090
6700	0.168	0.132	0.068	0.094	0.069	0.090
6800	0.168	0.142	0.086	0.108	0.076	0.090
6900	0.147	0.142	0.086	0.108	0.069	0.104
7000	0.168	0.142	0.086	0.108	0.069	0.104
7100	0.189	0.132	0.068	0.108	0.082	0.090
7200	0.168	0.152	0.086	0.108	0.076	0.104
7300	0.168	0.152	0.086	0.108	0.069	0.104
7400	0.189	0.141	0.086	0.108	0.076	0.104
7500	0.189	0.152	0.086	0.094	0.082	0.104
7600	0.189	0.152	0.086	0.094	0.082	0.104
7700	0.189	0.152	0.086	0.081	0.082	0.104
7800	0.189	0.152	0.086	0.108	0.076	0.104
7900	0.189	0.152	0.086	0.121	0.082	0.104
8000	0.189	0.162	0.086	0.121	0.076	0.104
8100	0.189	0.162	0.086	0.121	0.076	0.104
8200	0.211	0.152	0.086	0.121	0.090	0.104
8300	0.211	0.162	0.086	0.121	0.090	0.104
8400	0.211	0.172	0.086	0.121	0.082	0.104
8500	0.211	0.172	0.086	0.121	0.082	0.104
8600	0.211	0.162	0.086	0.135	0.082	0.104
8700	0.211	0.182	0.086	0.135	0.075	0.104
8800	0.211	0.172	0.086	0.121	0.075	0.119
8900	0.211	0.172	0.086	0.121	0.082	0.119
9000	0.211	0.172	0.086	0.135	0.083	0.119
9100	0.211	0.182	0.103	0.135	0.083	0.119
9200	0.211	0.182	0.086	0.135	0.083	0.119
9300	0.232	0.172	0.086	0.135	0.083	0.104
9400	0.211	0.172	0.086	0.135	0.090	0.119
9500	0.232	0.161	0.086	0.135	0.090	0.119
9600	0.232	0.151	0.086	0.135	0.082	0.119
9700	0.232	0.161	0.086	0.135	0.090	0.119
9800	0.232	0.182	0.086	0.148	0.090	0.119
9900	0.232	0.193	0.086	0.135	0.090	0.119
10000	0.232	0.182	0.086	0.135	0.090	0.119

III. Primary datasheets (Pressure vs. time for different metals)

Table D.5: Pressure *vs.* time for different concentrations of Pt.

Time	Specific Oxygen Uptake ($mgO_2/mgVSS$)					
(s)	0 mg/l	5 mg/l	10 mg/l	15 mg/l	20 mg/l	25 mg
0	0	0	0	0	0	0
100	-0.69	-0.52	-1.00	-1.00	-0.16	-0.51
200	-0.69	-0.52	-1.00	-0.50	-0.73	-1.00
300	-0.69	-0.52	-0.46	-1.00	-0.16	-0.49
400	-0.69	-0.52	-0.54	-0.50	-0.16	-0.49
500	-0.69	-0.52	-1.00	-1.00	-1.16	-1.00
600	-0.15	-0.52	-1.54	-0.50	-0.73	-1.00
700	-0.15	-0.52	-0.54	-0.50	-0.73	-0.49
800	-0.69	-0.52	-1.00	-0.50	-0.73	-1.00
900	-0.69	-1.00	-1.54	-1.00	-1.16	-1.00
1000	-0.15	-0.52	-1.54	-1.00	-1.16	-1.00
1100	-0.69	-0.52	-1.00	-0.50	-0.73	-1.00
1200	-1.15	-1.03	-1.00	-1.00	-1.16	-1.00
1300	-1.15	-1.52	-1.54	-1.50	-1.73	-1.00
1400	-0.61	-0.52	-1.00	-1.00	-1.16	-1.00
1500	-1.15	-1.00	-1.00	-0.50	-1.16	-1.00
1600	-1.69	-1.52	-1.46	-1.50	-1.16	-1.00
1700	-1.15	-1.52	-2.00	-1.00	-1.16	-1.49
1800	-0.15	-1.00	-1.54	-1.00	-1.16	-1.00
1900	-1.15	-1.52	-2.00	-1.00	-1.16	-1.00
2000	-1.15	-1.52	-2.00	-1.50	-1.16	-1.00
2100	-1.15	-1.52	-1.54	-1.00	-1.73	-1.00
2200	-0.61	-1.00	-1.00	-1.00	-1.16	-1.49
2300	-1.15	-1.52	-1.46	-1.50	-1.16	-1.49
2400	-1.15	-1.52	-2.00	-1.50	-1.73	-1.49
2500	-1.15	-1.52	-2.00	-1.50	-1.16	-1.49
2600	-1.15	-1.00	-1.54	-1.50	-1.16	-1.49
2700	-1.61	-1.52	-2.00	-1.50	-1.73	-1.51
2800	-1.08	-1.52	-2.00	-1.50	-1.73	-1.49
2900	-0.61	-1.52	-1.54	-1.00	-1.73	-1.49
3000	-1.61	-1.52	-2.00	-1.50	-1.16	-2.00
3100	-1.61	-2.52	-2.54	-2.00	-1.73	-2.00
3200	-1.61	-2.03	-2.54	-2.00	-1.73	-2.00
3300	-1.08	-1.52	-2.00	-1.00	-1.73	-2.00
3400	-1.61	-2.03	-2.00	-2.00	-2.16	-1.51
3500	-1.61	-2.03	-2.00	-2.00	-2.73	-2.00
3600	-1.08	-2.03	-2.00	-2.00	-2.31	-2.00
3700	-1.61	-1.52	-2.00	-1.50	-2.31	-2.00
3800	-1.61	-2.52	-2.54	-2.00	-2.16	-2.00
3900	-1.08	-2.52	-2.54	-2.00	-2.73	-2.00
4000	-1.08	-2.00	-2.00	-2.00	-2.16	-2.00
4100	-1.61	-2.00	-2.00	-2.00	-2.16	-2.00
4200	-1.61	-2.52	-2.00	-2.50	-2.73	-2.00
4300	-1.61	-2.52	-2.46	-2.00	-2.73	-2.00
4400	-1.61	-2.00	-2.00	-2.00	-2.73	-2.00
4500	-1.61	-2.52	-3.00	-2.50	-2.16	-2.00
4600	-2.08	-2.52	-3.00	-2.50	-2.73	-2.00
4700	-1.08	-2.52	-2.46	-2.50	-2.73	-2.00
4800	-1.61	-2.52	-2.00	-2.00	-2.16	-2.00

Table D.5 (cont'd): Pressure *vs.* time for different concentrations of Pt.

Time	Specific Oxygen Uptake ($mgO_2/mgVSS$)					
(s)	0 mg/l	5 mg/l	10 mg/l	15 mg/l	20 mg/l	25 mg
5000	-2.08	-2.52	-3.00	-3.00	-2.73	-2.51
5100	-1.54	-2.52	-2.54	-2.00	-2.73	-2.00
5200	-2.08	-2.52	-3.00	-2.50	-2.16	-2.00
5300	-2.08	-2.52	-3.00	-2.50	-2.73	-2.51
5400	-2.08	-2.52	-3.00	-3.00	-2.73	-2.51
5500	-2.08	-2.52	-3.00	-2.00	-2.73	-2.00
5600	-2.08	-3.03	-3.00	-2.50	-3.16	-2.00
5700	-2.08	-3.03	-3.54	-3.00	-3.16	-2.51
5800	-2.08	-2.52	-3.00	-3.00	-3.16	-2.00
5900	-2.08	-2.52	-3.00	-2.50	-2.73	-2.00
6000	-2.08	-3.52	-3.00	-2.50	-3.16	-2.51
6100	-2.08	-3.52	-3.54	-3.00	-3.73	-2.51
6200	-2.08	-3.52	-3.54	-3.00	-2.73	-2.51
6300	-2.08	-3.52	-3.00	-3.00	-3.16	-2.51
6400	-2.54	-3.52	-4.00	-3.50	-3.16	-2.51
6500	-2.00	-3.52	-4.00	-3.50	-3.73	-3.00
6600	-2.08	-3.00	-3.00	-3.00	-3.16	-2.51
6700	-2.54	-3.52	-4.00	-3.50	-3.16	-3.00
6800	-2.54	-3.52	-3.54	-3.50	-3.73	-2.51
6900	-2.54	-3.52	-3.54	-3.00	-3.73	-3.00
7000	-2.54	-3.52	-3.54	-3.00	-3.16	-3.00
7100	-2.54	-4.03	-4.00	-3.50	-3.16	-2.51
7200	-2.54	-3.52	-4.00	-4.00	-3.73	-2.51
7300	-2.54	-3.52	-4.00	-3.00	-3.16	-3.00
7400	-2.54	-3.52	-4.00	-3.50	-3.16	-2.51
7500	-2.54	-4.03	-4.54	-3.50	-3.73	-2.51
7600	-2.54	-4.52	-4.00	-4.00	-3.73	-3.00
7700	-2.00	-3.52	-4.00	-3.00	-3.73	-3.00
7800	-2.54	-4.52	-4.00	-3.50	-3.73	-3.00
7900	-3.00	-4.52	-4.00	-3.50	-3.73	-3.00
8000	-3.00	-4.52	-4.54	-3.50	-4.16	-3.00
8100	-2.54	-4.00	-3.54	-4.00	-3.73	-3.00
8200	-3.00	-4.03	-4.46	-4.00	-3.73	-3.00
8300	-3.00	-4.52	-4.00	-4.00	-3.73	-3.51
8400	-3.00	-4.00	-4.00	-4.00	-3.73	-3.00
8500	-2.54	-4.52	-4.00	-3.50	-3.73	-3.00
8600	-2.54	-4.52	-4.54	-4.00	-4.73	-3.00
8700	-3.00	-4.52	-4.54	-4.00	-4.73	-3.00
8800	-2.46	-4.00	-4.54	-4.00	-4.16	-3.00
8900	-3.00	-4.52	-4.46	-4.00	-4.16	-3.00
9000	-2.46	-4.52	-4.46	-4.00	-4.73	-3.00
9100	-2.46	-4.52	-5.00	-4.00	-4.16	-3.51
9200	-2.46	-4.52	-4.54	-4.00	-4.73	-3.00
9300	-3.00	-5.03	-5.00	-4.50	-4.16	-3.51
9400	-3.00	-5.03	-5.00	-4.00	-4.73	-3.51
9500	-3.00	-4.52	-4.00	-4.00	-4.73	-3.00
9600	-3.00	-4.52	-4.46	-4.00	-4.16	-3.00
9700	-3.00	-5.00	-4.00	-4.50	-4.73	-3.51
9800	-3.00	-4.52	-5.00	-5.00	-4.73	-3.51
9900	-2.92	-4.52	-4.00	-4.00	-4.16	-3.51
10000	-3.46	-5.00	-5.00	-4.50	-4.16	-3.51

Table D.6: Pressure *vs.* time for different concentrations of Pd.

Time	Specific Oxygen Uptake ($mgO_2/mgVSS$)					
(s)	0 mg/l	5 mg/l	10 mg/l	15 mg/l	20 mg/l	25 mg
0	0	0	0	0	0	0
100	-0.53	-0.49	-0.43	-0.47	-0.40	-0.46
200	-0.53	-1.46	-1.43	-1.49	-0.86	-2.00
300	-0.53	-2.94	-1.43	-2.51	-0.86	-1.46
400	-0.53	-2.43	-1.43	-3.51	-1.40	-1.46
500	-0.53	-2.94	-1.86	-3.51	-2.47	-1.00
600	-0.53	-2.92	-2.43	-3.00	-2.93	-2.46
700	-0.53	-3.43	-2.43	-3.51	-2.93	-2.46
800	-1.53	-3.43	-2.86	-4.00	-2.47	-2.46
900	-1.00	-3.43	-3.29	-4.00	-3.40	-2.46
1000	-2.00	-3.92	-3.86	-3.49	-3.93	-3.00
1100	-2.95	-4.40	-3.86	-4.51	-3.93	-3.00
1200	-3.47	-4.40	-3.86	-5.00	-3.47	-3.46
1300	-4.47	-4.40	-4.29	-5.49	-4.40	-3.46
1400	-6.05	-5.40	-4.86	-4.49	-4.93	-4.00
1500	-7.11	-5.89	-4.86	-6.00	-4.93	-4.00
1600	-7.58	-5.38	-4.86	-6.00	-4.93	-4.00
1700	-8.11	-5.89	-5.29	-5.49	-5.47	-4.00
1800	-8.11	-6.40	-5.86	-5.98	-5.93	-4.46
1900	-8.63	-7.40	-5.86	-6.49	-4.93	-5.00
2000	-9.11	-7.40	-5.86	-6.49	-5.47	-5.00
2100	-9.11	-6.92	-6.29	-5.98	-6.93	-5.00
2200	-9.11	-7.89	-6.86	-6.49	-5.93	-6.00
2300	-10.16	-8.40	-6.86	-7.00	-6.47	-6.00
2400	-10.63	-8.40	-6.86	-6.98	-6.47	-5.46
2500	-10.63	-7.92	-6.86	-6.98	-6.93	-6.00
2600	-10.63	-8.40	-6.86	-6.98	-7.47	-6.00
2700	-11.16	-9.40	-6.86	-6.98	-7.47	-6.00
2800	-11.16	-8.92	-6.86	-6.98	-7.47	-6.00
2900	-11.16	-8.92	-7.43	-7.47	-7.93	-6.46
3000	-11.16	-9.40	-7.86	-6.98	-7.47	-7.00
3100	-12.16	-9.92	-7.43	-7.98	-6.93	-7.00
3200	-11.68	-9.92	-7.86	-7.47	-7.93	-6.46
3300	-11.16	-9.92	-7.86	-7.47	-7.93	-7.00
3400	-11.68	-10.40	-8.43	-7.47	-7.93	-7.00
3500	-12.68	-10.40	-8.43	-7.47	-7.47	-7.00
3600	-11.68	-10.43	-8.43	-7.47	-8.47	-7.00
3700	-11.68	-10.92	-8.43	-6.96	-8.93	-8.00
3800	-12.68	-10.92	-8.43	-7.47	-8.47	-7.46
3900	-12.68	-10.92	-8.43	-7.96	-8.47	-7.46
4000	-12.68	-10.92	-8.86	-7.96	-8.93	-8.00
4100	-11.68	-11.40	-9.43	-7.96	-9.47	-8.00
4200	-12.21	-11.92	-9.00	-8.47	-8.47	-8.00
4300	-12.21	-11.43	-8.86	-7.96	-9.00	-8.00
4400	-12.21	-11.43	-9.43	-7.45	-9.47	-8.00
4500	-11.68	-11.92	-9.43	-7.45	-9.47	-8.00
4600	-12.21	-11.92	-9.00	-7.96	-9.47	-8.46
4700	-12.74	-11.92	-9.00	-8.45	-9.47	-8.00
4800	-12.21	-11.92	-10.00	-7.94	-10.47	-9.00
4900	-12.21	-12.92	-9.57	-8.45	-9.47	-9.00
5000	-12.74	-12.92	-10.00	-8.45	-10.00	-9.00

Table D.6 (cont'd): Pressure *vs.* time for different concentrations of Pd.

Time	Specific Oxygen Uptake ($mgO_2/mgVSS$)					
(s)	0 mg/l	5 mg/l	10 mg/l	15 mg/l	20 mg/l	25 mg
5100	-12.74	-12.43	-10.00	-8.45	-10.47	-9.00
5200	-12.21	-12.43	-10.00	-7.94	-10.47	-9.00
5300	-12.21	-12.92	-10.00	-8.45	-10.00	-9.46
5400	-12.74	-12.92	-9.57	-8.94	-10.00	-9.00
5500	-12.74	-12.92	-10.00	-8.43	-10.47	-8.91
5600	-11.74	-12.92	-10.57	-8.43	-10.47	-9.46
5700	-12.26	-13.40	-10.57	-8.45	-10.47	-9.46
5800	-12.74	-13.92	-10.00	-8.94	-10.47	-9.00
5900	-12.74	-13.43	-10.00	-8.43	-11.47	-9.00
6000	-11.74	-13.92	-10.57	-7.94	-11.00	-9.46
6100	-12.26	-13.92	-10.57	-8.94	-10.47	-9.46
6200	-12.74	-13.92	-10.14	-8.43	-11.00	-9.46
6300	-12.26	-13.43	-10.57	-8.92	-11.47	-9.46
6400	-11.74	-13.92	-11.14	-8.43	-11.47	-10.00
6500	-12.26	-14.40	-11.14	-8.94	-10.93	-10.00
6600	-12.26	-14.40	-11.14	-9.43	-11.00	-9.46
6700	-12.26	-13.92	-11.14	-8.92	-11.47	-10.46
6800	-11.74	-14.40	-11.14	-8.43	-11.47	-10.46
6900	-12.26	-14.40	-11.14	-8.92	-11.47	-10.46
7000	-12.26	-14.40	-11.14	-8.92	-12.00	-10.00
7100	-11.74	-13.92	-11.14	-8.92	-11.93	-10.46
7200	-11.74	-14.40	-11.71	-8.41	-11.47	-10.46
7300	-12.26	-14.92	-11.14	-8.92	-12.00	-10.46
7400	-12.26	-14.40	-11.14	-8.92	-12.00	-10.46
7500	-11.74	-14.40	-11.71	-8.92	-12.47	-10.46
7600	-11.74	-15.40	-11.71	-8.92	-11.47	-11.00
7700	-12.26	-14.40	-11.71	-8.92	-11.47	-11.00
7800	-12.79	-14.92	-11.71	-8.92	-12.47	-10.46
7900	-12.26	-14.40	-11.71	-8.92	-12.47	-11.46
8000	-12.26	-15.40	-11.29	-8.92	-12.47	-11.46
8100	-12.26	-15.40	-11.71	-9.41	-12.00	-10.91
8200	-12.26	-14.92	-11.71	-9.41	-12.47	-10.46
8300	-11.26	-14.89	-12.29	-8.90	-12.47	-11.46
8400	-12.26	-15.40	-12.29	-8.92	-11.93	-11.46
8500	-12.26	-15.40	-12.29	-9.41	-12.47	-11.46
8600	-11.79	-14.92	-12.29	-9.41	-12.93	-11.46
8700	-11.26	-15.40	-12.29	-8.90	-12.47	-11.46
8800	-11.79	-15.89	-12.29	-9.41	-12.47	-11.46
8900	-12.26	-15.40	-12.29	-9.41	-12.47	-11.46
9000	-11.26	-14.92	-12.29	-9.41	-12.93	-11.46
9100	-11.26	-15.89	-12.86	-8.90	-12.47	-11.91
9200	-11.79	-15.89	-12.43	-9.41	-12.47	-11.46
9300	-11.79	-15.40	-12.29	-9.41	-13.00	-11.46
9400	-11.26	-15.40	-12.86	-8.90	-12.93	-11.91
9500	-11.26	-15.89	-12.86	-9.41	-12.93	-12.46
9600	-11.79	-15.89	-12.86	-9.90	-12.47	-11.91
9700	-11.79	-15.89	-12.86	-9.41	-12.93	-11.46
9800	-11.26	-15.89	-12.86	-8.90	-12.93	-12.46
9900	-11.26	-15.89	-13.43	-9.41	-13.47	-12.46
10000	-11.79	-15.89	-12.43	-9.90	-12.47	-12.46

Table D.7: Pressure *vs.* time for different concentrations of Rh.

Time	Specific Oxygen Uptake ($mgO_2/mgVSS$)					
(s)	0 mg/l	5 mg/l	10 mg/l	15 mg/l	20 mg/l	25 mg
0	0.000	0.000	0.000	0.000	0.000	0.000
100	-2.000	-0.074	-1.935	-1.000	-0.487	-0.486
200	-4.000	-1.630	-3.968	-4.000	-1.974	-0.973
300	-6.000	-3.185	-5.000	-6.000	-2.966	-1.459
400	-7.000	-4.667	-6.516	-7.000	-3.957	-2.459
500	-7.000	-5.667	-7.000	-7.000	-5.462	-3.459
600	-8.000	-6.148	-7.516	-7.000	-5.966	-4.486
700	-9.000	-7.630	-8.032	-8.000	-6.974	-6.000
800	-10.000	-8.148	-9.032	-9.000	-7.974	-6.000
900	-10.000	-9.148	-9.516	-10.000	-8.974	-7.000
1000	-10.000	-8.630	-10.032	-10.000	-8.479	-7.000
1100	-12.000	-10.111	-10.516	-11.000	-8.983	-7.514
1200	-12.000	-10.630	-10.548	-11.000	-10.479	-8.514
1300	-12.000	-11.148	-11.548	-12.000	-10.479	-8.514
1400	-12.000	-11.630	-11.548	-12.000	-10.479	-9.000
1500	-13.000	-11.630	-12.032	-12.000	-10.983	-9.514
1600	-13.000	-12.630	-12.548	-13.000	-11.983	-10.514
1700	-13.000	-12.630	-12.548	-13.000	-12.479	-10.514
1800	-13.000	-13.111	-13.032	-13.000	-11.983	-10.514
1900	-14.000	-12.593	-13.032	-13.000	-12.487	-10.514
2000	-15.000	-14.111	-13.548	-14.000	-13.487	-11.027
2100	-15.000	-14.111	-14.032	-14.000	-12.983	-11.514
2200	-15.000	-14.111	-14.548	-14.000	-12.983	-11.514
2300	-15.000	-14.593	-14.548	-14.000	-13.487	-11.514
2400	-15.000	-14.593	-14.548	-15.000	-13.487	-12.514
2500	-15.000	-15.111	-14.548	-15.000	-14.487	-12.514
2600	-15.000	-15.111	-15.032	-15.000	-14.487	-12.514
2700	-16.000	-15.074	-15.065	-15.000	-13.991	-12.514
2800	-17.000	-15.593	-15.065	-16.000	-14.487	-13.027
2900	-16.000	-16.111	-15.548	-15.000	-15.487	-13.514
3000	-16.000	-15.593	-15.548	-15.000	-14.991	-13.514
3100	-16.000	-16.074	-15.548	-16.000	-14.991	-13.514
3200	-17.000	-16.593	-16.065	-16.000	-15.496	-13.514
3300	-17.000	-16.593	-16.065	-16.000	-15.991	-13.514
3400	-16.000	-16.593	-16.548	-16.000	-15.487	-13.514
3500	-17.000	-16.074	-16.548	-16.000	-14.991	-13.514
3600	-17.000	-17.074	-17.065	-16.000	-15.991	-14.514
3700	-18.000	-17.593	-17.065	-17.000	-16.487	-14.514
3800	-17.000	-17.593	-17.065	-17.000	-15.991	-14.514
3900	-18.000	-17.074	-17.065	-17.000	-15.991	-14.514
4000	-18.000	-18.074	-17.065	-17.000	-16.991	-15.514
4100	-17.000	-18.074	-17.065	-17.000	-16.991	-15.000
4200	-18.000	-18.074	-17.065	-17.000	-16.496	-15.000
4300	-18.000	-17.556	-17.065	-17.000	-16.496	-15.514
4400	-18.000	-18.074	-17.548	-17.000	-16.991	-15.514
4500	-18.000	-18.074	-17.548	-17.000	-16.991	-15.514
4600	-18.000	-18.074	-17.548	-17.000	-16.991	-15.514
4700	-19.000	-18.037	-17.548	-17.000	-16.991	-15.514
4800	-19.000	-19.074	-18.065	-18.000	-17.991	-16.000
4900	-19.000	-19.074	-18.065	-17.000	-17.991	-16.000
5000	-18.000	-18.556	-18.065	-17.000	-17.496	-16.000

Table D.7 (cont'd): Pressure *vs.* time for different concentrations of Rh.

Time	Specific Oxygen Uptake ($mgO_2/mgVSS$)					
(s)	0 mg/l	5 mg/l	10 mg/l	15 mg/l	20 mg/l	25 mg
5100	-19.000	-18.556	-18.065	-18.000	-17.496	-15.514
5200	-19.000	-19.074	-18.065	-18.000	-17.991	-16.514
5300	-19.000	-19.074	-18.548	-18.000	-17.991	-16.514
5400	-19.000	-19.074	-18.548	-17.000	-17.991	-16.000
5500	-20.000	-19.074	-18.065	-18.000	-17.991	-16.514
5600	-20.000	-20.074	-18.581	-18.000	-18.496	-17.000
5700	-19.000	-19.074	-18.548	-18.000	-18.496	-17.000
5800	-19.000	-19.556	-18.548	-18.000	-17.991	-17.000
5900	-20.000	-19.556	-18.065	-18.000	-18.000	-16.514
6000	-20.000	-20.074	-19.065	-19.000	-18.991	-17.514
6100	-20.000	-20.074	-19.065	-18.000	-18.991	-17.000
6200	-20.000	-19.556	-18.548	-18.000	-18.496	-17.000
6300	-21.000	-19.556	-19.065	-19.000	-18.496	-17.514
6400	-21.000	-20.074	-19.065	-19.000	-18.991	-17.514
6500	-20.000	-20.074	-19.065	-19.000	-18.991	-17.514
6600	-20.000	-20.074	-19.065	-18.000	-18.496	-17.514
6700	-21.000	-20.037	-19.065	-19.000	-18.496	-17.514
6800	-21.000	-21.074	-19.581	-19.000	-19.496	-18.000
6900	-20.000	-21.074	-19.065	-19.000	-18.991	-17.514
7000	-20.000	-20.556	-19.548	-19.000	-18.991	-17.514
7100	-21.000	-20.556	-20.065	-19.000	-18.991	-18.000
7200	-21.000	-21.074	-19.581	-19.000	-19.496	-18.000
7300	-21.000	-21.074	-19.548	-19.000	-19.496	-18.000
7400	-21.000	-20.556	-19.548	-19.000	-19.496	-18.000
7500	-21.000	-21.074	-19.581	-20.000	-19.496	-18.514
7600	-22.000	-21.074	-19.581	-20.000	-19.991	-18.514
7700	-21.000	-21.074	-20.065	-20.000	-19.991	-18.514
7800	-21.000	-21.074	-20.065	-19.000	-19.496	-18.514
7900	-22.000	-21.556	-20.065	-20.000	-19.496	-18.514
8000	-22.000	-21.556	-20.581	-20.000	-19.991	-18.514
8100	-21.000	-21.074	-20.581	-20.000	-19.991	-19.000
8200	-21.000	-21.556	-20.065	-20.000	-19.991	-19.000
8300	-21.000	-21.556	-20.581	-20.000	-19.991	-19.000
8400	-21.000	-21.556	-20.581	-20.000	-20.496	-19.514
8500	-21.000	-21.556	-20.065	-20.000	-20.496	-19.514
8600	-22.000	-21.556	-20.065	-20.000	-20.496	-19.514
8700	-22.000	-22.074	-20.581	-21.000	-20.496	-19.514
8800	-22.000	-22.074	-20.581	-21.000	-20.496	-19.514
8900	-22.000	-22.074	-21.065	-20.000	-20.991	-19.000
9000	-22.000	-21.556	-20.581	-21.000	-20.496	-19.514
9100	-22.000	-22.074	-20.581	-21.000	-20.991	-19.514
9200	-22.000	-22.074	-21.065	-21.000	-20.991	-20.000
9300	-22.000	-22.074	-21.065	-21.000	-20.991	-20.000
9400	-22.000	-22.074	-20.581	-21.000	-21.000	-20.000
9500	-23.000	-23.074	-20.581	-21.000	-21.496	-20.000
9600	-22.000	-23.074	-20.581	-21.000	-21.496	-20.000
9700	-22.000	-22.556	-21.065	-21.000	-21.496	-20.000
9800	-23.000	-22.556	-21.581	-21.000	-21.496	-20.000
9900	-23.000	-23.074	-21.581	-21.000	-21.496	-20.514
10000	-23.000	-23.074	-21.581	-21.000	-21.496	-20.000

Table D.8: Pressure *vs.* time for different concentrations of Ru.

Time	Specific Oxygen Uptake ($mgO_2/mgVSS$)					
(s)	0 mg/l	5 mg/l	10 mg/l	15 mg/l	20 mg/l	25 mg
0	0.00	0.00	0.00	0.00	0.00	0.00
100	-1.00	-0.10	0.00	-1.00	-0.88	-1.00
200	-1.00	-0.62	-1.00	-2.00	-0.88	-1.00
300	-1.00	-0.57	-1.00	-1.00	-0.88	-2.00
400	-1.00	-0.57	-1.00	-1.00	-0.88	-2.00
500	-2.00	-0.10	-1.00	-2.00	-1.35	-2.00
600	-1.00	-1.10	-1.00	-2.00	-0.88	-2.00
700	-1.00	-1.10	-1.00	-1.00	-0.88	-2.00
800	-2.00	-1.10	-1.00	-1.00	-1.35	-2.00
900	-2.00	-1.10	-1.00	-2.00	-1.75	-2.00
1000	-1.00	-1.10	-2.00	-2.00	-1.75	-2.00
1100	-2.00	-1.10	-2.00	-2.00	-0.88	-2.00
1200	-2.00	-0.57	-2.00	-2.00	-1.75	-2.00
1300	-2.00	-1.62	-2.00	-2.00	-1.75	-2.00
1400	-2.00	-1.62	-2.00	-2.00	-1.75	-3.00
1500	-2.00	-2.10	-2.00	-2.00	-1.75	-2.00
1600	-2.00	-2.10	-2.00	-3.00	-2.22	-2.00
1700	-2.00	-2.10	-2.00	-3.00	-1.75	-3.00
1800	-2.00	-2.10	-2.00	-3.00	-1.75	-3.00
1900	-3.00	-2.10	-2.00	-2.00	-1.75	-3.00
2000	-2.00	-2.10	-2.00	-4.00	-2.22	-3.00
2100	-2.00	-2.62	-3.00	-3.00	-2.22	-3.00
2200	-3.00	-2.10	-2.00	-3.00	-1.75	-3.00
2300	-4.00	-2.10	-2.00	-3.00	-2.22	-3.00
2400	-4.00	-2.62	-2.00	-3.00	-2.63	-3.00
2500	-3.00	-3.10	-3.00	-3.00	-2.22	-3.00
2600	-4.00	-2.57	-3.00	-3.00	-2.22	-3.00
2700	-4.00	-2.57	-2.00	-4.00	-3.10	-3.00
2800	-4.00	-3.10	-3.00	-4.00	-2.63	-4.00
2900	-3.00	-3.10	-3.00	-3.00	-2.63	-4.00
3000	-4.00	-3.10	-3.00	-3.00	-2.63	-4.00
3100	-4.00	-3.10	-3.00	-4.00	-3.10	-4.00
3200	-4.00	-4.10	-3.00	-4.00	-2.63	-4.00
3300	-4.00	-3.57	-3.00	-4.00	-2.63	-4.00
3400	-5.00	-3.57	-3.00	-4.00	-3.10	-3.00
3500	-4.00	-4.10	-3.00	-5.00	-3.10	-4.00
3600	-4.00	-4.10	-3.00	-4.00	-3.10	-4.00
3700	-4.00	-4.10	-3.00	-4.00	-2.63	-4.00
3800	-5.00	-3.57	-3.00	-5.00	-3.10	-4.00
3900	-5.00	-4.10	-3.00	-5.00	-3.10	-4.00
4000	-5.00	-4.10	-4.00	-5.00	-3.10	-4.00
4100	-5.00	-4.10	-3.00	-4.00	-3.10	-4.00
4200	-5.00	-4.10	-4.00	-5.00	-3.98	-4.00
4300	-5.00	-4.62	-4.00	-6.00	-3.50	-5.00
4400	-5.00	-5.10	-3.00	-5.00	-3.10	-4.00
4500	-6.00	-4.57	-4.00	-5.00	-3.57	-5.00
4600	-6.00	-5.10	-4.00	-6.00	-3.98	-5.00
4700	-6.00	-5.10	-4.00	-6.00	-3.98	-5.00
4800	-6.00	-5.10	-4.00	-5.00	-3.50	-5.00
4900	-7.00	-4.57	-4.00	-6.00	-3.98	-5.00
5000	-6.00	-5.10	-4.00	-6.00	-3.98	-5.00

Table D.8 (cont'd): Pressure *vs.* time for different concentrations of Ru.

Time	Specific Oxygen Uptake ($mgO_2/mgVSS$)					
(s)	0 mg/l	5 mg/l	10 mg/l	15 mg/l	20 mg/l	25 mg
5100	-6.00	-5.62	-4.00	-6.00	-3.98	-5.00
5200	-6.00	-5.10	-4.00	-6.00	-3.98	-6.00
5300	-7.00	-5.10	-4.00	-6.00	-4.45	-5.00
5400	-6.00	-5.62	-4.00	-6.00	-3.98	-6.00
5500	-6.00	-5.57	-4.00	-6.00	-3.98	-5.00
5600	-7.00	-5.57	-4.00	-6.00	-4.45	-5.00
5700	-7.00	-6.10	-4.00	-7.00	-3.98	-6.00
5800	-7.00	-6.10	-5.00	-6.00	-3.98	-6.00
5900	-7.00	-6.10	-5.00	-6.00	-3.98	-5.00
6000	-7.00	-6.10	-4.00	-7.00	-4.45	-6.00
6100	-7.00	-6.10	-5.00	-7.00	-4.45	-6.00
6200	-7.00	-6.10	-4.00	-7.00	-4.45	-6.00
6300	-7.00	-6.10	-4.00	-6.00	-4.45	-6.00
6400	-7.00	-6.57	-4.00	-8.00	-4.45	-6.00
6500	-7.00	-7.10	-5.00	-7.00	-4.45	-6.00
6600	-7.00	-6.57	-5.00	-7.00	-4.45	-6.00
6700	-8.00	-6.57	-4.00	-7.00	-4.45	-6.00
6800	-8.00	-7.10	-5.00	-8.00	-4.92	-6.00
6900	-7.00	-7.10	-5.00	-8.00	-4.45	-7.00
7000	-8.00	-7.10	-5.00	-8.00	-4.45	-7.00
7100	-9.00	-6.57	-4.00	-8.00	-5.32	-6.00
7200	-8.00	-7.57	-5.00	-8.00	-4.92	-7.00
7300	-8.00	-7.57	-5.00	-8.00	-4.45	-7.00
7400	-9.00	-7.05	-5.00	-8.00	-4.92	-7.00
7500	-9.00	-7.57	-5.00	-7.00	-5.32	-7.00
7600	-9.00	-7.57	-5.00	-7.00	-5.32	-7.00
7700	-9.00	-7.57	-5.00	-6.00	-5.32	-7.00
7800	-9.00	-7.57	-5.00	-8.00	-4.92	-7.00
7900	-9.00	-7.57	-5.00	-9.00	-5.32	-7.00
8000	-9.00	-8.10	-5.00	-9.00	-4.92	-7.00
8100	-9.00	-8.10	-5.00	-9.00	-4.92	-7.00
8200	-10.00	-7.57	-5.00	-9.00	-5.79	-7.00
8300	-10.00	-8.10	-5.00	-9.00	-5.79	-7.00
8400	-10.00	-8.57	-5.00	-9.00	-5.32	-7.00
8500	-10.00	-8.57	-5.00	-9.00	-5.32	-7.00
8600	-10.00	-8.10	-5.00	-10.00	-5.32	-7.00
8700	-10.00	-9.10	-5.00	-10.00	-4.85	-7.00
8800	-10.00	-8.57	-5.00	-9.00	-4.85	-8.00
8900	-10.00	-8.57	-5.00	-9.00	-5.32	-8.00
9000	-10.00	-8.57	-5.00	-10.00	-5.39	-8.00
9100	-10.00	-9.10	-6.00	-10.00	-5.39	-8.00
9200	-10.00	-9.10	-5.00	-10.00	-5.39	-8.00
9300	-11.00	-8.57	-5.00	-10.00	-5.39	-7.00
9400	-10.00	-8.57	-5.00	-10.00	-5.79	-8.00
9500	-11.00	-8.05	-5.00	-10.00	-5.79	-8.00
9600	-11.00	-7.52	-5.00	-10.00	-5.32	-8.00
9700	-11.00	-8.05	-5.00	-10.00	-5.79	-8.00
9800	-11.00	-9.10	-5.00	-11.00	-5.79	-8.00
9900	-11.00	-9.62	-5.00	-10.00	-5.79	-8.00
10000	-11.00	-9.10	-5.00	-10.00	-5.79	-8.00

Appendix E: MATLAB scripts and primary data sheets - Chapter 8.0

I. MATLAB scripts for implementation of ASM1_PGM

```
function dxdt = ASM1_PGM (t,x);
% This MATLAB function implements the ASM1_PGM. First it defines the relationships among
% different growth rates and the relevant parameters. Then, based on the Petersen matrix,
% stoichiometric relations of each reactant is combined. Finally mass balance over reactor is defined
% for each component.

% STEPS TO FOLLOW:

% 1. Define state variables.

% 2. Define parameters and their values.

% 3. Define processes: Growth rates of aerobes, anoxic, decays, hydrolysis, ammonification.

% 4. Combine processes and components using stoichiometry to find the fate of each component.

% 5. Apply the mass balance equation for each reactor type. e.g. CSTR, PBR etc.

% 6. Solve the equations and find the steady state values for all the state variables.

% 7. Plot the graphs using simulation and the actual experimental data in the same graph and hold
%    them for comparison.

% 8. Select some parameters and change their values of 5, 10, 15, 20, 50 and 100 percent (%) changes
%    to see the effect on the output.

% 9. Identify the most critical parameters based on the above sensitivity analysis.

% 10. CHECK UNITS AND THEIR CONSISTENCY in ALL VARIABLES AND PARAMETERS.

%-----------------------------------------------------------------------------------------------------------%
% STATE variables: Redefine for calculation simplification purposes. Mass balance equations will be
% solved in the same sequence to keep the integrity of each component in 9 x n global matrix.

S_S = x(1); S_TAN = x(2); S_TNO2 = x(3); S_NO3 = x(4);
X_H = x(5); X_AOB = x(6); X_NOB = x(7); X_ANX = x(8); X_S = x(9);


%--------------------------Common formulae, parameters and their respective values.-----------------%

V_C = 0.75/(1000); %1.5/(1000); % Volume of CSTR in m3.
V_P = 0.75/(1000); % Volume of PBR in m3.
R = 1; % Recycle ratio. Q_R/Q_F = R; Q_R = Recirculate flow rate, Q_F = Feed.

S_O = 2.5; %global S_O(j) ; % Dissolved oxygen content in the reactor in  g/m3.
S_PGM = 20; % PGM metal concentration in g/m3.

% Q_C Flow rate of CSTR in m3/d.
% Q_P Flow rate of PBR in m3/d.
```

```
Q_R = (2*1.2*60*24)/(1000*1000); % Return sludge flow rate of CSTR in m3/d.
% Maximum specific growth rates of different microbes.
mu_H_max = 8.72;      % Maximum heterotrophic growth rate in 1/d(Wyffels et al., 2004).
mu_AOB_max = 2.02;  % Maximum AOB growth rate in 1/d(Wyffels et al., 2004).
mu_NOB_max = 1.36;  % Maximum NOB growth rate in 1/d(Wyffels et al., 2004).
mu_ANX_max = 0.019;% Maximum ANX growth rate in 1/d(Van Hulle, 2005).

% Decay coefficients of different microbes.
b_H = 2.32;           % Heterotrophic decay coefficients in 1/d (Wyffels et al., 2004).
b_AOB = 0.19;         % AOB decay coefficients in 1/d (Wyffels et al., 2004).
b_NOB = 0.092;        % NOB decay coefficients in 1/d (Wyffels et al., 2004).
b_ANX = 0.0025;       % ANX decay coefficients in 1/d (Van Hulle, 2005).

% Yield coefficients of different microbes.
Y_H = 0.52;           % Heterotrophic yield in gCOD/gCOD (Wyffels et al., 2004)
Y_AOB = 0.15;         % AOB yield in gCOD/gN (Wyffels et al., 2004)
Y_NOB = 0.041;        % NOB yield in gCOD/gN (Wyffels et al., 2004)
Y_NO3 = 0.44;         % Heterotrophic yield in gCOD/gCOD (Wyffels et al., 2004)
Y_TNO2 = 0.44;        % Heterotrophic yield in gCOD/gCOD (Wyffels et al., 2004)
Y_ANX = 0.159;        % Anammox yield in gCOD/gN (Van Hulle, 2005).

% Anoxic coefficients for heterotrophs.
beta_NO2 = 0.6;       % Anoxic reduction factor (Wyffels et al., 2004).
beta_NO3=0.6;         % Anoxic reduction factor (Wyffels et al., 2004).

% Half-saturation, inhibition coefficients and other parameters.
K_OA = 0.235; % Saturation constant for S_O of X_AOB in gO2/m3(Wyffels et al., 2004).
K_NH3 = 0.85; % Saturation constant for S_NH3 of X_AOB in gN/m3(Wyffels et al., 2004).
K_OH = 0.2;    % Saturation constant for S_O of X_H in gO2/m3(Wyffels et al., 2004).
K_SH = 50;     % Saturation constant for S_S of X_H in gCOD/m3(Wyffels et al., 2004).
K_NO3 = 1;     % Saturation constant for S_S of X_H in gN/m3(Wyffels et al., 2004).
K_TNO2 = 1;   % Saturation constant for S_S of X_H in gN/m3(Wyffels et al., 2004).
K_ON = 1.5;    % Saturation constant for S_O of X_NOB in gO2/m3(Wyffels et al., 2004).
K_HNO2= 0.0009; % Saturation constant for S_HNO2 of X_AOB in gO2/m3(Wyffels et al., 2004).
K_TAN = 0.07; % Saturation constant for S_TAN of X_ANX in gO2/m3 (Van Hulle, 2005).
K_X = 0.03;    % Substrate constant for X_S in gCOD/gCOD (Van Hulle, 2005)
K_OAN = 0.01;% Inhibition coefficient for S_O of X_ANX in gO2/m3 (Van Hulle, 2005).
K_PGM = 33.34;        % Inhibition coefficient of Rh in g/m3 (Chapter 6).

k_H = 3;              % Maximum specific hydrolysis rate in gCOD/gCOD/d (Van Hulle, 2005)
f_i = 0.15;           % Production of X_I from decay gCOD/gCOD(Wyffels et al., 2004).
f_p = 0.1;            % Production of X_I from deacy (Van Hulle, 2005).
i_nxi = 0.02;         % N content of X_I in gN/gCOD(Wyffels et al., 2004).
i_nbm = 0.0583;       % N content of biomass in gN/gCOD(Wyffels et al., 2004).

%---------------------------------------- Aerobic Growth of heterotrophs ----------------------------------%

r_H_O2 = u_H_max*(S_O/(K_OH+S_O))*(S_S/(K_SH+S_S))*(K_PGM/(K_PGM+S_PGM))*X_H;


%---------------------------------- Anoxic Growth of heterotrophs on NO3----------------------------------%

r_H_NO3 = mu_H_max*beta_NO3*(K_OH/(K_OH+S_O))*(S_NO3/(K_NO3+S_NO3))*...
      (S_NO3/(S_TNO2+S_NO3))*(S_S/(K_SH+S_S))*(K_PGM/(K_PGM+S_PGM))*X_H;
```

```
%---------------------------------- Anoxic Growth of heterotrophs on TNO2-----------------------------%

r_H_TNO2 = mu_H_max*beta_NO2*(K_OH/(K_OH+S_O))*(S_TNO2/(K_TNO2+S_TNO2))*...
       (S_TNO2/(S_TNO2+S_NO3))*(S_S/(K_SH+S_S))*(K_PGM/(K_PGM+S_PGM))*X_H;

%---------------------------------- Aerobic Growth of autotrophs (AOB)--------------------------------%

r_AOB = mu_AOB_max*(S_O/(K_OA+S_O))*(S_TAN/(K_NH3+S_TAN))*...
     (K_PGM/(K_PGM+S_PGM))*X_AOB;

%-------------------------------Aerobic Growth of Nitrite oxidisers (NOB)-----------------------------%

r_NOB = mu_NOB_max*(S_O/(K_ON+S_O))*(S_TNO2/(K_HNO2+S_TNO2))*...
     (K_PGM/(K_PGM+S_PGM))*X_NOB;

%---------------------------------- Anammox Growth on NH4 and NO2 -----------------------------------%

r_ANX = mu_ANX_max*(K_OAN/(K_OAN+S_O))*(S_TAN/(K_TAN+S_TAN))*...
     (S_TNO2/(K_TNO2+S_TNO2))*(K_PGM/(K_PGM+S_PGM))*X_ANX;

%---------------------------------------Decay of heterotrophics-------------------------------------%

r_D_H = b_H*X_H;

%---------------------------------------- Decay of AOB ----------------------------------------------%

r_D_AOB = b_AOB*X_AOB;

%---------------------------------------- Decay of NOB ----------------------------------------------%

r_D_NOB = b_AOB*X_NOB;

%---------------------------------------- Decay of Anammox ------------------------------------------%

r_D_ANX = b_ANX*X_ANX;

%---------------------------------- Hydrolysis of entrapped organics ---------------------------------%

r_HD_O = k_H*((X_S/X_H)/(K_X+(X_S/X_H)))*X_H;

%-------------------------------------------------------------------------------------------------------%

% Component generation/disappearance rates  (+) Production; (-) Utilisation;

% Net rate of utilisation of oxygen.

r_S_O2 = (-1*(1-Y_H)/Y_H)*r_H_O2 + (-1*(3.43-Y_AOB)/Y_AOB)*r_AOB +...
   (-1*(1.14-Y_NOB)/Y_NOB)*r_NOB;

% Net rate of production of readily biodegradable organic substrates.

r_S_S = r_HD_O + (-1/Y_H)*r_H_O2 + (-1/Y_NO3)*r_H_NO3 + (-1/Y_TNO2)*r_H_TNO2;
```

```
% Net rate of production of total ammonium (formation - utilisation).

r_S_TAN = (-i_nbm)*r_H_O2 + (i_nbm-f_p*i_nxi)*r_D_H + (-i_nbm)*r_H_NO3 +...
   (-i_nbm)*r_H_TNO2 + (-1/Y_AOB-i_nbm)*r_AOB + (i_nbm-f_p*i_nxi)*r_D_AOB...
   + (-i_nbm*r_NOB) + (i_nbm-f_p*i_nxi)*r_D_NOB + (-1/Y_ANX - i_nbm)*r_ANX...
   + (i_nbm-f_p*i_nxi)*r_D_ANX;

% Net rate of production of TNO2 (formation - utilisation).

r_S_TNO2 = ((1-Y_NO3)/(1.14*Y_NO3))*r_H_NO3 + (-1*(1-Y_NO2)/(1.71*Y_NO2))...
        *r_H_TNO2 + (1/Y_AOB)*r_AOB + (-1/Y_NOB)*r_NOB +...
        (-1*(1.52+1/Y_ANX))*r_ANX;

% Net rate of production of NO3- (formation - utilisation).

r_S_NO3 = -(1-Y_NO3)/(1.14*Y_NO3)*r_H_NO3 + (1/Y_NOB)*r_NOB + 1.52*r_ANX;

% Nett rate of production of Nitrogen gas.

r_S_N2 = ((1-Y_NO2)/(1.71*Y_NO2))* r_H_TNO2 + (2/Y_NOB)* r_ANX;

% Net rate of growth of Heterotroph biomass.

r_X_H = r_H_O2 - r_D_H + r_H_NO3 + r_H_TNO2;

% Net rate of growth of AOB biomass.

r_X_AOB = r_AOB - r_D_AOB;

% Net rate of growth of NOB biomass.

r_X_NOB = r_NOB - r_D_NOB;

% Net rate of growth of Anammox biomass.

r_X_ANX = r_ANX - r_D_ANX;

% Net rate of production of slowly biodegradable substrates.

r_X_S = (-1)* r_HD_O + (1-f_i)* r_D_H + (1-f_i)*r_AOB + (1-f_i)*r_D_NOB ...
   + (1-f_i)*r_D_ANX;

% Net rate of production of inert particulates.

r_X_I = f_i*r_D_H + f_i*r_D_AOB + f_i*r_D_NOB + f_i*r_D_ANX;

%-----------------------------------------------------------------------------------------------------------------%

% MASS BALANCE OVER REACTOR AND CLARIFIER.

% Calculate the concentrations in g/m3 = mg/l.

global x0;

% Initial conditions for different influent conditions.
```

```
S_S_IN_CSTR = x0(1);
S_TAN_IN_CSTR = x0(2);
S_TNO2_IN_CSTR = x0(3);
S_NO3_IN_CSTR = x0(4);
X_H_IN_CSTR = x0(5);
X_AOB_IN_CSTR = x0(6);
X_NOB_IN_CSTR = x0(7);
X_ANX_IN_CSTR = x0(8);
X_S_IN_CSTR = x0(9);

% Form a set of differential algebraic equations (DAEs) for time domain analysis of various interested
% state variables. (Number of state variables = number of DAEs).

dS_S = (Q_R/(V_C*R))*(S_S_IN_CSTR - S_S) + r_S_S;                    % In g/m3/d.
dS_TAN = (Q_R/(V_C*R))*(S_TAN_IN_CSTR - S_TAN) + r_S_TAN;           % In g/m3/d.
dS_TNO2 = (Q_R/(V_C*R))*(S_TNO2_IN_CSTR - S_TNO2) + r_S_TNO2;       % In g/m3/d.
dS_NO3 = (Q_R/(V_C*R))*(S_NO3_IN_CSTR - S_NO3) + r_S_NO3;           % In g/m3/d.
dX_H = (Q_R/(V_C*R))*(X_H_IN_CSTR - X_H) + r_X_H;                   % In g/m3/d.
dX_AOB = (Q_R/(V_C*R))*(X_AOB_IN_CSTR - X_AOB) + r_X_AOB;           % In g/m3/d.
dX_NOB = (Q_R/(V_C*R))*(X_NOB_IN_CSTR - X_NOB) + r_X_NOB;           % In g/m3/d.
dX_ANX = (Q_R/(V_C*R))*(X_ANX_IN_CSTR - X_ANX) + r_X_ANX;           % In g/m3/d.
dX_S = (Q_R/(V_C*R))*(X_S_IN_CSTR - X_S) + r_X_S;                   % In g/m3/d.

dxdt = [dS_S dS_TAN dS_TNO2 dS_NO3 dX_H dX_AOB dX_NOB dX_ANX dX_S]';

% g/m3 = mg/l.
% ------------------------------------------------------------------------------------------------------------ %

% --------------------------STEADY STATE SIMULATION OF ASM1_PGM--------------------------- %

% Initial conditions for S_O(1); S_S(2); S_TAN(3); S_TNO2(4); S_NO3(5); X_H(6); X_AOB(7);
% X_NOB(8); X_ANX(9); X_N(10); X_S(11);

x0 = [10 69.2 0.03 67.8 523 261.75 157.05 5 52.35];

% Solve the set of DAEs described in ASM1_PGM.
[t, y] = ode15s('ASM1_PGM',[0 0.2], x0);


% Plot the parameters.
plot (t,y(:,1),'*',t,y(:,2),'+',t,y(:,3),'-',t,y(:,4),'s', t,y(:,5),'>', t,y(:,6),'h',t,y(:,7),'o',t,y(:,8),'v'), t,y(:,9),'-.')

xlabel('\fontname{Times New Roman}\bf{}\fontsize{11}Time (d)')
ylabel('\fontname{Times New Roman}\bf{}\fontsize{11}Concentration(mg/l)')
legend('Soluble organics','Ammonium-N','Nitrite-N','Nitrate-N',...
        'Heterotrophic biomass','AOB','NOB','Anammox',1)

% ------------------------------------------------------------------------------------------------------------ %
% ---------------------------DYNAMIC SIMULATION OF ASM1_PGM------------------------------ %

%---------------------------------------- EXPERIMENTAL DATA ----------------------------------------%
% This script simulates the dynamic behaviour of CSTR under different influent conditions over
% 80 days. This script simulate the output of different component in the CSTR and plot with the
% measured values.
% Read experimental data from MS Excel sheet.
```

```
% S_NH4_IN, S_NO3_IN, S_MLSS and COD etc. for the CSTR.
[t_days] = xlsread('CSTR_PBR_SMALL.xls','CSTR_PBR','B7:B42');
[S_S_IN_CSTR] = xlsread('CSTR_PBR_SMALL.xls','CSTR_PBR','J7:J42'); %J42');
[S_S_OUT_CSTR] = xlsread('CSTR_PBR_SMALL.xls','CSTR_PBR','N7:N42');
[S_TAN_IN_CSTR] = xlsread('CSTR_PBR_SMALL.xls','CSTR_PBR','G7:G42');
[S_TAN_OUT_CSTR] = xlsread('CSTR_PBR_SMALL.xls','CSTR_PBR','K7:K42');
[S_TNO2_IN_CSTR] = xlsread('CSTR_PBR_SMALL.xls','CSTR_PBR','H7:H42');
[S_TNO2_OUT_CSTR] = xlsread('CSTR_PBR_SMALL.xls','CSTR_PBR','L7:L42');
[S_NO3_IN_CSTR] = xlsread('CSTR_PBR_SMALL.xls','CSTR_PBR','I7:I42');
[S_NO3_OUT_CSTR] = xlsread('CSTR_PBR_SMALL.xls','CSTR_PBR','M7:M42');

[S_MLSS] = xlsread('CSTR_PBR_SMALL.xls','CSTR_PBR','E7:E42');

% Approximate biomass fractions based on MLSS found in the given wastewater.
[X_H_IN_CSTR] = (0.38*0.5)*[S_MLSS];
[X_AOB_IN_CSTR] = (0.38*0.25)*[S_MLSS];
[X_NOB_IN_CSTR] = (0.38*0.15)*[S_MLSS];
[X_ANX_IN_CSTR] = (0.38*0.05)*[S_MLSS];
[X_S_IN_CSTR] = (0.38*0.05)*[S_MLSS];

%-----------------------------------------------------------------------------------------------------------------------%

i = numel(t_days);

% Define the steady state matrices for different influent conditions.

[t_S]=[]; [S_SS]=[]; [S_TAN_SS]=[]; [S_TNO2_SS]=[]; [S_NO3_SS]=[];
[X_H_SS]=[]; [X_AOB_SS]=[]; [X_NOB_SS]=[]; [X_ANX_SS]=[]; [X_S_SS]=[];

for j = 1:1:i

   % Load relevant data to appropreate influent concentration matrix.

   S_S_IN_CSTR(j);
   S_TAN_IN_CSTR(j);
   S_TNO2_IN_CSTR(j);
   S_NO3_IN_CSTR(i);
   X_H_IN_CSTR(j);
   X_AOB_IN_CSTR(j);
   X_NOB_IN_CSTR(j);
   X_ANX_IN_CSTR(j);
   X_S_IN_CSTR(j);

   % Use each concentrations of influent data as initial conditions.
   global x0;

   x0 = [S_S_IN_CSTR(j) S_TAN_IN_CSTR(j) S_TNO2_IN_CSTR(j) S_NO3_IN_CSTR(j)...
         X_H_IN_CSTR(j) X_AOB_IN_CSTR(j) X_NOB_IN_CSTR(j) X_ANX_IN_CSTR(j)...
         X_S_IN_CSTR(j)];

   % Solve the ASM1_PGM2 for ADE to get time-varying dependencies of each component.
   [t, y] = ode15s('ASM1_PGM_SA',[0 2], x0);

   % Load time varying final concentrations.
   y1 = y(:,1); y2 = y(:,2); y3 = y(:,3); y4 = y(:,4); y5 = y(:,5);
```

```
    y6 = y(:,6); y7 = y(:,7); y8 = y(:,8); y9 = y(:,9); %y10 = y(:,10);

    % Get the steady state concentration in the reactor for each component.
    [t_S] = [t_S; t_days(i)];
    [S_SS] = [S_SS; y1(40)];
    [S_TAN_SS] = [S_TAN_SS; y2(40)];
    [S_TNO2_SS] = [S_TNO2_SS; y3(40)];
    [S_NO3_SS] = [S_NO3_SS; y4(40)];
    [X_H_SS] = [X_H_SS; y5(40)];
    [X_AOB_SS] = [X_AOB_SS; y6(40)];
    [X_NOB_SS] = [X_NOB_SS; y7(40)];
    [X_ANX_SS] = [X_ANX_SS; y8(40)];
    [X_S_SS] = [X_S_SS; y9(40)];

end

% ----------Plot desired parameters ----------%

% Model vs. measured of AMMONIUM output in the reactor.
subplot(2,2,1); plot (t_days,S_TAN_SS,'*-',t_days,S_TAN_OUT_CSTR,'+--')

xlabel('\fontname{Times New Roman}\bf{}\fontsize{11}Time (d)')
ylabel('\fontname{Times New Roman}\bf{}\fontsize{11}NH_4^+-N(mg/l)')
legend('Model','Measured',2)
% Model vs. measured of NITRATE output in the reactor.
subplot(2,2,2); plot (t_days,S_NO3_SS,'*-',t_days,S_NO3_OUT_CSTR,'+--')

xlabel('\fontname{Times New Roman}\bf{}\fontsize{11}Time (d)')
ylabel('\fontname{Times New Roman}\bf{}\fontsize{11}NO_3 ^--N(mg/l)')
legend('Model','Measured',2)

% Model vs. measured of NITRITE output in the reactor.
subplot(2,2,3); plot (t_days,S_TNO2_SS,'*-',t_days,S_TNO2_OUT_CSTR,'+--')

xlabel('\fontname{Times New Roman}\bf{}\fontsize{11}Time (d)')
ylabel('\fontname{Times New Roman}\bf{}\fontsize{11}NO_2 ^--N(mg/l)')
legend('Model','Measured',2)


% Model vs. measured of TOTAL COD output in the reactor.
subplot(2,2,4); plot (t_days,S_SS,'*-',t_days,S_S_OUT_CSTR,'+--')

xlabel('\fontname{Times New Roman}\bf{}\fontsize{11}Time (d)')
ylabel('\fontname{Times New Roman}\bf{}\fontsize{11}Total COD(mg/l)')
legend('Model','Measured',2)

% ----------%
```

II. Mixed liquor suspended solids and mixed liquor volatile suspended liquor

Table E1: MLSS and VSS fractions in the simulated PMR wastewaters.

MLSS	**FS**	**MLVSS**	$\frac{MLVSS}{MLSS}$
mg/l	**mg/l**	**mg/l**	
2160	1420	740	0.34
2040	1430	610	0.30
2020	1300	720	0.36
1800	1180	620	0.34
1710	1140	570	0.33
1580	1090	490	0.31
1850	1210	640	0.35
1660	1090	570	0.34
1440	1030	410	0.28
2100	1010	1090	0.52
1390	720	670	0.48
1320	900	420	0.32
1235	525	710	0.57
1155	655	500	0.43
1235	740	495	0.40
1355	840	515	0.38
1275	825	450	0.35
Mean			**0.38**
Standard deviation			**0.08**

III. Primary data sheets for sensitivity analysis

Table E2: Effect of Y_H on $[NH_4^+-N]$ in dynamic simulation of the CSTR.

Time (day)	Measured $[NH_4^+-N]$ (mg/l)	Model prediction and error of $[NH_4^+-N]$ in mg/l ($Y_H = 0.52$)							
		1 % of Y_H		5 % of Y_H		10 % of Y_H		15 %of Y_H	
		Model	Error	Model	Error	Model	Error	Model	Error
0	35.0	66.5	-31.5	43.6	-8.6	30.4	4.6	20.2	14.8
5	23.1	51.3	-28.2	32.8	-9.7	6.2	16.9	7.1	16.0
7	28.8	45.8	-17.0	33.3	-4.5	8.9	19.9	6.7	22.1
9	22.8	41.7	-18.9	27.6	-4.8	10.4	12.4	5.4	17.4
11	8.2	27.4	-19.2	18.2	-10.0	10.1	-1.9	5.6	2.6
13	8.7	23.1	-14.4	13.7	-5.0	7.6	1.1	4.4	4.3
18	5.3	18.6	-13.3	4.3	1.0	1.0	4.3	2.2	3.1
20	8.6	20.8	-12.2	6.0	2.6	5.6	3.0	2.8	5.8
23	15.5	13.2	2.3	3.6	11.9	2.2	13.3	3.2	12.3
30	2.6	31.5	-28.9	13.5	-10.9	7.3	-4.7	5.5	-2.9
36	12.8	18.4	-5.6	12.0	0.8	9.1	3.7	8.5	4.3
38	3.9	17.7	-13.8	3.6	0.3	2.9	1.0	2.8	1.1
40	9.1	54.9	-45.8	38.8	-29.7	20.2	-11.1	3.4	5.7
42	9.8	56.5	-46.7	44.0	-34.2	27.3	-17.5	16.3	-6.5
44	11.3	33.3	-22.0	19.0	-7.7	10.4	0.9	6.1	5.2
46	11.2	56.5	-45.3	41.8	-30.6	25.9	-14.7	10.8	0.4
48	12.0	44.1	-32.1	34.9	-22.9	23.6	-11.6	16.9	-4.9
50	9.3	51.1	-41.8	51.1	-41.8	51.1	-41.8	51.1	-41.8
52	8.1	45.0	-36.9	35.3	-27.2	25.7	-17.6	16.5	-8.4
54	10.0	42.1	-32.1	29.7	-19.7	14.1	-4.1	4.8	5.2
56	1.8	38.7	-36.9	26.1	-24.3	15.4	-13.6	10.6	-8.8
58	14.5	42.6	-28.1	27.2	-12.7	13.3	1.2	7.4	7.1
60	27.7	46.7	-19.0	30.8	-3.1	11.9	15.8	5.6	22.1
62	25.2	47.4	-22.2	34.6	-9.4	19.2	6.0	12.2	13.0
64	31.6	51.0	-19.4	37.8	-6.2	20.2	11.4	10.5	21.1
66	21.0	44.6	-23.6	21.9	-0.9	3.7	17.3	1.4	19.6
68	7.7	39.1	-31.4	25.8	-18.1	14.8	-7.1	9.7	-2.0
70	4.6	37.9	-33.3	22.2	-17.6	9.4	-4.8	5.4	-0.8
72	6.0	40.9	-34.9	22.1	-16.1	2.5	3.5	1.2	4.8
74	3.4	36.9	-33.5	18.1	-14.7	6.3	-2.9	3.1	0.3
76	5.7	42.0	-36.3	29.7	-24.0	17.7	-12.0	11.4	-5.7
78	8.0	39.1	-31.1	21.6	-13.6	7.4	0.6	3.3	4.7
80	4.3	41.6	-37.3	27.8	-23.5	6.6	-2.3	3.8	0.5
82	20.1	62.2	-42.1	49.5	-29.4	23.5	-3.4	4.8	15.3
84	18.7	67.8	-49.1	49.6	-30.9	26.3	-7.6	2.2	16.5
86	29.5	76.9	-47.4	58.1	-28.6	32.7	-3.2	4.6	24.9
Mean	13.5	42.1	**-28.6**	28.1	**-14.6**	14.7	**-1.2**	8.3	**5.2**

Table E3: Effect of Y_H on [NO_3^--N] in dynamic simulation of the CSTR.

Time (day)	Measured [NO_3^--N] (mg/l)	Model prediction and error of [NO_3^--N] in mg/l (Y_H = 0.52)							
		1 % of Y_H		5 % of Y_H		10 % of Y_H		15 % of Y_H	
		Model	Error	Model	Error	Model	Error	Model	Error
0	111.2	70.6	40.6	94.0	17.2	107.5	3.7	117.8	-6.6
5	155.4	46.8	108.6	65.7	89.7	93.0	62.4	92.0	63.4
7	151.2	72.7	78.5	85.5	65.7	110.6	40.7	112.7	38.5
9	147.4	69.0	78.4	83.6	63.9	101.2	46.2	106.3	41.1
11	98.6	65.4	33.2	75.0	23.6	83.3	15.3	87.9	10.7
13	88.0	68.2	19.8	77.7	10.3	83.7	4.3	86.7	1.3
18	222.2	57.7	164.5	72.4	149.8	75.8	146.4	74.5	147.7
20	77.2	51.8	25.4	67.0	10.2	67.4	9.8	70.2	7.0
23	101.4	38.6	62.8	48.0	53.4	49.1	52.3	48.1	53.3
30	204.6	67.9	136.7	86.3	118.3	92.5	112.1	94.2	110.4
36	73.0	40.6	32.4	47.4	25.6	50.4	22.6	51.0	22.0
38	131.0	117.0	14.1	130.6	0.4	131.1	-0.1	131.2	-0.2
40	258.6	100.9	157.7	116.3	142.3	134.2	124.4	151.0	107.6
42	192.8	121.1	71.8	133.2	59.6	149.6	43.2	160.1	32.7
44	209.2	119.9	89.3	134.1	75.1	142.3	66.9	146.3	62.9
46	188.4	123.1	65.3	137.5	50.9	153.2	35.2	168.2	20.2
48	250.1	142.1	108.1	151.0	99.1	162.1	88.0	168.5	81.6
50	266.2	116.1	150.1	116.1	150.1	116.1	150.1	116.1	150.1
52	284.8	133.7	151.1	143.1	141.7	152.4	132.4	161.3	123.5
54	292.0	129.6	162.4	141.5	150.6	156.6	135.4	165.7	126.4
56	294.5	132.6	161.9	145.2	149.3	155.8	138.7	160.2	134.3
58	227.1	127.6	99.6	143.1	84.0	157.0	70.1	162.5	64.7
60	167.2	93.2	74.0	109.1	58.2	128.0	39.2	133.8	33.4
62	136.8	74.4	62.4	87.3	49.5	102.7	34.1	109.5	27.3
64	156.4	76.4	80.0	89.5	66.9	107.0	49.4	116.4	40.0
66	220.5	93.0	127.5	115.4	105.2	133.5	87.1	134.9	85.7
68	289.6	126.3	163.3	139.6	150.0	150.4	139.2	155.2	134.4
70	282.4	134.2	148.2	149.9	132.5	162.5	119.9	166.1	116.3
72	310.9	152.6	158.4	171.4	139.6	192.1	118.8	192.8	118.2
74	341.0	160.0	180.9	179.1	161.8	190.9	150.1	193.5	147.4
76	322.9	131.3	191.6	143.6	179.3	155.5	167.4	161.5	161.4
78	292.0	145.1	147.0	162.3	129.7	176.3	115.7	179.7	112.3
80	301.6	148.8	152.9	162.8	138.8	184.6	117.0	187.4	114.2
82	178.0	104.4	73.6	117.4	60.7	144.2	33.9	164.2	13.8
84	215.8	98.6	117.2	116.1	99.7	138.6	77.2	163.6	52.2
86	301.6	110.8	190.8	128.7	173.0	152.9	148.7	181.1	120.5
Mean	209.5	101.7	**107.8**	115.7	**93.8**	129.0	**80.5**	135.3	**74.2**

Table E4: Effect of Y_{AOB} on $[NH_4^+-N]$ in dynamic simulation of the CSTR.

Time (day)	Measured $[NH_4^+-N]$ (mg/l)	Model prediction and error of $[NH_4^+-N]$ in mg/l (Y_AOB = 0.19)							
		90 % of Y_{AOB}		95 % of Y_{AOB}		105 % of Y_{AOB}		110 % of Y_{AOB}	
		Model	Error	Model	Error	Model	Error	Model	Error
0	35.0	40.4	-5.4	40.9	-5.9	51.7	-16.7	61.1	-26.1
5	23.1	7.2	15.9	6.6	16.5	37.3	-14.2	46.0	-22.9
7	28.8	0.8	28.0	2.4	26.4	35.7	-6.9	40.4	-11.6
9	22.8	2.0	20.8	2.0	20.8	32.6	-9.8	38.4	-15.6
11	8.2	0.1	8.1	1.1	7.1	18.3	-10.1	24.4	-16.2
13	8.7	0.1	8.6	0.9	7.8	6.9	1.8	16.4	-7.7
18	5.3	0.4	4.9	3.1	2.2	9.2	-3.9	15.2	-9.9
20	8.6	0.2	8.4	2.7	5.9	13.3	-4.7	18.1	-9.5
23	15.5	0.1	15.4	0.6	14.9	0.6	14.9	4.8	10.7
30	2.6	9.6	-7.0	3.0	-0.4	8.4	-5.8	24.3	-21.7
36	12.8	0.2	12.6	1.7	11.1	11.2	1.6	16.3	-3.5
38	3.9	0.0	3.9	0.1	3.8	3.2	0.7	11.2	-7.3
40	9.1	10.7	-1.6	13.2	-4.1	25.0	-15.9	29.3	-20.2
42	9.8	27.6	-17.8	29.3	-19.5	30.3	-20.5	38.9	-29.1
44	11.3	0.8	10.5	0.9	10.4	1.8	9.5	15.2	-3.9
46	11.2	25.0	-13.8	27.5	-16.3	29.0	-17.8	38.5	-27.3
48	12.0	20.2	-8.2	25.7	-13.7	27.2	-15.2	21.3	-9.3
50	9.3	51.1	-41.8	51.1	-41.8	51.1	-41.8	51.1	-41.8
52	8.1	24.0	-15.9	25.3	-17.2	27.7	-19.6	23.0	-14.9
54	10.0	11.2	-1.2	12.1	-2.1	16.5	-6.5	17.8	-7.8
56	1.8	4.8	-3.0	8.9	-7.1	9.2	-7.4	22.5	-20.7
58	14.5	0.9	13.6	1.5	13.0	17.2	-2.7	34.4	-19.9
60	27.7	8.1	19.6	7.2	20.5	22.0	5.7	33.9	-6.2
62	25.2	17.9	7.3	14.5	10.7	17.2	8.0	32.2	-7.0
64	31.6	17.4	14.2	19.5	12.1	18.6	13.0	32.3	-0.7
66	21.0	0.1	20.9	0.1	20.9	13.6	7.4	27.4	-6.4
68	7.7	8.0	-0.3	9.6	-1.9	14.6	-6.9	24.3	-16.6
70	4.6	1.9	2.7	3.0	1.6	6.7	-2.1	26.0	-21.4
72	6.0	0.2	5.8	0.3	5.7	9.7	-3.7	21.0	-15.0
74	3.4	0.2	3.2	0.3	3.1	15.4	-12.0	18.0	-14.6
76	5.7	8.2	-2.5	12.3	-6.6	14.2	-8.5	25.2	-19.5
78	8.0	1.1	6.9	0.9	7.1	8.5	-0.5	16.9	-8.9
80	4.3	8.6	-4.3	5.9	-1.6	27.7	-23.4	34.7	-30.4
82	20.1	18.6	1.5	21.0	-0.9	29.6	-9.5	43.6	-23.5
84	18.7	10.3	8.4	23.7	-5.0	28.2	-9.5	38.3	-19.6
86	29.5	17.9	11.6	30.0	-0.5	34.7	-5.2	44.0	-14.5
Mean	13.5	9.9	**3.6**	11.4	**2.1**	20.1	**-6.6**	28.5	**-15.0**

Table E5: Effect of Y_{AOB} on $[NO_3^-\text{-N}]$ in dynamic simulation of the CSTR.

Time (day)	Measured $[NO_3^-\text{-N}]$ (mg/l)	Model prediction and error of $[NO_3^-\text{-N}]$ in mg/l (Y_{AOB} = 0.19)							
		90 % of Y_{AOB}		95 % of Y_{AOB}		105 % of Y_{AOB}		110 % of Y_{AOB}	
		Model	Error	Model	Error	Model	Error	Model	Error
0	111.2	94.6	16.6	95.6	15.6	85.7	25.5	76.1	35.1
5	155.4	88.1	67.3	91.3	64.1	61.1	94.3	52.2	103.2
7	151.2	116.0	35.2	116.3	34.9	83.1	68.1	78.3	72.9
9	147.4	107.0	40.4	109.2	38.2	78.5	68.9	72.5	74.9
11	98.6	93.0	5.6	92.5	6.1	74.9	23.7	68.6	30.0
13	88.0	91.4	-3.4	90.6	-2.6	84.5	3.5	74.8	13.2
18	222.2	76.4	145.8	73.5	148.7	67.3	154.9	61.2	161.0
20	77.2	72.8	4.4	70.3	6.9	59.4	17.8	54.5	22.7
23	101.4	51.2	50.2	50.7	50.7	50.7	50.7	46.6	54.8
30	204.6	88.1	116.5	96.5	108.1	91.4	113.2	75.2	129.4
36	73.0	59.5	13.5	57.9	15.1	48.3	24.7	43.0	30.0
38	131.0	133.9	-2.9	133.8	-2.8	130.8	0.2	123.1	7.9
40	258.6	138.9	119.7	138.9	119.7	130.0	128.6	125.7	132.9
42	192.8	145.8	47.0	145.8	47.0	146.9	45.9	138.1	54.7
44	209.2	149.6	59.6	151.3	57.9	151.2	58.0	137.5	71.7
46	188.4	150.3	38.1	149.6	38.8	150.2	38.2	140.5	47.9
48	250.1	162.9	87.3	158.8	91.4	158.6	91.5	164.7	85.4
50	266.2	116.1	150.1	116.1	150.1	116.1	150.1	116.1	150.1
52	284.8	151.6	133.2	151.6	133.2	150.6	134.2	155.5	129.3
54	292.0	155.9	136.1	156.7	135.3	154.5	137.5	153.2	138.8
56	294.5	163.3	131.2	160.9	133.6	162.2	132.4	148.5	146.0
58	227.1	166.2	60.9	167.6	59.5	153.0	74.1	135.6	91.5
60	167.2	127.3	39.9	130.4	36.8	117.7	49.5	105.7	61.5
62	136.8	100.6	36.2	105.6	31.2	104.8	32.0	89.4	47.4
64	156.4	106.0	50.5	105.8	50.7	108.8	47.6	94.8	61.6
66	220.5	133.6	86.9	136.3	84.3	123.3	97.2	109.8	110.8
68	289.6	154.1	135.5	154.2	135.3	150.7	138.9	140.8	148.8
70	282.4	166.7	115.7	167.4	115.0	165.4	117.0	145.8	136.6
72	310.9	190.5	120.5	192.3	118.6	184.8	126.2	173.2	137.8
74	341.0	194.5	146.5	196.2	144.8	181.5	159.5	178.9	162.1
76	322.9	161.6	161.3	159.3	163.6	159.1	163.8	147.8	175.1
78	292.0	178.8	113.2	181.4	110.6	175.1	116.9	166.5	125.5
80	301.6	179.7	121.9	184.4	117.2	162.9	138.7	155.8	145.8
82	178.0	144.2	33.8	144.2	33.8	139.3	38.8	125.0	53.0
84	215.8	149.0	66.9	138.7	77.2	138.6	77.2	129.2	86.6
86	301.6	161.6	140.0	152.9	148.7	152.9	148.7	144.5	157.1
Mean	209.5	131.1	**78.4**	131.2	**68.5**	123.7	**85.8**	115.2	**94.2**

Table E6: Effect of K_{NH3} on [NH_4^+-N] in dynamic simulation of the CSTR.

Time (day)	Measured [NH_4^+-N] (mg/l)	Model prediction and error of [NH_4^+-N] in mg/l (K_NH3 = 0.52)							
		50 % of K_{NH3}		90 % of K_{NH3}		125 % of K_{NH3}		150 % of K_{NH3}	
		Model	Error	Model	Error	Model	Error	Model	Error
0	35.0	32.4	2.6	30.9	4.1	27.4	7.6	27.0	8.0
5	23.1	8.4	14.7	6.1	17.0	9.9	13.2	9.3	13.8
7	28.8	7.6	21.2	9.0	19.8	12.5	16.3	13.5	15.3
9	22.8	7.5	15.3	11.4	11.4	12.1	10.7	15.5	7.3
11	8.2	7.0	1.2	10.1	-1.9	11.4	-3.2	13.6	-5.4
13	8.7	4.3	4.4	7.9	0.8	7.3	1.4	6.5	2.2
18	5.3	0.4	4.9	2.2	3.1	4.5	0.8	8.6	-3.3
20	8.6	0.6	8.0	3.7	4.9	5.1	3.5	10.6	-2.0
23	15.5	1.3	14.2	1.7	13.8	0.4	15.1	2.4	13.1
30	2.6	10.6	-8.0	5.9	-3.3	8.4	-5.8	9.8	-7.2
36	12.8	6.2	6.6	8.3	4.5	11.2	1.6	12.2	0.6
38	3.9	0.5	3.4	2.5	1.4	2.1	1.8	3.0	0.9
40	9.1	19.7	-10.6	19.7	-10.6	16.1	-7.0	17.4	-8.3
42	9.8	26.2	-16.4	25.4	-15.6	26.7	-16.9	27.2	-17.4
44	11.3	4.1	7.2	9.2	2.1	13.0	-1.7	13.7	-2.4
46	11.2	27.1	-15.9	27.5	-16.3	26.4	-15.2	26.5	-15.3
48	12.0	23.4	-11.4	24.5	-12.5	26.5	-14.5	26.6	-14.6
50	9.3	51.1	-41.8	51.1	-41.8	51.1	-41.8	51.1	-41.8
52	8.1	25.6	-17.5	25.7	-17.6	24.0	-15.9	25.0	-16.9
54	10.0	13.6	-3.6	14.0	-4.0	13.9	-3.9	16.5	-6.5
56	1.8	12.9	-11.1	14.6	-12.8	17.8	-16.0	19.2	-17.4
58	14.5	5.2	9.3	11.5	3.0	14.7	-0.2	18.3	-3.8
60	27.7	6.5	21.2	10.6	17.1	14.6	13.1	17.2	10.5
62	25.2	8.7	16.5	17.5	7.7	22.8	2.4	24.2	1.0
64	31.6	19.8	11.8	20.1	11.5	21.9	9.7	24.8	6.8
66	21.0	0.1	20.9	2.8	18.2	5.8	15.2	8.2	12.8
68	7.7	12.9	-5.2	14.5	-6.8	17.9	-10.2	19.1	-11.4
70	4.6	3.0	1.6	8.4	-3.8	12.2	-7.6	14.8	-10.2
72	6.0	0.3	5.7	1.8	4.2	4.3	1.7	6.3	-0.3
74	3.4	1.2	2.2	5.2	-1.8	8.7	-5.3	10.9	-7.5
76	5.7	16.4	-10.7	16.2	-10.5	19.8	-14.1	22.1	-16.4
78	8.0	1.6	6.4	6.2	1.8	10.0	-2.0	12.6	-4.6
80	4.3	4.1	0.2	6.2	-1.9	7.7	-3.4	7.5	-3.2
82	20.1	23.1	-3.0	23.4	-3.3	23.7	-3.6	23.9	-3.8
84	18.7	25.9	-7.2	26.3	-7.6	26.5	-7.8	18.8	-0.1
86	29.5	32.3	-2.8	32.7	-3.2	32.9	-3.4	33.1	-3.6
Mean	13.5	12.5	**1.0**	14.3	**-0.8**	15.9	**-2.4**	17.1	**-3.6**

Table E7: Effect of K_{NH3} on [NO_3^--N] in dynamic simulation of the CSTR.

Time (day)	Measured [NO_3^--N] (mg/l)	Model prediction and error of [NO_3^--N] in mg/l (K_NH3 = 0.52)							
		50 % of K_{NH3}		90 % of K_{NH3}		125 % of K_{NH3}		150 % of K_{NH3}	
		Model	Error	Model	Error	Model	Error	Model	Error
0	111.2	105.4	5.8	107.0	4.3	110.6	0.6	111.0	0.3
5	155.4	90.7	64.7	93.1	62.3	89.2	66.2	89.8	65.6
7	151.2	111.9	39.3	110.4	40.8	106.8	44.4	105.9	45.3
9	147.4	104.1	43.3	100.1	47.3	99.5	47.9	95.9	51.5
11	98.6	86.4	12.2	83.3	15.3	82.0	16.6	79.8	18.8
13	88.0	87.1	0.9	83.4	4.6	84.0	4.0	84.8	3.2
18	222.2	76.4	145.8	74.6	147.6	72.2	150.0	67.9	154.3
20	77.2	72.5	4.7	69.3	7.9	67.9	9.3	62.2	15.0
23	101.4	50.0	51.4	49.6	51.8	50.9	50.5	48.9	52.5
30	204.6	89.1	115.5	94.0	110.6	91.4	113.2	89.9	114.7
36	73.0	53.4	19.6	51.2	21.8	48.2	24.8	47.2	25.8
38	131.0	133.4	-2.4	131.5	-0.5	131.8	-0.8	131.0	0.0
40	258.6	134.2	124.4	134.6	124.0	138.8	119.8	137.7	120.9
42	192.8	150.5	42.3	151.5	41.3	150.4	42.4	150.0	42.8
44	209.2	148.7	60.5	143.5	65.7	139.7	69.5	139.0	70.2
46	188.4	151.6	36.9	151.3	37.1	152.7	35.7	152.7	35.7
48	250.1	162.1	88.0	161.1	89.0	159.2	90.9	159.2	90.9
50	266.2	116.1	150.1	116.1	150.1	116.1	150.1	116.1	150.1
52	284.8	152.3	132.5	152.4	132.4	154.3	130.5	153.4	131.4
54	292.0	156.6	135.4	156.6	135.4	157.1	134.9	154.5	137.5
56	294.5	158.1	136.4	156.6	137.9	153.3	141.2	151.9	142.6
58	227.1	165.2	61.9	158.8	68.3	155.6	71.5	151.9	75.2
60	167.2	133.2	34.0	129.3	38.0	125.2	42.0	122.6	44.6
62	136.8	113.4	23.4	104.4	32.4	99.0	37.8	97.6	39.2
64	156.4	107.0	49.4	107.0	49.4	105.4	51.0	102.4	54.0
66	220.5	137.8	82.7	134.3	86.2	131.2	89.3	128.8	91.7
68	289.6	152.2	137.4	150.8	138.8	147.2	142.3	146.1	143.5
70	282.4	169.0	113.4	163.6	118.8	159.7	122.7	157.0	125.4
72	310.9	194.0	116.9	192.8	118.1	190.3	120.7	188.2	122.7
74	341.0	196.0	144.9	192.0	149.0	188.4	152.6	186.1	154.9
76	322.9	156.5	166.4	157.0	165.9	153.4	169.5	151.0	171.9
78	292.0	182.1	109.9	177.4	114.6	173.5	118.5	170.9	121.1
80	301.6	187.1	114.5	185.0	116.6	183.5	118.1	183.7	117.9
82	178.0	144.2	33.9	144.2	33.9	144.2	33.9	144.2	33.9
84	215.8	138.6	77.2	138.6	77.2	138.6	77.2	147.3	68.6
86	301.6	152.9	148.7	152.9	148.7	152.9	148.7	152.9	148.7
Mean	209.5	131.1	**78.4**	129.4	**80.1**	127.9	**81.6**	126.6	**82.8**

Table E8: Effect of K_{OA} on $[NH_4^+-N]$ in dynamic simulation of the CSTR.

Time (day)	Measured $[NH_4^+-N]$ (mg/l)	Model prediction and error of $[NH_4^+-N]$ in mg/l (K_{OA} = 0.235)							
		50 % of K_{OA}		90 % of K_{OA}		125 % of K_{OA}		150 % of K_{OA}	
		Model	Error	Model	Error	Model	Error	Model	Error
0	35.0	38.0	-3.0	34.8	0.3	32.7	2.3	28.1	6.9
5	23.1	8.3	14.8	11.8	11.3	8.7	14.4	4.4	18.7
7	28.8	5.1	23.7	10.2	18.6	10.7	18.1	8.7	20.1
9	22.8	5.2	17.6	7.5	15.3	11.4	11.4	10.0	12.8
11	8.2	4.2	4.0	8.0	0.2	8.0	0.2	9.8	-1.6
13	8.7	2.7	6.0	4.7	4.0	6.0	2.7	6.6	2.1
18	5.3	2.2	3.1	0.6	4.7	0.7	4.6	0.9	4.4
20	8.6	4.3	4.3	1.6	7.0	1.9	6.7	1.3	7.3
23	15.5	1.2	14.3	1.7	13.8	2.8	12.7	1.4	14.1
30	2.6	6.2	-3.6	11.7	-9.1	7.4	-4.8	6.9	-4.3
36	12.8	4.0	8.8	6.5	6.3	7.0	5.8	7.4	5.4
38	3.9	0.3	3.6	0.8	3.1	1.2	2.7	1.4	2.5
40	9.1	18.8	-9.7	21.1	-12.0	20.0	-10.9	20.2	-11.1
42	9.8	26.4	-16.6	26.6	-16.8	25.2	-15.4	25.5	-15.7
44	11.3	1.3	10.0	5.6	5.7	6.2	5.1	8.2	3.1
46	11.2	27.6	-16.4	23.3	-12.1	27.0	-15.8	26.3	-15.1
48	12.0	26.2	-14.2	25.0	-13.0	23.5	-11.5	23.6	-11.6
50	9.3	51.1	-41.8	51.1	-41.8	51.1	-41.8	51.1	-41.8
52	8.1	25.8	-17.7	25.4	-17.3	26.0	-17.9	25.7	-17.6
54	10.0	12.9	-2.9	13.5	-3.5	12.3	-2.3	14.1	-4.1
56	1.8	9.6	-7.8	9.0	-7.2	13.1	-11.3	14.1	-12.3
58	14.5	7.6	6.9	4.7	9.8	8.0	6.5	11.0	3.5
60	27.7	2.3	25.4	2.8	24.9	6.8	20.9	10.2	17.5
62	25.2	11.1	14.1	15.5	9.7	18.2	7.0	19.0	6.2
64	31.6	21.0	10.6	22.5	9.1	20.0	11.6	20.0	11.6
66	21.0	0.1	20.9	0.5	20.5	1.2	19.8	2.0	19.0
68	7.7	11.3	-3.6	11.8	-4.1	10.7	-3.0	14.0	-6.3
70	4.6	3.3	1.3	2.9	1.7	5.5	-0.9	7.3	-2.7
72	6.0	0.2	5.8	0.4	5.6	0.7	5.3	1.0	5.0
74	3.4	0.8	2.6	1.6	1.8	2.9	0.5	4.1	-0.7
76	5.7	12.7	-7.0	12.5	-6.8	16.6	-10.9	16.1	-10.4
78	8.0	0.2	7.8	1.7	6.3	3.3	4.7	5.0	3.0
80	4.3	6.7	-2.4	8.4	-4.1	7.1	-2.8	5.0	-0.7
82	20.1	22.1	-2.0	22.9	-2.8	23.3	-3.2	23.6	-3.5
84	18.7	16.5	2.2	25.7	-7.0	26.2	-7.5	26.5	-7.8
86	29.5	19.5	10.0	32.1	-2.6	32.6	-3.1	32.9	-3.4
Mean	13.5	11.6	**1.9**	12.9	**0.5**	13.5	**0.0**	13.7	**-0.2**

Table E9: Effect of K_{OA} on $[NO_3^-N]$ in dynamic simulation of the CSTR.

Time (day)	Measured $[NO_3^-N]$ (mg/l)	Model prediction and error of $[NO_3^-N]$ in mg/l (K_{OA}= 0.235)							
		50 % of K_{OA}		90 % of K_{OA}		125 % of K_{OA}		150 % of K_{OA}	
		Model	Error	Model	Error	Model	Error	Model	Error
0	111.2	99.3	11.9	103.0	8.2	105.2	6.0	110.0	1.3
5	155.4	90.6	64.8	87.2	68.2	90.5	64.9	94.9	60.5
7	151.2	114.4	36.8	109.2	42.0	108.7	42.5	110.8	40.4
9	147.4	106.5	40.9	104.2	43.2	100.2	47.3	101.6	45.8
11	98.6	89.4	9.2	85.5	13.1	85.5	13.1	83.6	15.0
13	88.0	88.8	-0.8	86.7	1.3	85.3	2.7	84.7	3.3
18	222.2	74.5	147.7	76.2	146.0	76.1	146.1	75.9	146.3
20	77.2	68.7	8.5	71.5	5.7	71.2	6.0	71.8	5.4
23	101.4	50.1	51.3	49.7	51.7	48.6	52.8	49.9	51.5
30	204.6	93.7	110.9	88.0	116.6	92.4	112.2	92.9	111.7
36	73.0	55.6	17.4	53.1	19.9	52.6	20.4	52.1	20.9
38	131.0	133.6	-2.6	133.2	-2.2	132.8	-1.8	132.6	-1.6
40	258.6	134.3	124.4	132.6	126.0	134.2	124.4	134.2	124.4
42	192.8	149.5	43.3	149.9	42.9	151.7	41.1	151.6	41.2
44	209.2	151.7	57.5	147.0	62.2	146.7	62.5	144.7	64.5
46	188.4	150.2	38.2	155.3	33.1	151.9	36.6	152.8	35.6
48	250.1	158.7	91.4	160.3	89.8	162.1	88.0	162.1	88.0
50	266.2	116.1	150.1	116.1	150.1	116.1	150.1	116.1	150.1
52	284.8	151.6	133.2	152.4	132.5	152.0	132.8	152.4	132.4
54	292.0	156.7	135.3	156.7	135.4	158.3	133.7	156.6	135.4
56	294.5	161.0	133.5	162.2	132.3	158.1	136.4	157.2	137.4
58	227.1	161.7	65.4	165.7	61.4	162.4	64.7	159.4	67.7
60	167.2	137.1	30.1	137.3	29.9	133.2	34.0	129.7	37.5
62	136.8	110.1	26.7	106.1	30.7	103.7	33.1	103.0	33.8
64	156.4	105.1	51.3	104.1	52.3	107.0	49.4	107.3	49.1
66	220.5	137.1	83.4	136.7	83.8	136.0	84.5	135.2	85.3
68	289.6	153.3	136.3	153.2	136.3	154.7	134.8	151.3	138.3
70	282.4	168.0	114.4	169.2	113.2	166.6	115.8	164.7	117.6
72	310.9	193.9	117.1	194.2	116.8	194.0	117.0	193.7	117.3
74	341.0	196.2	144.8	195.7	145.3	194.4	146.6	193.1	147.9
76	322.9	159.8	163.1	160.6	162.3	156.5	166.4	157.2	165.7
78	292.0	184.1	108.0	182.1	109.9	180.5	111.5	178.7	113.3
80	301.6	184.5	117.1	182.8	118.8	184.1	117.5	186.3	115.4
82	178.0	144.2	33.9	144.2	33.9	144.2	33.9	144.2	33.9
84	215.8	147.3	68.6	138.6	77.2	138.6	77.2	138.6	77.2
86	301.6	164.9	136.7	152.9	148.7	152.9	148.7	152.9	148.7
Mean	209.5	131.7	**77.8**	130.6	**78.8**	130.2	**79.2**	130.1	**79.4**

Appendix F: Primary data sheets - Chapter 9.0

Table F1: Ammonium and nitrate at influent and effluent in PBR-CSTR-PBR configuration.

Time	NH_4^+-N (mg/l)		NO_3^--N (mg/l)	
(d)	Influent	Effluent	Influent	Effluent
0	59.70	1.6	544.00	6.27
2	47.20	1.7	443.17	4.58
4	44.90	2.1	426.80	5.00
6	81.40	1.9	469.90	5.08
8	66.30	1.0	479.84	4.35
10	66.20	0.8	437.65	4.96
12	75.80	1.1	579.23	6.19
14	83.00	4.3	699.21	4.66
16	151.20	8.3	645.78	4.68
18	152.40	8.9	188.90	4.62
21	92.80	7.2	332.96	6.72
26	158.80	4.0	216.11	32.31
28	135.40	7.0	283.98	22.94
32	80.80	12.4	222.35	19.57
35	143.20	14.4	209.14	16.22
38	130.60	15.0	236.35	10.70
40	127.40	13.8	228.77	8.52
45	82.80	13.4	280.53	57.66
47	80.40	13.0	391.89	78.29
49	70.20	13.6	339.38	20.80
51	74.00	12.4	332.53	20.89
53	77.00	12.2	411.07	15.64
58	79.60	11.6	71.77	5.31
57	78.10	14.1	28.56	6.15
60	73.20	11.3	288.30	4.36
63	150.00	11.3	380.43	6.67
68	118.00	11.6	377.34	6.12
71	96.80	12.0	455.19	7.72
73	93.60	12.0	527.17	9.02
75	194.40	12.3	540.22	8.48

Table F2: The pH and MLSS variation in CSTR and $PBR_{Secondary}$ under PBR-CSTR-PBR configuration.

Time	CSTR		PBR
(d)	MLSS*	pH	pH
0	2160	6.49	8.18
2	2040	6.87	8.15
4	2020	7.09	8.19
6	2050	6.96	8.23
8	1890	6.38	8.06
10	1800	6.53	8.04
12	1710	6.22	7.94
14	1730	6.19	7.61
16	1580	6.09	7.23
18	1850	6.61	6.83
21	1660	6.30	7.25
26	1440	6.93	6.73
28	2100	6.87	6.60
32	1480	6.73	6.60
35	1390	7.21	6.60
38	1320	7.12	6.67
40	1525	7.05	6.92
45	1235	7.52	7.06
47	1155	7.43	6.97
49	1235	7.39	6.96
51	-	7.60	7.02
53	-	7.50	6.98
58	-	7.67	7.02
57	1355	7.64	7.26
60	1275	7.62	7.21
63	1215	7.75	7.26
68	1235	7.68	7.23
71	1315	7.50	7.29
73	1320	7.28	7.21
75	1220	7.14	7.25

* MLSS in mg/l.

Table F3: Nitrate accumulation / reduction in clarifiers of CSTR and $PBR_{Secondary}$.

Time (d)	CSTR		$PBR_{Secondary}$	
	NO_3^--N (mg/l)		NO_3^--N (mg/l)	
	Out	Clarifier	Out	Clarifier
0	586.54	544.00	6.27	7.10
2	460.18	443.17	4.58	5.41
4	439.48	426.80	5.00	7.89
6	479.84	469.90	5.08	9.17
8	469.90	479.84	4.35	10.84
10	435.82	437.65	4.96	18.06
12	576.81	579.23	6.19	4.94
14	708.04	699.21	4.66	5.21
16	667.76	645.78	4.68	4.86
18	210.88	188.90	4.62	5.60
21	370.20	332.96	6.72	7.72
26	108.04	216.11	32.31	23.22
28	275.99	283.98	22.94	28.83
32	203.27	222.35	19.57	29.54
35	214.32	209.14	16.22	20.05
38	232.53	236.35	10.70	13.45
40	238.29	228.77	8.52	8.59
45	274.87	280.53	57.66	51.86
47	413.22	391.89	78.29	76.40
49	338.00	339.38	20.80	6.17
51	306.48	332.53	20.89	4.62
53	407.73	411.07	15.64	5.69
58	295.44	71.77	5.31	8.94
57	314.08	28.56	6.15	6.15
60	295.44	288.30	4.36	4.36
63	357.85	380.43	6.67	6.67
68	349.20	377.34	6.12	6.12
71	472.21	455.19	7.72	7.72
73	535.83	527.17	9.02	9.02
75	375.80	540.22	8.48	9.94